Lincoln Silva Carneiro

SISTEMÁTICA E DIVERSIFICAÇÃO DOS GÊNEROS *HYLOPEZUS* E *MYRMOTHERA* (AVES: GRALLARIIDAE)

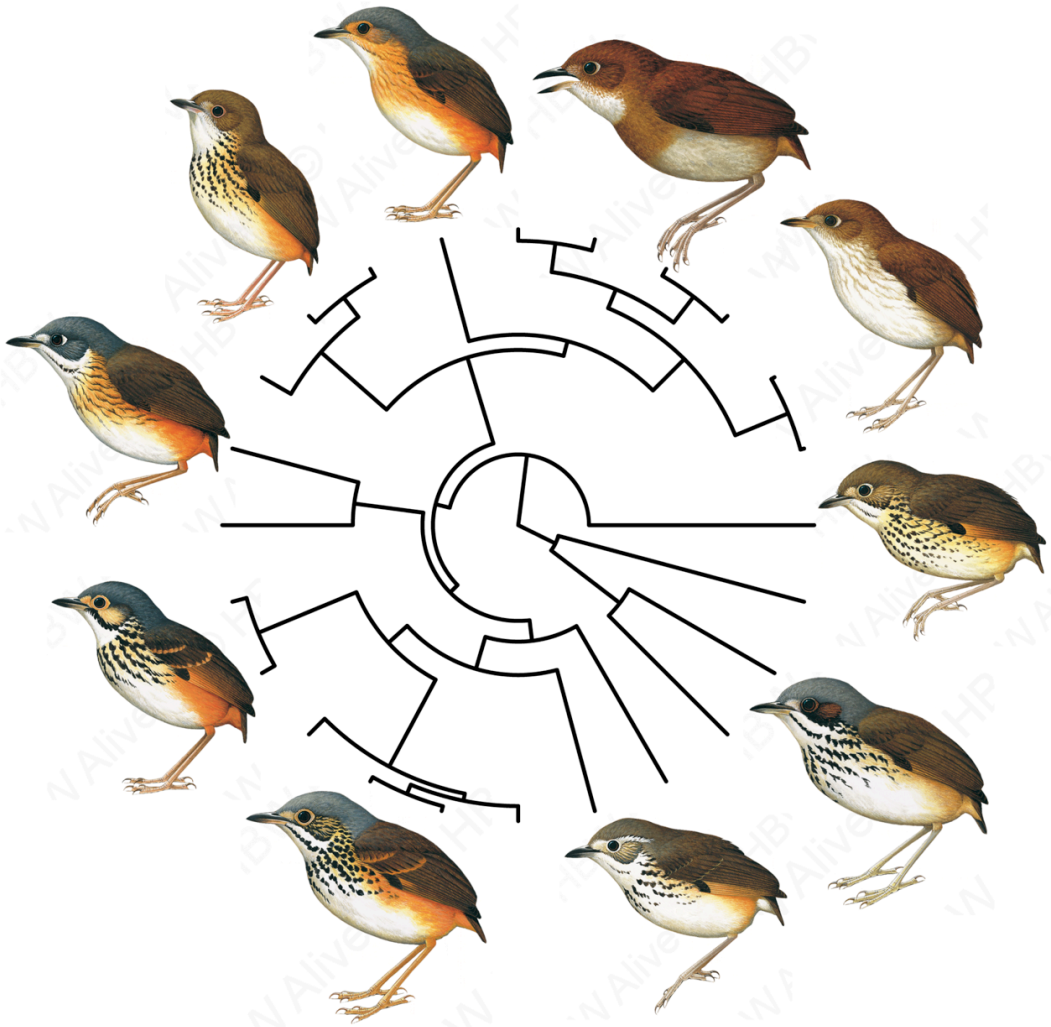

UNIVERSIDADE FEDERAL DO PARÁ/ MUSEU PARAENSE EMÍLIO GOELDI

MUSEU PARAENSE EMÍLIO GOELDI
UNIVERSIDADE FEDERAL DO PARÁ
PROGRAMA DE PÓS-GRADUAÇÃO EM ZOOLOGIA
CURSO DE MESTRADO EM ZOOLOGIA

SISTEMÁTICA E DIVERSIFICAÇÃO DOS GÊNEROS *HYLOPEZUS* E *MYRMOTHERA* (AVES: GRALLARIIDAE)

Aluno: Lincoln Silva Carneiro

Tese apresentada ao Programa de Pós-graduação em Zoologia, Curso de Doutorado, do Museu Paraense Emílio Goeldi e Universidade Federal do Pará como requisito para obtenção do grau de doutor em Zoologia.

Orientador: Dr. Alexandre Aleixo

BELÉM – PARÁ
2015

*"*Uma longa viagem de mil milhas

inicia-se com o movimento de um pé*"*

Lao-Tsé

LINCOLN SILVA CARNEIRO

SISTEMÁTICA E DIVERSIFICAÇÃO DOS GÊNEROS *HYLOPEZUS* E *MYRMOTHERA* (AVES: GRALLARIIDAE)

_____

Dr. Alexandre Aleixo
Orientador
Departamento de Zoologia, Museu Paraense Emílio Goeldi

_____

Dra. Teresa Cristina Sauer de Ávila-Pires
Titular
Departamento de Zoologia, Museu Paraense Emílio Goeldi

_____

Dra. Camila Cherem Ribas
Titular
Instituto Nacional de Pesquisas da Amazônia

_____

Dr. Pericles Sena do Rêgo
Titular
Universidade Federal do Pará

_____

Dr. Alexander Charles Lees
Titular
Museu Paraense Emílio Goeldi

_____

Dr. José de Sousa e Silva Júnior
Suplente
Museu Paraense Emilio Goeldi

_____

Dra. Sofia Alexandre Marques Silva
Suplente
Museu Paraense Emilio Goeldi

AGRADECIMENTOS

Gostaria de agradecer a todas pessoas e instituições que contribuíram direta e indiretamente para que esse trabalho se concretizasse.

Quero agradecer ao Museu Paraense Emílio Goeldi, à Universidade Federal do Pará e ao programa de pós-graduação. A Capes pelo suporte financeiro durante estes quatro anos de pesquisas.

A todos os curadores de diversas instituições Nacionais e Internacionais: Natan Rice (ANSP), John Bates (FMNH), Carla Fontana (PUC), Cristina Miyake (LGEMA), Ao Field Museum of Natural History (FMNH), na figura do Dr. Jonh Bates; aos Drs. Paul Sweet e Joel Cracraft, do American Museum of Natural History (AMNH); ao Dr. Nathan Rice, da Academy of Natural Sciences of Drexel University (ANSP); ao Dr. Terry Chesser, do National Museum of Natural History (NMNH); à Dra. Cristina Miyake (LGEMA); à Dra. Carla Fontana, da Pontifícia Universidade Católica do RS (PUC-RS); ao Dr. Mark Robbins, do Kansas University Natural History Museum (KUNHM); Donna Ditmann e Robb Brumfield (LSU).

A Terry Chesser e Joel Cracraft por me ajudarem na obtenção de financiamento que possibilitou a analise das peles depositadas nas principais coleções dos EUA. E por me receberem em suas respectivas instituições. E aos diversos colaboradores que gentilmente nos cederam vocalizações e tecidos de todo Neotrópico, em especial ao Dr. Gustavo Bravo pela parceria neste trabalho e pelas importantes amostras moleculares que nos cedeu.

Aos amigos do Museu Paraense Emilio Goeldi e aos meus colegas de Doutorado Youzef Bitar, André Ravetta, Leandra Cardoso, João Carlos, Adriano Maciel, Marcela Lima, Laura Miglio, Guilherme Dutra. Leonardo Trevellin. Aos amigos da ornitologia do Goeldi que ajudaram diretamente na consecução do trabalho e na preparação da Tese: Leonardo Miranda, Lucas Araújo, Leonardo Moura, Tibério Burlamaqui, Sidnei Dantas, Sofia Silva e Eduardo Portes. A Fátima Lima, cujo trabalho bem feito permite que encontremos todas as informações da coleção de Aves do MPEG, e pelos agradáveis cafés da tarde que certamente tonaram a rotina de trabalho muito mais

agradável. Ao pessoal do laboratório de Biologia Molecular do MPEG, especialmente à Joice, Cintia e ao meu amigo Geraldo Lima pela ajuda com a bancada.

Um agradecimento Especial ao meu 'compadre' Ângelo Dourado, pela amizade, pelas conversas e apoio nos momentos mais complicados e pelas ajudas com as coordenadas e com os mapas, valeu mano. À Marcelo Sturaro e Pedro Peloso, pela amizade e pelas conversas sobre biologia evolutiva e sistemática, que sem duvida, contribuíram para melhorar as ideias contidas na Tese. Ao Pedro Peloso, também pela revisão de parte do manuscrito.

À Liza Maria Veiga, *in memoriam*, pelo incentivo para iniciar nessa maravilhosa e árdua jornada que foi o doutorado, pela paciência e dedicação, sou muito grato por tudo que compartilhei com ela.

Agradeço ao meu orientador Alexandre Aleixo, pela oportunidade e pela confiança que depositou em min. Por ter abraçado esse trabalho sem restrições não medindo esforços pra garantir as condições necessárias a sua realização. Pelo incentivo, pela orientação e por todas as construtivas conversas que me fizeram entender melhor a sistemática e a taxonomia das aves, muito obrigado chefe!

À minha família, que sem dúvida é a razão de tudo: em especial meus pais Francisco Carneiro e Maria de Fátima e a minha segunda mãe tia Edith que lutaram muito pra que isso tudo fosse possível, ao meu irmão: Faisal e as maravilhosas sobrinhas que me deu Duda e Sarah. Quero também agradecer à nova família que ganhei, Rozilda e Vicente Borges, Amanda e Monike que me acolheram e me apoiaram muito nessa fase final.

Um agradecimento especialíssimo a minha namorada Mazillene Borges, pelo carinho, amor, apoio e motivação. Pela compreensão durante os momentos mais críticos e por todo o suporte que tem me dado, obrigado meu amor!

MUITO OBRIGADO!

Sumário

Introdução Geral

Os avanços recentes no campo da sistemática de aves, especialmente com a inclusão de caracteres moleculares e vocais, tem levado a uma melhor compreensão dos processos históricos que geraram a diversidade de aves do Neotrópico e a um grande número de rearranjos sistemáticos e taxonômicos (Zink & Blackwell-Rago, 2000; Aleixo, 2002; D'Horta *et al*., 2008; Zimmer, 2008; Navarro-Sigüenza *et al*., 2008; Rheindt *et al*., 2008).

Atualmente, existem diversas hipóteses que tentam explicar a diversidade presente e sua distribuição espacial, entre as principais podemos citar: a Hipótese paleogeográfica (Emsley, 1965); o modelo das barreiras ripárias (Wallace, 1852; Gascon *et al*., 2000); a hipótese dos refúgios (Haffer, 1969; 1997); a hipótese dos rios-refúgios (Ayres, 1992); e a hipótese de perturbação-vicariância (Colinvaux, 1993). Embora essas varias hipóteses biogeográficas tenham sido formuladas, apenas poucos estudos têm testado os padrões filogenéticos dos táxons Neotropicais (Derryberry *et al*., 2011; Patel *et al*., 2011; d'Horta *et al*., 2012; Ribas, *et al*., 2011; Smith *et al*., 2013, Bryson *et al*., 2014). E apesar do grau de complexidade das hipóteses propostas, alguns estudos (Bates *et al*., 1998; Tobias, *et al*., 2008; Antonelli, *et al*., 2010) tem proposto que a história evolutiva da biota neotropical pode ter sido influenciada por um mosaico de diferentes modelos ao longo do tempo, sugerindo um passado ainda mais complexo do que o previsto pelas hipóteses existentes.

Táxons proximamente relacionados e que ocupam uma mesma área biogeográfica ou um mesmo bioma, representam modelos promissores para testar tais hipóteses, uma vez que permitem a identificação e comparação dos diferentes processos históricos que levaram a sua diferenciação (Aleixo & Rossetti, 2007; Antonelli, *et al*., 2010). Os gêneros *Hylopezus* e *Myrmothera*, atendem estes requisito, já que alguns de seus táxons ocorrem amplamente no Neotropico e são simpátricos em algumas áreas (Krabbe & Schulenberg, 2003; Remsen *et al*., 2012), permitindo, assim, uma análise comparativa dos efeitos dos eventos históricos sobre essas linhagens filogeneticamente próximas e co-distribuídas.

Os gêneros *Hylopezus* e *Myrmothera* foram inicialmente alocados na família Formicariidae (Ridgway 1909; Lowery & O'neil 1969), mas estudos moleculares recentes (Irestedt *et al*., 2002; Chesser *et. al*, 2004; Rice, 2005a,b) demonstraram a

parafilia deste grupo e realocaram estes dois gêneros na família Grallariidae (Sclater & Salvin 1873), juntamente com os gêneros *Grallaricula* e *Grallaria* (Irestedt *et al*., 2002; Chesser *et*. *al*, 2004; Rice, 2005a,b). Os gêneros *Hylopezus* e *Myrmothera* formam uma linhagem bem apoiada que tem como grupo irmão o gênero *Grallaricula* (Rice, 2005a,b), e esse clado, por sua vez, tem como grupo irmão *Grallaria* (Krabbe *et al*., 1999, Irestedt *et al*., 2002, Chesser *et*. *al*, 2004, Rice, 2005 2005a,b).

O gênero *Hylopezus* foi descrito por Ridgway (1909) e distribui-se na região Neotropical, estendendo-se desde Honduras até o nordeste da Argentina (Krabbe &Schulenberg 2003). Até recentemente, eram reconhecidas oito espécies biológicas no gênero, *H*. *macularius*, *H*. *perspicillatus*, *H*. *fulviventris*, *H*. *berlepschi*, *H*. *ochroleucus*, *H*. *auricularis*, *H*. *nattereri* e *H*. *dives* (Peters 1976, Ridgely & Tudor, 1994, Krabbe & Schulenberg, 2003; Remsen *et al*., 2012). Entretanto, Carneiro *et al*., (2012), com base em caracteres morfológicos, vocais e moleculares descreveram uma nova espécie, *H*. *whittakeri*, e elevaram três subespécies do complexo *macularius* ao nível de espécie (*H*. *macularius*, *H*. *dilutus*, *H*. *paraensis*). Portanto, atualmente o gênero *Hylopezus* comporta 11 espécies e 12 subespécies (Krabbe & Schulenberg, 2003; Carneiro *et al*., 2012), a saber:

- *Hylopezus* (m.)Ridgway1909
- *Hylopezus perspicillatus* (Lawrence) 1861
- *Hylopezus perspicillatus intermedius* (Ridgway)1884 - Ocorre do leste de Honduras até o Oeste do Panamá.
- *Hylopezus perspicillatus lizanoi* (Cherrie) 1891 - Distribuido do sul da Costa Rica até o Oeste do Panamá.
- *Hylopezus perspicillatus pallidior* Todd1919 – Colombia, vales do alto rio Sinú.
- *Hylopezus perspicillatus periophthalmicus* (Salvadori & Festa)1898 - Ocorre do oeste da Colombia até o Noroeste do Equador (Chocó).
- *Hylopezus perspicillatus perspicillatus* (Lawrence) 1861 - Distribuido do leste do Panamá até o Noroeste da Colombia
- *Hylopezus macularius* (Temminck) 1830
- *Hylopezus dilutus* (Hellmayr) 1910
- *Hylopezus paraensis* (Snethlage) 1910
- *Hylopezus whittakeri* Carneiro *et al*., 2012

- *Hylopezus auricularis* Gyldenstolpe1941
- *Hylopezus dives* (Salvin) 1865
- *Hylopezus dives barbacoae* Chapman 1914 - Ocorre do leste do Panamá até a costa sul da Colombia.
- *Hylopezus dives dives* (Salvin) 1865 - Ocorre do leste de Honduras até o sul da Costa Rica.
- *Hylopezus dives flammulatus* Griscom1928 – Noroeste do Panamá.
- *Hylopezus fulviventris* (Sclater, PL)1858
- *Hylopezus fulviventris caquetae* Chapman 1923 – Disrtibuido na região sudeste da Colombia.
- *Hylopezus fulviventris fulviventris* (Sclater, PL) 1858 – Leste do Equador ao norte do Peru.
- *Hylopezus berlepschi* (Hellmayr)1903
- *Hylopezus berlepschi berlepschi* (Hellmayr)1903 – Sul da Amazonia brasileira do leste do Purús até a margem oeste do Tocantins.
- *Hylopezus berlepschi yessupi* (Carriker) 1930 – Leste do Peru até a margem oeste do Purús.
- *Hylopezus ochroleucus* (Wied-Neuwied)1831
- *Hylopezus nattereri* (Pinto) 1937

O gênero *Myrmothera* foi descrito por Vieillot (1816), e distribui-se exclusivamente na bacia amazônica (Krabbe & Schulenberg 2003). São atualmente reconhecidas duas espécies para o gênero, *M. campanisona e M. simplex* (Peters, 1976, Ridgely & Tudor, 1994, Krabbe & Schulenberg, 2003 e Remsen *et al.,* 2012), porém ambas são espécies politípicas e possuem apreciável variação vocal e de plumagem. De acordo com Krabbe & Schulenberg (2003), este gênero possui atualmente 10 subespécies:

- Myrmothera (*f.*) Vieillot 1816
- *Myrmothera campanisona* (Hermann) 1783
- *Myrmothera campanisona campanisona* (Hermann) 1783: Sudeste da Venezuela e Guianas.
- *Myrmothera campanisona dissors* Zimmer 1934: Leste da Colombia, Sul da

Venezuela e Noroeste do Brasil.

- *Myrmothera campanisona minor* (Taczanowski) 1882: Leste do Peru (Sul do rio Amazonas), Oeste do Brasil (Leste do rio Purús) e Extremo Noroeste da Bolivia.
- *Myrmothera campanisona modesta* (Sclater, PL) 1855: Base leste dos andes da Colombia (Sul de Meta)
- *Myrmothera campanisona signata* Zimmer 1934: Leste do Equador e Nordeste do peru (Norte do rio Amazonas)
- *Myrmothera campanisona subcanescens* Todd 1927: Brasil, Sul do rio Amazonas, do leste do rio Madeira ao oeste do rio Xingu.
- Myrmothera simplex (Salvin & Godman) 1884
- *Myrmothera simplex duidae* Chapman 1929: Sul da Venezuela (Duida e Neblina).
- *Myrmothera simplex guaiquinimae* Zimmer & Phelps, WH 1946: Sudeste da Venezuela e Sudeste da Bolivia.
- *Myrmothera simplex pacaraimae* Phelps, WH Jr & Dickerman 1980: Sul da Bolivia, Monte Paracaima.
- *Myrmothera simplex simplex* (Salvin & Godman) 1884: Sudeste da Venezuela, Monte Roraima.

Trabalhos recentes indicam a existência de uma pronunciada variação vocal em vários complexos de espécies dos gêneros *Hylopezus* e *Myrmothera* (Maijer 1998, Krabbe & Schulenberg 2003, Carneiro *et al.,* 2012), contrastando com o tratamento taxonômico atual, que é baseado majoritariamente em caracteres morfológicos e de plumagem (Ridgway 1909; Lowery & O'Neill 1969) que nesses dois gêneros são crípticos e de difícil diagnose (Cadena *et al.,* 2007, Carneiro *et al.,* 2012). Esses dados evidenciam a falta de conhecimento das relações filogenéticas entre os táxons desses dois gêneros, fato que impossibilita a caracterização acurada da história evolutiva a da real diversidade deste grupo.

O objetivo principal do presente estudo foi contribuir para o entendimento das relações filogeneticas dentro da família Grallaridae, especialmente dentro dos gêneros *Hylopezus* e *Myrmothera*, que representam o enfoque central do trabalho. Adicionalmente, utilizamos uma abordagem filogenética para investigar a evolução dos caracteres

fenotípicos destes dois gêneros, no intuito de melhor compreender os processos que moldaram a diversidade desse grupo na região Neotropical. O uso de dados morfológicos, moleculares e vocais para a caracterização espacial e temporal da diversificação dos gêneros *Hylopezus* e *Myrmothera* permitiu uma compreensão mais completa dos processos de especiação, biogeografia histórica e fluxo gênico envolvendo as linhagens destes gêneros, e constitui em ultima analise, um acréscimo ao conhecimento a cerca dos processos de diversificação da região Neotropical.

2. OBJETIVOS

2.1 – Objetivo Geral

Realizar uma revisão Sistemática e taxonômica dos gêneros *Hylopezus* e *Myrmothera*, com base em dados morfológicos, vocais e moleculares, e propor hipóteses sobre a história evolutiva e biogeográfica desse grupo.

2.2 – Objetivos específicos

- Verificar a validade dos táxons reconhecidos atualmente para o grupo;
- Verificar o monofiletismo de *Hylopezus* e *Myrmothera* como atualmente compreendidos e buscar as relações entre os táxons desse grupo;
- Inferir a história evolutiva do grupo e o tempo de divergência entre os clados;
- Reconstruir as possíveis áreas ancestrais dos táxons desse grupo;
- Através das topologias obtidas, inferir as relações entre as áreas de ocorrência das espécies do grupo, na tentativa compreender o relacionamento entre biomas e dentro deles;
- Investigar a evolução fenotípica do grupo e contrasta-la com as relações sistemáticas resgatadas pelas filogenias.
- Caracterizar os táxons que vierem a ser reconhecidos e analisar sua distribuição geográfica;
- Verificar o grau de concordância dos padrões filogeográficos entre as diferentes populações co-distribuídas, relacionando-os a eventos históricos comuns que possam explicá-los.

2. Referências Bibliográficas.

ALEIXO, A. 2012. Molecular systematics and the role of "varzea" – "terra-firme" ecotone in the diversification of *Xiphorhynchus* woodcreepers (Aves: Dendrocolaptidae). **The Auk** 119: 621 – 640.

ALEIXO, A. e ROSSETTI, D. F. 2007. Avian gene tree, landscape evolution, and geology: towards a modern synthesis of Amazonian history biogeography?. **J. Onithol**. 148: 443 – 453.

ANTONELLI, A.; QUIJADA-MASCAREÑAS, A.; CRAWFORD, A. J.; BATES, J. M.; VELAZCO, P. M; WÜSTER, W. 2010. Molecular studies and phylogeography of Amazonian tetrapods and their relation to geological and climatic models. In Amazonia: landscape and species evolution A look into the past**.** Blackwell Publishing Ltd. p. 384-405.

BATES, J. M., HACKETT, S. J. & CRACRAFT, J. 1998. Area-relationships in the Neotropical lowlands: an hypothesis based on raw distributions of passerine birds. **Journal of Biogeography, 25**: 783–793.

BRUMFIELD, R. T.; TELLO, J. G.; CHEVIRON, Z. A.; CARLING, M. D.; CROCHET, N. & ROSENBERG, K. V. 2007. Phylogenetic conservatism and antiquity of a tropical specialization: Army-ant-following in the typical antbirds (Thamnophilidae). **Mol. Phylogenet. Evol**. 45 1-13.

CADENA, C. D., B. LOPEZ-LANUS, J. M. BATES, N. KRABBE, N. H. RICE, F. G. STILES, J. D. PALACIO, AND P. SALAMAN. 2007. A rare case of interspecific hybridization in the tracheophone suboscines: Chestnut-naped Antpitta *Grallaria nuchalis* Chestnut-crowned Antpitta *G. ruficapilla* in a fragmented Andean landscape. **Ibis** 10: 1-12.

CARNEIRO, L. S, GONZAGA, L. P, RÊGO, P. S, SAMPAIO, I, SCHNEIDER, H. AND ALEIXO, A. 2012. Systematic revision of the spotted antpitta *Hylopezus macularius* (grallariidae), with description of a cryptic new species from brazilian amazonia. **Auk**. 129(2): 338 – 351.

CHESSER, R. T. 2004. Molecular systematics of New World suboscine birds. **Molecular Phylogenetics and Evolution** 32: 11-24.

CHEVIRON, Z. A.; HACKETT, S. J. & CAPPARELLA, A. P. 2005. Complex evolutionary history of a Neotropical lowland forest bird (*Lepidothrix coronata*) and its implications for historical hypotheses of the origin of Neotropical avian diversity. **Molecular Phylogenetics and Evolution, 36**: 338–357.

COLINVAUX, P. 1993. Pleistocene biogeography and diversity in tropical forests of South America. In **Biological Relationships between Africa and South America.** GOLDBLATT, P. (ed.). New Haven: Yale University Press. p. 99-473.

CRACRAFT, J. 1985. Historical biogeography and patterns of diferention within the South America avifauna: Areas of endemism. **Ornithological Monographs** 36: 49 – 89.

D'HORTA, F. M., SILVA, J.M.C., RIBAS, C. Species limits and hybridization zones in *Icterus cayanensis chysocephalus* group (Aves: Icteridae). **Biological Journal of the Linnean Society** 95: 583 – 597. 2008.

DRUMMOND, A.J., RAMBAUT, A. BEAST: Bayesian evolutionary analysis by sampling trees. **BMC Evolutionary Biology** 7: 214. 2007.

EMSLEY, M.G. 1965. Speciation in *Heliconius* (Lep., Nymphalidae): Morphology and geographic distribution. **Zoologica** (N.Y.) **50**: 191-254.

GASCON, C., MALCOLM, J. R., PATTON, J. L., SILVA, M. N. F., BOGART, J. P., LOUGHEED, S. C., PERES, C A, NECKEL, S., BOAG, P. T. 2000. Riverine barriers and the geographic distribution of Amazonian species. **PNAS** 97: 13672-13677.

HACKETT, S.J. 1996. Molecular phylogenetics and biogeography of tanagers in the genus *Ramphocelus* (Aves). **Molecular Phylogenetics and Evolution** 5 (2). 368-382.

HAFFER, J. 1985. Avian zoogeography of the neotropical lowland. **Ornithological Monographs** 36: 113-146.

HAFFER, J. 1996. Speciation in Amazonian forest birds. **Science** 165: 131-137.

HAFFER, J. 1997. Alternative models of vertebrate speciation in Amazonia: an overview. **Biodiversity and Conservation, 6**: 451-476.

IRESTEDT, M., J. FJELDSÅ, U. S. JOHANSSON, AND P. G. P. ERICSON. 2002. Systematic relations and biogeography of the tracheophone suboscines (Aves: Passeriformes). **Molecular Phylogenetics and Evolution** 23: 499-512.

ISLER, M. L., P. R. ISLER, AND B. M. WHITNEY. 1998. Use of vocalizations to establish species limits in antbirds (Passeriformes: Thamnophilidae). **Auk** 115: 577-590.

KRABBE, N Agro, D.J.; Rice, N.H.; Jacome, M.; Navarrete, L. & Sornoza M., F. (1999): A new species of antpitta (Formicariidae: *Grallaria*) from the southern Ecuadorian Andes. **The Auk** 116(4): 882-890.

KRABBE, N., AND T. S. SCHULENBERG. 2003. Family Formicariidae (ground-antbirds). Pag. 682-731 *in* Handbook of the Birds of the World, Vol. 8. Broadbills to tapaculos. (J. del Hoyo et al., Eds.). Lynx Edicions, Barcelona.

LOWERY, G. H. J., AND J. P. O´NEILL. 1969. A new species of *Grallaria* from Peru, and a revision of the subfamily Grallarinae. **Auk** 86: 1–12.

MAIJER, S. 1998. Rediscovery of *Hylopezus* (*macularius*) *auricularis*: distinctive song and habitat indicate species rank. **Auk** 115:1072-1073.

MARKS, B.D., HACKETT,S.J. e CAPPARELLA, A.P. 2002. Historical relationship among Neotropical lowland forest areas of endemism as determined by mitochondrial DNA sequence variation within the Wedge-billed Woodcreeper (Aves: Dendrocolaptidae: *Glyphorhynchus spirurus*). **Molecular Phylog. Evol**. 24: 153 – 167.

MCGUIRE, J. A.; WITT, C. C.; ALTSHULER, D. L. & REMSEN JR, J. V. 2007. Phylogenetic Systematics and Biogeography of Hummingbirds: Bayesian and Maximum Likelihood Analyses of Partitioned Data and Selection of an Appropriate Partitioning Strategy. **Systematic Biology, 56**(5):837–856.

NAVARRO-SIGÜENZA, A. G., A. T. PETERSON, A. NYARI, G. M. GARCÍA-DERAS, AND J. GARCÍA-MORENO. 2008. Phylogeography of the *Buarremon* brush-finch com- plex (Aves, Emberizidae) in Mesoamerica. **Molecular Phylogenetics and Evolution** 47:21–35.

OLSSON, U., ALSTRÖM, P., GELANG, M., ERICSON, P.G.P. & SUNDBERG, P. 2006. Phylogeography of Indonesian and Sino-Himalayan region bush warblers (*Cettia*, Aves). ***Molecular Phylogenetics and Evolution***, 41, 556-565.

PETERS, J. L. 1976. Check-list of birds of the world. Vol. VII. Cambridge: Harvard University Press.

RAIKOW, R.J. 1994. A phylogeny of the woodcreepers (Dendrocolptidae). **The Auk** 111 (1): 104 – 114p.

Remsen, J. V., Jr., C. D. Cadena, A. Jaramillo, M. Nores, J. F. Pacheco, M. B. Robbins, T. S. Schulenberg, F. G. Stiles, D. F. Stotz, and K. J. Zimmer. 2012. [Version: 25 January 2012.] A classification of the bird species of South America. **American Ornithologists' Union**. [Online.] Available at www.museum.lsu. edu/~Remsen/SACCBaseline.html.

RHEINDT, F.E., NORMAM, J.A. e CHRISTIDIS, L. 2008. Genetics differentiation acroos the Andes in two pan-Neotropical tyrant-flycatcher specie. **Emu** 108 (3): 261 – 268.

RIBAS, C.C., ALEIXO, A., NOGUEIRA, A.C.R., MIYAKI, C.Y. & CRACAFT, J. 2011. A palaeobiogeographic model for biotic diversification within Amazonia over the past three million years. ***Proceedings of the Royal Society, Biological Sciences***, 279, 681-689.

RIBAS, C. C. & MIYAKI, C. Y. 2007. Análise comparativa de padrões de diversificação em quatro gêneros de psitacídeos neotropicais. **Revista Brasileira de Ornitologia, 15**: 245-252.

RICE, N.H**.** 2005. Phylogenetic relationships of antpitta genera (Passeriformes: Formicariidae). **The Auk** 122: 673–683.

RICE, N.H**.** 2005. Further evidence for paraphyly of the Formicariidae (Passeriformes). **The Condor** 107:910–915.

RIDGELY, R.S. e TUDOR, G. The birds of South America: the oscines passerines. Univ. Texas Press. 516p. 1994.

RIDGWAY, R. 1909. New genera, species and subspecies of Formicariidae, Furnariidae, and Dendrocolaptidae. **Proc. Biol. Soc. Washington**, 22: 69-74.

SANMARTÍN, I., MARK, P.V.D. & RONQUIST, F. 2008. Inferring dispersal: a bayesian approach to phylogeny-based island biogeography, with special reference to the Canary Islands. ***Journal of Biogeography***, 35, 428-449.

SILVA, J.M.C., SOUSA, M.C. & CASTELLETTI, C.H.M. 2004. Areas of endemism for passerine birds in the Atlantic forest, South America. *Global* ***Ecology and Biogeography***, 13, 85-92.

SLADE, R. W.; MORITZ, C.; HEIDEMAN, A. & HALE, P. T. 1993. Rapid assessment of single-copy nuclear DNA variation in diverse species. **Molecular Ecology,** 2: 359-373.

TOBIAS, J.A., BATES, J.M., HACKETT, S.J., SEDDON, N. 2008. Comment on the latitudinal gradient in recent speciation and extinction rates of birds and mammals. **Science** 319, 901c.

TOBIAS, J.A.; SEDDON, N.; SPOTTISWOODE, C. N; PILGRIM, J, D; FISHPOOL, L. D. C;.COLLAR, N. J. 2010. Quantitative criteria for species delimitation. **Ibis** 12: 1-23.

WALLACE, A. R. 1852. On the monkeys of the Amazon. **Proceedings of the Zoological Society of London, 20**: 107-110.

WILLIS, E. O. 1967. Behavior of Bicolored Antbirds. University of California **Publications in Zoology** 79: 1–132.

ZIMMER, K. J. 2008. The White-eyed foliage gleaner (Furnariidade: *Automolus*) is two species. **The Wilson Journal of Ornithology** 120 (1): 10-25.

ZINK, R.M. e BLACKWELL-RAGO. 2000 Species limits and recents population history in the curved-billed thrasher. **The Condor** 102: 881 – 886.

Capítulo 1

Sistemática molecular e biogeografia historica de duas linhagens de 'antpittas' (Aves, Grallaridae) no Neotrópico

"Molecular systematics and historical biogeography of two lineages of antpittas (Aves, Grallariidae) across the Neotropics[1]"

[1] Esse capítulo está no formato de manuscrito e será submetido ao periódico "Journal of Biogeography". O co-autor Gustavo Bravo não revisou a presente versão.

Molecular systematics and historical biogeography of two lineages of antpittas (Aves, Grallariidae) across the Neotropics

Lincoln Carneiro,[1,4] Gustavo Bravo,[2] and Alexandre Aleixo[3]

[1]*Curso de Pós-Graduação de Zoologia, Universidade Federal do Pará–Museu Paraense Emílio Goeldi, Belém, Pará, Brazil;* [2] *Secção de Aves, Museu de Zoologia, Universidade de São Paulo (MZUSP), Caixa Postal 42.494, CEP 04218–970, São Paulo, SP, Brasil; and* [3]*Coordenação de Zoologia, Museu Paraense Emílio Goeldi, Caixa Postal 399, CEP 66040-170, Belém, Pará, Brazil.*

[4]Address correspondence to this author. E-mail: lincoln_carneiro@yahoo.com.br

ABSTRACT

Aim to infer the phylogenetic relationships, divergence time history, and diversification of the avian neotropical antpitta genera *Hylopezus* and *Myrmothera* (Grallariidae).

Location Central and South America.

Methods We sampled 144 individuals of the 12 currently recognized species in *Hylopezus* and *Myrmothera* and 5 outgroup species. We generated multilocus sequence data (3139 base pairs) from two mitochondrial (ND2 and ND3) and three nuclear genes (TGFB2, MUSK and BF5) to infer phylogenetic relationships and reconstruct time-calibrated species trees. These chronograms were used to calculate diversification rates and reconstruct ancestral areas for these two genera.

Results The phylogenetic analyses recovered 19 lineages clustered into two major clades, both distributed in Central and South America. *Hylopezus nattereri*, previously considered a subspecies of *H. ochroleucus*, was consistently recovered in a separate clade of uncertain phylogenetic relationships within the *Grallaricula* / *Hylopezus* / *Myrmothera* clade. Divergence time estimates for the group suggested that antpittas probably originated in Central America during the Oligocene, and that the diversification within the *Hylopezus* / *Myrmothera* clade was highest in the late Miocene. The spatio-temporal pattern suggests that a complex sequence of events,

possibly related to the Andean uplift and infilling of former sedimentation basins as well as erosion cycles, shaped the current distribution and diversity of lineages in this group.

Main conclusions Our reconstruction of the diversification history of the *Hylopezus* and *Myrmothera* genera provided an additional scenario for the evolution of the Neotropical biota. The recovered spatio-temporal pattern may reflect an evolutionary history influenced by several independent palaeogeological events such as the Andean uplift, marine incursions, as well as the formation of the modern Amazon drainage. Apparently this diversification took place during the late Miocene to Pliocene, hence coinciding with the onset of major changes to the Amazon drainage, which could have allowed the colonization and diversification of *Hylopezus* / *Myrmothera* throughout Amazonia. Our biogeographic reconstructions pointed to an ancestral distribution centered in western Amazonia, with a subsequent dispersion eastward starting on the early Miocene. We suggest a new taxonomic classification for the species in the genera *Hylopezus* and *Myrmothera* that conforms with the evolutionary history of the group.

Keywords

Ancestral area reconstruction, Amazonia, diversification rates, Neotropics, Systematics, Taxonomy.

INTRODUCTION

Inferring patterns of diversification within widespread lineages provide insights into broad-scale processes that generate biodiversity (Avise, 2000). This approach is especially difficult in the Neotropics, given the extreme geological complexity and the high diversity and endemicity in this region (Cracraft & Prum, 1988; Graham, 1997; Burnham & Graham, 1999). Nonetheless, studies on the origins and diversification of several taxa provide examples of how geological processes (Bryson *et al*., 2012), climate change (Weir & Schluter, 2004), niche conservatism (Smith *et al*., 2012) and the colonization of novel regions (Simpson, 1980) influence lineage dynamics.

One particularly important mean of developing strong hypotheses for broad and general biogeographic patterns is the simultaneous analysis and comparison of multiple independent lineages that are codistributed throughout a region (Nelson & Platnick, 1980; Lomolino *et al*., 2006; Castoe *et al*., 2009). To this end, a realistic approach is to uncover phylogenetic patterns of independent lineages and then test specific hypotheses regarding the historical and ecological processes that have shaped species diversity in these lineages (Beheregaray, 2008; Riddle *et al*., 2008). Antpittas range through nearly the entire Neotropical region, making this group excellent to investigate the effects of historical and ecological processes across different biogeographic provinces on lineage diversification.

In recent years, new aspects of land surface evolution were evoked to explain biogeographic patterns in the Amazon basin, such as changes in drainage patterns and sedimentation within the large wetlands that existed in western Amazon during the Miocene (Wesselingh *et al*., 2002), and the role of Andean uplift on drainage patterns of the lowlands (Antonelli & Sanmartín, 2011; Hoorn et al., 2010; Hoorn *et al*., 2013). The uplift of the Andes also triggered climate changes across the continent (Insel *et al*., 2009), as this mountain belt formed a barrier that retained moisture from the Atlantic Ocean. Thus, these events, which occurred before the Pleistocene, seem to have been important for the evolution of the Neotropical biota (Antonelli *et al*., 2009; Batalha-Filho *et al*., 2014; Lohmann *et al*., 2013; Weir & Price, 2011). However, lineage diversification events seem to have occurred throughout the Tertiary and Quaternary, including the Pleistocene (Rull, 2008, 2011a, 2011b).

The hypothesis by Wallace (1852) that rivers could be barriers to dispersal and that this could lead to speciation, received new attention as geological evidence suggested a recent (Plio-Pleistocene) establishment of the Amazon basin as a trans-continental drainage emptying into the Atlantic Ocean (Campbell *et al*., 2006; Latrubesse *et al*., 2010). This scenario has been shown to be congruent with recent divergences of avian populations across the main Amazonian rivers (Fernandes *et al*., 2012; Maldonado-Coelho *et al*., 2013; Ribas *et al*., 2012a).

The family Grallaridae has 51 recognized species divided in four genera, *Grallaria*, *Grallaricula*, *Myrmothera* and *Hylopezus* (Remsem *et al*., 2015). The relationships between these genera were proposed based on molecular phylogenies (Rice, 2005; Moyle *et al*., 2009; Ohlson *et al*., 2013) and are also partially supported by morphological characters (Lowery & O'Neill, 1969; Galvão & Gonzaga, 2011). In those studies with better sampling, *Hylopezus* and *Myrmothera* are recovered as sister taxa, and *Grallaricula* as their closest relative, with this entire clade as sister group of *Grallaria* (Rice, 2005; Moyle *et al*., 2009; Ohlson *et al*., 2013).

Within the two sister genera *Hylopezus* and *Myrmothera* geographical variation in song structure has been documented for several species. As an example, three taxa in the *H. macularius* complex, which are morphologically nearly undistinguishable from each other, differ conspicuously in their vocalizations (Carneiro *et al*., 2012). The importance of vocal characters as a premating isolating mechanism in Grallariidae was highlighted in a study showing that vocalizations appears to have a strong genetic basis in this family (Cadena *et al*., 2007). This evidence suggests that some of the species in the group might, in fact, consist of more than a single taxon / evolutionary unit, i.e. they represent species complexes. Several antpittas have very restricted ranges, many sing for only a few months of the year, and large parts of their areas of occurrence remain inaccessible, making it plausible that even more species remain to be discovered or recognized as such based on multi-character taxonomic studies (Krabbe & Schulenberg, 2003).

In this study, we infer the phylogenetic relationships, divergence time and biogeography of the *Hylopezus* and *Myrmothera* genera, using mitochondrial DNA (mtDNA) and nuclear loci. We infer phylogeographical structure and estimate a time-calibrated species trees for these genera with a comprehensive taxon sampling. We

then estimate the ancestral range of each divergence event and tested for temporal shifts in diversification rates. To uncover the evolutionary history of antpittas we wanted to answer three main questions: (i) what are the phylogenetic relationships among genera and species of *Hylopezus* and *Myrmothera* antpittas?; (ii) how these relationships correspond to currently defined systematic limits?; and (iii) can the timing and sequence of speciation events in these lineages be associated with described events in the landscape history of Neotropics?

MATERIALS AND METHODS

Taxon sampling and molecular phylogeny

To infer the phylogenetic relationships within *Hylopezus* and *Myrmothera*, we sequenced 144 tissue samples (77 *Hylopezus*, 62 *Myrmothera* and 5 outgroups) from throughout their distributions (Figs. 1 & 2; see also Table S2 in supplementary material). Our sampling spanned the geographical distributions of all 12 currently recognized species within these genera (Krabbe & Schulenberg, 2003; Carneiro *et al*., 2012). We included in our analyzes species of the two other genera of the Grallariidae family, *Grallaricula* (*G. flavirostris* and *G. nana*) and *Grallaria* (*G. rufula*, *G. ruficapilla* and *G. guatimalensis*), as outgroups, hence covering all currently recognized genera of the family (Krabbe & Schulenberg, 2003; Rice, 2005).

Total genomic DNA was extracted using a DNeasy tissue extraction kit (Qiagen, Valencia, CA, USA). For most samples, we sequenced the mitochondrial genes – NADH dehydrogenase subunit 2 (ND2: 1041 base pairs, bp), and NADH dehydrogenase subunit 3 (ND3: 351 bp); representing the main lineages inferred from our complete mtDNA data (see below). We also sequenced three nuclear introns – transforming growth factor beta 2 intron 5 (TGFB2: 625 bp); the 3rd intron of the Z-linked muscle-specific kinase (MUSK: 582 bp); and a fragment of the beta-fibrinogen intron 5 (FGB-I5: 549 bp). For primers details (see Appendix; Table S1)

PCR conditions were as follows: an initial denaturation step at 94 °C for 3 min and 30 s; followed by 35 cycles at 94 °C for 35 s, annealing temperature for 40 s and 72 °C for 1 min; plus a final extension step at 72 °C for 5 min. Annealing temperatures were as follows: ND3, and ND2-56 °C; MUSK, and FGB-I5- 63 °C; and TGFB2-60 °C. The PCR products were cleaned using PEG 8000 20% NaCl 2,5 M. Amplifications

were cycle-sequenced using a BigDye 3.1 Terminator kit (BigDye, Applied Biosystems, Foster City, CA) and the same primers used for amplification. Cycle sequencing reactions were cleaned with ethanol EDTA precipitation, and resuspended in Hi-Di formamide. Sequences were then visualized through an ABI 3730 automated DNA sequencer.

Electropherograms were inspected, assembled in contigs and edited in Geneious 7.1.5 (Biomatters, www.geneious.com). Heterozygous sites were coded according to IUPAC when double peaks were present in both strands of the same individual's electropherograms. Sequences were aligned with MAFFT using the default parameters, and further inspected and corrected visually.

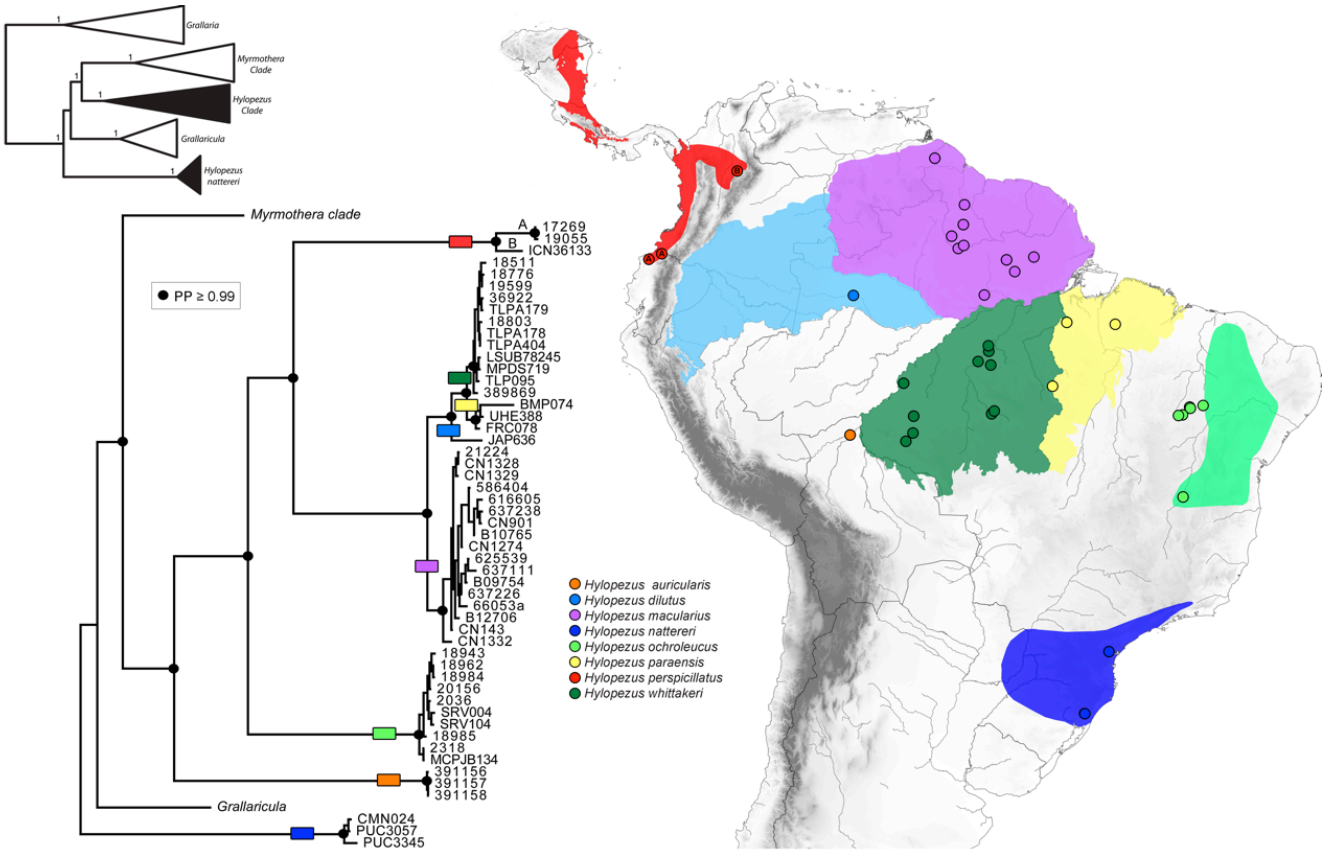

Figure 1 Multilocus Bayesian phylogeny of the so-called 'core *Hylopezus*' (see results) based on mtDNA (ND2 and ND3) and nDNA (TGFB2, MUSK, FGB-I5) genes (Complete phylogeny: top left; Black highlighted lineages: bottom left); and map showing the distributions of the seven currently recognized species belonging to this clade in addition to *H. nattereri* (Krabbe & Schulenberg, 2003; Carneiro *et al*., 2012) with the localities of the specimens sampled denoted as dots (right). Capital letters above branches denote major geographical lineages. Significant nodal Bayesian posterior probabilities (PP) are indicated by black circles. Additional locality data can be found in Appendix S2.

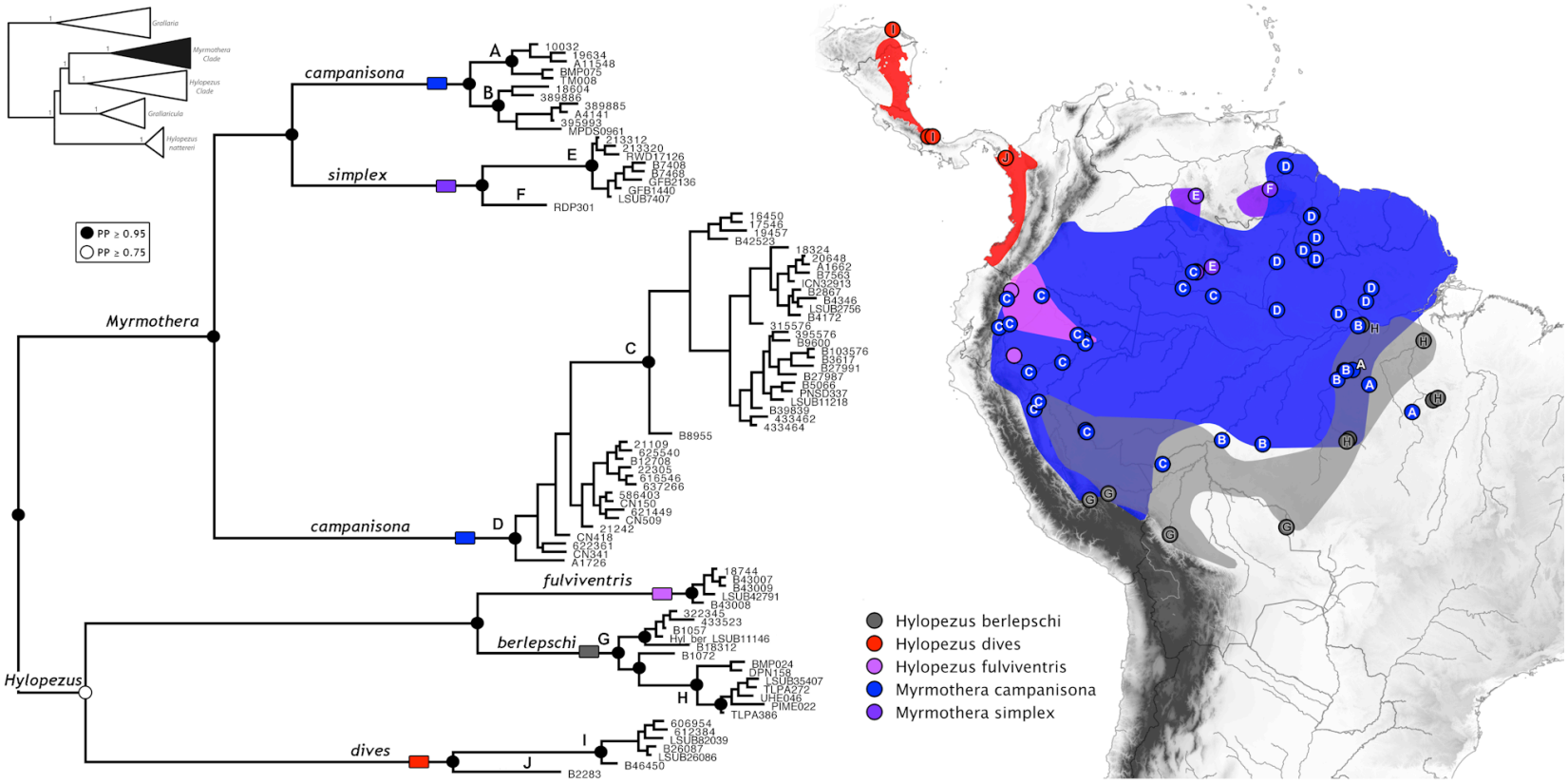

Figure 2 Multilocus Bayesian phylogeny of the so-called 'extended *Myrmothera*' clade (see results) based on mtDNA (ND2 and ND3) and nDNA (TGFB2, MUSK, FGB-I5) genes (Complete phylogeny: top left; Black highlighted lineage: bottom left); and map showing the distributions of the five currently recognized species belonging to this clade (Krabbe & Schulenberg, 2003) with the localities of the specimens sampled denoted as dots (right). Capital letters above branches denote major geographical lineages. Significant nodal Bayesian posterior probabilities (PP) are indicated by black circles. Additional locality data can be found in Appendix S2.

Phylogeographical estimation

To assess the genetic structure and delimitate geographical lineages, we generated a multilocus phylogeny including all individuals sampled (n = 144 including outgroups) using Bayesian inference (BI) on MrBayes 3.2.1 (Ronquist *et al*., 2012). Lineages were defined as genetically distinct geographical clusters with strong support values (≥ 0.95 Bayesian posterior probability; Huelsenbeck & Rannala, 2004; Bryson *et al*., 2014). Single divergent samples from unique geographical areas were also referred to as lineages for convenience. The evolutionary models were selected with PartitionFinderV1.1.1 (Lanfear *et al*., 2012) using the Bayesian information criterion (BIC) (Minin *et al*., 2003; Posada, 2008). The optimal partition scheme and substitution models for our dataset were chosen based on comparisons limited to following schemes: (i) data combined into a single partition; (ii) mitochondrial and nuclear loci analyzed separately; (iii) genes analyzed separately; (iv) 1st and 2nd codon positions analyzed separately from 3rd codon positions; (v) all codon analyzed separately.

Two independent runs of 20 million generations with four chains of Markov chain Monte Carlo (MCMC) each were performed, and trees were sampled every 1000 generations. Output parameters were visualized using Tracer 1.6 (Rambaut & Drummond, 2007) to ascertain stationarity and convergence (Effective Sample Size – ESS values > 200). The first 25% of generations were discarded as burn-in. MrBayes analyses were carried out in the CIPRES Science Gateway (Miller *et al*., 2010).

Species trees and divergence time estimation

We used BEAST 1.7.4 (Drummond *et al*., 2012), to reconstruct a time-calibrated multilocus species tree using individuals from each phylogeographical lineage recovered and the five outgroups. We used a Yule speciation prior and relaxed uncorrelated lognormal clock for each gene tree (Drummond *et al*., 2006). We considered the same partitions and models used in the phylogeographical reconstructions, as estimated in PartitionFinderV1.1.1. To calibrate our species tree, we used the ND2 substitution rate of 1.25 x 10^{-2} substitutions/site/Myr (2.5% change between lineages per Myr) from Smith & Klicka (2010). We specified a lognormal distribution and a relatively wide logarithmic standard deviation of 0.2 for each gene,

thus encompassing alternative substitution rates (e.g. Lerner *et al*., 2011). We performed two independent runs with 150 million generations each, with parameters sampled every 1000 generations. Tracer was used to check for convergence between runs, likelihood stationarity, appropriate burn-in, and adequate effective sample sizes (> 200). After discarding the first 15 million generations (10%) as burn-in, the parameter values of the samples from the posterior distribution were summarized on the maximum clade credibility tree using TreeAnnotator 1.7.4 (Drummond & Rambaut, 2007), and the consensus species tree with the divergence times was visualized and edited in FigTree 1.4 (http:// tree.bio.ed.ac.uk/software/figtree/).

Ancestral area reconstruction

To reconstruct the biogeographic history of antpittas across the Neotropics, we used BioGeoBEARS (BioGeography with Bayesian (and likelihood) Evolutionary Analysis in R Scripts; Matzke, 2013; http://cran. r-project.org/web/packages/BioGeoBEARS/index.html). This package implements many models in a common likelihood framework, so that standard statistical model selection procedures can be applied to let the data choose the best model (Matzke 2013). We performed six different BioGeoBears analyses, the models included the Dispersal-Extinction Cladogenesis Model (DEC), a likelihood version of the Dispersal-Vicariance Analysis ("DIVALIKE"), and a version of the Bayesian inference of historical biogeography for discrete areas (BAYAREALIKE), as well as "+J" versions of these three models, which include founder-event speciation, an important process left out of most inference methods (Matzke, 2013). These biogeographic processes are implemented in a maximum likelihood (DEC, DEC+J, DIVALIKE, DIVALIKE+J) or Bayesian (BAYAREALIKE, BAYAREALIKE+J) framework, as free parameters estimated from the data. We defined nine geographical areas for the BioGeoBEARS analysis, based on evidence available for historical relationships between relevant geographic areas in the Neotropics (Hoorn *et al*., 2010; Morrone, 2014), and the current distribution of antpittas. These biogeographic regions were adapted from (Silva *et al*., 2005; Ribas *et al*., 2012b; Borges & Silva 2012; Morrone, 2014) as follows: Andes, Chocó, Central America, Tepuis, Guiana Shield, Western Amazon, Eastern Amazon, Atlantic Forest, and Caatinga (See Appendix S3 for biogeographic setting details). Our multilocus species tree was used to infer the

ancestral area probability, which was computed for each node and subsequently plotted on the majority-rule chronogram (Fig. 4). Finally, we compared the six different models for statistical fit in two ways, using Likelihood values and Akaike Information Criterion (AIC), both implemented in the BioGeoBEARS R package (Matzke, 2013).

Diversification rates

We analyzed temporal shifts in diversification rates within *Hylopezus* and *Myrmothera* genera (excluding outgroups) using maximum likelihood-based diversification-rate analysis (Rabosky, 2006a) and divergence dates estimated from both the multilocus and the mtDNA datasets. The fits of different birth–death models implementing two constant rates (pure birth and birth–death) and three variable rates (exponential and logistic density-dependent and two-rate pure birth) were computed with Laser 2.4 (Rabosky, 2006b). Model fit was measured using AIC scores, and the significance of the change in AIC scores between the best rate-constant and best rate-variable model was determined through simulations implemented in Laser. Log-likelihood and AIC values were calculated for three models (SPVAR, EXVAR and BOTHVAR; Rabosky & Lovette, (2008) that allow differential extinction and speciation rates. We generated lineage-through-time (LTT) plots to visualize the tempo of diversification within the *Hylopezus* / *Myrmothera* clade inferred from our multilocus species tree and mtDNA chronogram reconstructions.

RESULTS

Phylogeographic estimation

The BI recovered 20 evolutionary lineages within *Hylopezus* and *Myrmothera* genera, distributed in two major clades and one separate lineage with a single member, *H. nattereri* (Figs. 1 & 2). The 'core *Hylopezus*' clade contained 8 lineages from seven currently recognized *Hylopezus* species (Fig. 1), whereas the 'extended *Myrmothera*' clade comprises 11 lineages from 5 species, including 3 taxa currently allocated in *Hylopezus* (Krabbe & Schulenberg, 2003), showing that the genus *Hylopezus*, as currently defined, is polyphyletic (Fig. 2). Support for each one of these two major

clades was high (PP = 1), and the BI recovered the 'core *Hylopezus*' clade as sister to the 'extended *Myrmothera*' clade (PP = 1). Furthermore, *Hylopezus nattereri* was recovered with high support (PP = 1) as a distinct lineage within the *Hylopezus* / *Myrmothera* + *Grallaricula* clade, but of uncertain phylogenetic affinities, as demonstrated by the low posterior probability associated with the node uniting *Grallaricula* and the *Hylopezus* / *Myrmothera* clades (Figs. 1 & 2).

Our reconstructions revealed all species currently recognized in the *Hylopezus* / *Myrmothera* clade as monophyletic, except for the paraphyly found within the genus *Myrmothera*. The widespread lowland Amazonian endemic *Myrmothera campanisona* includes four distinct paraphyletic lineages subdivided in two groups: one comprising Guiana Shield and Western Amazon Forest lineages (C and D), and another (A and B) comprising Eastern Amazon Forest lineages (East of Tapajos River), with the latter more closely related to the remaining species of the genus, the highland Tepui endemic *M. simplex* (Fig. 2). We also found deep divergences between some populations across the entire *Hylopezus* / *Myrmothera* clade, and most of them represent geographically isolated lineages (Figs. 1 & 2). The optimal partition scheme and the best-fit models used on the BI are described in details on supplementary material (Table S4).

Species trees and divergence time estimation

Complete genetic data could not be obtained for some specimens used in our multilocus species tree analyses. In particular, we could not obtain FGB-I5 sequences from *H. dilutus*, and any nuclear data for the two divergent lineages of *H. perspicillatus* (A and B) (Fig. 3), so these lineages were represented solely from mtDNA data. Our multilocus species tree produced a time-calibrated phylogenetic reconstruction with overall high resolution and nodal support (80% of nodes with PP > 0.95; Fig. 3). Additionally, our multilocus and mtDNA chronogram topologies were similar and differed only in the placement of *H. dives* and on the relationships between the *Grallaricula* and members of the *Hylopezus* / *Myrmothera* clades (Figure 3). *Hylopezus dives* was placed as sister of *H. fulviventris* + *H. berlepschi* (multilocus species tree, PP = 0.65) or as sister to the *Myrmothera* lineages (mtDNA chronogram, PP = 0.67; Fig. 3).

The multilocus species tree also yielded high support for a relationships that was poorly supported in the mtDNA reconstruction: 'core *Hylopezus*' and 'extended *Myrmothera*' clades were recovered as sister groups.

Estimates of time divergence differed between mtDNA and the multilocus species tree (Fig. 3). The split of *Grallaria* from all other taxa, for example, differed by 2.5 Myr. Mean estimated divergence dates in the mtDNA chronogram were older, and 95% highest posterior density (HPD) intervals were wider than those of the multilocus species tree estimates, as expected (Edwards & Beerli, 2000; Bryson *et al*., 2014).

The multilocus species tree suggested an Eocene divergence of the *Grallaria* genus from the remaining species of the family (mean estimated date 43.29 Ma, 95% HPD: 51.03–36.09 Ma). The main clades subsequently diverged throughout the Oligocene, as follows: i) *H. nattereri* diverged at *c*. 30.3 Ma (95% HPD: 35.5–25.4 Ma); ii) the *Grallaricula* clade originated at *c*. 28.3 Ma (95% HPD: 32.9–23.8 Ma); and iii) the *Hylopezus* / *Myrmothera* clade appeared at *c*. 24.8 Ma (95% HPD: 29.8–20.1 Ma). Diversification within the 'core *Hylopezus*' clade began with the early divergence of *H. auricularis* at *c*. 22.5 Ma (95% HPD: 26.9–18.4 Ma), and continued on through the Miocene with the *H. ochroleucus* divergence at *c*. 16.1 Ma (95% HPD: 20.1–12.1 Ma). The estimates for divergence within the 'core *Hylopezus*' during the Pliocene onwards differed between mtDNA and the multilocus analyses due to differences between the number of lineages sampled in each analysis (Fig. 3). Within the 'extended *Myrmothera*' clade divergence began during the Miocene at *c*. 15.7 Ma (95% HPD: 18.5–12.9 Ma), but concentrated throughout the Pliocene and into the Quaternary; three divergences occurred within the Pliocene, whereas six spanned through the Pliocene and Quaternary (Fig. 3).

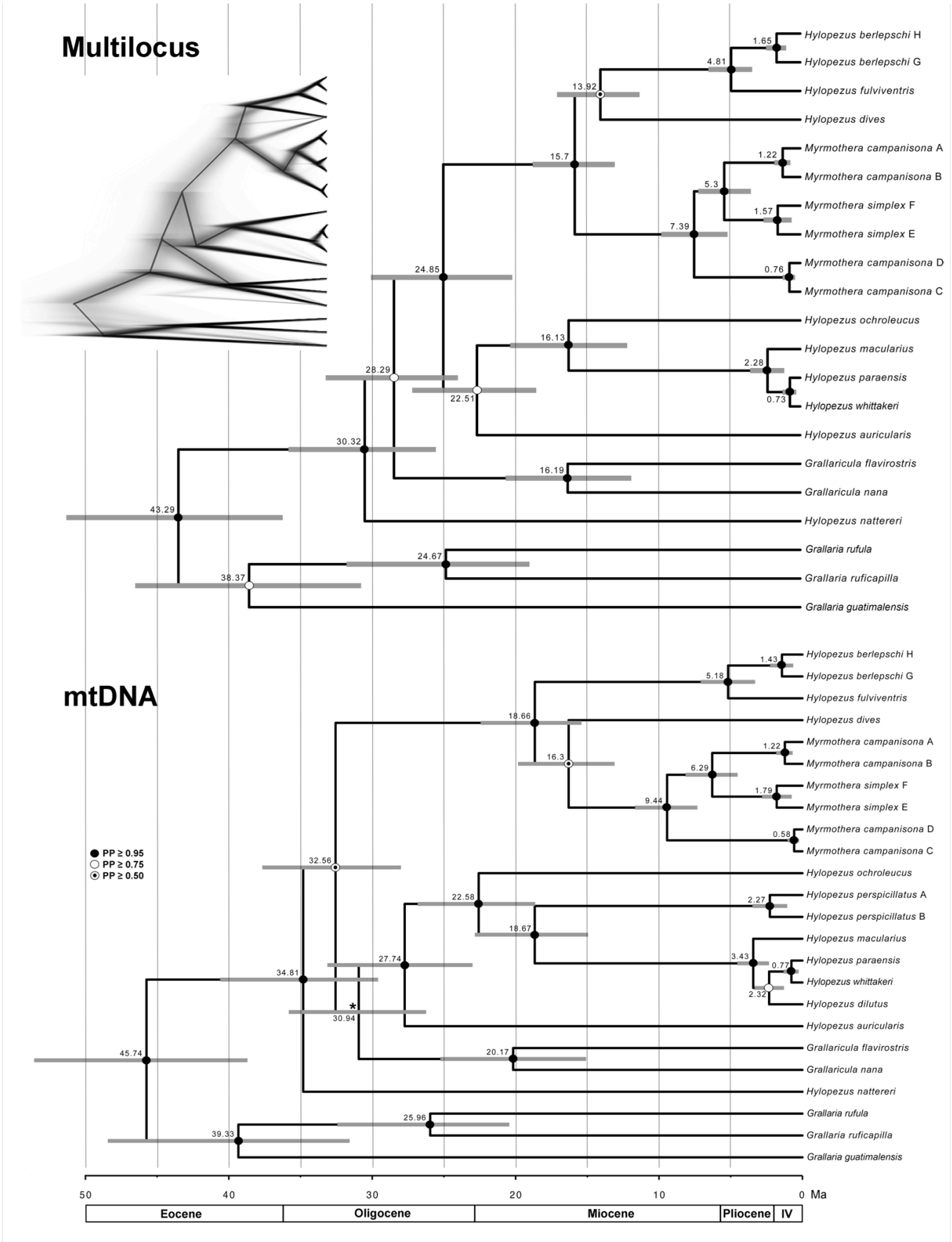
Multilocus
Hylopezus berlepschi H
Hylopezus berlepschi G
Hylopezus fulviventris
Hylopezus dives
Myrmothera campanisona A
Myrmothera campanisona B
Myrmothera simplex F
Myrmothera simplex E
Myrmothera campanisona D
Myrmothera campanisona C
Hylopezus ochroleucus
Hylopezus macularius
Hylopezus paraensis
Hylopezus whittakeri
Hylopezus auricularis
Grallaricula flavirostris
Grallaricula nana
Hylopezus nattereri
Grallaria rufula
Grallaria ruficapilla
Grallaria guatimalensis
1.65
4.81
13.92
15.7
1.22
5.3
1.57
7.39
0.76
24.85
16.13
2.28
28.29
22.51
0.73
30.32
16.19
43.29
24.67
38.37
mtDNA
PP ≥ 0.95
PP ≥ 0.75
PP ≥ 0.50
Hylopezus berlepschi H
Hylopezus berlepschi G
Hylopezus fulviventris
Hylopezus dives
Myrmothera campanisona A
Myrmothera campanisona B
Myrmothera simplex F
Myrmothera simplex E
Myrmothera campanisona D
Myrmothera campanisona C
Hylopezus ochroleucus
Hylopezus perspicillatus A
Hylopezus perspicillatus B
Hylopezus macularius
Hylopezus paraensis
Hylopezus whittakeri
Hylopezus dilutus
Hylopezus auricularis
Grallaricula flavirostris
Grallaricula nana
Hylopezus nattereri
Grallaria rufula
Grallaria ruficapilla
Grallaria guatimalensis
1.43
5.18
18.66
16.3
1.22
6.29
1.79
9.44
0.58
32.56
22.58
2.27
18.67
3.43
0.77
27.74
34.81
2.32
30.94
*
45.74
20.17
25.96
39.33
50
40
30
20
10
0 Ma
Eocene
Oligocene
Miocene
Pliocene
IV

Figure 3 Reconstructions for antpittas estimated from multilocus (species tree) and mtDNA (chronogram) datasets using *Beast. Bars indicate 95% highest posterior densities of divergence dates. The mean estimated dates are shown above nodes and the scale bar is in millions of years ago (Ma). Bayesian posterior probability (PP) support for nodes are indicated by coded dots according to the figure legend, with nodes receiving less than 0.50 support marked with an asterisk. IV = Quaternary. The inset (upper left) figure is the result of the superposition of all gene trees and has the same topology of the multilocus tree (generated by DensiTree 2.0.1).

Diversification rates

Birth–death likelihood analyses of lineage diversification rates within the *Hylopezus* / *Myrmothera* clade failed to reject the null hypothesis of rate constancy for both datasets (P = 0.85, multilocus species tree; P = 0.89, mtDNA chronogram). We obtained two best-fit rate-constant models; birth-death for the mtDNA, and pure birth for the multilocus dataset (Table 1). The lineage diversification rate in antpittas remained constant through time, with diversification rates estimated at 0.0780 (multilocus) and 0.0273 (mtDNA) divergence events per lineage per million years. Models considering variable rates of extinction and speciation did not provide a better fit to the data (Table 1). The lineage-through-time plot also suggested a near constant rate during most of the 35 million year history of the group (Fig. 3).

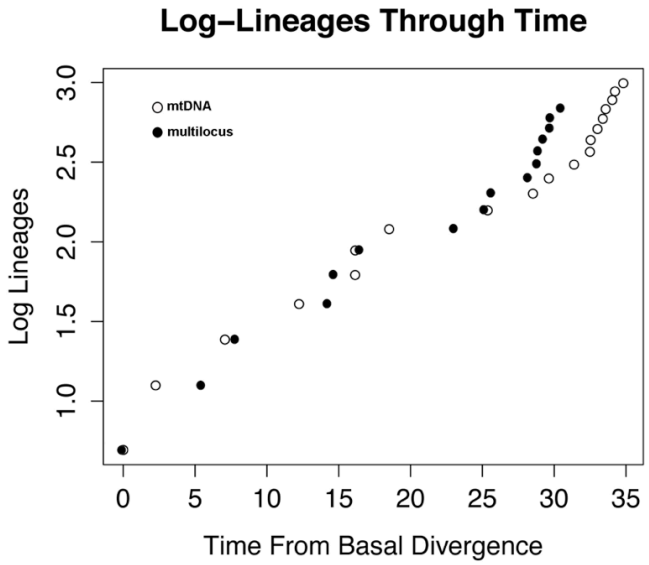

Figura 4 Lineage through time plot (LTT) of *Hylopezus* and *Myrmothera* inferred from a timetree generated by BEAST based on our multilocus species tree reconstruction and the mtDNA chronogram.

Table 1 Summary of diversification models fitted to the branching times derived from multilocus species tree and mtDNA chronogram reconstructions for the *Hylopezus* / *Myrmothera* clade (outgroup excluded). Log-likelihood (lnL) values and Akaike information criterion (AIC) scores for each model are provided. The AIC scores from the best-fitting constant or variable model were determined using simulations and are shown in bold. Rate-variable models were exponential and logistic density-dependent (DDX, DDL), two-rate pure birth (Yule2), time-varying speciation (SPVAR), time-varying extinction (EXVAR), and time-varying speciation and extinction (BOTHVAR).

	Rate-constant models		Rate-variables models					
	Pure birth	Birth-death	DDX	DDL	Yule2	SPVAR	EXVAR	BOTHVAR
Multilocus								
lnL	-21.81258	-21.0345	-21.70614	-21.81262	-20.4486	-20.91266	-21.03461	-20.87921
AIC	**45.62516**	46.069	47.41227	47.62524	46.8972	47.82531	48.06921	49.75842
mtDNA								
lnL	-25.67072	-24.6466	-25.5992	-25.6707	-23.7637	-24.3371	-24.6466	-24.1418
AIC	53.3414	**53.2931**	55.0584	55.3415	53.5274	54.6743	55.2932	56.2836

Ancestral area reconstruction

Of the six biogeographic models evaluated, the best fit to our dataset of antpittas was BAYAREALIKE + J (ln *L* = -64.55), whereas BAYAREALIKE (ln *L* = -87.37) was less likely (LRT = 45.63, $p < 0.05$). The most likely ancestral area reconstruction, and the parameters and scores from each model implemented are given below (Fig. 4; Table 2). For node pie charts likelihoods of ancestral areas see Figure S5 in supplementary material.

Table 2 Models and parameters from each of the analyses in BioGeoBEARS. Dispersal (d), Extinction (e), Founder (J), values of Log-Likelihood (ln *L*) and Akaike Information Criterion (AIC) scores from each model implemented.

Model	Parameters	d	e	j	ln *L*	AIC
DEC	2	0.0068	0.010	0	-76.19	156.4
DEC+J	3	0.0037	0.0001	0.095	-65.4	136.8
DIVALIKE	2	0.0064	0.0001	0	-69.63	143.3
DIVALIKE+J	3	0.0046	0.0001	0.065	-65.44	136.9
BAYAREALIKE	2	0.0122	0.081	0	-87.37	178.7
BAYAREALIKE+J	3	0.0024	0.0001	0.074	**-64.55**	**135.1**

This biogeographic reconstruction indicated an Andes/Chocó origin for *Grallaria* and for the ancestor that originated the remaining groups of the family. Our analysis suggested an early dispersal event during the Oligocene, which separated the Atlantic forest endemic *H. naterreri* from the remaining lineages. Still during the Oligocene, the diversification of the lineage that originated the genus *Grallaricula* took place. The most likely origin for the *Hylopezus* / *Myrmothera* clade (node *D*) was Western Amazonia. From this area, the clades the members of the *Hylopezus* / *Myrmothera* clade appear to have colonized the remaining sectors of Amazonia and the Tepuis, as well as Trans-Andean South America, Central America and the northeastern Brazilian *Caatinga* biome (Fig. 5). However, it is important to bear in mind that this ancestral area reconstruction should be interpreted with caution, as some nodes were not completely solved in our phylogenetic reconstructions and some lineages were not included in the species tree.

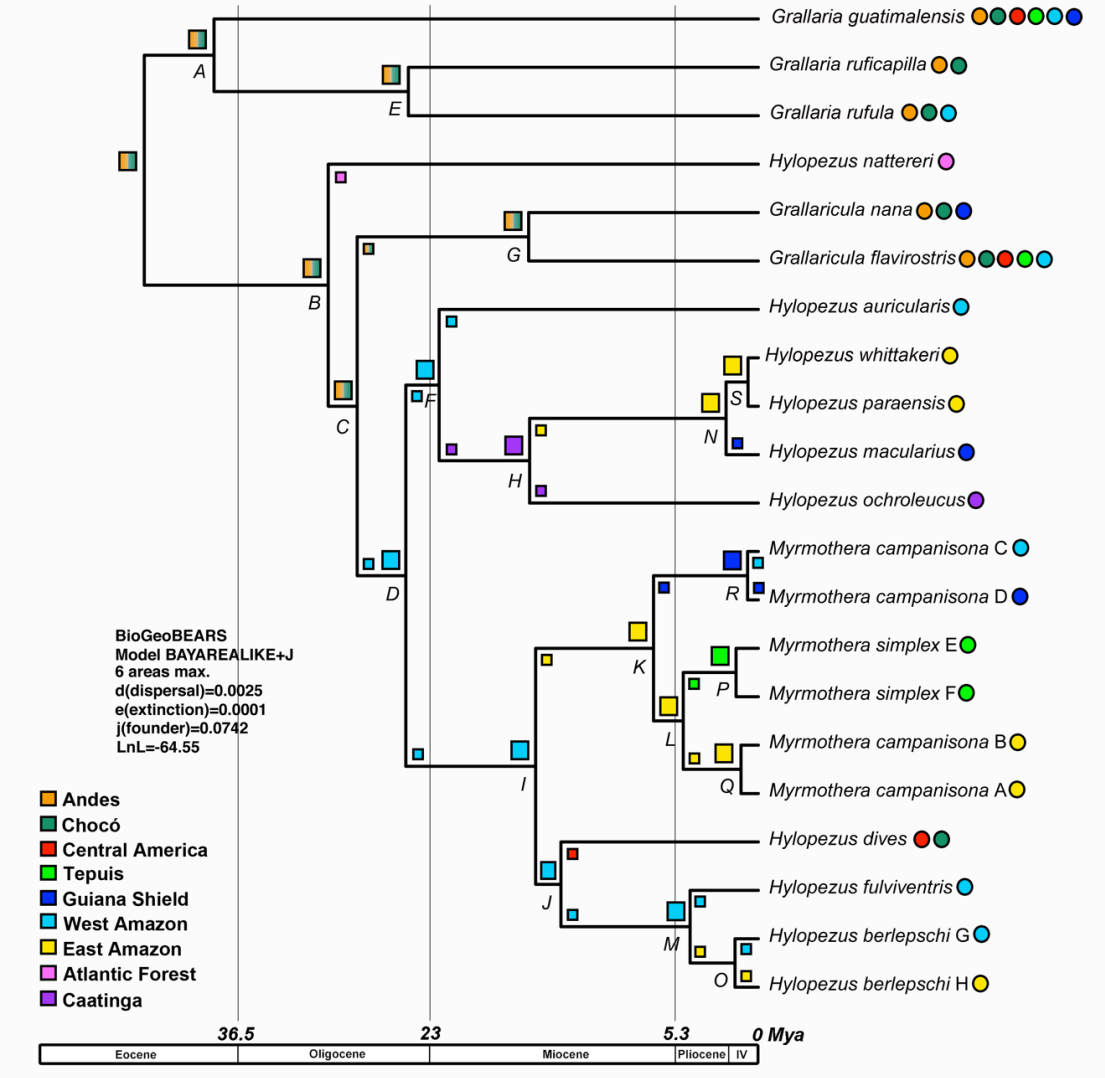

Figure 5 Time-calibrated species trees generated by BEAST and ancestral area reconstructions provided by BioGeoBEARS, both derived from the multilocus dataset. The best-fit model for our phylogenetic reconstruction was BAYAREALIKE + J (lnL = -64.55, AIC = 135.1). The most likely area states are shown to the left of the each node; smaller squares denote states just after speciation. Ranges that are combinations of two areas are represented by mixed color square. The color-coded circles at the tips represent the current areas occupied by each lineage. IV = Quaternary. Only the most probable area states are shown. (Node pie charts likelihoods of ancestral areas and additional details in Appendix S5).

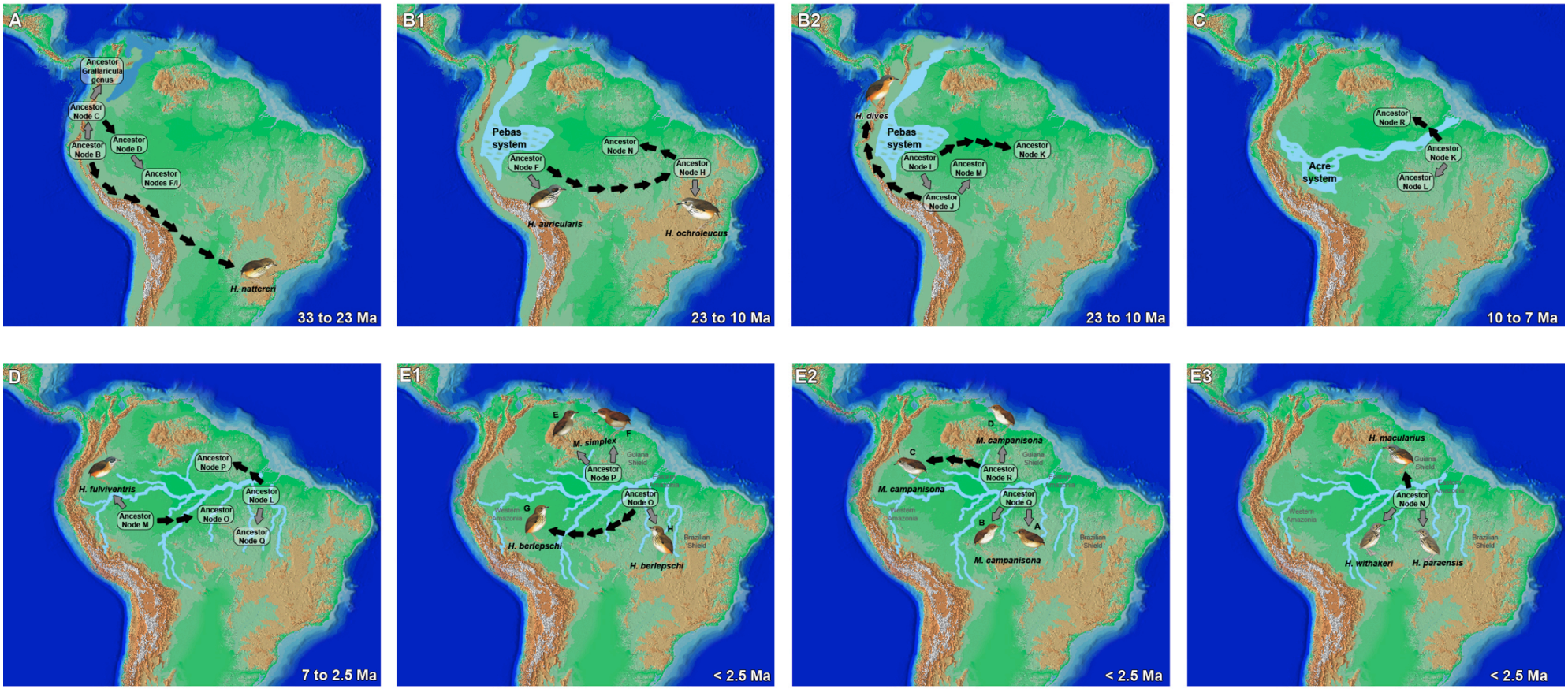

Figure 6 Hypothesized paleoscenarios for the evolution of the *Hylopezus* / *Myrmothera* clade. Palegeographic maps follow Hoorn *et al*. (2010). (A) Oligocene: Andes uplifting and a major marine incursion in northwestern South America. (B1; B2) Early Miocene: Mountain building in the Central and Northern Andes (~12 Ma) and wetland propagation into Western Amazonia (Pebas system). (C) Late Miocene: accelerated mountain building in the Central and Northern Andes. Initial establishment of the transcontinental Amazon basin, with western Amazonia still holding wetlands (Acre system). (D) Late Miocene to Pliocene: The megawetland disappeared and upland *terra firme* rainforests expanded into western Amazonia; closure of Panama Isthmus, establishment of modern drainage of Amazon river (Late Pliocene to Pleistocene; Campbell *et al*., 2006; Latrubesse *et al*., 2010) and final phase of Andean uplift. (E1; E2; E3) Quaternary: the modern Amazon river established and Andean cordillera uplifted. All currently extant *Hylopezus* and *Myrmothera* species diversified. The ancestors and the respective node codes follow Fig. 5. Arrows represent divergences in lineages, with gray and black arrows indicating divergences within and between distinct biogeographic areas, respectively. Illustrations are courtesy of Lynx Edicions (Handbook of the birds of the world, Vol. 8, 2003).

DISCUSSION

Phylogenetic and biogeographic patterns recovered in this study reinforce the spatial and temporal complexity of biological diversification in the Neotropics. Our results disagree with the current phylogenetic and taxonomic status of the genera *Hylopezus* and *Myrmothera*. Patterns of lineage diversification within this group also reveal much about the historical processes that have shaped biological diversification throughout the Neotropics since the Oligocene.

Given our data, and assuming the monophyly of the Grallariidae as supported by several studies (Rice, 2005; Moyle *et al*., 2009; Galvão & Gonzaga, 2011; Ohlson *et al*., 2013), our ancestral area reconstructions suggest that the group originated in the Andes/Chocó area, which coincides with the family stronghold, whereby most species are distributed in these areas but specially along the Andes (Krabbe & Schulenberg, 2003). Of the 51 currently recognized species in Grallariidae, at least 30 occur in the Andes and the Chocó. However, it is critical to note that the Grallariidae have had a long history in both Central and South America, and that our sampling and ancestral area reconstruction are focused on *Hylopezus* and *Myrmothera*, where most species are distributed in South America.

Most Grallariidae inhabit humid forest. Indeed, most species in the *Hylopezus* / *Myrmothera* clade are found in wet forest, whereas a few others, such as *Hylopezus ochroleucus* and *Hylopezus nattereri*, occur in both humid and deciduous forest. Some species tolerate considerable habitat disturbance, and a couple of them seem to prefer disturbed habitats, i.e., *Hylopezus berlepschi* and *Hylopezus auricularis* (Krabbe & Schulenberg, 2003). Nonetheless, these life strategies seem to be more related to historical and ecological processes affecting habitat selection, rather than having a strict phylogenetic component.

The diversification rates that we estimated were constant. The rate constancy for the clades provides an alternative perspective on avian diversification in the Neotropics, compared with previous studies that coupled elevated rates of speciation with particular palaeogeographical or palaeoclimatic events (e.g. Weir & Schluter, 2004; Weir, 2006; Chaves *et al*., 2011; but see Zink *et al*., 2004), and reiterates the importance of using well-sampled phylogeographical datasets when comparing rates

of diversification on tropical regions (Ribas *et al*., 2012b). Our data are consistent with other recent observations showing a steady lineage accumulation up to the present among Neotropical endemic bird lineages (Derryberry *et al*., 2011; Patel *et al*., 2011; d'Horta *et al*., 2012; Smith *et al*., 2013, Bryson *et al*., 2014).

Origin and diversification of the *Hylopezus* / *Myrmothera* clade in the Neotropics

At the middle of the Oligocene (*c*. 30 Ma), *H. nattereri* diverged from the remaining *Hylopezus* and *Myrmothera* lineages (Fig. 3); this result suggest that *H. nattereri* should be treated as a highly divergent and independent lineage within Grallariidae, probably in a separate genus (so far, apparently unnamed).

The divergence of the 'core *Hylopezus* clade' (which includes *H. auricularis, H. ochroleucus, H. perspecillatus, H. macularius, H. dilutus, H. whittakeri*, and *H. paraensis*; see Fig. 1) started at the end of the Oligocene (*c*. 22 Ma) in Western Amazonia and procceded thereof to other parts of South America, eventually reaching Central America. Independently, during the middle of the Miocene (*c*. 15 Ma), the 'extended *Myrmothera* clade' (comprising *M. campanisona*, *M. simplex*, *H. dives*, *H. berlepschi*, and *H. fulviventris*; see Fig. 2) also began to diversify first in western Amazonia, reaching later on trans-Andean South America and Central America (Figs. 5 & 6).

Despite, the relatively high number of taxa in Grallaridae (51 species), a small number, essentially restricted to *Hylopezus* and *Myrmothera* (approximately 13 lineages, including *Grallaria varia*), occur in the lowlands. This imbalance between Neotropical highland and lowland lineages can be related to the extinction of deep branches in Grallariidae, as has also been inferred for other Suboscines lineages (Ohlson *et al.,* 2013). On the other hand, niche conservatism can restrict lineage distribution and diversification to narrow geographic areas and environmental conditions (Giehl & Jarenkow, 2012). Thus, niche conservatism coupled with an overall low dispersal ability reported for Grallariidae (Stratford & Stouffer, 2015) could explain the relatively fewer number of extant lowland taxa in this family, when compared to some other widespread Neotropical lineages of similar ages (Derryberry *et al*., 2011; Ohlson *et al.,* 2013), without necessarily resorting to events of extinction.

The diversification analysis indicated a best topological-fit to a pure birth model (Lnl

and AIC; Table 1) and a lineage diversification rate constant through time within the *Hylopezus* / *Myrmothera* clade (Fig. 4). This diversification pattern mirrors those documented for other Neotropical avian endemic groups that exhibited a similar pattern of constant diversification throughout the late Tertiary and Quaternary (Derryberry *et al*., 2011; d'Horta *et al*., 2013; Patel *et al*., 2011).

The lack of any significant shift in the diversification rate through time in the *Hylopezus* / *Myrmothera* clade suggests that this group represents an old and apparently ecologically specialized lineage, less prone to intense diversification compared to other New World suboscines relatives whose origin date to a similar period, such as the Furnariidae, with ca. 300 taxa and well documented episodes of diversification in the lowlands and highlands (Derryberry *et al*., 2011). Despite this relative poor diversity, the *Hylopezus* / *Myrmothera* clade phylogeny matches a complex sequence of landscape changes through the last 33 million years in the Neotropics (Fig. 5). These events include the uplift of the Andes (Hoorn *et al*., 2010), marine incursions (Antonelli & Sanmartín, 2011; Hoorn *et al*., 2010), the Plio-Pleistocene formation of flat depositional basins and the consequent establishment of the east-draining Amazon River (Ribas *et al*., 2012b).

Diversification in the Amazon basin

Expansion out of Andes/Chocó and into Amazon basin during the late Oligocene (Figs. 3 & 5) provided new opportunities for diversification within the Grallariidae. Despite reaching the Amazon basin some 24 to 25 Ma, most of the diversification within the *Hylopezus* / *Myrmothera* clade occurred more recently and at a near-constant rate. Posterior credibility intervals for 12 of the 15 (80%) divergences in our multilocus species tree encompass Pliocene and Quaternary dates. The predominance of taxa representing deep *Hylopezus* and *Myrmothera* lineages in Western Amazonia (e.g., *H. auricularis*) is consistent with our estimates of ancestral areas of diversification for the *Hylopezus* / *Myrmothera* clade, which point Western Amazonia as the source of colonization events to other parts of the basin and neighboring areas (Figs. 3, 5, & 6). Starting in the late Miocene and Pliocene, remarkable changes in the Amazonian landscape and the consolidation of the modern Amazonian drainage

(Hoorn *et al*., 2010) allowed the group to colonize (disperse) and diversify along the Amazon Basin (Figs. 3 & 5).

Diversification of the Atlantic Forest lineage

One of the basal-most lineages in the *Hylopezus* / *Myrmothera* clade consists of the lone "*Hylopezus*" endemic to the Atlantic Forest of southeastern South America: *H. nattereri* (Fig. 1). The origin of this lineage predates that of the *Hylopezus* / *Myrmothera* clade and was estimated as dating back to the Oligocene (Figs. 3 and 5). Recent studies showed that the Atlantic Forest holds ancient lineages that date to the mid-Tertiary, as verified for birds (Derryberry *et al*., 2011), mammals (Fabre *et al*., 2013; Galewski *et al*., 2005) and frogs (Fouquet *et al*., 2012). This endemic Atlantic Forest lineage has an Andean/Chocó sister group, and probably reached southeastern South America through the southern Andes, as it is restricted to humid subtropical and montane forests (Krabbe & Schulenberg, 2003).

Uplift of the Andes and diversification of antpittas

Our ancestral area reconstructions suggest that *H. dives* originated from a western Amazonian ancestor that diversified in Trans-Andean South America / Central America after having crossed the Andes before its major uplift (mean estimated date 13.9 Ma, 95% HPD: 11.2–16.8 Ma; Fig. 2, lineage J). After this initial split, *H. dives* populations split across the Panamá isthmus (Fig. 2). However, it is important to note the poor support recovered for the *H. dives* node in both chronograms, and the topology differences between mtDNA and multilocus trees (Fig. 3). The dispersion across the Andes inferred for the ancestor of *H. dives* is consistent with the mountain building pattern of the cordillera, whereby orogeny followed a south to north direction (Hoorn *et al*., 2010). This pattern has also been invoked to explain the diversification of other avian groups across and along the Andes (Chaves *et al*., 2011; Ribas *et al*., 2007).

Systematics implications

Results from our dense range-wide sampling and molecular dataset shed new light

into the systematics of antpittas. The 11 species currently recognized within this group can be further divided into 5 additional geographically and genetically structured evolutionary units (Figs. 1 & 2).

At a broader level, our multilocus species tree reconstruction strongly suggests that *Myrmothera* forms a monophyletic group with three species currently placed in *Hylopezus* genus (*H. dives*, *H. fulviventris*, and *H. berlepschi* ; Fig. 3). The clade formed by *H. auricularis*, *H. ochroleucus*, *H. whittakeri*, *H. paraensis*, and *H. macularius*, recovered by the multilocus species tree, probably also comprise *Hylopezus*' type species: *H. perspicillatus*. Even though we had no success with the amplification of any nuclear markers for this taxon, it was recovered with high support within this clade according to both the concatenated Bayesian tree and the mtDNA chronogram (Figs. 1, 2 & 3). Finally, the Atlantic forest endemic *H. nattereri* was recovered as an old and isolated lineage, not closely related to the remaining *Hylopezus* and *Myrmothera* species (Fig. 3). Nevertheless, *H. nattereri* was regarded until recently as a subspecies of *H. ochroleucus* based on mostly on plumage characters, being split later on based on voice (Krabbe & Schulenberg, 2003). Our phylogenetic estimates support the notion that plumage similarities between *H. nattereri* and *H. ochroleucus* could be result of convergence or simply retention of ancestral characters.

Therefore, *Hylopezus,* as presently configured, is polyphyletic. At a minimum, the following taxonomical recommendations are in order: 1) the clade formed by *H. berlepschi*, *H. dives* and *H. fulviventris* renders *Myrmothera* paraphyletic, therefore merging this '*Hylopezus*' group into *Myrmothera* Hermann, 1783, would solve this problem; and 2) we also recommend the recognition of *H. nattereri* as a separate (monotypic) genus to be named elsewhere, given its large phylogenetic distance from the remaining taxa of the *Hylopezus* / *Myrmothera* clade (Figs. 2 & 3). Future studies should provide more densely sampled phylogenies of the genera *Grallaricula* and *Grallaria*, therefore allowing for a more accurate positioning of *H. nattereri* in the family phylogeny.

Finally, because the *Hylopezus*' type species is *H. perspicillatus*, the following species must remain in this genus: *H. auricularis*, *H. ochroleucus*, *H. perspicillatus, H. macularius, H. dilutus, H. whittakeri*, and *H. paraensis*.

Conclusions

Our analyses provided an additional scenario for the evolution and biological diversification in the Neotropical region. The spatio-temporal pattern recovered herein for the *Hylopezus* / *Myrmothera* clade may reflect an evolutionary history influenced by several independent external events such as the Andean uplift (Hoorn *et al*., 2010), marine incursions (Antonelli & Sanmartín, 2011), as well as river formation (Ribas *et al*., 2012a). Nevertheless, it is intriguing that most diversification within this group appeared to have occurred so recently. Apparently, the onset of diversification took place only in the late Miocene to Pliocene, when remarkable changes to the Amazon River drainage took place (Hoorn *et al*., 2010), allowing for episodes of colonization and diversification throughout the Amazonian Basin all the way through the Quaternary (Figs. 3 & 5). Our biogeographic inferences recovered a distribution centered in western Amazonia basin, with a later dispersion towards eastern Amazonia during the early Miocene (Figs. 3 & 4) (Hoorn *et al*., 2010). However, Amazonian antpittas apparently have strict ecological requirements, and limited ability to colonize new areas, and these facts could explain the relatively few number of extant taxa in the group when compared to other Neotropical lowland lineages of similar age. Finally, our phylogenetic hypothesis also support a new taxonomy for the genera *Hylopezus* and *Myrmothera*.

Appendix A. Supplementary material

Table S1. List of primers used in the study.

Gene	Primmer	Reference
NADH dehydrogenase subunits 2 (ND2, 1041 bps)	L5215 H6313	Hackett, 1996 Sorenson *et al*., 1999
NADH dehydrogenase subunits 3 (ND3, 351 bps)	L5215 H6313	Hackett, 1996 Sorenson *et al*., 1999
Transforming growth factor beta 2 intron 5 (TGFB2, 625 bps)	L6625/H7005	Hafner *et al*., 1994
Beta-fibrinogen intron 5 (FGB-I5, 549 bps)	FIB5L/FIB5H	Driskell & Christidis, 200
3rd intron of the Z-linked muscle-specific kinase (MUSK, 582 bp)	MUSK-F/MUSK-R	Kimball *et al*., 2009

Table S2. General information on the tissue samples sequenced in the present study. Voucher numbers refer to deposit at ornithological collections. Taxonomy follows Remsen et al. (2015), except to *H. macularius* complex, which follows Carneiro et al. (2012).

Taxon	Locality	Voucher
Myrmothera simplex	Venezuela: Amazonas; Sierra de Tapirapeco; Cerro Tamacuari; 1270m	AMNH - GFB2136
Myrmothera simplex	Venezuela: Amazonas; Pico Cardonas; Elev. 1250M Rainforest, Valley N. Base	AMNH - RWD17126
Myrmothera simplex	Venezuela: Bolivar; La Escalera, KM 122 on El dorado-ST. Eleanea Road	AMNH - RDP301
Myrmothera simplex	Venezuela: Amazonas; Cerro Yavi	AMNH - 213312
Myrmothera simplex	Venezuela: Amazonas; Cerro de la Neblina; CAMP VII 1800-1900M	AMNH - GFB1440
Myrmothera simplex	Venezuela: Amazonas; Cerro Yavi	AMNH - 213320
Myrmothera simplex	Venezuela, Amazonas Territory, CERRO DE LA NEBLINA CAMP VII 1800M	LSUMZ - B7408
Myrmothera simplex	Venezuela, Amazonas Territory, CERRO DE LA NEBLINA CAMP VII 1800M	LSUMZ - B7468
Myrmothera campanisona	Brazil: Pará: FLOTA de Faro, ca 70 km NW de Faro	MPEG - CN150
Myrmothera campanisona	Brazil: Pará: Juruti, Projeto Juruti/Alcoa, Platô Capiranga, trilha 196	MPEG - MPDS0961
Myrmothera campanisona	Brazil: Pará: Alenquer, ESEC Grão-Pará	MPEG - CN509
Myrmothera campanisona	Brazil: Pará: Alenquer, ESEC Grão-Pará	MPEG - CN418
Myrmothera campanisona	Brazil: Pará: Rio Xingu, margem direita, Caracol (área 2)	MPEG - BMP075
Myrmothera campanisona	Brazil: Pará: Óbidos, Flota do Trombetas	MPEG - CN341
Myrmothera campanisona	Brazil: Pará: Altamira, Floresta Nacional de Altamira	MPEG - TM008
Myrmothera campanisona	Rio Juruá, Marechal Taumaturgo, Nossa Senhora Aparecida	MPEG - PNSD337
Myrmothera campanisona	Rio Branco, margem esquerda, Caracaraí, próximo BR 174	MPEG - MPDS040
Myrmothera campanisona	Brazil: Amazonas, São Gabriel da Cachoeira, PPBIO	MPEG - 20648
Myrmothera campanisona	Brazil: Pará: Itaituba, margem direita Rio Tapajós, Comunidade Penedo	MPEG - 19634
Myrmothera campanisona	Brazil: Pará, Jacareacanga, margem esquerda Rio Tapajós, Vila Mamãe-anã	MPEG - 18604
Myrmothera campanisona	Brazil: Pará: Estern margin Rio Tapajós e direita do Jamanxin SW Itaituba	INPA - A10032

Myrmothera campanisona	RR, Parque Nacional Viruá, margem esquerda do Rio Branco, "grid"	INPA - A1726
Myrmothera campanisona	Brazil: Amazonas, 110 km ENE Santa Isabel do Rio Negro	INPA - A1662
Myrmothera campanisona	RO, Porto Velho; margem direita do Rio Jaci; Três Praias	INPA - A4141
Myrmothera campanisona	PA, Margem direita do Rio Tapajós; 147 km sudoeste de Itaituba, J	INPA - A11548
Myrmothera campanisona	Guyana, Potaro-Siparuni, Iwokrama Reserve; ca. 41 road km, SW Kurupukari	ANSP - 21109
Myrmothera campanisona	Guyana, Iwokrama Reserve; Kobacalli Landing	ANSP - 21242
Myrmothera campanisona	Guyana, Potaro-Siparuni,Iwokrama Reserve; ca. 6-8 road mi. SW Kurupukari	ANSP - 22305
Myrmothera campanisona	Ecuador, Morona-Santiago,Santiago	ANSP - 16450
Myrmothera campanisona	Ecuador, Morona-Santiago,5 km SW Taisha	ANSP - 17546
Myrmothera campanisona	Ecuador, Napo, Zancudo Cocha	ANSP - 18324
Myrmothera campanisona	Ecuador, Napo, Pasohurco; km 57 on Hollin-Loreto Road	ANSP - 19457
Myrmothera campanisona	Brazil, Rondonia, Cachoeira Nazare, W bank Rio Jiparana, 100m	FMNH - 389886
Myrmothera campanisona	Brazil, Rondonia, Cachoeira Nazare, W bank Rio Jiparana, 100m	FMNH - 389885
Myrmothera campanisona	Peru: Madre de Dios: Moskitania, 13.4 km NNW Atalaya, l bank Alto Madre de Dios	FMNH - 433464
Myrmothera campanisona	Brazil, Acre, Reserva Extravista Alto Jurua, Rio Tejo,	FMNH - 395576
Myrmothera campanisona	Brazil, Rondonia, Cachoeira Nazare, W bank Rio Jiparana, 100m	FMNH - 395993
Myrmothera campanisona	Peru, Madre de Dios, Moskitania, 13.4 km NNW Atalaya, l bank Alto Madre de Dios	FMNH - 433462
Myrmothera campanisona	Parabara Savannah	KU - B12708
Myrmothera campanisona	Upper Essequibo River	USNM - 625540
Myrmothera campanisona	Parabara Savannah	USNM - 622361
Myrmothera campanisona	Upper Takutu - Upper Essequibo, lower Rewa River	USNM - 637266
Myrmothera campanisona	Barima-Waini, Baramita, In Former North West Region	USNM - 621449
Myrmothera campanisona	Barima-Waini, Baramita, In Former North West Region	USNM - 586403
Myrmothera campanisona	Gunn'S Landing, West Bank Upper Essequibo River	USNM - 616546
Myrmothera campanisona	Peru, Loreto Department, S bank Maranon R., Est. Biol. Pithecia	LSUMZ - B3617
Myrmothera campanisona	Bolivia, Pando Department, Nicolás Suarez; 12 km by road S of Cobija	LSUMZ - B9600
Myrmothera campanisona	Bolivia, Pando Department, Nicolás Suarez; 12 km by road S of Cobija	LSUMZ - B8955

Myrmothera campanisona	Peru, Loreto Department, Ca. 86 km SE Juanjui on E bank upper Rio Pauya	LSUMZ - B39839
Myrmothera campanisona	Peru, Loreto Department, Ca 7 km S Jeberos	LSUMZ - B42523
Myrmothera campanisona	Peru, Loreto Department, 1 km N Rio Napo, 157 km by river NNE Iquitos	LSUMZ - B2867
Myrmothera campanisona	Peru, Loreto Department, 79 km WNW Contamana, ca	LSUMZ - B27991
Myrmothera campanisona	Peru, Loreto Department, S Rio Amazonas, ca 10km SSW mouth Rio Napo	LSUMZ - B5066
Myrmothera campanisona	Peru, Loreto Department, S bank Maranon River, Est. Biol. Pithecia.	LSUMZ - B103576
Myrmothera campanisona	Peru, Loreto Department, Lower Rio Napo region, E bank Rio Yanayacu, N Iquitos.	LSUMZ - B4346
Myrmothera campanisona	Peru, Loreto Department, Lower Rio Napo region, E. bank Rio Yanayacu, N Iquitos	LSUMZ - B4172
Myrmothera campanisona	Peru, Loreto Department, 79 km WNW Contamana, ca	LSUMZ - B27987
Myrmothera campanisona	Venezuela, Amazonas Territory, CERRO DE LA NEBLINA BASE CAMP 140M	LSUMZ - B7563
Hylopezus whittakeri	Pará, Jacareacanga, margem direita Rio Tapajós, Comunidade São Martim	MPEG - 18511
Hylopezus whittakeri	Pará, Itaituba, leste do Tapajós, Rio Ratão	MPEG - 18776
Hylopezus whittakeri	Pará, Itaituba, leste do Tapajós, Jatobá	MPEG - 18803
Hylopezus whittakeri	Pará, Jacareacanga, margem direita Rio Crepori	MPEG - 19599
Hylopezus whittakeri	Alvorada d'Oeste, Linha 64, Br 429 Km 87	MPEG - 38808
Hylopezus whittakeri	Cachoeira Nazaré, west bank Rio Ji-paraná	MPEG - 39819
Hylopezus whittakeri	Cachoeira Nazaré, west bank Rio Ji-paraná	MPEG - 39820
Hylopezus whittakeri	Cachoeira Nazaré, west bank Rio Ji-paraná	MPEG - 39821
Hylopezus whittakeri	Município de Humaitá, T. Indígena Parintintin, Aldeia Traíra-Chororó	MPEG - MPDS719
Hylopezus whittakeri	Paranaíta, margem direita Rio Paranaíta, Fazenda Rio Paranaíta	MPEG - TLP178
Hylopezus whittakeri	Paranaíta, margem direita Rio Paranaíta, Fazenda Rio Paranaíta	MPEG - TLP(A)179
Hylopezus whittakeri	Paranaíta, margem esquerda Rio Paranaíta, Fazenda Aliança	MPEG - TLP(A)404
Hylopezus whittakeri	Paranaíta, Rio Teles Pires, margem direita	MPEG - TLP(C)095
Hylopezus perspicillatus	Colombia: Santander, Flores Blancas	LSUMZ - 36133
Hylopezus perspicilatus	Ecuador, Esmeraldas, 20 road km NNW Alto Tambo	ANSP - 17269
Hylopezus perspicilatus	Ecuador, Esmeraldas, 30 km S Chontaduro; W bank Rio Verde	ANSP - 19055
Hylopezus paraensis	Rio Gurupi, Carutapera, Fazenda Santa Bárbara	MPEG - 36922

Hylopezus paraensis	Brazil: Rondonia, Cachoeira Nazare, W bank Rio Jiparana	FMNH - 389869
Hylopezus paraensis	Rio Xingu, margem direita, Senador José Porfírio	MPEG - UHE388
Hylopezus paraensis	Paragominas, Fazenda Rio Capim, CIKEL	MPEG - FRC078
Hylopezus paraensis	Rio Xingu, margem direita, Caracol (área 2)	MPEG - BMP074
Hylopezus ochroleucus	Piauí, São Raimundo Nonato, PN Serra da Capivara, Serra Vermelha	MPEG - 18943
Hylopezus ochroleucus	Piauí, Caracol, PN Serra das Confusões, Projeto Cajugaia	MPEG - 18962
Hylopezus ochroleucus	Piauí, Cristino Castro, PN Serra das Confusões, Baixo Japecanga	MPEG - 18984
Hylopezus ochroleucus	Piauí, Cristino Castro, PN Serra das Confusões, Baixo Japecanga	MPEG - 18985
Hylopezus ochroleucus	Piauí, Caracol, P. N. Serra das Confusões, Centro de Visitantes	MPEG - 20156
Hylopezus ochroleucus	Morro Cabeça no Tempo, Serra Vermelha	MPEG - SRV104
Hylopezus ochroleucus	Curimatá, Serra Vermelha	MPEG - SRV004
Hylopezus ochroleucus	Brazil: Minas Gerais; Mocambinho, Jaíba	LGEMA - 2318
Hylopezus ochroleucus	Brazil: Minas Gerais; Mocambinho, Jaíba	LGEMA - 2036
Hylopezus nattereri	Quatro Barras, Corvo	MPEG - CMN024
Hylopezus nattereri	Condominio Alpes- São Francisco de Paula, RS	PUCRS - PUC3057
Hylopezus nattereri	CPCN Pró-Mata, São Francisco de Paula-RS	PUCRS - PUC3345
Hylopezus macularius	Guyana, Iwokrama Reserve; Kobacalli Landing	ANSP - 21224
Hylopezus macularius	Alenquer, ESEC Grão-Pará	MPEG - 66053
Hylopezus macularius	Northwest District, Baramita	KU - B09754
Hylopezus macularius	Acari Mountains, N side	KU - B10765
Hylopezus macularius	Parabara Savannah	KU - B12706
Hylopezus macularius	Barima-Waini, Baramita, In Former North West Region	USNM - 586404
Hylopezus macularius	Parabara Savannah	USNM - 616605
Hylopezus macularius	Gunn'S Landing, 10 km SSE	USNM - 625539
Hylopezus macularius	Upper Takutu - Upper Essequibo, Upper Rewa River	USNM - 637111
Hylopezus macularius	Upper Takutu - Upper Essequibo, Upper Rewa River	USNM - 637226
Hylopezus macularius	Upper Takutu - Upper Essequibo, lower Rewa River	USNM - 637238

Hylopezus macularius	FLOTA de Faro, ca 70 km NW de Faro	MPEG - CN143
Hylopezus macularius	Almeirim, REBIO Maicuru	MPEG - CN901
Hylopezus macularius	Óbidos, ESEC Grão-Pará	MPEG - CN1274
Hylopezus macularius	Óbidos, ESEC Grão-Pará	MPEG - CN1329
Hylopezus macularius	Óbidos, ESEC Grão-Pará	MPEG - CN1328
Hylopezus macularius	Óbidos, ESEC Grão-Pará	MPEG - CN1332
Hylopezus fulviventris	Ecuador, Napo, 20 road km W of Coca; south bank Rio Payamino	ANSP - 18744
Hylopezus fulviventris	Peru, Loreto Department, Ca 54 km NNW mouth Rio Morona on east bank	LSUMZ - B43007
Hylopezus fulviventris	Peru, Loreto Department, Ca 54 km NNW mouth Rio Morona on west bank	LSUMZ - B43008
Hylopezus fulviventris	Peru, Loreto Department, Ca 54 km NNW mouth Rio Morona on west bank	LSUMZ - B43009
Hylopezus fulviventris	Peru: Loreto ; Ca 54 km NNW mouth of Rio Morona, on east bank	LSUMZ – 42791
Hylopezus dives	Panama, Darién Province, Cana on E slope Cerro Pirré	LSUMZ - B2283
Hylopezus dives	Honduras, Gracias a Dios t, Las Marias, Rio Platano, 25 km S Caribbean Sea	LSUMZ - B26087
Hylopezus dives	Panama, Bocas del Toro Province, Rio Changuinola Arriba, W bank	LSUMZ - B46450
Hylopezus dives	Bocas Del Toro, Tierra Oscura	USNM - 606954
Hylopezus dives	Bocas Del Toro, Tierra Oscura	USNM - 612384
Hylopezus dives	Honduras: Gracias a Dios ; Las Marias, on Rio Platano, 25 km S Caribbean Sea	LSUMZ – 26086
Hylopezus dives	Costa Rica: Limón; Limón, Reserva Biológica Hitoy Cerere	LSUMZ – 82039
Hylopezus dilutus	Maraã, Lago Cumapi	MPEG - JAP636
Hylopezus berlepschi	Bolivia, La Paz t, Rio Beni, ca 20 km by river N. Puerto Linares	LSUMZ - B1057
Hylopezus berlepschi	Bolivia, La Paz t, Rio Beni, ca 20 km by river N. Puerto Linares	LSUMZ - B1072
Hylopezus berlepschi	Bolivia, Santa Cruz t, Velasco; Parque Nacional Noel Keonpff Mercado	LSUMZ - B18312
Hylopezus berlepschi	Peru: Madre Dios; Hacienda Amazonia	FMNH - 322345
Hylopezus berlepschi	Peru: Madre Dios; Moskitania, 13.4 km NNW of Atalaya	FMNH - 433523
Hylopezus berlepschi	Rio Juruá, Marechal Taumaturgo, Nossa Senhora Aparecida	MPEG - PNSD325
Hylopezus berlepschi	Rio Xingu, Altamira, Ilha da Taboca, UHE Belo Monte	MPEG - UHE046
Hylopezus berlepschi	Rio Xingu, margem direita, Área 1	MPEG - BMP017

Hylopezus berlepschi	Rio Xingu, margem direita, Área 1	MPEG - BMP024
Hylopezus berlepschi	Santarém, Retiro	MPEG - PIME022
Hylopezus berlepschi	Paranaíta, Rio Teles Pires, margem esquerda	MPEG - TLP(A)272
Hylopezus berlepschi	Paranaíta, margem direita Rio Paranaíta, Fazenda Paranaíta	MPEG - TLP(A)386
Hylopezus berlepschi	Município de Ourilândia do Norte	MPEG - DPN158
Hylopezus berlepschi	Peru: Ucayali ; SE slope Cerro Tahuayo, ca km ENE Pucallpa	LSUMZ – 11146
Hylopezus berlepschi	Brazil: Pará; E. bank R.Teles Pires, 4 km from the mouth of the Rio Sao benedito	LSUMZ – 35407
Hylopezus auricularis	Bolívia: Beni; Riberalta	FMNH - 391156
Hylopezus auricularis	Bolívia: Beni; Riberalta	FMNH - 391157
Hylopezus auricularis	Bolívia: Beni; Riberalta	FMNH - 391158
Grallaricula nana	Colombia: North of Santander, PNN Tamá, Orocué	LSUMZ – AMC960
Grallaricula flavirostris	Colombia: Antioquia, Anorí, Alto El Chaquiral	LSUMZ - 4774
Grallaria rufula	Peru: Cajamarca, Quebrada Lanchal, ca 8 Km ESE Sallique	LSUMZ – 32257
Grallaria ruficapilla	Colombia: Caldas; Aranzazu, Hacienda Termópilas	LSUMZ – 1666
Grallaria guatimalensis	Panama: Darien, Cana on E slope Cerro Pirré	LSUMZ – 2331

Table S3. Biogeographic regions used in the BioGeoBears analyses.

CA: Central America includes Caribbean slope from eastern Honduras, western coast of Costa Rica and Panamá;

AN: includes Northern and Central Andes Cordillera;

CH: Pacific coast of northern Ecuador and Colombia;

TE: Northwestern South America, on the Guianan Shield, between Venezuela, Colombia, Guyana, Suriname and northern Brazil, where there are sandy plateaus or Tepuis higher than 2,000 m altitude (Morrone 2014);

WA: includes Rondônia, Imeri, Napo and Negro centers of endemism (Silva et al., 2005; Borges and Silva 2012), i.e., the areas west of the Branco and Madeira rivers in Amazonia;

EA: We combined the Belém, Xingu, Tapajós and Madeira centers of endemism (Silva et al., 2005);

GS: includes north of the Amazon River, east of the Rio Branco, and east of the Orinoco River (Silva et al., 2005; Morrone 2014);

CT: Northeastern Brazil, including the states of Bahia, Ceara, Minas Gerais, and Piaui Adapted from Morrone 2014;

Table S4. Best partitioning scheme and the best-fit models selected for each partition evaluated in PartitionFinder by yhe Bayesian Information Criterion (BIC).

Subset	Best model	Subset partitions	Subset sites
1	HKY+I	FGB-I5_pos1, FGB-I5_pos2	1-556\3, 2-556\3
2	F81+I	FGB-I5_pos3	3-556\3
3	HKY+G	MUSK_pos1, MUSK_pos2	557-1139\3, 558-
4	K80+G	Musk_pos3	559-1139\3
5	GTR+I+G	ND2_pos1, ND2_pos2	1140-2180\3, 1141-
6	GTR+I+G	ND2_pos3	1142-2180\3
7	HKY+I+G	ND3_pos1, ND3_pos2	2181-2531\3, 2182-
8	GTR+G	ND3_pos3	2183-2531\3
9	HKY+I	TGFB2_pos1, TGFB2_pos2	2532-3139\3, 2533-
10	K80+G	TGFB2_pos3	2534-3139\3

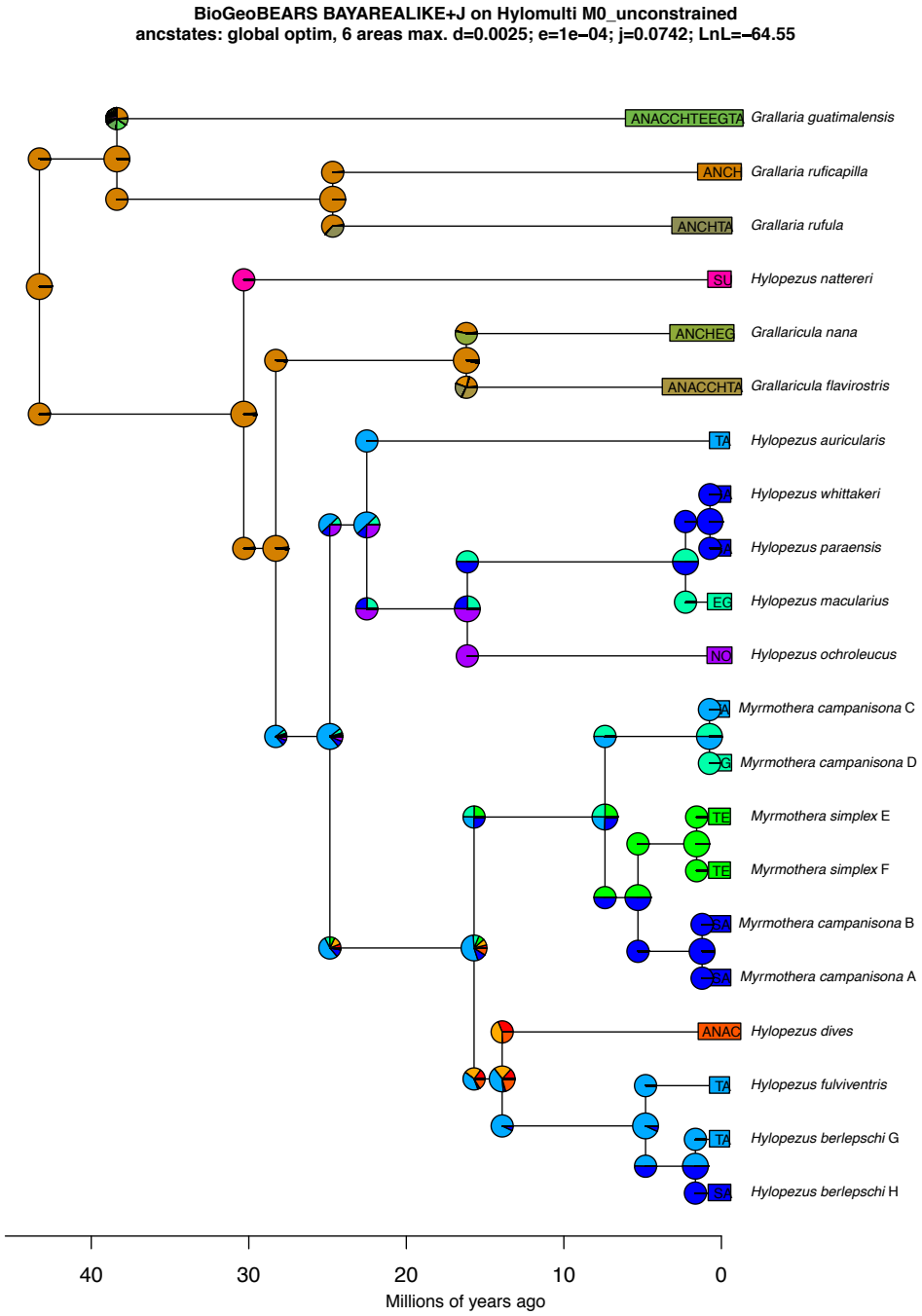

Figure S5. Time-calibrated species trees generated by BEAST and ancestral area reconstructions provided by BioGeoBEARS, both derived from the multilocus dataset. The best-fit model for our phylogenetic reconstruction was BAYAREALIKE + J (lnL = -64.55, AIC = 135.1). Node pie charts likelihoods of ancestral areas of the each node; See Appendix S3, and Figure 5 for biogeographic setting details.

REFERENCES

Antonelli, A., Nylander, J.A.A., Persson, C. & Sanmartín, I. (2009) Tracing the impact of the Andean uplift on Neotropical plant evolution. *Proceedings of National Academy of Science USA*, **106**, 9749–9754.

Antonelli, A. & Sanmartín, I. (2011) Why are there so many plant species in the Neotropics? *Taxon*, **60**, 403–414.

Avise, J.C. (2000) *Phylogeography: the history and formation of species*. Harvard University Press, Cambridge, MA.

Batalha-Filho, H., Pessoa, R.O., Fabre, P.-H., Fjeldså, J., Irestedt, M., Ericson, P.G.P., Silveira, L.F. & Miyaki, C.Y. (2014) Phylogeny and historical biogeography of gnateaters (Passeriformes, Conopophagidae) in the South America forests. *Molecular Phylogenetics and Evolution*, **79**, 422–432.

Beheregaray, L.B. (2008). Twenty years of phylogeography: the state of the field and the challenges for the Southern Hemisphere. *Mol. Ecol*. **17**, 3754–3774.

Borges, S.H. & da Silva, J.M.C. (2012) A new area of ende- mism for Amazonian birds in the Rio Negro Basin. Wilson *Journal of Ornithology*, **124**, 15–23.

Bryson, R.W. Jr, Riddle, B.R., Graham, M.R., Smith, B.T. & Prendini, L. (2012) As old as the hills: montane scorpions in southwestern North America reveal ancient associations between biotic diversification and landscape history. *PLoS ONE*, **8**, e52822.

Bryson, R.W. Jr, Chaves, J., Smith, B.T., Miller, M. J., Winker, K., Pérez-Emán. J. L. & Klicka, J. (2014) Diversification across the New World within the 'blue' cardinalids (Aves: Cardinalidae). *Journal of biogeography*, **41**, 587–599.

Burnham, R. J., & Graham, A. (1999) The history of Neotropical vegetation: new developments and status. *Annals of the Missouri Botanical Garden*, **86**, 546–589.

Cadena, C.D., López-Lanús, B., Bates, J.M., Krabbe, N., Rice, N.H., Stiles, F.G., Palacio, J.D. & Salaman, P. (2007) A rare case of interspecific hybridization in the tracheophone suboscines: Chestnut-naped Antpitta *Grallaria nuchalis* × Chestnut-

crowned Antpitta *G. ruficapilla* in a fragmented Andean landscape. *Ibis*, **149**,814–825.

Campbell K.E., Jr., Frailey, C.D. & Romero-Pittman, L. (2006) The Pan-Amazonian Ucayali Peneplain, late Neogene sedimentation in Amazonia, and the birth of the modern Amazon River system. *Palaeogeography Palaeoclimatology Palaeoecology* **239**, 166–219.

Carneiro, L. S., Gonzaga, L. P., Rêgo, P. S., Sampaio, I., Schneider, H., & Aleixo, A. (2012) Systematic revision of the spotted antpitta (Grallariidae: *Hylopezus macularius*), with description of a cryptic new species from brazilian Amazonia. *The Auk*, **129**, 338–351.

Castoe, T.A., Daza, J.M., Smith, E.N., Sasa, M.M., Kuch, U., Campbell, J.A., Chippindale, P.T. & Parkinson, C.L. (2009) Comparative phylogeography of pitvipers suggests a consensus of ancient Middle American highland biogeography. *Journal of Biogeography*, **36**, 88–103.

Chaves, J.A., Weir, J.T. & Smith, T.B. (2011) Diversification in *Adelomyia* hummingbirds follows Andean uplift. *Molecular Ecology*, **20**, 4564–4576.

Cracraft, J. & Prum, R.O. (1988) Patterns and processes of diversification: speciation and historical congruence in some Neotropical birds. *Evolution*, **42**, 603–620.

d'Horta, F.M., Cuervo, A.M., Ribas, C.C., Brumfield, R.T. & Miyaki, C.Y. (2012) Phylogeny and comparative phylogeography of *Sclerurus* (Aves: Furnariidae) reveal constant and cryptic diversification in an old radiation of rainforest understorey specialists. *Journal of Biogeography*, **40**, 37–49.

Derryberry, E.P., Claramunt, S., Derryberry, G., Chesser, R.T., Cracraft, J., Aleixo, A., Perez-Eman, J., Remsen, J.V., Jr & Brumfield, R.T. (2011) Lineage diversification and morphological evolution in a large-scale continental radiation: the Neotropical ovenbirds and woodcreepers (Aves: Furnariidae). *Evolution*, **65**, 2973–2986.

Driskell, A.C. & Christidis, L. (2004) Phylogeny and evolution of the Australo-Papuan honeyeaters (Passeriformes, Meliphagidae). *Molecular Biology and*

Evolution, **31**, 943–960.

Drummond, A.J. & Rambaut, A. (2007) BEAST: Bayesian evolutionary analysis by sampling trees. *BMC Evolutionary Biology*, **7**, 214.

Drummond, A.J., Ho, S.Y.W., Phillips, M.J. & Rambaut, A. (2006) Relaxed phylogenetics and dating with confidence. *PLoS Biology*, **4**, e88.

Drummond, A.J., Suchard, M.A., Xie, D. & Rambaut, A. (2012) Bayesian phylogenetics with BEAUti and the BEAST 1.7. *Molecular Biology and Evolution*, **29**, 1969–1973.

Edwards, S.V. & Beerli, P. (2000) Perspective: gene divergence, population divergence, and the variance in coales- cence time in phylogeographic studies. *Evolution*, **54**, 1839–1854.

Fabre, P.-H., Galewski, T., Tilak, M.-K. & Douzery, E.J.P. (2013) Diversification of South American spiny rats (Echimyidae): a multigene phylogenetic approach. *Zoologica Scripta*, **42**, 117–134.

Fernandes, A.M., Wink, M. & Aleixo, A. (2012) Phylogeography of the chestnut-tailed antbird (*Myrmeciza hemimelaena*) clarifies the role of rivers in Amazonian biogeography. *Journal of Biogeography*, **39**, 1524–1535.

Fouquet, A., Recoder, R., Teixeira Jr., M., Cassimiro, J., Amaro, R.C., Camacho, A., Damasceno, R., Carnaval, A.C., Moritz, C. & Rodrigues, M.T. (2012) Molecular phylogeny and morphometric analyses reveal deep divergence between Amazonia and Atlantic Forest species of *Dendrophryniscus*. *Molecular Phylogenetics and Evolution*, **62**, 826–838.

Graham, A. (1997) Neotropical plant dynamics during the Cenozoic-diversification, and the ordering of evolutionary and speciation processes. *Syst. Bot*. **22**, 139– 150.

Galewski, T., Mauffrey, J.F., Leite, Y.L., Patton, J.L. & Douzery, E.J. (2005) Ecomorphological diversification among South American spiny rats (Rodentia; *Echimyidae*): a phylogenetic and chronological approach. *Molecular Phylogenetics and Evolution*, **34**, 601–615.

Galvão, A. & Gonzaga, L.P. (2011) Morphological support for placement of the Wing-banded Antbird *Myrmornis torquata* in the Thamnophilidae (Passeriformes: Furnariides). *Zootaxa*, **3122**, 37–67.

Giehl, E.L.H. & Jarenkow, J.A. (2012) Niche conservatism and the differences in species richness at the transition of tropical and subtropical climates in South America. *Ecography*, **35**, 933–943.

Hackett, S.J. (1996) Molecular phylogenetics and biogeography of tanagers in the genus *Ramphocelus* (Aves). *Molecular Phylogenetics and Evolution*. **5**, 368–382.

Hafner, M.S., Sudman, P.D., Villablanca, F.X., Spradling, T.A., Demastes, J.W. & Nadler, S.A. (1994) Disparate rates of molecular evolution in the cospeciating hosts and parasites. *Science*, **265**, 1087–1090.

Hoorn, C., Wesselingh, F.P., ter Steege, H., Bermudez, M.A., Mora, A., Sevink, J., Sanmartın, I., Sanchez-Meseguer, A., Anderson, C.L., Figueiredo, J.P., Jaramillo, C., Riff, D., Negri, F.R., Hooghiemstra, H., Lundberg, J., Stadler, T., Searkinen, T. & Antonelli, A. (2010) Amazonia through time: Andean uplift, climate change, landscape evolution and biodiversity. *Science*, **330**, 927–931.

Hoorn, C., Mosbrugger, V., Mulch, A. & Antonelli, A. (2013) Biodiversity from mountain building. *Nature Geoscience*, **6**, 154.

Huelsenbeck, J.P. & Rannala, B. (2004) Frequentist properties of Bayesian posterior probabilities of phylogenetic trees under simple and complex substitution models. *Systematic Biology*, **53**, 904–913.

Insel, N., Poulsen, C. & Ehlers, T. (2009) Influence of the Andes Mountains on South American moisture transport, convection, and precipitation. *Climate Dynamics*, **35**, 1477–1492.

Kimball, R.T., Braun, E.L., Barker, F.K., Bowie, R.C.K., Braun, M.J., Chojnowski, J.L., Hackett, S.J., Han, K.L., Harshman, J., Heimer-Torres, V., Holznagel, W., Huddleston, C.J., Marks, B.D., Miglia, K.J., Moore, W.S., Reddy, S., Sheldon, F.H., Smith, J.V., Witt, C.C. & Yuri, T. (2009) A well-tested set of primers to amplify regions spread across the avian genome. *Molecular Phylogenetics and Evolution*, **50**,

654–660.

Krabbe, N., & Schulenberg, T. S. (2003) Family Rhinocryptidae (tapaculos). *Handbook of the Birds of the World 8*. (ed. By J. del Hoyo, A. Elliott and D. A. Christie), pp. 748–787. Lynx Edicions, Barcelona.

Lanfear, R., Calcott, B., Ho, S.Y.W., Guindon, S. (2012) PartitionFinder: combined selection of partitioning schemes and substitution models for phylogenetic analyses. *Mol. Biol. Evol*. **29**, 1695–1701.

Latrubesse, E.M., Cozzuol, M., Silva-Caminha, S.A.F., Rigsby, C.A., Absy, M.A. & Jaramillo, C. (2010) The late Miocene paleogeography of the Amazon Basin and the evolution of the Amazon River system. *Earth-Sciece Review*, **99**, 99–124.

Lerner, H.R.L., Meyers, M., James, H.F., Hofreiter, M. & Fleischer, R.C. (2011) Multilocus resolution of phylogeny and timescale in the extant adaptive radiation of Hawaiian honeycreepers. *Current Biology*, **21**, 1838–1844.

Lohmann, L.G., Bell, C.D., Calió, M.F. & Winkworth, R.C. (2013) Pattern and timing of biogeographical history in the Neotropical tribe Bignonieae (Bignoniaceae). *Botanical Journal of Linnean Society*, **171**, 154–170.

Lomolino, M.V., Riddle, B.R., Brown, J.H. (2006). Biogeography. Sinauer Associates, Sunderland, Mass.

Lowery, G.H., O'Neill, J.P. (1969). A new species of antpitta from Peru and a revision of the subfamily Grallariinae. *Auk*. **86**, 1–12.

Maldonado-Coelho, M., Blake, J.G., Silveira, L.F., Batalha-Filho, H. & Ricklefs, R.E. (2013) Rivers, refuges and population divergence of fire-eye antbirds (*Pyriglena*) in the Amazon Basin. *Journal Evolutionary Biology*, **26**, 1090–1107.

Matzke, N.J. (2013) Probabilistic historical biogeography: new models for founder-event speciation, imperfect detection, and fossils allow improved accuracy and model-testing. *Frontiers Biogeography*, **5**, 242–248.

Miller, M.A., Pfeiffer, W. & Schwartz, T. (2010) *Creating the CIPRES Science Gateway for inference of large phylogenetic trees. Proceedings of the Gateway*

Computing Environments Workshop (GCE 2010), pp. 1–8. Institute of Electrical and Electronics Engineers, Piscataway Township, NJ.

Minin, V., Abdo, Z., Joyce, P. & Sullivan, J. (2003) Performance-based selection of likelihood models for phylogeny estimation. *Systematics Biology*, **52**, 674–683.

Morrone J. J. (2014) Biogeographical regionalisation of the Neotropical region. *Zootaxa*. **3782**:1–110.

Moyle, R. G., Chesser, R. T., Brumfield, R. T., Tello, J. G., Marchese, D. J., & Cracraft, J. (2009) Phylogeny and Phylogenetic Classification of the Antbirds, Ovenbirds, Woodcreepers, and Allies (Aves: Passeriformes: Infraorder Furnariides). *Cladistics*, **25**, 1–5.

Nelson, G. & Platnick, N. 1980. A vicariance approach to historical biogeography. *Bioscience*, **30**, 339–343.

Ohlson J. I., M. Irestedt, P. G. P. Ericson, and J. Fjeldsa˚. (2013) Phylogeny and classification of the New World suboscines (Aves, Passeriformes). *Zootaxa*. **3613**:1–35.

Patel, S., Weckstein, J.D., Patan_e, J.S.L., Bates, J.M. & Aleixo, A. (2011) Temporal and spatial diversification of *Pteroglossus* araçaris (Aves: Ramphastidae) in the Neotropics: constant rate of diversification does not support a Pleistocene radiation. *Molecular Phylogenetics and Evolution*, **58**, 105–115.

Posada, D. (2008) jModelTest: phylogenetic model averaging. *Molecular Biology and Evolution*, **25**, 1253–1256.

Rabosky, D.L. (2006a) Likelihood methods for inferring temporal shifts in diversification rates. *Evolution*, **60**, 1152–1164.

Rabosky, D.L. (2006b) LASER: a maximum likelihood toolkit for detecting temporal shifts in diversification rates from molecular phylogenies. *Evolutionary Bioinformatics Online*, **2**, 257–260.

Rabosky, D.L. & Lovette, I.J. (2008) Density dependent diversification in North American wood warblers. *Proceedings of the Royal Society B: Biological Sciences*,

275, 2363–2371.

Rambaut, A. & Drummond, A.J. (2007) Tracer v1.5. Available at: http://beast.bio.ed.ac.uk/Tracer.

Remsen, J.V. Jr., Areta, J.I., Cadena, C.D., Jaramillo, A., Nores, M., Pacheco, J.F., Perez-Eman, J., Robbins, M.B., Stiles, F.G., Stotz, D.F. & Zimmer, K.J. (2015) A classification of the bird species of South America. *American Ornithologists' Union*. Available at: http://www.museum.lsu.edu/~Remsen/SACCBaseline.html.

Ribas, C.C., Moyle, R.G., Miyaki, C.Y. & Cracraft, J. (2007) The assembly of montane biotas: linking Andean tectonics and climatic oscillations to independent regimes of diver- sification in Pionus parrots. *Proceedings of the Royal Society B: Biological Sciences*, **274**, 2399–2408.

Ribas, C.C., Aleixo, A., Nogueira, A.C.R., Miyaki, C.Y. & Cracraft, J. (2012a) A palaeobiogeographic model for biotic diversification within Amazonia over the past three million years. *Proceedings of the Royal Society B: Biological Sciences*, **279**, 681–689.

Ribas, C.C., Maldonado, M.C., Smith, B.T., Cabanne, G.S., d'Horta, F.M. & Naka, L.N. (2012b) Towards an integrated historical biogeography of the Neotropical lowland avi- fauna: combining diversification analysis and landscape evolution. *Ornitologıa Neotropical*, **23**, 187–206.

Rice, N.H. (2005). Phylogenetic relationships of antpitta genera (Passeriformes: Formicariidae). *Auk.* **122**, 673–683.

Riddle, B.R., Dawson, M.N., Hadly, E.A., Hafner, D.J., Hickerson, M.J., Mantooth, S.J., Yoder, A.D. (2008). The role of molecular genetics in sculpting the future of integrative biogeography. *Prog. Phys. Geogr*. **32**, 173–202.

Ronquist, F., Teslenko, M., van der Mark, P., Ayres, D.L., Darling, A., Ho€hna, S., Larget, B., Liu, L., Suchard, M.A. & Huelsenbeck, J.P. (2012) MrBayes 3.2: efficient Bayesian phylogenetic inference and model choice across a large model space. *Systematic Biology*, **61**, 539–542.

Rull, V. (2008) Speciation timing and Neotropical biodiversity: the Tertiary-Quaternary debate in the light of molecular phylogenetic evidence. *Molecular Ecology*, **17**, 2722–2729.

Rull, V. (2011a) Neotropical biodiversity: timing and potential drivers. *Trends in Ecology and Evolution*, **26**, 508–513.

Rull, V. (2011b) Origins of biodiversity. *Science*, **331**, 398–399.

Silva, J.M.C., Rylands, A.B. & Fonseca, G.A.B., 2005. The Fate of the Amazonian Areas of Endemism. *Conservation Biology*, **19**, 689–694.

Simpson, G.G. (1980) *Splendid isolation: the curious history of South American mammals*. Yale University Press, New Haven, CT.

Smith, B.T. & Klicka, J. (2010) The profound influence of the Late Pliocene Panamanian uplift on the exchange, diversification, and distribution of New World birds. *Ecography*, **33**, 333–342.

Smith, B.T., Bryson, R.W., Jr, Houston, D.D. & Klicka, J. (2012) An asymmetry in niche conservatism contributes to the latitudinal species diversity gradient in New World vertebrates. *Ecology Letters*, **15**, 1318–1325.

Smith,B.T., Ribas,C.C., Whitney,B.W., Hernandez-Baños, B.E. & Klicka, J. (2013) Identifying biases at different spatial and temporal scales of diversification: an example using the Neotropical parrotlet genus Forpus. *Molecular Ecology*, **22**, 483–494.

Sorenson, M. D., Ast, J.C., Dimcheff,D.E., Yuri, T. & MinDell, D.P. (1999) Primers for a PCR-based approach to mitochondrial genome sequencing in birds and other vertebrates. *Molecular Phylogenetics and Evolution*, **12**, 105–114.

Stratford, J. A. & Stouffer, P. C. (2015) Forest fragmentation alters microhabitat availability for Neotropical terrestrial insectivorous birds. *Biological Conservation* (in press).

Wallace, A.R. (1852) On the monkeys of the Amazon. *Proceedings of the Zoological Society of London*, **20**, 107–110.

Weir, J.T. (2006) Divergent patterns of species accumulation in lowland and highland tropical birds. *Evolution*, **60**, 842–855.

Weir, J.T. & Schluter, D. (2004) Ice sheets promote speciation in boreal birds. *Proceedings of the Royal Society B: Biological Sciences*, **271**, 1881–1887.

Weir, J.T. & Price, M. (2011) Andean uplift promotes lowland speciation through vicariance and dispersal in *Dendrocincla* woodcreepers. *Molecular Ecology*, **20**, 4550– 4563.

Wesselingh, F.P., Räsänen, M.E., Irion, G., Vonhof, H.B., Kaandorp, R., Renema, W., Romero Pittman, L. & Gingras, M. (2002) Lake Pebas: a palaeoecological reconstruction of a Miocene, long-lived lake complex in western Amazonia. *Cainozoic Research*, **1**, 35–81.

Zink, R.M., Barber, B. & Klicka, J. (2004) The tempo of avian diversification during the Quaternary. *Proceedings of the Royal Society B: Biological Sciences*, **359**, 215–220.

Capítulo 2

Adaptação morfológica impulsiona a evolução vocal em 'antpittas' (Aves, Grallariidae)

"Morphological adaptation drives vocal evolution in antpittas (Aves, Grallariidae)[2]"

[2] Esse capítulo está no formato de manuscrito e será submetido ao periódico "Evolituon". O co-autor Gustavo Bravo não revisou a presente versão.

Morphological adaptation drives vocal evolution in antpittas (Aves, Grallariidae)

Lincoln Carneiro,[1,3] Gustavo Bravo[2] and Alexandre Aleixo[3]

[1]*Curso de Pós-Graduação de Zoologia, Universidade Federal do Pará–Museu Paraense Emílio Goeldi, Belém, Pará, Brazil;* [2] *Secção de Aves, Museu de Zoologia, Universidade de São Paulo (MZUSP), Caixa Postal 42.494, CEP 04218–970, São Paulo, SP, Brasil; and* [3]*Coordenação de Zoologia, Museu Paraense Emílio Goeldi, Caixa Postal 399, CEP 66040-170, Belém, Pará, Brazil.*

[4]Address correspondence to this author. E-mail: lincoln_carneiro@yahoo.com.br

ABSTRACT

Mating signals may diversify as a byproduct of morphological adaptation to habitat, potentially driving speciation. In the present study, we explored the interplay between morphological and vocal evolution in a suboscine passerine avian lineage, the antpittas (Grallaridae), using phenotypic and molecular datasets. We evaluate the effect of body size, beak morphology, and habitat on the evolution of vocal traits. Our results suggest that habitat is strongly correlated with body size, and that the latter is correlated with beak shape. Additionally, we found that lineages inhabiting 'dense forest' evolved toward larger body and beak sizes. Therefore, body size, beak morphology and habitat affect antpittas' vocalizations. More specifically, larger birds tend to produce slower-paced and lower-pitched vocalizations, and inhabit more closed forest. Thus, it is difficult to separate the effects of acoustic and morphological adaptation, since these processes seem to act in the same direction to forge antpittas' vocalizations.

Keywords: Convergent evolution, phylogenetic comparative analyses, Neotropics, suboscine birds.

INTRODUCTION

Identifying phenotypic diversity among lineages provide explanations about the evolutionary mechanisms that generate the different patterns of variation. Similarity that occurs across lineages that have a relatively recent common ancestor is often described as phylogenetic niche conservatism (PNC; Losos 2008; Wiens et al. 2010; Crisp and Cook 2012; Smith et al. 2012), However, when distantly related taxa evolve independently to become more similar to each other, the pattern is attributed to convergent evolution (Stayton 2006; Losos 2011). Therefore, distinguishing PNC from convergent evolution, as well as identifying the driving forces behind them represents a fundamental step toward understanding the mechanisms underlying phenotypic diversity (Bravo et al. 2014).

Phylogenetic comparative methods can be used to quantify the degree of ecological and phenotypic similarity among related species while accounting for phylogenetic relatedness; this allows distinguishing ancestral from derived similarity and identifying potential routes to the latter (e.g., Stayton 2006; Revell et al. 2007; Sidlauskas 2008). Phylogenetic comparative methods do not only represent a powerful quantitative tool to test whether such similarity is consistent with PNC or convergent evolution, but they also offer the possibility of revealing the potential role of natural selection and adaptation in driving phenotypic evolution among close relatives (Cooper et al. 2010).

To assess the phenotypic diversity within Hylopezus and Myrmothera genera (Grallariidae), we integrate a comprehensive molecular phylogeny (including *Hylopezus*, *Myrmothera* and *Grallaricula* genera) with acoustic, morphometric and ecological data within a comparative approach. Because morphological and acoustic traits can be subject to different evolutionary processes (Seddon 2005; Mason et al. 2015), we take into account variation in body size, body shape, frequency and temporal measures of vocalizations, to identify potential mechanisms of evolution for each character. Also, we considered ecological correlates of phenotypic similarity to assess their importance in explaining phenotypic diversification in antpittas.

The components of ecomorphological variation in birds have been addressed in various studies from a morphologic (Schulenberg 1983; Fitzpatrick 1985; Miles and

Ricklefs 1984; Bravo et al. 2014), acoustic (e.g., Baptista and Trail 1992; Price 2008; Tietze et al. 2015), and a combined perspective (Seddon 2005; Derryberry et al. 2012; Mason et al. 2015). Strong correlations between ecology, morphology and acoustic traits have been reported.

Divergence of mating signals are suggested to lead to reproductive isolation, and hence to speciation (West-Eberhard 1983; Panhuis et al. 2001). However, the processes by which populations diverge are far from understood (Wells and Henry 1998; Boughman 2002). Divergence may be result of divergent ecological adaptation (Dobzhansky 1951; Mayr 1963), maybe as a by-product of morphological adaptation (Podos 2001) or else by direct adaptation to the signaling environment (Boughman 2002). Adaptation to divergent ecologies can affect song structure indirectly when there is selection for changes in phenotypic traits, which are functionally related to sound production, such as body size or beak. For example, body mass has a strong negative relationship with song frequency in many avian lineages (Ryan and Brenowitz 1985; Badyaev and Leaf 1997; Palacios and Tubaro 2000; Seddon 2005).

Despite these findings, ecological adaptation only explains a small proportion of the variation in song structure (Badyaev and Leaf 1997; Buskirk 1997). Furthermore, this approach is insufficient to explain the song similarity among closely related species with differing ecologies (Ryan and Brenowitz 1985), or the pronounced differences in the songs of cryptic species with similar ecological requirements (e.g., *Phylloscopus* warblers: Irwin et al. 2001 and Tietze et al. 2015; tyrant flycatchers: Zimmer et al. 2001, Hylopezus complex: Carneiro et al. 2012).

In view of this we carried out a comparative analysis examining the factors affecting song diversification in antpittas, including ecological, morphological and acoustical traits. Antpittas are ideal subjects for this type of analysis because, as suboscines, song development is not thought to be dependent on learning (Isler et al. 1998) and thus is presumably unaffected by the confounding influence of cultural evolution. Furthermore, many species have weakly differentiated plumages and all species live in habitats with poor light conditions, therefore increasing the reliance on acoustic signals.

In this study, the following questions were addressed: (i) is there any correlation

between morphological and acoustical (frequency and temporal measures) traits in antpittas?; (ii) are vocal characters (particularly frequency parameters) influenced by habitat choice in antpittas?; (iii) are loudsongs of closely related sympatric species more divergent from each other than those of closely related species living in allopatry?

MATERIALS AND METHODS

Study Species

The *Hylopezus* / *Myrmothera* clade in Grallariidae (Carneiro *et al*. unpubl. ms. Chapter 1) includes small to medium-sized sedentary insectivore birds that inhabit forest, montane forest, bamboo, deciduous and *caatinga* woodland, and scrub; they occur throughout the Neotropics but are largely confined to the lowlands (Krabbe and Schulenberg, 2003). Antpittas in general seem to be morphologically conserved, but genetically and vocally diverse (Carneiro et al. 2012). A loud and distinctive song consisting of multiple notes delivered in a stereotyped pattern, define antpittas's vocalization. These vocalizations have been called ''loudsongs'' (sensu Willis 1967; Seddon 2005; Carneiro et al. 2012), because they differ from the traditional definition of song, i.e. complex male vocalizations used in mate advertisement (Catchpole and Slater 1995), although they are probably functionally analogous (Seddon 2005). Loudsongs are assumed to be entirely innate in the antpittas, give their close relationship to another suboscine family, the antbirds (Thamnophilidae) for which evidence of innate vocalizations were recentely provide (Touchton et al. 2014).

Molecular data

To recover the phylogenetic relationships within the *Hylopezus* / *Myrmothera* clade, we analyzed 139 samples of the ingroup (77 *Hylopezus* and 62 *Myrmothera*) from throughout their distributions (Figs 1 and 2, and see Table S1 in supplementary material). Our sampling spanned the geographical distributions and several populations of all 12 currently recognized species within these genera (Krabbe and Schulenberg, 2003; Carneiro et al. 2011). We included in our analyses species of the two other genera of the Grallariidae family, *Grallaricula* and *Grallaria*, as outgroups, representing all currently recognized genera in the family (Krabbe and Schulenberg, 2003; Rice, 2005).

Total genomic DNA was extracted using a DNeasy tissue extraction kit (Qiagen, Valencia, CA, USA). For most samples, we sequenced the mitochondrial genes – NADH dehydrogenase subunit 2 (ND2), (1041 base pairs, bp), and NADH dehydrogenase subunit 3 (ND3), 351 bp; representing the main lineages inferred from our complete mtDNA data (see below). We also sequenced three nuclear introns – transforming growth factor beta 2 intron 5 (TGFB2), 625 bp; the 3rd intron of the Z-linked muscle-specific kinase (MUSK), 582 bp; and 549 bp of beta-fibrinogen intron 5 (FGB-I5). PCR conditions, amplification and sequencing reactions following (Carneiro et al. unpubl. ms. Chapter 1)**.**

Electropherograms were inspected, assembled in contigs and edited in Geneious 7.1.5 (Biomatters, www.geneious.com). Heterozygous sites were coded according to IUPAC code when double peaks were present in both strands of the same individual's electropherograms. Sequences were aligned using MAFFT using the default parameters, and further inspected and corrected visually.

Phylogeographical estimation

To assess the genetic structure and delimitate geographical lineages, we generated a multilocus phylogeny including all individuals sampled (n = 144 including outgroups) using Bayesian inference (BI) on MrBayes 3.2.1 (Ronquist et al. 2012). Lineages were defined as genetically distinct geographical clusters with strong support values (≥ 0.95 Bayesian posterior probability; Huelsenbeck and Rannala, 2004; Bryson et al. 2014). Single divergent samples from unique geographical areas were also referred to as lineages for convenience. The evolutionary models were selected with PartitionFinderV1.1.1 (Lanfear et al. 2012) using the Bayesian information criterion (BIC) (Minin et al. 2003; Posada, 2008). The optimal partition scheme and substitution models for our dataset were chosen based on comparisons limited to following schemes: (i) data combined into a single partition; (ii) mitochondrial and nuclear loci analyzed separately; (iii) genes analyzed separately; (iv) 1st and 2nd codon positions analyzed separately from 3rd codon positions; (v) all codon analyzed separately.

Two independent runs of 20 million generations with four chains of Markov chain Monte Carlo (MCMC) each were performed, and trees were sampled every 1000

generations. Output parameters were visualized using Tracer 1.6 (Rambaut and Drummond, 2007) to ascertain stationarity and convergence (Effective Sample Size – ESS values > 200). The first 25% of generations were discarded as burn-in. MrBayes analyses were carried out in the CIPRES Science Gateway (Miller et al. 2010).

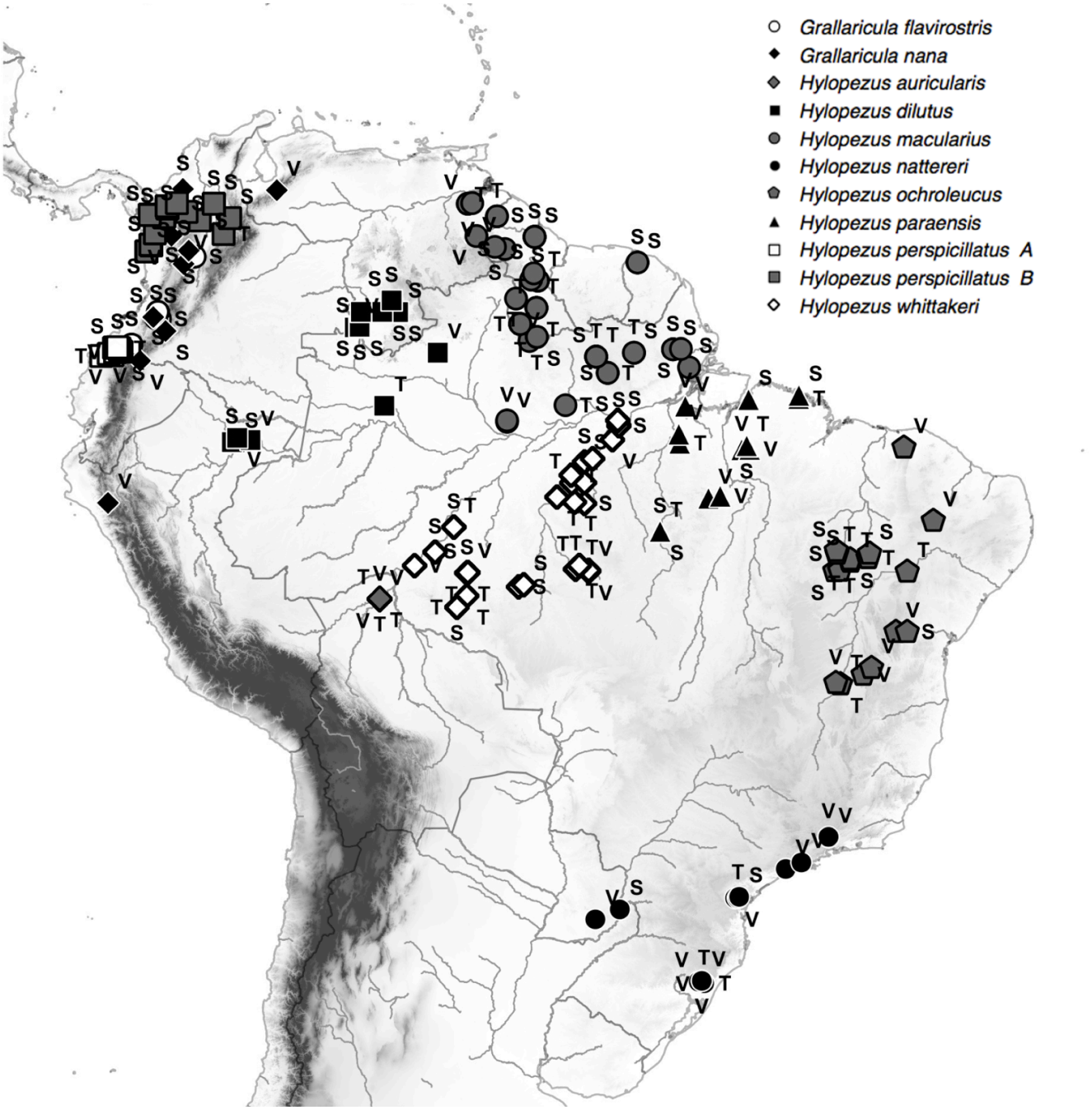

Figure. 1. Geographic distribution of specimens, vocalizations, and tissues of the 'core *Hylopezus*' clade and *Grallaricula* taxa analyzed in the present study. For nomenclature details see (Carneiro et al. unpubl. ms. Chapter 1). Letters next to a symbol represent materials available for that given locality: S = skins; V = vocalizations; T = tissues. Additional locality data can be found in Appendix S1.

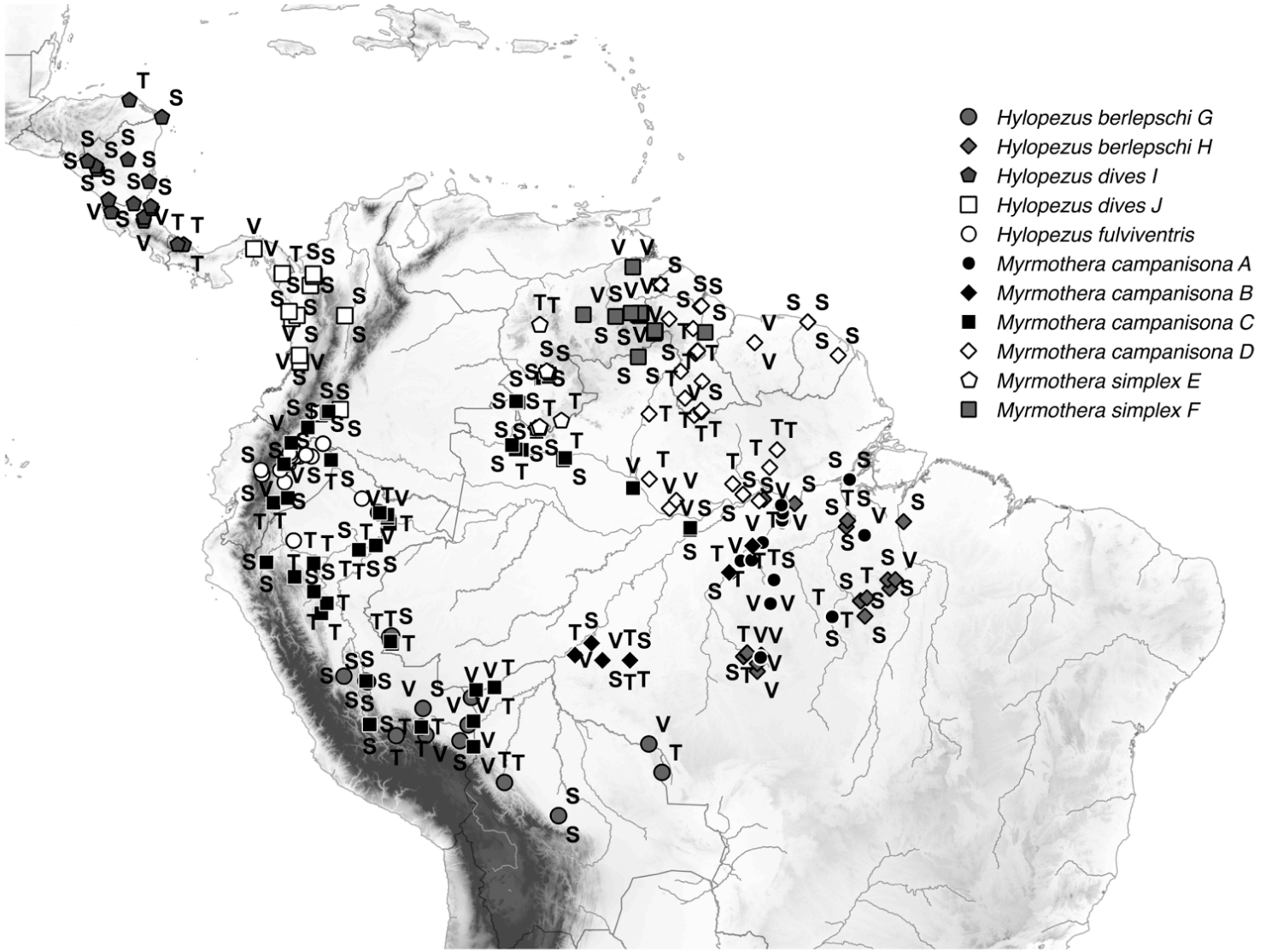

Figure. 2. Geographic distribution of specimens, vocalizations, and tissues of members of the "extended *Myrmothera*" clade analyzed in the present study. For nomenclature details see (Carneiro et al. unpubl. ms. Chapter 1). Letters next to a symbol represent materials available for that given locality: S = skins; V = vocalizations; T = tissues. Additional locality data can be found in Appendix S1.

Morphological data

We examined 327 study skins, belonging to all lineages of the *Hylopezus* / *Myrmothera* clade recovered by our phylogeographic estimation, except *Hylopezus auricularis*, excluded from all morphological analyses due to the lack of available specimens. For comparative purposes, we also examined skins of two *Grallaricula* species, recovered as the outgroup to the *Hylopezus* / *Myrmothera* clade (Carneiro et al. unpubl. ms. Chapter 1). Measurements of the following six morphological characters, representing size and shape, were taken to the nearest 0.1 mm with an electronic caliper: wing length, tail length, tarsus length, bill length from the distal points of the nostrils to the tip of the bill, bill depth, and width at the distal point of the nostrils.

To assess the morphological constraints, we quantified the size and shape components of variation within the group (i.e. all species included in the phylogenetic tree). A vector and a matrix describing size and shape variation, respectively, were estimated from the log-transformed averaged dataset following the approach described by Mosimann (1970) and Mosimann and James (1979). The size of each species is the mean of the six log-transformed morphological variables of the species, adapted from Bravo et al. (2014). We used the size vector as a proxy for body size.

The shape vector for each species was calculated by subtracting the size of the species from each trait (Mosimann 1970; Mosimann and James 1979). Because values of size and shape do not depend on inferences based on phylogenetic relatedness and values for other taxa, size and shape quantification do not require accounting for phylogenetic independence or explicit incorporation for phylogeny (Claramunt 2010; Bravo et al. 2014).

To assess beak variation potentially associated with mechanical patterns of song production, we multiplied bill length, depth, and width, which approximates to bill volume, and then used the logarithm as an overall measure of beak, following the method proposed by Derryberry et al.(2012). To minimize measurement errors, only one person (L. Carneiro) took all measurements.

Acoustic data

We analyzed 129 different recordings, from 95 localities throughout the Neotropics, belonging to all currently recognized species of *Hylopezus* and *Myrmothera*, except for a few lineages (see below). For comparative purposes, we also examined recordings of *Grallaricula nana*, recovered as the outgroup to the *Hylopezus* / *Myrmothera* clade (Carneiro et al. unpubl. ms. Chapter 1). The vocalizations are deposited in the following archives: MLS = Macaulay Library of Natural Sounds, Cornell Laboratory of Ornithology, Ithaca, New York; XC = Xeno-canto (www.xenocanto.org/), and PAC = Personal archives (Table S1).

Three lineages recovered in the phylogeographic analyses were not included in the bioacoustics analysis, as follows: *Grallariculla flavirostris* (which has a loudsong with less than three notes, precluding the measurement of some acoustic variables) and *H. perspicillatus* B and *M. simplex* E due to the lack of available vocalizations (To population details see results). The remaining 19 lineages were compared using the 14 acoustic measures described below (Fig. 3; Table 1). The number of notes per loudsong and pace (Number of notes per second) were square-root transformed; all other loudsong were log-transformed prior to analysis. For each species, only one loudsong per individual was used in the analyses, to avoid pseudoreplication. Songs measurements were made using spectrograms and refer to the fundamental harmonic, which in all vocalizations analyzed was also the dominant one. Spectrograms were produced from all recordings and their structure was quantified using a variety of standard time and frequency measurements, following the method proposed by Seddon (2005) (for details see Fig. 3; Table 1). Spectrograms and all song measurements were carried out using RAVEN PRO, version 1.5 (Cornell Laboratory of Ornithology, Ithaca, New York). Spectrograms were produced using the following settings in RAVEN (Window type: Hamming; window size: 1.300 samples; time grid: 95% overlap; and DFT size: 32.768 samples), when necessary; background noise was removed through lowpass and highpass filtering.

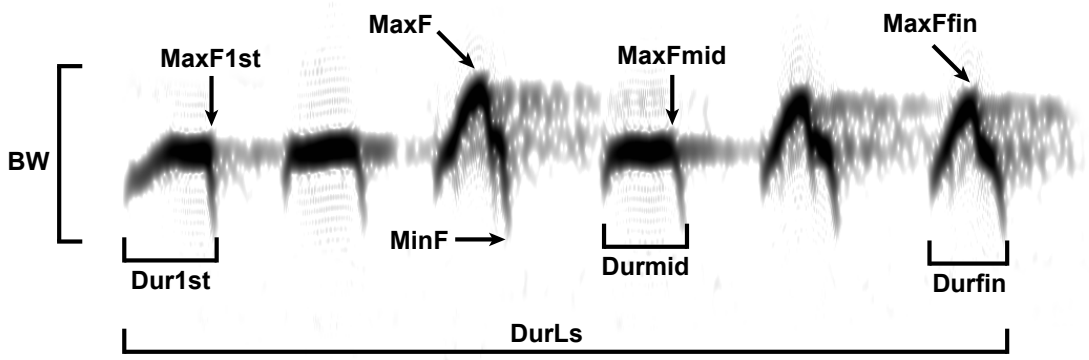

Figure. 3. Annotated spectrogram of the Spotted Antpitta *Hylopezus macularius*, loudsong (Guyana, Rupununi; MLS 73054). Loudsong structure was quantified by adaptation of the method proposed by Seddon (2005).

Phylogenetic principal component analysis

To asses the evolution of morphological and bioacustics characters throughout the phylogeny we used the Phylogenetic Principal Component Analysis (hereafter pPCA; Jombart et al. 2010b). It was implemented using the R package 'adephylo' (Jombart et al. 2010a), as described by Jombart et al. (2010b). pPCA is designed to investigate phylogenetic patterns in sets of quantitative traits. The analysis returns principal components maximizing the product of variance of the scores and their phylogenetic autocorrelation (Moran's I), therefore reflecting life histories that are phylogenetically structured.

The method describes the multivariate patterns and processes involved in the changes of continuous characters, distinguishing between combinations of characters that show a positive phylogenetic autocorrelation (global patterns) from those that appear to change independently from a shared evolutionary history, with a negative phylogenetic autocorrelation (local patterns; Webster et al. 2012).

To calculate phylogenetic proximities, we used the modification of Abouheifs proximity, as proposed by Jombart et al. (2010b). For this metric, using the non-

ultrametric Bayesian tree resulted in a matrix of phylogenetic proximities. We then investigated phylogenetic structures inspecting the eigenvalues and the phylogenetic autocorrelations of the traits using pPCA.

Because of correlations among traits dimensions we used phylogenetic principal components from pPCA to reduce the morphologic and acoustic datasets into a small number of mutually independent variables. For acoustic measures, two independent pPCA were performed, one only with frequency related variables, and other only with temporal features (Table 1). We assessed normality of morphometric and acoustic data with Kolmogorov-Smirnov tests and combined both sexes in the analyses because there was no evidence of sexual dimorphism for any character. In all tests, statistical significance was accepted at $P \leq 0.05$.

Habitat Designations

To evaluate the habitat effects on antpittas' loudsong structure, we separate the lineages in two habitat groups: 'primary' (Dense upland forest) and 'secondary' (more disturbed or less structured forest habitats, including montane forest, bamboo, deciduous and *caatinga* woodland). To assign species to different habitat types we used Krabbe and Schulenberg (2003) and our own field experience. We use these species categories to implement phylogenetic general linear models (pGLS) and investigate the effects of habitat, morphology, and their interactions on antpittas loudsong structure. Habitat designations for each lineage included in this study are available through the supporting information (Table S2).

Comparative analysis

Testing for phylogenetic signal was conducted for all measure variables (Table 1). The strength of phylogenetic signal was inferred using the K statistic, Blomberg's K is a measure of signal strength where K = 0 means a random distribution (i.e. no signal, total phylogenetic independence) and K = 1 a character state distribution as expected under a Brownian motion model of evolution (i.e. strong phylogenetic signal), while K values greater than 1 indicate strong phylogenetic signal and conservatism of traits (Blomberg et al. 2003). This analysis was carried out in R (package phytools v1.6-1, Revell, L. J. 2012).

To test whether mechanisms consistent with adaptive evolution have produced phenotypic divergence over time, we followed a model-based approach (Anderson 2008) that assessed which models of phenotypic evolution provide a better fit to the phenotypic data given the phylogeny. We evaluated four models that have different implications for understanding the mechanisms generating phenotypic diversity, as follows: 1) BM —The Brownian motion is a model proposed by Felsenstein (1973), which assumes that the correlation structure among trait values is proportional to the extent of shared ancestry for pairs of species; 2) OU— the Ornstein-Uhlenbeck model (Butler and King 2004), which fits a random walk with a central tendency and attraction strength proportional to the parameter α, where α represents the rate of adaptation to optima (Ingram and Mahler, 2013); 3) EB — the Early-burst model (Harmon et al. 2010) also called the ACDC model (accelerating- decelerating; Blomberg et al. 2003). Set by the a rate parameter, EB fits a model where the rate of evolution increases or decreases exponentially through time; and finally 4) White — the white-noise (non-phylogenetic) model, which assumes the data come from a single normal distribution with no covariance structure among species, and is sometimes associated to neutral evolution (Hunt 2006; Estes and Arnold 2007). These four models provide opportunities for finding patterns that are consistent with a role of adaptive processes in driving ecomorphological evolution (Bravo et al. 2014).

We also calculated Pagel's lambda and tested each variable for the best evolutionary model given the phylogeny by choosing the model through the lowest AICc (sample size-corrected Akaike information criterion) value out of Brownian motion, Ornstein–Uhlenbeck, early-burst, and white-noise (nonphylogenetic) models (R package geiger v2.0.3, Harmon et al. 2008).

As related taxa tend to resemble each other, it cannot a priori be assumed independence between the tips of the tree. However, traits under correlated evolution should hold when phylogenetic information is incorporated using independent contrasts (Felsenstein 1985; Harvey and Pagel 1991). To address this problem, the caper package (R package caper, Orme et al. 2012) implements the methods originally provided in the programs CAIC (Purvis and Rambaut, 1995) and MacroCAIC (Agapow and Isaac, 2002). These two programs calculate phylogenetic independent contrasts in a set of variables and then use linear models of those

contrasts to test for evolutionary relationships.

In order to correlate bioacoustic measures with morphological traits and ecological data, phylogenetic generalized linear models were formulated in R (pGLS; R package caper, Orme et al. 2012). Correlations were performed between several pairs of traits; habitat, song and morphological variables as well as their respective pPCA's were compared.

Vocal recognition and character displacement

To test whether sympatry promote vocal character displacement driven by competition and how it affects vocal recgnition, we adapted the method proposed by Seddon (2005), and analyzed 14 species that had both a close relative in sympatry and one in allopatry (Table S3, Appendix). Allopatric species were defined as those with mutually exclusive distribution ranges, whereas sympatric species were those that overlapped their ranges by at least 50%. All species compared occurred in the same vegetation stratum and within similar habitats, therefore minimizing the influence of habitat-dependent selection, and maximizing the likelihood that defined sympatric species are in direct contact (Seddon, 2005). When more than one closely related species from a suitable habitat occurred allopatrically or sympatrically, we tested all possible combinations. The 14 separate acoustic measurements were taken from spectrograms comprising three or more notes. Loudsong divergence between species pairs was quantified first using separate acoustic measurements and then using the first principal components (pPCA) derived from frequency and temporal variables separately (Tables 1 and 2). Finally, to assess whether any loudsong divergence in sympatry was accompanied by parallel changes in morphology, we compared the body size and beak morphology of sympatric and allopatric species pairs.

In all cases, we subtracted 'pair-members' loudsong values from one another and then used paired tests (Wilcoxon signed-rank) to examine whether the difference in loudsong structure across all the trios, morphological measures, and pPCA values, was greater between sympatric than allopatric species pairs.

Testing for convergent evolution

We used the SURFACE package (Ingram and Mahler 2013) implemented in R, to test whether acoustic and morphological similarities within the antpittas might be attributed to convergent evolution. SURFACE uses stepwise Akaike Information Criterion first to locate regime shifts on a tree, then to identify whether shifts are towards convergent regimes (Ingram and Mahler 2013). The model selection procedure starts with only one adaptive regime and then increases the number of peaks in a stepwise fashion. To detect convergent adaptive peaks, SURFACE tests whether corrected AIC (AICc) values improve as it allows collapsing compatible adaptive regimes found in different branches. Therefore, it assumes that all clades of the tree can be evolving around different optima (i.e. adaptive regimes) under an Ornstein-Uhlenbeck (OU) process, allowing the identification of those clades that are convergent (Bravo et al. 2014).

We ran SURFACE using the morphological and acoustic traits pointed by pPCA as that best describes each character, and as the method assumes that traits have independent rates of adaptation and diffusion. If some traits show strong evolutionary correlations to each other on the pPCA, only one was used.

Evolution over time

To evaluate the rate of morphological and acoustic evolution in relation to lineage diversification, we conducted disparity-through-time analyses (DTT; Harmon et al. 2003), as implemented in the Geiger package v.1.3 (Harmon et al. 2008) in R. In this analyses, the observed average phenotypic disparity was compared to that expected according to a pure Brownian motion (BM) model (Harmon et al. 2003, 2008), and the difference was quantified by the morphological disparity index (MDI).

Negative MDI values are generally interpreted as evidence for an early burst in trait evolution, supporting the adaptive character of the diversification process in this clade (Harmon et al. 2010; Slater et al. 2010). Positive MDI values should represent traits or

clades that accumulated disparity during their recent history (Bravo et al. 2014). We compared observed relative disparity with the mean expectation of 10.000 simulations under Brownian motion. We adopted this method to measure acoustic data disparity, once the acoustic data are continuous and meets the test requirements.

To perform DTT analyses, we used a time-calibrated tree (Carneiro et al. unpubl. ms. Chapter 1) pruned using the ape package v.2.3 (Paradis et al. 2004) in R, and only the lineages available to morphological and acoustic data were sustained. Morphological (size and shape) and acoustic traits (frequency and temporal variables) were carried out in DTT analysis.

RESULTS

Phylogenetic tree

The phylogenetic analyses based on Bayesian methods recovered 20 evolutionary lineages within the *Hylopezus* / *Myrmothera* clade, distributed in two major clades and one separate lineage with a single member, *H. nattereri* (Fig. 1 and 2 in Carneiro et al. unpubl. ms. Chapter 1). This topology corroborates previous results showing *Hylopezus* as a polyphyletic genus (Carneiro et al. unpubl. ms. Chapter 1). Support for each one of the two major sub-clades within the *Hylopezus* / *Myrmothera* clade was strong (PP = 1). Furthermore, *H. nattereri* was recovered as a distinct lineage of uncertain basal relationships, but within a monophyletic group that also includes the *Hylopezus* / *Myrmothera* clade and the *Grallaricula* genus (PP = 1). The taxonomic implications of these findings will be discussed elsewhere (Carneiro et al. unpub. ms. Chapter 3).

We also found deep divergences between some populations, and most of them represent geographically isolated lineages, which were included in our morphological and acoustical analyses: *H. perspicillatus* (lineages A and B); *M. campanisona* (lineages A, B, C and D); *M. simplex* (lineages E and F); *H. berlepschi* (lineage G and H); *H. dives* (lineages I and J). The complete bayesian phylogeny was pruned using the ape package v.2.3 (Paradis et al. 2004) in R, and only one specimen per lineage was kept. To avoid underestimating the phenotypic diversity of the ingroup lineages or introducing some bias in the analyzes, the outgroup *Grallaria* was not included in our phenotypic analyses due also to the small number of taxa sampled compared to

the real diversity of the genus.

Phylogenetic principal component analysis

Size and shape pPCA

In the morphological pPCA, on size corrected variables and size vector, only the first global principal component was retained. This PC explained 58.4% of variation in the variables, and demonstrates a positive phylogenetic autocorrelation (Moran's I = 0.62; Jombart et al. 2010b). Most of the morphological changes detected were associated with size vector and wing shape (Fig. 4). Evaluating the trait loadings reveals that this PC has a strong positive loading of size and strong negative loading of wing morphology (Fig. 5). The high phylogenetic autocorrelation for this PC is indicative of trait patterns gradually changing with phylogenetic distance.

Inspecting the size vector and shape wing on the phylogeny demonstrates morphological consistency within some lineages (Fig. 4), however there are indications of morphological variation associated with the environment, since taxa of analogous habitats ('primary'; Dense forest or 'secondary'; Less structured forest habitats) were more similar to each other than expected by the phylogeny (Table S2).

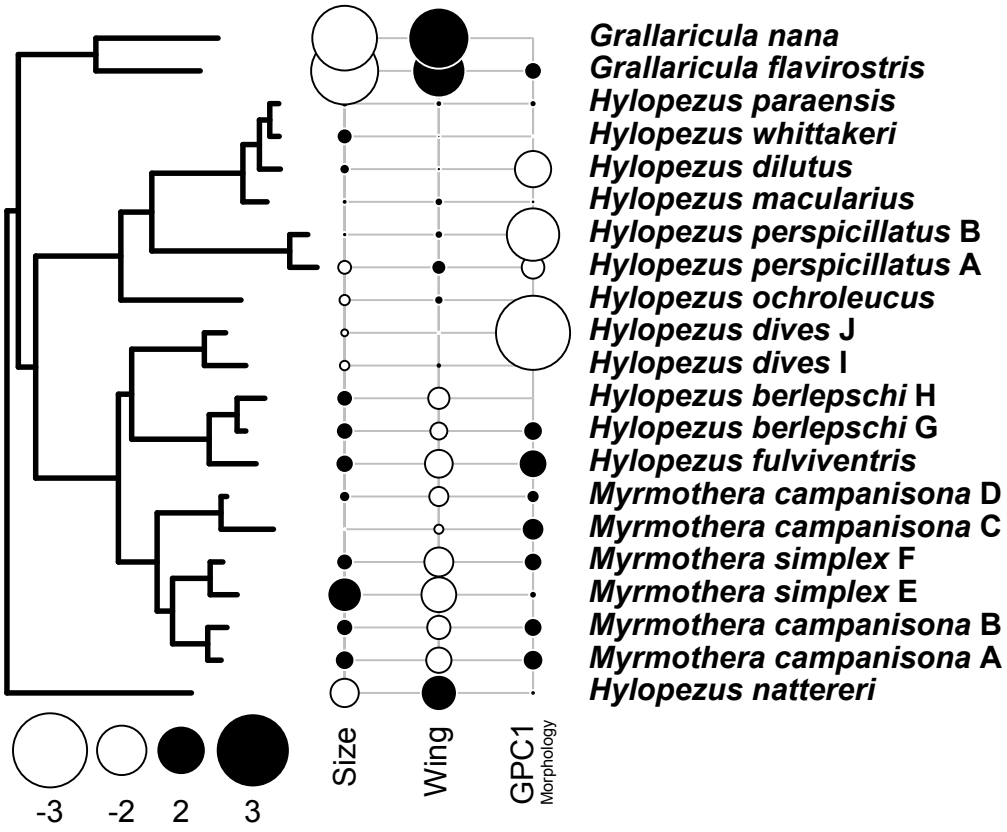

Figure. 4. Traits that contribute strongly with the first PC score for the morphological data. Black circles are positive scores and white circles are negative scores. Size of the circles indicates magnitude of the score. GPC1: The First global component from the morphological pPCA.

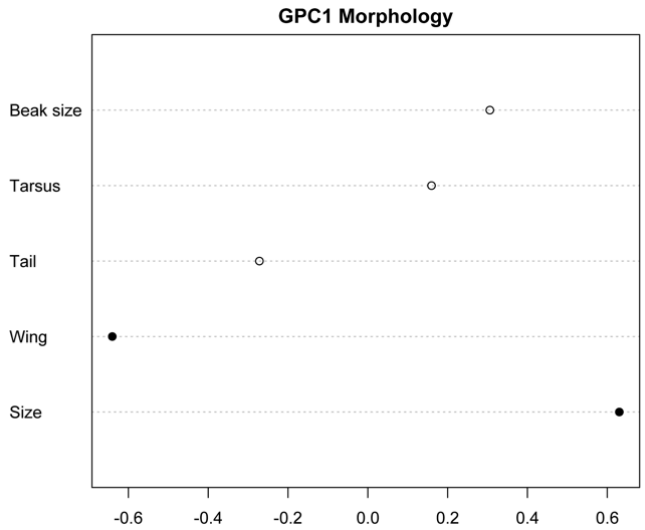

Figure. 5. Contributions to the morphology retained PC, showing direction and weight

for each character. Black dots represent characters that contribute strongly to each PC.

Acoustic pPCA

In the acoustic pPCAs, on frequency-related variables, two global principal components were selected (Fig. 6). The first global PC explained 88.1% of variation in the frequency traits and had a positive phylogenetic autocorrelation (Moran's I = 0.44). Most of these frequency variations were associated with strong negative loading of the maximum frequency variables ("MaxFfin"; "MaxFpen"; "MaxFmid"; "MaxF"), which seem by the loadings inspection, closely related (Fig. 7). The second global PC explained 10,8% of frequency variation. Inspecting the trait loadings reveals that this PC has a strong positive loading to "MinF" and "PeakFreq" and a strong negative loading of "BW" (Fig. 7); the phylogenetic autocorrelation for this PC is I = 0.20.

On time-related data, again two principal components were retained, however, in this case, one global and one local. The first, global PC, represents 69.5% of total PC variation, and it has a positive phylogenetic autocorrelation of I = 0.30. This PC has a strong positive relation to "Dur1st" and a strong negative loading of "Pace" (Fig. 7). The second shape PC represents 21.4% of total variation and had a negative autocorrelation of I = - 0.18; the time variation was negatively related to "Dur1st" and strongly positive related to "Dur" (Fig. 7).

Mapping PCs on the phylogeny demonstrates some acoustic consistency, especially within minor closely related groups, such as in *Myrmothera* (Fig. 6). However, the major acoustic pattern cannot be explained only by phylogenetic relationships (Fig. 6), as demonstrated by the moderate indices of phylogenetic autocorrelation of the PCs (Moran's I).

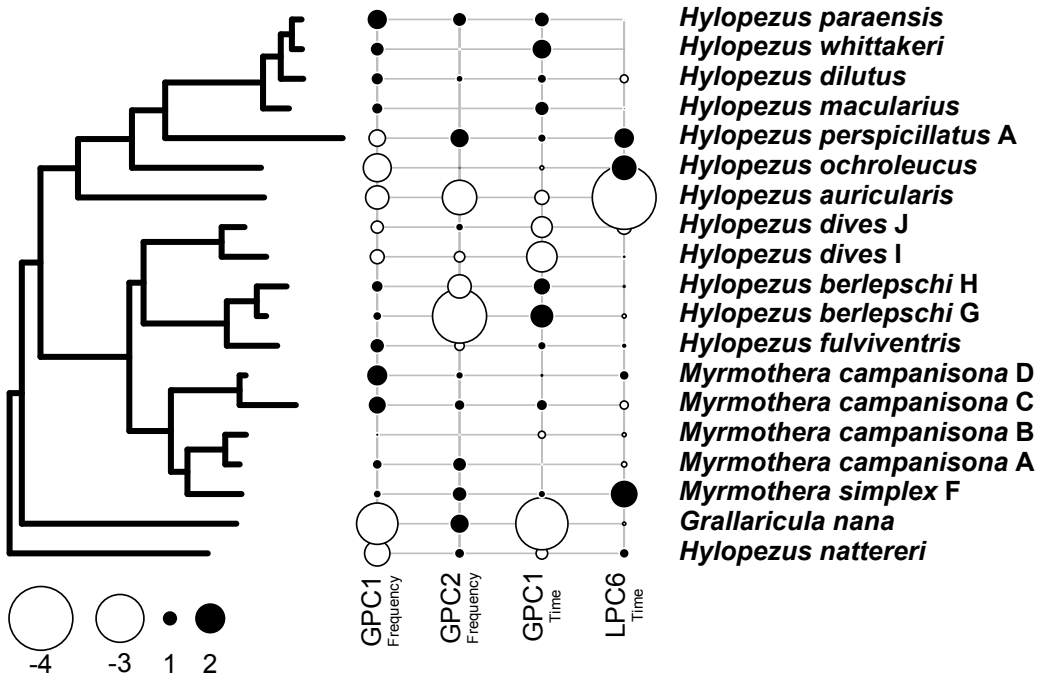

Figure. 6. Scores for each taxon for the four acoustic PCs. Black circles are positive scores and white circles are negative scores. Size of the circles indicates magnitude of the score. GPC1 and GPC2 (Frequency): The First and second global components from the frequency pPCA. GPC1 and LPC6 (Time): The First global and the sixth local components from the time pPCA.

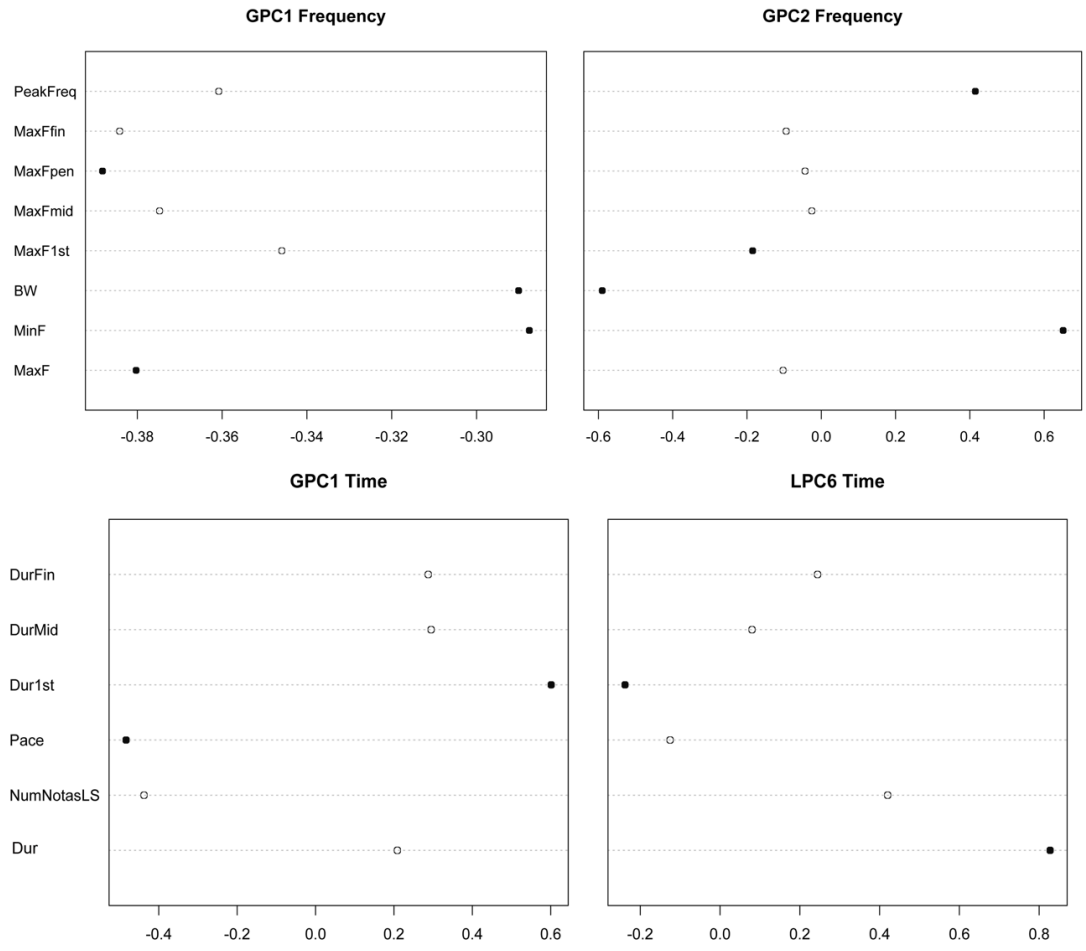

Figure. 7. Contributions to acoustic examined PCs, showing direction and weight for each character. Black dots represent characters that contribute strongly to each PC.

Comparative analyses

The phylogenetic signal for measured traits varied with Blomberg's K between slightly over 0.3 and more than 2.3 (Table 1). The higher phylogenetic signals (Blomberg's K: 0.9 - 2.3) were detected for the morphological measurements. These values indicate strong phylogenetic signal and conservatism of traits (Blomberg et al. 2003). A strong phylogenetic signal was also found for all vocal frequency parameters, except bandwidth and GPC2 frequency, whereas for temporal parameters, a moderate signal was found (Blomberg's K: 0.3 – 0.8). The pagel's λ was highly correlated with K values (Table 1), and the values were closer to 1 except for LPC6time, since local PCs has, by definition, a negative phylogenetic autocorrelation (Jombart et al. 2010b). Almost all traits evolved under the Ornstein–Uhlenbeck model

(or Brownian motion) model, and only the GPC2 frequency and the LPC6time evolved under a White Noise model (Table 1).

We found a negative correlation between body size and wing length, and a positive relationship between body size and beak (Fig. 8A and B; Table 3). Body size was furthermore negatively correlated with general frequency parameters of song (MaxF, MinF, peak frequency and with the GPC1Frequency; Table 3), and significantly associated with two temporal measures, negatively to pace and positively with GPC1time. This indicates that larger species tend to perform loudgsongs with lower frequencies and delivery a smaller number of notes per second (Table 3; Fig. 8).

The explanatory variable, habitat, was correlated with 11 parameters, including eight related to frequency (MaxF, MinF, MaxF1st, MaxFmid, MaxFpen, MaxFfin, PeakFreq and GPC1Freq), two related to morphology (size and wing), and one associated with time (GPC1time; Table 3).

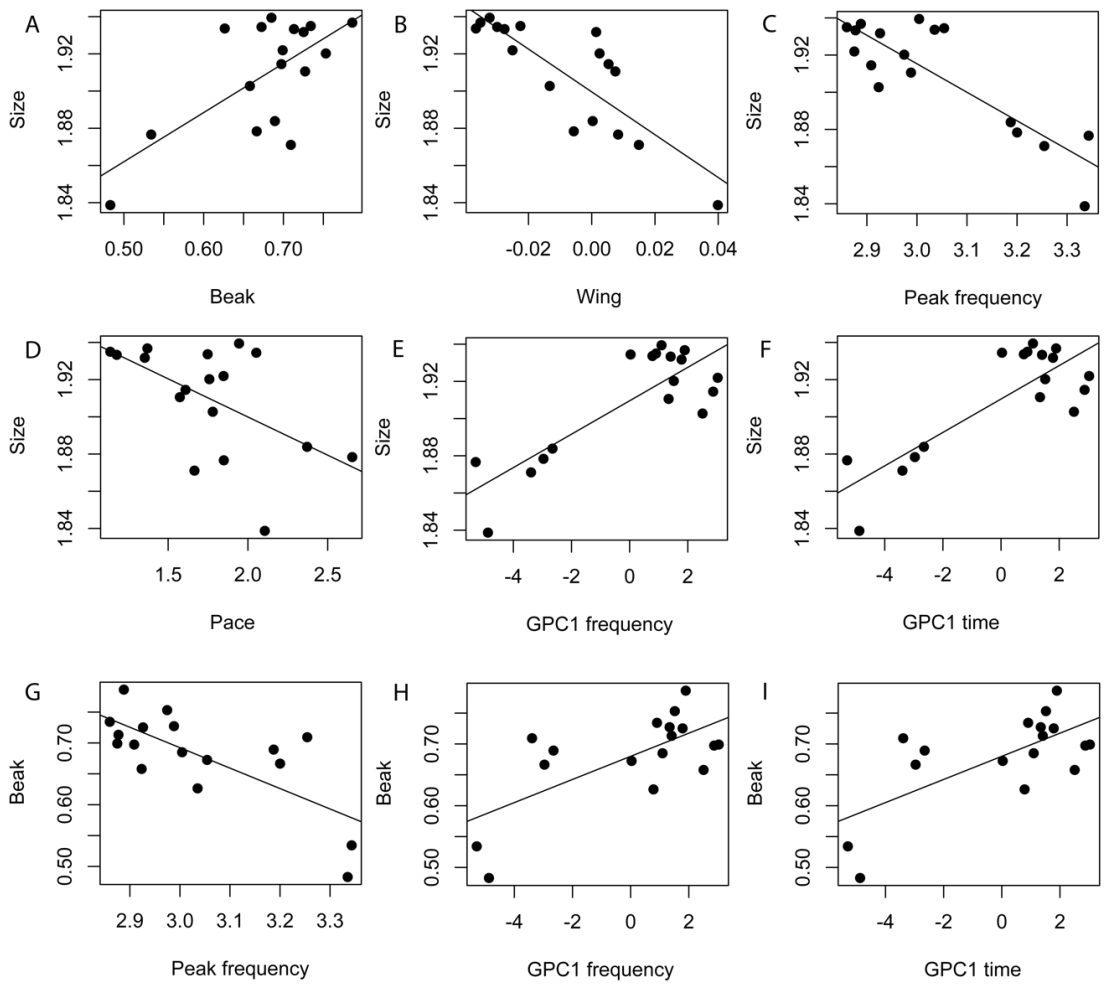

Figure 8. Bivariate correlations of morphological and acoustic variables: (A) Body size on beak, (B) body size on wing, (C) body size on peak frequency, (D) body size on pace, (E) body size on GPC1 frequency, (F) body size on GPC1 time, (G) beak on peak frequency, (H) beak on GPC1 frequency, (I) beak on GPC1 time. For trait definitions see Table 1; for coefficients of correlation and significance levels, see Table 3.

Table 1. Loudsong / morphology parameter definition and phylogenetic signal.

Category	Trait	Unit	Definition	*K*	*P*	λ	Model
Frequency	MaxF	KHz	Maximum frequency of loudsong	1.594	0.001	0.999	OU
	MinF	KHz	Minimum frequency of loudsong	1.041	0.001	0.966	OU (BM)
	BW	KHz	Bandwidth, measured as the difference between maximum and minimum	0.433	0.060	0.730	BM
	MaxF1st	KHz	Maximum frequency of first note	1.477	0.001	0.996	BM (OU)
	MaxFmid	KHz	Maximum frequency of middle note	1.606	0.001	0.999	OU
	MaxFpen	KHz	Maximum frequency of penult note	1.666	0.001	0.999	OU
	MaxFfin	KHz	Maximum frequency of final note	1.853	0.001	0.999	OU
	Peak Frequency	KHz	Frequency with maximum energy of loudsong	1.854	0.001	0.999	OU (BM)
Duration	DurLs	Sec	Duration of loudsong	0.408	0.050	0.000	BM (White)
	NumNotesLS	Sec	Number of notes per loudsong	0.780	0.002	0.976	OU (BM)
	Pace	Sec	Number of notes per second	0.845	0.002	0.978	OU (BM)
	Dur1st	Sec	Duration of first note	0.696	0.003	0.898	OU (BM)
	Durmid	Sec	Duration of middle note	0.489	0.054	0.814	BM
	Durfin	Sec	Duration of final note	0.612	0.015	0.956	OU (BM)
Morphology	Size	Mm	Proxy for body size	1.714	0.001	0.991	OU (BM)
	Wing	Mm	Wing length	2.321	0.001	0.999	EB (BM, OU)
	Tarsus	Mm	Tarsus length	1.522	0.001	0.954	OU (BM, EB)
	Tail	Mm	Tail length	0.905	0.005	0.999	OU (BM)
	Beak	Mm	Proxy for beak volume	1.607	0.001	0.999	OU (BM)
Derived	GPC1morphology		First global component from a pPCA analysis of measures 15–19	1.503	0.001	0.976	BM (OU)
	GPC1frequency		First global component from a pPCA analysis of measures 1–8	1.655	0.001	0.999	OU
	GPC2frequency		Second global component from a pPCA analysis of measures 1–8	0.341	0.184	0.621	White

	GPC1time	First global component from a pPCA analysis of measures 9–14	0.820	0.004	0.992	OU (BM)
	LPC6time	Sixth local component from a pPCA analysis of measures 9–14	0.382	0.075	0.000	White
Explanatory	Habitat	Habitat type (see text)	*	*	*	*

Definitions of loudsong and morphology parameters used for analysis with phylogenetic signal (Blomberg's K with P value, Pagel's **λ**), estimated model of evolution (BM: Brownian motion, EB: Early burst, OU: Ornstein–Uhlenbeck, White: white noise; alternative models in parentheses, if ΔAICc < 1).

Table 2. Mean (± SD) differences between antpittas species in sympatric and allopatric pairs for 16 temporal and frequency loudsong, and two morphological variables. Statistics are derived from Wilcoxon signed-ranks tests; $n = 9$ trios. Bold denotes *P*-values that were significant ($P < 0.05$).

Trait	**Simpatric pairs**	**Allopatric pairs**	**Statistics**
Maximum frequency of loudsong (MaxF)	0.06 ± 0.04	0.04 ± 0.02	0.425
Minimum frequency of loudsong (MinF)	0.16 ± 0.11	0.12 ± 0.11	0.496
Bandwidth, difference between maximum and minimum (BW)	0.17 ± 0.11	0.15 ± 0.08	0.570
Maximum frequency of first note (MaxF1st)	0.06 ± 0.04	0.05 ± 0.02	0.425
Maximum frequency of middle note (MaxFmid)	0.06 ± 0.03	0.04 ± 0.01	0.164
Maximum frequency of penult note (MaxFpen)	0.06 ± 0.03	0.04 ± 0.02	0.128
Maximum frequency of final note (MaxFfin)	0.05 ± 0.03	0.03 ± 0.01	0.054
Frequency with maximum energy of loudsong (Peak frequency)	0.08 ± 0.03	0.03 ± 0.02	**0.007**
Duration of loudsong (DurLS)	0.13 ± 0.08	0.06 ± 0.05	0.054
Number of notes (NumNotesLS)	0.47 ± 0.28	0.26 ± 0.26	0.362
Number of notes per second (Pace)	0.55 ± 0.16	0.13 ± 0.09	**0.003**
Duration of first note (Dur1st)	0.18 ± 0.09	0.13 ± 0.04	0.910
Duration of middle note (DurMid)	0.09 ± 0.06	0.09 ± 0.04	0.652
Duration of middle note (DurFin)	0.09 ± 0.06	0.09 ± 0.04	0.652
Proxy for body size (Size)	0.012 ± 0.010	0.005 ± 0.007	0.164
Proxy for beak volume (Beak)	0.035 ± 0.047	0.029 ± 0.017	0.359
First global component from a pPCA analysis of frequency measures	0.97 ± 0.60	0.55 ± 0.62	0.203
First global component from a pPCA analysis of temporal measures	1.75 ± 1.21	1.22 ± 1.03	0.359

.

Table 3. Correlation between variables.

	Size	**Beak**	**Habitat**
MaxF	**-0.144****	**-0.310***	**- 3.636***
MinF	**- 0.080***	-0.147	**- 2.276***
BW	- 0.028	-0.064	- 3.105
MaxF1st	**- 0.158****	**-0.335***	**- 3.990***
MaxFmid	**- 0.160****	**-0.311***	**- 3.730***
MaxFpen	**- 0.149****	**-0.323***	**- 3.550***
MaxFfin	**- 0.157****	**-0.359****	**- 3.640***
Peak Frequency	**- 0.143*****	**-0.308***	**- 3.094****
DurLs	0.019	-0.127	0.729
NumNotesLS	- 0.022	-0.053	- 1.083
Pace	**- 0.042***	-0.048	- 0.844
Dur1st	0.041	0.036	3.562
Durmid	0.068	- 0.009	5.016
Durfin	0.091	- 0.009	3.192
Size	-	**1.670****	**19.55****
Wing	**-1.498*****	-0.936	**-33.014****
Tarsus	**-0.642*****	**-1.881*****	-27.79
Tail	-0.139	**-1.356*****	-7.521
Beak	**0.248****	-	10.372
GPC1morphology	0.008	**0.066****	- 0.388
GPC1frequency	**0.007****	**0.016***	**- 0.764***
GPC2frequency	- 0.003	- 0.007	0.512
GPC1time	**0.007****	**0.016***	**0.189***
LPC6time	- 0.001	- 0.013	- 0.373

Coefficients of correlation. *P < 0.05, **P < 0.01, ***P < 0.001. Values in bold indicate traits that contributed significantly to the phylogenetic generalized linear model (pGLS).

Vocal recognition and character displacement

For 14 of 16 acoustic traits measured, the average difference was greater between the loudsongs of sympatric than allopatric species pairs. However only two variables were significant, peak frequency and pace (Table 2). This was confirmed using phylogenetic principal components to describe loudsong structure: the mean difference in PC values was greater between the loudsongs of sympatric than allopatric pairs (Table 2; Fig. 9).

However it is important to note that eight of nine allopatric pairs are members of species complexes (Table S3; Fig. 1), and these taxa are therefore more closely related to their allopatric congeners than to a sympatric one. Similarly, given the remarkable vocal differences among related taxa that co-occur and whose ecological requirements and distributions overlap, is likely that vocal traits are under character displacement influence (Table 2; Fig. 9).

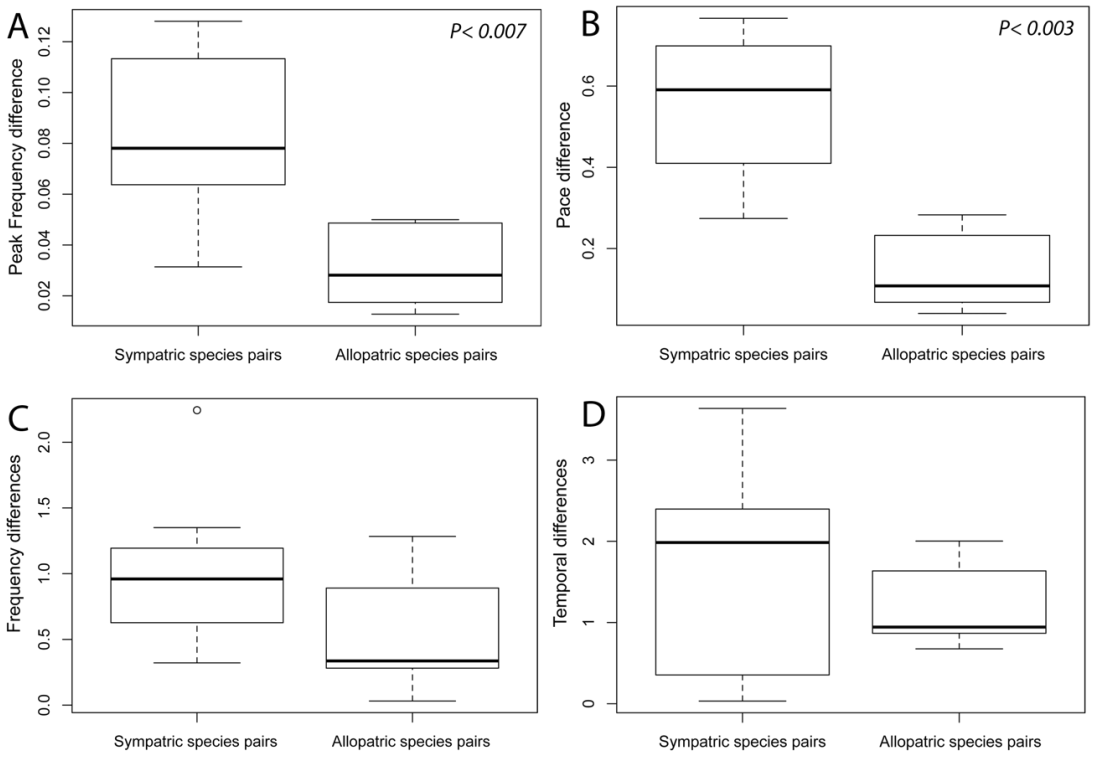

Figure. 9. Boxplots illustrating loudsong differences between sympatric and allopatric species pairs for (A) Peak frequency, (B) Pace, (C) GPC1frequency and GPC1time

(see Table 2 for measure details). The lower and upper boundaries of the boxes represent first and second interquartile ranges, respectively, the horizontal bar shows the median, and the lower and upper bars relate to the 10th and 90th percentiles, respectively. *P*-values are derived from a Wilcoxon signed-ranks tests (see text); $n = 9$ trios (Table S3).

Testing convergent evolution

Size and shape

SURFACE analyses support a scenario in which both size and shape evolve around adaptive peaks. Four shifts of regime were identified to occur. The most informative model included three independent adaptive regimes (k'), however, only one appear after multiple shifts on independent branches (k' conv) and is thus considered to exhibit true convergence (Fig. 10A; loglik Size = 48.38, loglik Wing = 63.11, loglik Tail = 47.53, loglik Tarsus = 54.04, loglik Beak = 42.59; α Size = 19.66, α Wing = 6.68, α Tail = 26.51, α Tarsus = 15.10, α Beak = 25.17; σ^2 Size = 0.033, σ^2 Wing = 0.005, σ^2 Tail = 0.043, σ^2 Tarsus = 0.016, σ^2 Beak = 0.067, σ^2; AICc = -430.12; where the parameters α and σ^2 represent respectively, the rate of adaptation to optima and the rate of stochastic evolution; Ingram and Mahler, 2013). The AICc improved from -416.72 to -430.12, between the forward and backward phases (ΔAICc = 13.4; for comparison, the AICc of the Brownian motion model was -406.52; Fig. 10B).

The true convergent regime includes three taxa that inhabit different types of more disturbed areas: *Hylopezus ochroleucus*, from semi-deciduous woodland, including *caatinga* and *Hylopezus nattereri* and *Grallaricula nana*, both of which inhabit montane forest, favoring bamboo thickets (Fig. 10A). Inferred adaptive peaks of body and beak for this convergent regime are below observed values for all species, excepted *G. flavirostris*, which suggests that, contrary to other members of the group, these three independent lineages are evolving toward smaller body and beak sizes (Fig. 10C and D). However, wing size appears to be inversely proportional to the body size (Fig. 10C).

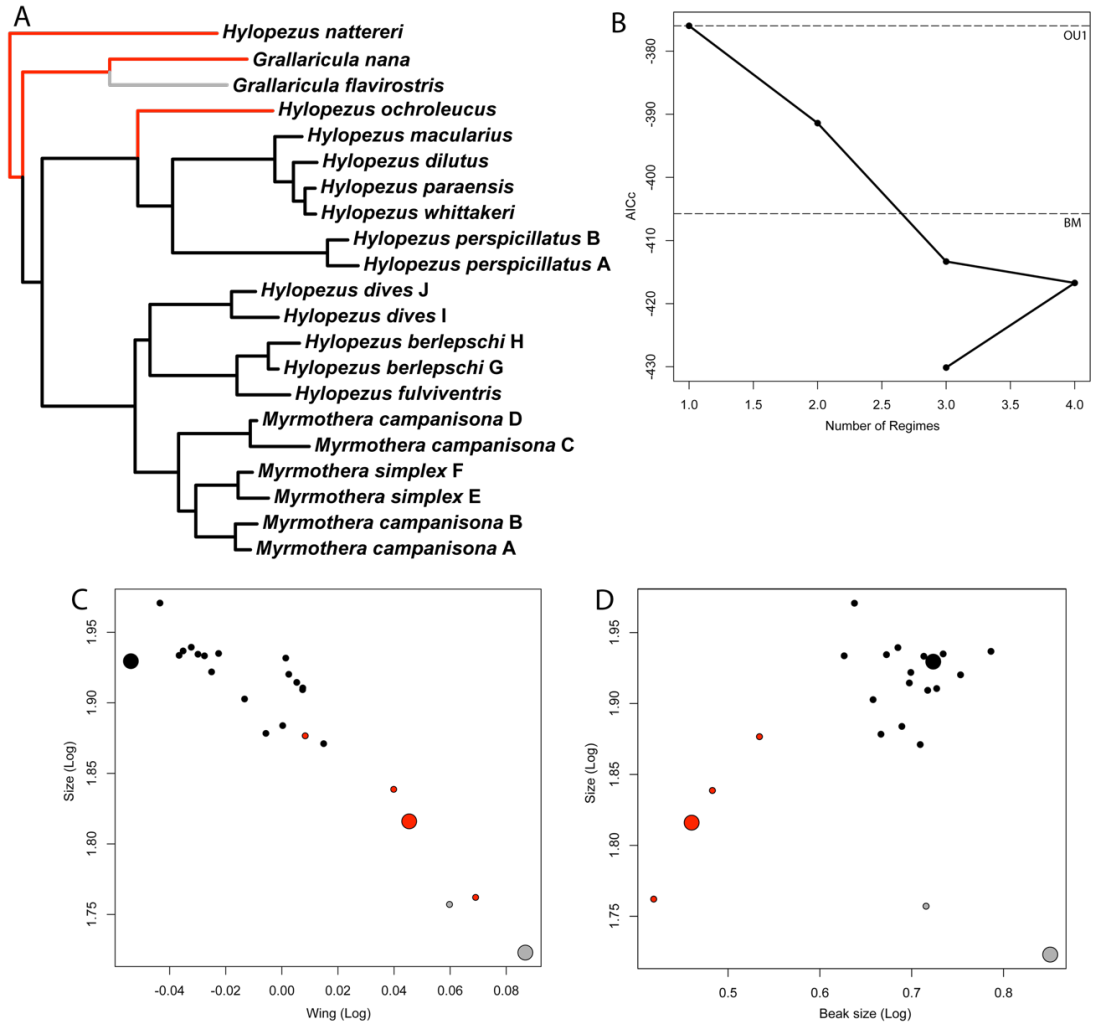

Figure. 10 Convergent adaptive regimes of the antpittas related to morphological traits. (A) *Hylopezus* / *Myrmothera* clade cladogram with adaptive regimes identified by SURFACE. Red branches represent convergent adaptive regime and black and gray branches denote non-convergent regimes. (B) Change in AICc during the forward and backward phases of the SURFACE analysis (Hansen model), and comparison with values obtained for the Brownian motion (BM) and single-regime OU (OU1) models. (C and D) Trait values for each species (small circles) and estimated optima (large circles), with regime colours matching those in the tree.

Acoustic traits

Different regimes were found by SURFACE for each acoustic dataset (temporal and frequency traits). The final Hansen model for temporal measures included four shifts of regime and three distinct regimes ($\Delta k = 1$) and $c = 2$ convergent shifts (Fig. 11A).

However, only one appears after multiple shifts in independent branches and is thus considered to exhibit true convergence (loglik Pace = 2.17, loglik Dur = 22.41, loglik Dur1st = 16.88; α Pace = 16.73, α Dur = 69.28, α Dur1st = 42.20; σ^2 Pace = 2.31, σ^2 Dur = 0.80, σ^2 Dur1st = 0.94, AICc = -24.39).

For the frequency measures, five shifts of regime were identified to occur. The most informative model included 3 independent adaptive regimes (*k'*), two of which appear after multiple shifts in independent branches (*k'* conv) and are thus considered to exhibit true convergence (loglik MinF = 13.45, loglik MaxF = 31.88, loglik MaxF1st = 31.93, loglik MaxFpen = 33.04, loglik PeakFreq = 31.29, loglik BW = 12.23; α MinF = 37.11, α MaxF = 46.10, α MaxF1st = 39.07, α MaxFpen = 46.38, α PeakFreq = 29.23, 1 α BW = 56.96; σ^2 MinF = 1.22, σ^2 MaxF = 0.20, σ^2 MaxF1st = 0.18, σ^2 MaxFpen = 0.18, σ^2 PeakFreq = 0.15, σ^2 BW = 1.98; AICc = -205.38).

The temporal traits appear to be highly conserved and it is difficult to map these characters on the phylogeny, but pace and the GPC1 time were negatively correlated to antpittas' body size (Table 3; Fig. 8), although this relationship was not clearly recovered by the convergence test (Fig. 11A). For the frequency related traits, the two true convergent regimes appear to be strongly correlated with habitat conditions, and showed a clear relationship between environmental structure and frequency measures (Fig. 12A; Table 3). Inferred adaptive peaks of frequency for these convergent regimes suggest that lineages related to dense undergrowth of humid or flooded forest are evolving onto lower frequencies while lineages that inhabits more open areas, like semi-deciduous woodland, open understory or thickets of bamboo are evolving toward higher frequencies (Fig. 12C and D).

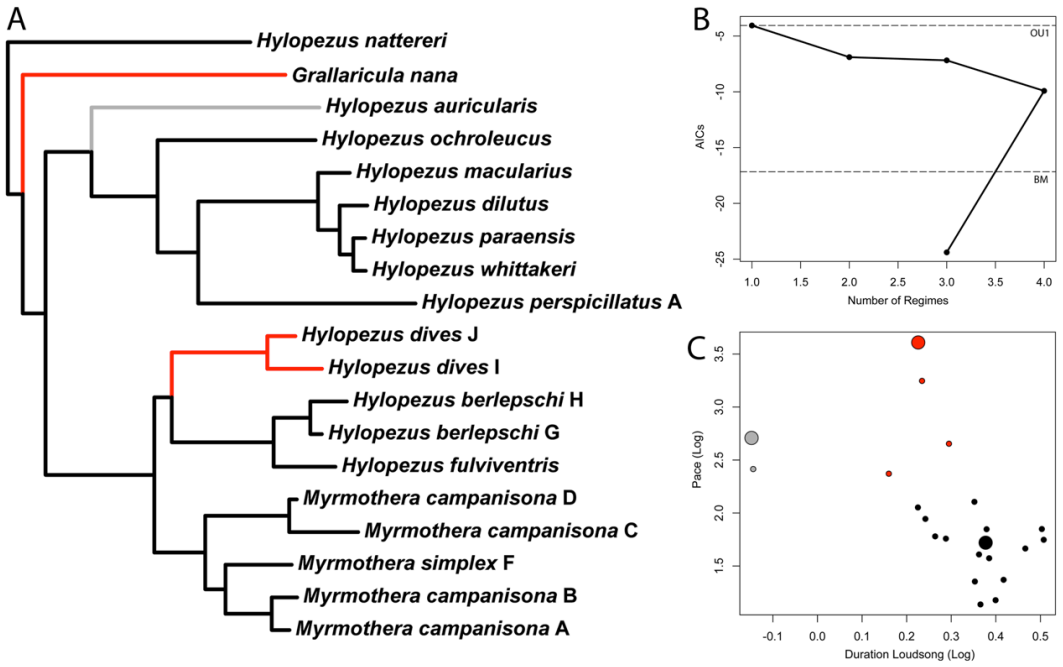

Figure. 11. Convergent adaptive regimes of the antpittas related to loudsong duration. (A) *Hylopezus* / *Myrmothera* clade cladogram with adaptive regimes identified by SURFACE. Red branches represent convergent adaptive regime and black and gray branches denote non-convergent regimes. (B) Change in AICc during the forward and backward phases of the SURFACE analysis (Hansen model), and comparison to values obtained for the Brownian motion (BM) and single-regime OU (OU1) models. (C and D) Trait values for each species (small circles) and estimated optima (large circles), with regime colours matching those in the tree.

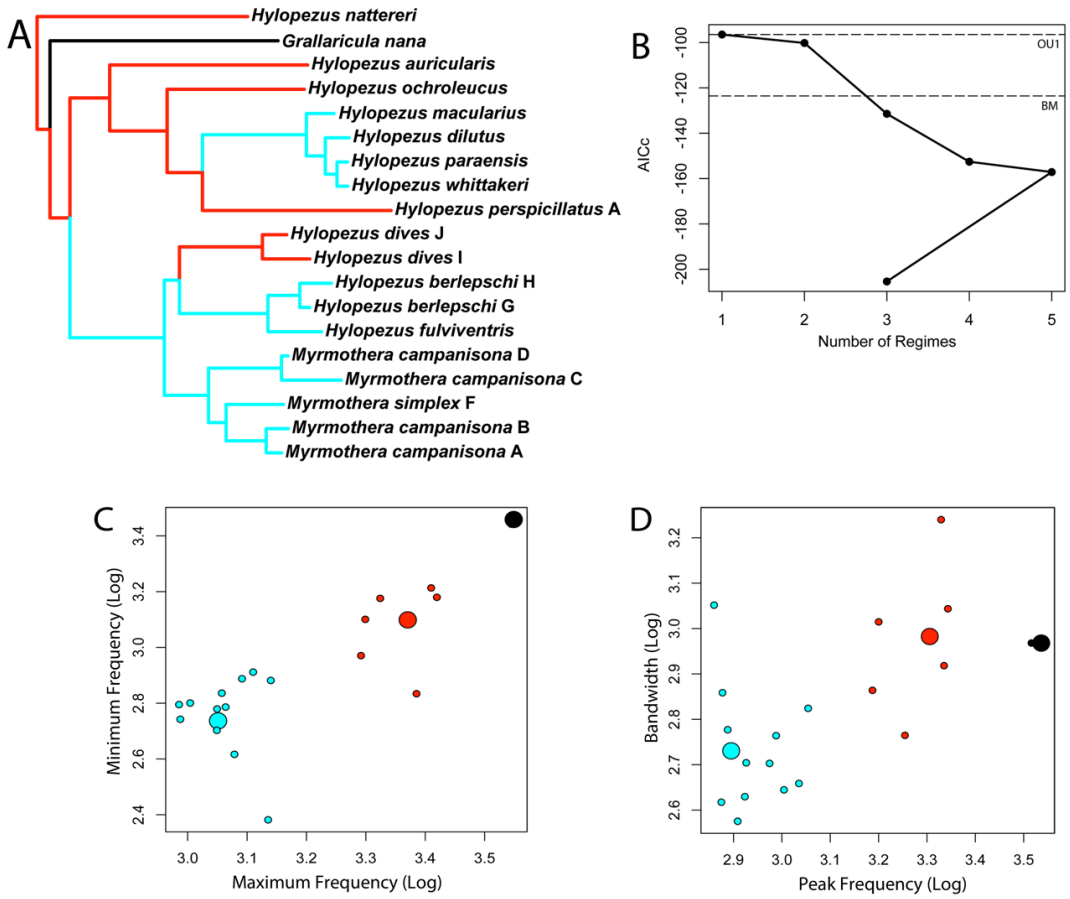

Figure. 12. Convergent adaptive regimes of the antpittas related to loudsong frequency. (A) *Hylopezus* / *Myrmothera* clade cladogram with adaptive regimes identified by SURFACE. Colored branches represent convergent adaptive regimes and black branch denote non-convergent regime. (B) Change in AICc during the forward and backward phases of the SURFACE analysis (Hansen model), and comparison to values obtained for the Brownian motion (BM) and single-regime OU (OU1) models. (C and D) Trait values for each species (small circles) and estimated optima (large circles), with regime colours matching those in the tree.

Evolution over time

Subclade disparity through time was lower than expected under a Brownian motion model to body size evolution (Fig. 13A). This is confirmed quantitatively by a negative MDI of -0.22, which generally describe clades that accumulated disparity during their early history (i.e. disparity distributed primarily among subclades). On

the other hand, body shape disparity was concentrated primarily within subclades, as demonstrated by the positive MDI values of 0.38, indicating that clades accumulated disparity during their recent history (Fig. 13B). We compared observed relative disparity with the mean expectation of 10.000 simulations under Brownian motion.

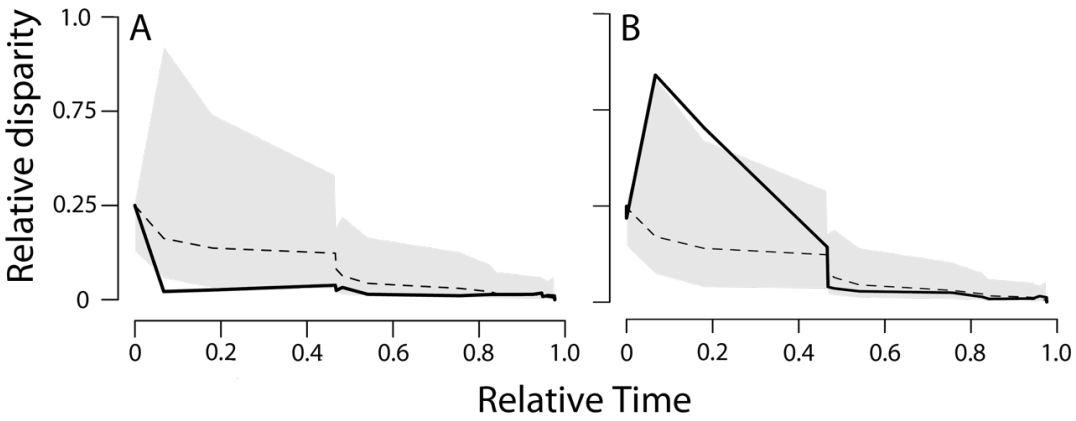

Figure 13. Mean of disparity through time (DTT) for antpittas body size (A) and body shape (B). Solid line represents observed disparity, dashed line represents the mean of 10 000 simulations of character evolution on the antpittas phylogeny under Brownian motion. The grey shaded area indicates the 95% DTT range for the simulated data.

The mean of disparity through time related to loudsong frequency and duration traits, were close to zero (MDI values; frequency = 0.0009; duration = 0.016). This result suggests that vocalizations of antpittas could have evolved approximately under a Brownian motion process (Fig. 14A and B).

Despite an overall pattern of continuous decrease through time, subclade disparity shows one increase in frequency, coincident with the origination of *Hylopezus* / *Myrmothera* clade at approximately 25 Ma (approx. 0.1 - 0.2 relative time; Fig. 14A; For details see Carneiro et al. unpubl. ms. Chapter 1), and another increase related to duration, at approximately 15 Ma (approx. 0.5 relative time; Fig. 14B), coincident with the radiations of 'core *Hylopezus*', 'extended *Myrmothera*' and *Grallaricula* (For details see Carneiro et al. unpubl. ms. Chapter 1).

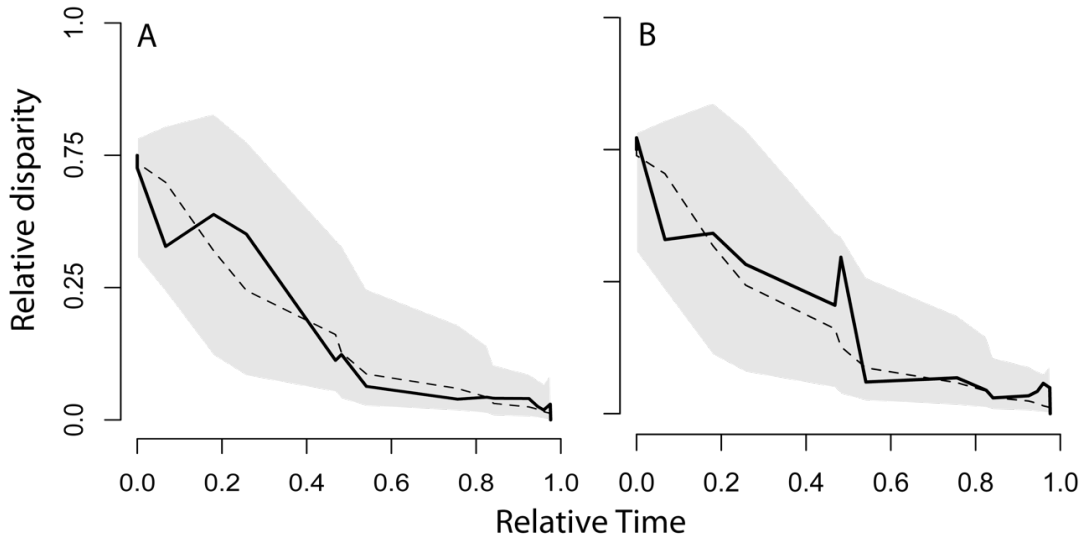

Figure 14. Mean of disparity through time (DTT) for antpittas related to loudsong frequency (A) and duration (B). Solid line represents observed disparity, dashed line represents the mean of 10 000 simulations of character evolution on the antpittas phylogeny under Brownian motion. The grey shaded area indicates the 95% DTT range for the simulated data.

DISCUSSION

Morphological evolution

The phylogenetic relationship of antpittas' morphologies recovered by the pPCA demonstrates the conserved morphology pattern within the group, but nonetheless that morphological variation is associated with environmental conditions (Fig. 4; Table S2). Our pPCA layout shows that taxa inhabiting analogous habitats ('primary'; Dense forest or 'secondary'; Less structured forest habitats) were more similar to each other than expected by the phylogeny, particularly in body size and wing shape (Fig. 4; Table 3). These results were corroborated by the strongly significant relationship between body size, wing shape and habitat, recovered by the pGLS analyses (Table 3).

On the other hand, the convergence test implemented by SURFACE did not recover all lineages that inhabits 'secondary areas' such as convergent adaptive group, it is possible that the remaining morphological characters included in SURFACE analyses (beak, tail and tarsus), has masked the correlation between body size and habitat, indicated by the other analyzes. Nevertheless, the convergence regime recovered includes three taxa that inhabit different types of open areas (Fig. 10A; Table S2). Our results suggest that lineages that inhabit 'dense forest' evolved toward larger body and beak (Fig. 4; Fig. 10C and D). However, wing size appears to be inversely proportional to body size, and this effect seems to be a tendency of larger size and smaller wings in forest taxa against smaller size and larger wings in open habitat lineages (Fig. 8A and B; Fig. 10C and D).

The relative contribution of shape variation antpittas is lower than that of body size variation (Fig. 4 and 5). This suggests that phenotypic similarities among the disparate antpittas lineages reflect evolutionary constraints on body shape, and despite their different body sizes, they are similar in their ecological requirements and use the same resources (e.g., prey items, microhabitat). This findings agree with the idea, suggested for other terrestrial vertebrate groups, that convergent evolution is primarily observed in body shape as a result of adaptation in allopatry mediated by ecological factors such as energetics, locomotion and food item (e.g., Grant et al. 2004; Harmon et al. 2005; Wiens et al. 2006). Our DTT analysis indicate a body size disparity

accumulated during the early antpittas' evolutionary history, and this likely dates back to the time when the group colonized the lowlands of the Amazon and the Atlantic Forest, at approximately 25 Mya (Fig. 14A; For details see Carneiro et al. unpubl. ms. Chapter 1), with changes in body size coincident with the occupation of these new habitats outside of the Andes. However, a combination of several ecological and environmental factors not directly assessed in our analyses is likely to influence these evolutionary associations between body size and habitat attributes. Differential effects of these factors along with stochastic processes would partially explain the observed variation in body size among species (Bravo et al. 2014).

Vocal evolution

Effect of body size and beak morphology on antpittas' vocalizations

The speciation theory regards mating signal divergence as a by-product of genetic differentiation in allopatry, through drift and/or adaptation to divergent ecologies (Dob- zhansky 1951; Mayr 1963). Consistent with the ecological adaptation hypothesis are data showing correlated evolution among morphology and mating signal characteristics. Such correlations arise if natural selection favors modifications in traits functionally related to the production of mating signals. In birds, body size and beak morphology are under strong selective pressures relating to diet (Gibbs and Grant 1987) and our results showed that in antpittas both these traits influence loudsong structure: body size and beak volume had a strong negative relationship with loudsong frequency, and body size was negatively correlated with pace pattern (Fig. 8; and Table 3). That these relationships were retained after controlling for phylogeny suggests that the evolution of loudsong structure in antpittas is correlated with morphology.

Negative correlations between body size and song frequency are concordant with the widely accepted notion that body mass is negatively correlated with various measures of acoustic frequencies, particularly minimum, maximum, and peak frequencies (Wallschlager, 1980; Ryan and Brenowitz, 1985; Tubaro and Mahler, 1998; Seddon 2005, Mason et al. 2015). There is a functional relationship; the frequency that a vibrating structure, in this case the syringeal membrane, can most efficiently produce is affected by the mass of the structure itself (Bowman, 1979; Wallschlager, 1980;

Shy, 1983). Thus, larger antpittas have more massive syrinxes that produce lower frequencies with greater efficacy.

In addition to acoustic frequencies, we found that body size was correlated with pace, and temporal loudsong features (GPC1 time). This is consistent with the findings of previous studies on the effect of habitat and body mass (Ryan and Brenowitz, 1985; Wiley, 1991; Badyaev and Leaf, 1997, Mason et al. 2015); however, the functional relationships that undergo these correlations are less easy to explain. The pGLS recovered a strongly positive correlation between body size and beak volume, thus larger species tend to have larger beaks, this should therefore lead to a decrease in the ability to produce notes rapidly.

Beak shape also influenced acoustic parameters related to frequencies, and this agrees with previous studies (Podos et al. 2004; Huber and Podos, 2006; Derryberry et al. 2012); however, these correlations have received different support from empirical results (Palacios and Tubaro, 2000; Farnsworth and Lovette, 2005). Therefore, the allometric relationship between body size and beak shape could confound the correlations between size and loudsong characters. Thus, it is difficult identifying whether morphological constraints related on vocal characters considered here are due to body size (i.e. syrinx size), related to physiological constraints associated beak size and shape, or a mixed of these two possibilities.

The correlation between beak morphology and acoustic frequencies suggests that the beak plays an important role in determining the frequency of antpittas loudsongs. The same pattern was reported by Palacios and Tubaro (2000) and Derryberry et al. (2012). Interestingly, in these studies a correlation between beak size and song frequency was found in woodcreepers (family: Dendrocolaptidae), a suboscine family with great interspecific variation in beak shape. In antpittas, despite the small magnitude of variation, a consistent relationship between beak and acoustic frequency was detect. Given the conserved morphology of antpittas, and the similarity of ecological requirements of members of this group, it is unlikely that the song diversification has occurred as a by-product of adaptation to different foraging niches as found in Darwin's finches (Podos 2001).

Overall, the present study suggests that in the antpittas, morphology and the acoustic

features of loudsongs have evolved in a correlated way. However, the extent to which antpittas match beak configuration (e.g., vocal sac) to the acoustic properties of their songs (e.g., peak frequency) as shown in Darwin's finches (Podos et al. 2004), needs to be further investigated. If performance-related loudsong properties are also used in species recognition and mate choice, correlated evolution of beak morphology and loudsong structure might facilitate reproductive isolation and speciation in this diverse assemblage.

Additional selective pressures in antpittas vocalizations

The need for accurate species identification is likely to be important, particularly in dense forest-dwelling lineages, where dim light conditions render visual signals less effective, and where many species are poorly differentiated by plumage (Seddon 2005). The speciation theory predicts that mating signals will diverge in sympatry because selection against the production of unfit hybrids favors traits that reliably signal species identity (Dobzhansky 1951; Lewontin 1974; Liou and Price 1994). Birdsongs have long been predicted to diverge by this process but evidence for this has hitherto been scarce (Irwin and Price 1999; Seddon 2005).

Our findings demonstrate that on average differences were greater between the loudsongs of sympatric than allopatric species pairs. This was significant for two variables, peak frequency and pace (Table 2). And the pattern was confirmed by phylogenetic principal components, where mean difference in PC values, corrected by phylogenies, was greater between the loudsongs of sympatric than allopatric pairs (Table 2; Fig. 9). Therefore, this supports the idea that the need for species recognition may drive vocal evolution in birds.

However it is important to note that eight of the nine allopatric pairs tested are members of species complexes (Table S3; Fig. 1), and that these taxa are more closely related to their allopatric congeners than to a sympatric one. This suggests that the patterns of vocal congruence detected could be mistaken by differences in evolutionary history of the taxa. Nevertheless, given the remarkable vocal difference among related taxa that co-occur and whose ecological requirements and distributions overlap, is likely that vocal traits are under character displacement influence (Table 2; Fig 8).

Demonstrations of more pronounced song differences in sympatry than allopatry are consistent with the idea that the need for species discrimination selects for vocal divergence. As far as could be determined, loudsong divergence was not accompanied by morphological divergence (Table 2). Moreover, all species occupied similar ecological niches, suggesting that loudsong divergence is not a by-product of ecological character displacement, but may have been driven either by reinforcement or by disruptive sexual selection (Panhuis et al. 2001; Seddon 2005).

Conclusions

Our antpitta's comparative approach sheds light on the role that morphology and habitat selection play in the evolution of acoustic signals in suboscine birds. Our findings suggest that antpitta's vocalizations are driven by morphological atributes, such as body size and beak shape. These characters seem to impact the vocal evolution of antpittas more than acoustic inter-habitat differences. In antpittas there has been an evolutionary response to selection for species discrimination; this underscores the potential of interactions among closely related sympatric species to drive song divergence. Furthermore, the strong correlations between song structure, morphology, and habitat suggest that, as proposed by traditional theories of speciation, ecological adaptation may indeed drive signal evolution. Future studies could expand upon the work presented here by including the remaining lineages of Grallariidae (with an extensive sampling of the genera *Grallaricula* and *Grallaria*), where a broader phenotypic variation could disentangle whether the strong correlations observed here are due to mechanical constraints associated with ecological adaptation.

Appendix. Supplementary material

Table S1. General information of specimens, vocalizations, and tissues analyzed in the present study. Voucher numbers refer to deposit at ornithological collections. Taxonomy follows Remsen et al. (2015), except to *H. macularius* complex, which follows Carneiro et al. (2012).

LINEAGE	SOURCE	LOCALITY	VOUCHER
Myrmothera simplex F	Morphology	Venezuela: Bolivar, Roraima	169839-ANSP
Myrmothera simplex F	Morphology	Venezuela: Mt. Auyan. Tepui Plateau	323541-AMNH
Myrmothera simplex F	Morphology	Venezuela: Roraima. Philipp Camp.	236690-AMNH
Myrmothera simplex F	Morphology	Venezuela: Mt. Auyan. Tepui Plateau	323544-AMNH
Myrmothera simplex F	Morphology	Venezuela: Mt. Auyan. Tepui Plateau	323543-AMNH
Myrmothera simplex F	Morphology	Venezuela: Bolivar, Serra Pacaraima, Cerro Urutami	812901-AMNH
Myrmothera simplex F	Morphology	Venezuela: Bolivar, Serra Pacaraima, Cerro Urutami	812902-AMNH
Myrmothera simplex F	Morphology	Venezuela: Bolivar, Serra Pacaraima, Cerro Urutami	812900-AMNH
Myrmothera simplex F	Morphology	Venezuela: Cerro Guaiguinima, Falda N. O.	383248-USNM
Myrmothera simplex F	Morphology	Guyana; Mount Roraima, North Slope,	626929-USNM
Myrmothera simplex F	Morphology	Guyana; Mount Roraima, North Slope,	626774-USNM
Myrmothera simplex F	Morphology	Guyana; Mount Roraima, North Slope,	626921-USNM
Myrmothera simplex F	Morphology	Guyana; Mount Roraima, North Slope,	626869-USNM
Myrmothera simplex F	Morphology	Guyana; Cuyuni-Mazaruni, Paruima, ca. 19 KM, at Mt. Holitipu,	639140-USNM
Myrmothera simplex F	Morphology	Brit. Guiana: Roraima	156333-AMNH
Myrmothera simplex F	Vocal	Venezuela: Rio Cuyuni; km 124; Sierra de Lema	MLS62408
Myrmothera simplex F	Vocal	Venezuela: At highest elevation on Escalera	MLS60984
Myrmothera simplex F	Vocal	Venezuela: Escalera, South of las Claritas	MLS60983
Myrmothera simplex F	Vocal	Venezuela: 112.0 km S of El Dorado	MLS52919
Myrmothera simplex F	Vocal	Venezuela: 112.0 km S of El Dorado	MLS52916
Myrmothera simplex F	Vocal	Venezuela: 45.0 km S of Las Claritas	MLS49522

Myrmothera simplex F	Vocal	Venezuela: 45.0 km S of Las Claritas	MLS49521
Myrmothera simplex F	Vocal	Venezuela: 25.0 km S of Las Claritas	MLS49339
Myrmothera simplex F	Vocal	Venezuela: La Escalera	MLS30418
Myrmothera simplex F	Vocal	Guyana: north slope Mt Roraima	MLS134902
Myrmothera simplex E	Morphology	Venezuela: Amazonas, Mount Duida, Desfiladero	323087-USNM
Myrmothera simplex E	Morphology	Venezuela: Mt. Duida. Sinmit Central Camp.	245926-AMNH
Myrmothera simplex E	Morphology	Venezuela: Mt. Duida. Cumbre 2. Cabeceras del Valle	270928-AMNH
Myrmothera simplex E	Morphology	Venezuela: Mt. Duida. Cabeceras del Valle	270924-AMNH
Myrmothera simplex E	Morphology	Venezuela: Mt. Duida. Valley head, Summit	270921-AMNH
Myrmothera simplex E	Morphology	Venezuela: Mt. Duida. Cumbre 13. Desfiladero	270926-AMNH
Myrmothera simplex E	Morphology	Venezuela: Mt. Duida. Cumbre 2. Cabeceras del Valle	270920-AMNH
Myrmothera simplex E	Morphology	Venezuela: Mt. Duida. Sunmit Privisional Camp.	270925-AMNH
Myrmothera simplex E	Morphology	Venezuela: Mt. Duida. Cumbre 2. Cabeceras del Valle	270923-AMNH
Myrmothera simplex E	Morphology	Venezuela: Terr. Amazonas. Valley N Base Pico Cardona	816753-AMNH
Myrmothera simplex	*Molecular*	Venezuela: Amazonas; Sierra de Tapirapeco; Cerro Tamacuari; 1270m	AMNH - 2136
Myrmothera simplex	*Molecular*	Venezuela: Amazonas; Pico Cardonas; Elev. 1250M Rainforest, Valley N. Base	AMNH - 17126
Myrmothera simplex	*Molecular*	Venezuela: Bolivar; La Escalera, KM 122 on El dorado-ST. Eleanea Road	AMNH - RDP301
Myrmothera simplex	*Molecular*	Venezuela: Amazonas; Cerro Yavi	AMNH - 213312
Myrmothera simplex	*Molecular*	Venezuela: Amazonas; Cerro de la Neblina; CAMP VII 1800-1900M	AMNH - 1440
Myrmothera simplex	*Molecular*	Venezuela: Amazonas; Cerro Yavi	AMNH - 213320
Myrmothera simplex	*Molecular*	Venezuela, Amazonas Territory, CERRO DE LA NEBLINA CAMP VII 1800M	LSUMZ - B7408
Myrmothera simplex	*Molecular*	Venezuela, Amazonas Territory, CERRO DE LA NEBLINA CAMP VII 1800M	LSUMZ - B7468
Myrmothera campanisona D	Vocal	Venezuela: 10.0 km E of Rio Grande	MLS49340
Myrmothera campanisona D	Vocal	Brazil: Amazonas, 25.0 km N of Manaus	MLS32418
Myrmothera campanisona D	Vocal	Suriname: Foengoe island	MLS2136
Myrmothera campanisona D	Vocal	Suriname: Foengoe island	MLS2131
Myrmothera campanisona D	Vocal	Guyana: Upper Takutu-Upper Essequibo, Sipu RIver	MLS134399

Myrmothera campanisona D	Vocal	Brazil: Amazonas, ZF-3, Reserva 41	MLS113138
Myrmothera campanisona D	Vocal	Guyana: Upper Takutu-Upper Essequibo, 20.0 km E of Nappi Village	MLS70074
Myrmothera campanisona C	Vocal	Ecuador: Sucumb√≠os, 12.0 km N of Lumbaqui	MLS74784
Myrmothera campanisona C	Vocal	Venezuela: Amazonas, Rio Negro region; Pica San Carlos-Solano	MLS62420
Myrmothera campanisona C	Vocal	Bolivia: La Paz, Alto Rio Madidi Camp	MLS52374
Myrmothera campanisona C	Vocal	Bolivia: Pando, SW of Cobija; Camino Mucden	MLS38929
Myrmothera campanisona C	Vocal	Brazil: Amazonas, 25.0 km N of Manaus	MLS32418
Myrmothera campanisona C	Vocal	Peru: Loreto, north bank Rio Napo; Quebrada; Sucusari	MLS29114
Myrmothera campanisona C	Vocal	Peru: Madre de Dios	MLS13288
Myrmothera campanisona C	Vocal	Brazil: Amazonas, Parque Nacional Jau	MLS117014
Myrmothera campanisona B	Vocal	Brazil: Ariquemes, Rondônia. 25km north of town	XC90425
Myrmothera campanisona B	Vocal	Brazil: Parque Nacional da Amazônia	XC90424
Myrmothera campanisona B	Vocal	Brazil: Parque Nacional da Amazônia	XC90423
Myrmothera campanisona B	Vocal	Brazil: Rondônia, Cachoeira Nazare; west bank of Rio Jiparana	MLS40235
Myrmothera campanisona B	Vocal	Brazil: Pará, Parque Nacional da Amazonia; southwest of Itaituba	MLS35671
Myrmothera campanisona A	Vocal	Brazil: Belterra, Bacia 357, PA	XC94889
Myrmothera campanisona A	Vocal	Brazil: Tapajós National Forest	XC90422
Myrmothera campanisona A	Vocal	Brazil: Cristalino Jungle Lodge, MT	XC68792
Myrmothera campanisona A	Vocal	Brazil: Cristalino Jungle Lodge, MT	XC5707
Myrmothera campanisona A	Vocal	Brazil: Cristalino Jungle Lodge, MT	XC38478
Myrmothera campanisona A	Vocal	Brazil: Novo Progresso, state of Pará	XC28243
Myrmothera campanisona A	Vocal	Brazil: Novo Progresso, state of Pará.	XC119378
Myrmothera campanisona A	Vocal	Brazil: Pará, Floresta Nacional de Tapajos; Base de Sucupira, BR-163	MLS115082
Myrmothera campanisona A	Vocal	Brazil: Pará, Floresta Nacional de Tapajos; BR-163	MLS114910
Myrmothera campanisona A	Vocal	Brazil: Mato Grosso, Cristalino Ecological Institute; Trilha da Castaneira	MLS110055
Myrmothera campanisona	*Molecular*	Brazil: Pará: FLOTA de Faro, ca 70 km NW de Faro	MPEG - CN150
Myrmothera campanisona	*Molecular*	Brazil: Pará: Juruti, Projeto Juruti/Alcoa, Platô Capiranga, trilha 196	MPEG - 0961

Myrmothera campanisona	*Molecular*	Brazil: Pará: Alenquer, ESEC Grão-Pará	MPEG - CN509
Myrmothera campanisona	*Molecular*	Brazil: Pará: Alenquer, ESEC Grão-Pará	MPEG - CN418
Myrmothera campanisona	*Molecular*	Brazil: Pará: Rio Xingu, margem direita, Caracol (área 2)	MPEG - BMP075
Myrmothera campanisona	*Molecular*	Brazil: Pará: Óbidos, Flota do Trombetas	MPEG - CN341
Myrmothera campanisona	*Molecular*	Brazil: Pará: Altamira, Floresta Nacional de Altamira	MPEG - TM008
Myrmothera campanisona	*Molecular*	Rio Juruá, Marechal Taumaturgo, Nossa Senhora Aparecida	MPEG - PNS337
Myrmothera campanisona	*Molecular*	Rio Branco, margem esquerda, Caracaraí, próximo BR 174	MPEG - MPD040
Myrmothera campanisona	*Molecular*	Brazil: Amazonas, São Gabriel da Cachoeira, PPBIO	MPEG - 20648
Myrmothera campanisona	*Molecular*	Brazil: Pará: Itaituba, margem direita Rio Tapajós, Comunidade Penedo	MPEG - 19634
Myrmothera campanisona	*Molecular*	Brazil: Pará, Jacareacanga, margem esquerda Rio Tapajós, Vila Mamãe-anã	MPEG - 18604
Myrmothera campanisona	*Molecular*	Brazil: Pará: Estern margin Rio Tapajós e direita do Jamanxin SW Itaituba	INPA - A10032
Myrmothera campanisona	*Molecular*	RR, Parque Nacional Viruá, margem esquerda do Rio Branco, "grid"	INPA - A1726
Myrmothera campanisona	*Molecular*	Brazil: Amazonas, 110 km ENE Santa Isabel do Rio Negro	INPA - A1662
Myrmothera campanisona	*Molecular*	RO, Porto Velho; margem direita do Rio Jaci; Três Praias	INPA - A4141
Myrmothera campanisona	*Molecular*	PA, Margem direita do Rio Tapajós; 147 km sudoeste de Itaituba, J	INPA - A11548
Myrmothera campanisona	*Molecular*	Guyana, Potaro-Siparuni, Iwokrama Reserve; ca. 41 road km, SW Kurupukari	ANSP - 21109
Myrmothera campanisona	*Molecular*	Guyana, Iwokrama Reserve; Kobacalli Landing	ANSP - 21242
Myrmothera campanisona	*Molecular*	Guyana, Potaro-Siparuni,Iwokrama Reserve; ca. 6-8 road mi. SW Kurupukari	ANSP - 22305
Myrmothera campanisona	*Molecular*	Ecuador, Morona-Santiago,Santiago	ANSP - 16450
Myrmothera campanisona	*Molecular*	Ecuador, Morona-Santiago,5 km SW Taisha	ANSP - 17546
Myrmothera campanisona	*Molecular*	Ecuador, Napo, Zancudo Cocha	ANSP - 18324
Myrmothera campanisona	*Molecular*	Ecuador, Napo, Pasohurco; km 57 on Hollin-Loreto Road	ANSP - 19457
Myrmothera campanisona	*Molecular*	Brazil, Rondonia, Cachoeira Nazare, W bank Rio Jiparana, 100m	FMNH - 389886
Myrmothera campanisona	*Molecular*	Brazil, Rondonia, Cachoeira Nazare, W bank Rio Jiparana, 100m	FMNH - 389885
Myrmothera campanisona	*Molecular*	Peru: Madre de Dios: Moskitania, 13.4 km NNW Atalaya	FMNH - 433464
Myrmothera campanisona	*Molecular*	Brazil, Acre, Reserva Extravista Alto Jurua, Rio Tejo,	FMNH - 395576
Myrmothera campanisona	*Molecular*	Brazil, Rondonia, Cachoeira Nazare, W bank Rio Jiparana, 100m	FMNH - 395993

Myrmothera campanisona	*Molecular*	Peru, Madre de Dios, Moskitania, 13.4 km NNW Atalaya	FMNH - 433462
Myrmothera campanisona	*Molecular*	Guyana: Parabara Savannah	KU - B12708
Myrmothera campanisona	*Molecular*	Guyana: Upper Essequibo River	USNM - 625540
Myrmothera campanisona	*Molecular*	Guyana: Parabara Savannah	USNM - 622361
Myrmothera campanisona	*Molecular*	Upper Takutu - Upper Essequibo, lower Rewa River	USNM - 637266
Myrmothera campanisona	*Molecular*	Barima-Waini, Baramita, In Former North West Region	USNM - 621449
Myrmothera campanisona	*Molecular*	Barima-Waini, Baramita, In Former North West Region	USNM - 586403
Myrmothera campanisona	*Molecular*	Gunn'S Landing, West Bank Upper Essequibo River	USNM - 616546
Myrmothera campanisona	*Molecular*	Peru, Loreto Department, S bank Maranon R., Est. Biol. Pithecia	LSUMZ - B3617
Myrmothera campanisona	*Molecular*	Bolivia, Pando Department, Nicolás Suarez; 12 km by road S of Cobija	LSUMZ - B9600
Myrmothera campanisona	*Molecular*	Bolivia, Pando Department, Nicolás Suarez; 12 km by road S of Cobija	LSUMZ - B8955
Myrmothera campanisona	*Molecular*	Peru, Loreto Department, Ca. 86 km SE Juanjui on E bank upper Rio Pauya	LSUMZ - B39839
Myrmothera campanisona	*Molecular*	Peru, Loreto Department, Ca 7 km S Jeberos	LSUMZ - B42523
Myrmothera campanisona	*Molecular*	Peru, Loreto Department, 1 km N Rio Napo, 157 km by river NNE Iquitos	LSUMZ - B2867
Myrmothera campanisona	*Molecular*	Peru, Loreto Department, 79 km WNW Contamana, ca	LSUMZ - B27991
Myrmothera campanisona	*Molecular*	Peru, Loreto Department, S Rio Amazonas, ca 10km SSW mouth Rio Napo	LSUMZ - B5066
Myrmothera campanisona	*Molecular*	Peru, Loreto Department, S bank Maranon River, Est. Biol. Pithecia.	LSUMZ - 103576
Myrmothera campanisona	*Molecular*	Peru, Loreto Department, Lower Rio Napo region, E bank Rio Yanayacu,	LSUMZ - B4346
Myrmothera campanisona	*Molecular*	Peru, Loreto Department, Lower Rio Napo region, E. bank Rio Yanayacu	LSUMZ - B4172
Myrmothera campanisona	*Molecular*	Peru, Loreto Department, 79 km WNW Contamana, ca	LSUMZ - B27987
Myrmothera campanisona	*Molecular*	Venezuela, Amazonas Territory, CERRO DE LA NEBLINA BASE CAMP 140M	LSUMZ - B7563
Mymothera Campanisona D	Morphology	Guyana: Bartica Grove	90595-USNM
Mymothera Campanisona D	Morphology	Guyana: Iwokrana Reserve; ca 41 rd. KM SW Kurupukari; 100m	188777-ANSP
Mymothera Campanisona D	Morphology	Brit. Guyana: Ourumme	51071-ANSP
Mymothera Campanisona D	Morphology	Brit. Guiana: Riv Takutu	492333-AMNH
Mymothera Campanisona D	Morphology	Brazil: R. Amazon, N. Bank, Faro: R. Jamunda, Castanhal	283954-AMNH
Mymothera Campanisona D	Morphology	Brit. Guiana: Riv Takutu	492332-AMNH

Mymothera Campanisona D	Morphology	Brit. Guiana: Tumatumari, Potaro River	125716-AMNH
Mymothera Campanisona D	Morphology	Brit. Guiana: Kartabo	805766-AMNH
Mymothera Campanisona D	Morphology	Brit. Guiana: Kartabo	805765-AMNH
Mymothera Campanisona D	Morphology	Brit. Guiana: Kartabo	805764-AMNH
Mymothera Campanisona D	Morphology	French Guiana: Jamanaio, Mana R.	233860-AMNH
Mymothera Campanisona D	Morphology	French Guiana: Jamanaio, Mana R.	233861-AMNH
Mymothera Campanisona D	Morphology	Cayenne: Ipousin, Approuaque R.	492334-AMNH
Mymothera Campanisona D	Morphology	French Guiana: Jamanaio, Mana R.	233862-AMNH
Mymothera Campanisona D	Morphology	Brazil: R. Amazon, N. Bank, Faro: R. Jamunda, Castanhal	283953-AMNH
Mymothera Campanisona D	Morphology	Brazil: R. Amazon, N. Bank, Faro: Boca R. Pirarucu	283955-AMNH
Mymothera Campanisona D	Morphology	Brazil: R. Amazon, N. Bank, Faro: R. Jamunda, Castanhal	283952-AMNH
Mymothera Campanisona D	Morphology	Brazil: R. Amazon, N. Bank, Faro: R. Jamunda, Castanhal	283951-AMNH
Mymothera Campanisona D	Morphology	Guyana; Upper Essequibo River, 01º35´N 058º38´W, 225M	625540-USNM
Mymothera Campanisona C	Morphology	Peru: Sandia, Huacamayo	103264-ANSP
Mymothera Campanisona C	Morphology	Peru: Sandia, Huacamayo	103265-ANSP
Mymothera Campanisona C	Morphology	Peru: Sandia, Huacamayo	103263-ANSP
Mymothera Campanisona C	Morphology	Peru: Shapaja; Rio Huallaga	117470-ANSP
Mymothera Campanisona C	Morphology	Peru: Dept. Loreto, S bank of Rio maraño on rio Samiria	177840-ANSP
Mymothera Campanisona C	Morphology	Peru: Dept. Loreto, S bank of Rio maraño on rio Samiria	177841-ANSP
Mymothera Campanisona C	Morphology	Peru: Lower Rio Marañon, Pomará	185760-AMNH
Mymothera Campanisona C	Morphology	Peru: Oroja, R. Amazonas	231936-AMNH
Mymothera Campanisona C	Morphology	Peru: Oroja, R. Amazonas	231937-AMNH
Mymothera Campanisona C	Morphology	Peru: N. E. Rio Negro, W. Of Moyabamba	234693-AMNH
Mymothera Campanisona C	Morphology	Peru: Boca R. Umbamba	240341-AMNH
Mymothera Campanisona C	Morphology	Peru: Pomará, Rio Maraño	182048-AMNH
Mymothera Campanisona C	Morphology	Peru: Prov. Huánuco, Chuchurras	492338-AMNH
Mymothera Campanisona C	Morphology	Peru: Mta Rosa, Alto Ucayali	240340-AMNH

Mymothera Campanisona C	Morphology	Peru: Lagarto, Alto Ucayali	239274-AMNH
Mymothera Campanisona C	Morphology	Brazil: Amazonas, Rio Maturaca	326448-USNM
Mymothera Campanisona C	Morphology	Brazil: Venezuela, Brazo Casiquiare, Cano Caripo, below	327110-USNM
Mymothera Campanisona C	Morphology	Brazil: Salto Do Hua, Rio Maturaca	326446-USNM
Mymothera Campanisona C	Morphology	Brazil: Salto Do Hua, Rio Maturaca	326449-USNM
Mymothera Campanisona C	Morphology	Guyana: North West; Baramita, 07º22´N, 60º29´W 125 M	586403-USNM
Mymothera Campanisona C	Morphology	Brazil: Venezuela, Chapazon, Brazo Casiquiare	327111-USNM
Mymothera Campanisona C	Morphology	Brazil: Serra Imeri, near Salto Do Hua	326450-USNM
Mymothera Campanisona C	Morphology	Colombia: Putumayo, Umbria	160036-ANSP
Mymothera Campanisona C	Morphology	Brazil: Amazonas, Rio Maturaca	143135-ANSP
Mymothera Campanisona C	Morphology	Venezuela: Rio Negro	8193-ANSP
Mymothera Campanisona C	Morphology	Brazil: Rio Negro, Javanari	310745-AMNH
Mymothera Campanisona C	Morphology	Brazil: Rio Madeira, Rosarinho	282119-AMNH
Mymothera Campanisona C	Morphology	Venezuela: La Laja. Rio Orinoco, Ven, MT. Duida	273000-AMNH
Mymothera Campanisona C	Morphology	Venezuela: Caño Seou. Rio Orinoco, Serra Duida	272999-AMNH
Mymothera Campanisona C	Morphology	Venezuela: Rio Cassiquiare, L. bank, El Merey	423644-AMNH
Mymothera Campanisona C	Morphology	Colombia: Caqueta, La Murelia (R. Bodoquera)	116349-AMNH
Mymothera Campanisona C	Morphology	Colombia: Caqueta, La Murelia (R. Bodoquera)	116348-AMNH
Mymothera Campanisona C	Morphology	Colombia: Bogota?	492340-AMNH
Mymothera Campanisona C	Morphology	Colombia: Caqueta, Florencia	116347-AMNH
Mymothera Campanisona C	Morphology	Colombia: Caqueta, Florencia	116346-AMNH
Mymothera Campanisona C	Morphology	Brazil: Rio Madeira, Rosarinho, Lago sampaio	282120-AMNH
Mymothera Campanisona C	Morphology	Venezuela: Playa dil Rio Bare, Mte. Duida	273003-AMNH
Mymothera Campanisona C	Morphology	Brazil: Rio Negro, São Gabriel	276106-AMNH
Mymothera Campanisona C	Morphology	Venezuela: Campamento del Medio, Mt Duida	270917-AMNH
Mymothera Campanisona C	Morphology	Brazil: Rio Negro, Cacao Pereria Igarapé	313086-AMNH
Mymothera Campanisona C	Morphology	Venezuela: La Laja. Rio Orinoco, Ven, MT. Duida	273001-AMNH

Mymothera Campanisona C	Morphology	Brazil: Rio Negro, Tatú	AMNH
Mymothera Campanisona C	Morphology	Venezuela: Rio Cassiquiare, R. bank, Opposite El Merey	423645-AMNH
Mymothera Campanisona C	Morphology	Venezuela: Rio Huaynia junction with Rio Cassiquiare, R. Bank	423646-AMNH
Mymothera Campanisona C	Morphology	Venezuela: Campamento del Medio, Mt Duida	273002-AMNH
Mymothera Campanisona C	Morphology	Brazil: Rio Negro, São Gabriel	276105-AMNH
Mymothera Campanisona C	Morphology	Venezuela: Rio Cassiquiare, L. bank, El Merey	417394-AMNH
Mymothera Campanisona C	Morphology	Venezuela: Rio Cassiquiare, R. bank, Opposite El Merey	417393-AMNH
Mymothera Campanisona C	Morphology	Peru: Rio Apurimac, Luisiana (12º39´S, 73º 44´W)	819711-AMNH
Mymothera Campanisona C	Morphology	Peru: Rio Apurimac, HDA. Luisiana, ca. 500m	788334-AMNH
Mymothera Campanisona B	Morphology	Brazil: Rio Tapajós, Limoal	288618-AMNH
Mymothera Campanisona B	Morphology	Brazil: Calama, Rio Machados (Confl. Of R. Madeira)	492336-AMNH
Mymothera Campanisona B	Morphology	Brazil: Rondonia, Mun. Porto Velho, Fazenda Rio Candeias	35156-MPEG
Mymothera Campanisona B	Morphology	Brazil: Pará, Mun. Juruti, Plato Capiranga, Trilha 196	60975-MPEG
Mymothera Campanisona B	Morphology	Brazil: Pará, Mun. Jacareacanga, Vila mamãe-anã	75730-MPEG
Mymothera Campanisona B	Morphology	Brazil: Rondonia, Cachoeira Nazaré, west bank Rio Jiparaná	39823-MPEG
Mymothera Campanisona B	Morphology	Brazil: Rondonia, Cachoeira Nazaré, west bank Rio Jiparaná	39824-MPEG
Mymothera Campanisona B	Morphology	Brazil: Rondonia, Cachoeira Nazaré, west bank Rio Jiparaná	39825-MPEG
Mymothera Campanisona B	Morphology	Brazil: Rondonia, Cachoeira Nazaré, west bank Rio Jiparaná	39826-MPEG
Mymothera Campanisona B	Morphology	Brazil: Rondonia, Cachoeira Nazaré, west bank Rio Jiparaná	39827-MPEG
Mymothera Campanisona A	Morphology	Brazil: Rio Tapajós, Igarape Brabo	286762-AMNH
Mymothera Campanisona A	Morphology	Brazil: Rio Tapajós, Aramanay	288757-AMNH
Mymothera Campanisona A	Morphology	Brazil: Rio Tapajós, Igarape Brabo	286760-AMNH
Mymothera Campanisona A	Morphology	Brazil: Pará, Mun. Itaituba, Prox. Penedo MI4	76458-MPEG
Mymothera Campanisona A	Morphology	Brazil: Pará, Rod. Transamazônica, Km 25, Rio Tapacurazinho	34421-MPEG
Mymothera Campanisona A	Morphology	Brazil: Pará, Rod. Transamazônica, Km 25, Rio Tapacurazinho	47846-MPEG
Mymothera Campanisona A	Morphology	Brazil: Pará, Rio Xingu, Caracol	65325-MPEG
Mymothera Campanisona A	Morphology	Brazil: Pará, Altamira, Flona de Altamira	63897-MPEG

Mymothera Campanisona A	Morphology	Brazil: Pará,Mun. Altamira, Rio Xingu Margem Esquerda	55488-MPEG
Mymothera Campanisona A	Morphology	Brazil: Pará,Mun. Altamira, Rio Xingu Margem Esquerda	55489-MPEG
Hylopezus whittakeri	Morphology	Brazil: Calama, Rio Machados, Confl. Of Rio Madeira	492297-AMNH
Hylopezus whittakeri	Morphology	Brazil: Rio Tapajós, Limoal	288617-AMNH
Hylopezus whittakeri	Morphology	Pará. santarém-cuiabá km 84 (santarém ruropolís).	47847-MPEG
Hylopezus whittakeri	Morphology	Mato grosso. rio aripijanã. dardanelos	34420-MPEG
Hylopezus whittakeri	Morphology	Mato grosso. rio aripijanã. dardanelos nucleo pioneiro humbolt	45606-MPEG
Hylopezus whittakeri	Morphology	RO. alvorada d'oeste linha 64 br 429 km 87	38808-MPEG
Hylopezus whittakeri	Morphology	Rondônia. cachoeira nazaré. west bank of rio jiparaná	MG39819-MPEG
Hylopezus whittakeri	Morphology	Rondônia. cachoeira nazaré. west bank of rio jiparaná	MG39820-MPEG
Hylopezus whittakeri	Morphology	Rondônia. cachoeira nazaré. west bank of rio jiparaná	MG39821-MPEG
Hylopezus whittakeri	Morphology	AM. mun. humaitá. t. i. parintintin; aldeia traíra-chororó	58757-MPEG
Hylopezus whittakeri	Morphology	brasil. pará. belterra. flona do tapajós. base sucupira.	56099-MPEG
Hylopezus whittakeri	Morphology	MT-Mun.Paranaitá, Faz. Rio Paranaitá, Margem direita do Rio Paranaitá.	MG67501-MPEG
Hylopezus whittakeri	Morphology	MT-Mun.Paranaitá, Faz. Aliança, Margem esquerda do Rio Paranaitá.	MG69333-MPEG
Hylopezus whittakeri	Morphology	MT-Mun.Paranaitá, Rio Teles Pires Margem direita.	MG69334-MPEG
Hylopezus whittakeri	Morphology	Brazil: Pará. r tapajós. fordlândia	58838-MZUSP
Hylopezus whittakeri	Morphology	Brazil: Pará. rio jamary	21895-MNRJ
Hylopezus whittakeri	Morphology	Brazil: Santarem, R. Amazon	21365-CMNH
Hylopezus whittakeri	Morphology	Brazil: Colonia de Mojui, Santarem	22035-CMNH
Hylopezus whittakeri	Morphology	Brazil: Colonia de Mojui, Santarem	22034-CMNH
Hylopezus whittakeri	Morphology	Brazil: Colonia de Mojui, Santarem	21729-CMNH
Hylopezus whittakeri	Morphology	Brazil: Colonia de Mojui, Santarem	21826-CMNH
Hylopezus whittakeri	Morphology	Brazil: Vila Braga, R. Tapajos	22994-CMNH
Hylopezus whittakeri	Morphology	Brazil: Vila Braga, R. Tapajos	23119-CMNH
Hylopezus whittakeri	Morphology	Brazil: Miriti tuba, R. Tapajos	24624-CMNH
Hylopezus whittakeri	Morphology	Brazil: Santarem, R. Amazon	25166-CMNH

Hylopezus whittakeri	Morphology	Brazil: Vila Braga, R. Tapajos	313767-USMN
Hylopezus whittakeri	Vocal	Brazil: Porto Velho, Rondonia	XC189546
Hylopezus whittakeri	Vocal	Brazil: Mato Grosso, Reserva Ecologica Cristalino, Trilha de Jozias	MLS89010
Hylopezus whittakeri	Vocal	Brazil: Mato Grosso, W of Rio Cristalino, Reserva Ecologica Cristalino	MLS88479
Hylopezus whittakeri	Vocal	Brazil: Mato Grosso, S of Rio Teles Pires	MLS52318
Hylopezus whittakeri	Vocal	Brazil: Mato Grosso, 25.0 km N of Alta Floresta	MLS48111
Hylopezus whittakeri	Vocal	Brazil: Mato Grosso, 20.0 km N of Alta Floresta	MLS48068
Hylopezus whittakeri	Vocal	Brazil: Rondônia, Cachoeira Nazare; west bank of Rio Jiparana	MLS40236
Hylopezus whittakeri	Vocal	Brazil: Pará, Floresta Nacional de Tapajos; Base de Sucupira, BR-163	MLS115081
Hylopezus whittakeri	*Molecular*	Pará, Jacareacanga, margem direita Rio Tapajós, Comunidade São Martim	MPEG - 18511
Hylopezus whittakeri	*Molecular*	Pará, Itaituba, leste do Tapajós, Rio Ratão	MPEG - 18776
Hylopezus whittakeri	*Molecular*	Pará, Itaituba, leste do Tapajós, Jatobá	MPEG - 18803
Hylopezus whittakeri	*Molecular*	Pará, Jacareacanga, margem direita Rio Crepori	MPEG - 19599
Hylopezus whittakeri	*Molecular*	Alvorada d'Oeste, Linha 64, Br 429 Km 87	MPEG - 38808
Hylopezus whittakeri	*Molecular*	Cachoeira Nazaré, west bank Rio Ji-paraná	MPEG - 39819
Hylopezus whittakeri	*Molecular*	Cachoeira Nazaré, west bank Rio Ji-paraná	MPEG - 39820
Hylopezus whittakeri	*Molecular*	Cachoeira Nazaré, west bank Rio Ji-paraná	MPEG - 39821
Hylopezus whittakeri	*Molecular*	Município de Humaitá, T. Indígena Parintintin, Aldeia Traíra-Chororó	MPEG - MPD719
Hylopezus whittakeri	*Molecular*	Paranaíta, margem direita Rio Paranaíta, Fazenda Rio Paranaíta	MPEG - TLP178
Hylopezus whittakeri	*Molecular*	Paranaíta, margem direita Rio Paranaíta, Fazenda Rio Paranaíta	MPEG - TLP179
Hylopezus whittakeri	*Molecular*	Paranaíta, margem esquerda Rio Paranaíta, Fazenda Aliança	MPEG - TLP404
Hylopezus whittakeri	*Molecular*	Paranaíta, Rio Teles Pires, margem direita	MPEG - TLP095
Hylopezus perspicillatus B	Morphology	Colombia: Cordoba, Socorre, Rio Sinu, 1.5 mi below mouth Rio Verde	411881-USNM
Hylopezus perspicillatus B	Morphology	Colombia: Cordoba, Socorre, Rio Sinu, 1.5 mi below mouth Rio Verde	411887-USNM
Hylopezus perspicillatus B	Morphology	Colombia: Cordoba, Socorre, Rio Sinu, 1.5 mi below mouth Rio Verde	411886-USNM
Hylopezus perspicillatus B	Morphology	Colombia: Cordoba, Quebrada Salvajin, Rio Esmeralda, Upper Rio Sinu	411888-USNM
Hylopezus perspicillatus B	Morphology	Colombia: Cordoba, Quebrada Salvajin, Rio Esmeralda, Upper Rio Sinu	411890-USNM

Hylopezus perspicillatus B	Morphology	Colombia: Cordoba, Quebrada Salvajin, Rio Esmeralda, Upper Rio Sinu	411879-USNM
Hylopezus perspicillatus B	Morphology	Colombia: Antioquia, Hacienda Belen, 8 mi W of Segovia	402484-USNM
Hylopezus perspicillatus B	Morphology	Colombia: Antioquia, Hacienda Belen, 8 mi W of Segovia	402481-USNM
Hylopezus perspicillatus B	Morphology	Colombia: Antioquia, Hacienda Belen, 8 mi W of Segovia	402482-USNM
Hylopezus perspicillatus B	Morphology	Colombia: Antioquia, El Real, Rio Nechi	402485-USNM
Hylopezus perspicillatus B	Morphology	Colombia: Antioquia, Taraza, Rio Taraza, 12 km NW Pto. Antioquia	402486-USNM
Hylopezus perspicillatus B	Morphology	Colombia: Bolivar, Santa Rosa, Simiti, 15 mi W	398006-USNM
Hylopezus perspicillatus B	Morphology	Colombia: Bolivar, Santa Rosa, Simiti, 15 mi W	398004-USNM
Hylopezus perspicillatus B	Morphology	Colombia: Cordoba, Socorre, Rio Sinu, 1.5 mi below mouth Rio Verde	411884-USNM
Hylopezus perspicillatus B	Morphology	Colombia: Santander, Conchal, 8 mi NE, Hacienda Santana, on railroad to Wilches	411892-USNM
Hylopezus perspicillatus B	Morphology	Colombia: Santander, Conchal, 8 mi NE, Hacienda Santana, on railroad to Wilches	411891-USNM
Hylopezus perspicillatus B	Morphology	Colombia: Bolivar, Santa Rosa, Simiti, 15 mi W	398005-USNM
Hylopezus perspicillatus B	Morphology	Colombia: Bolivar, Santa Rosa, Simiti, 15 mi W	398007-USNM
Hylopezus perspicillatus B	Morphology	Colombia: Antioquia, Hacienda Belen, 8 mi W of Segovia	402483-USNM
Hylopezus perspicillatus B	Morphology	Colombia: Antioquia, Hacienda Belen, 8 mi W of Segovia	402479-USNM
Hylopezus perspicillatus B	Morphology	Colombia: Cordoba, Quebrada Salvajin, Rio Esmeralda, Upper Rio Sinu	411878-USNM
Hylopezus perspicillatus B	Morphology	Colombia: Cordoba, Quebrada Salvajin, Rio Esmeralda, Upper Rio Sinu	411889-USNM
Hylopezus perspicillatus B	Morphology	Colombia: Cordoba, Quebrada Salvajin, Rio Esmeralda, Upper Rio Sinu	411882-USNM
Hylopezus perspicillatus B	Morphology	Colombia: Cordoba, Quebrada Salvajin, Rio Esmeralda, Upper Rio Sinu	411880-USNM
Hylopezus perspicillatus B	Morphology	Colombia: Cordoba, Socorre, Rio Sinu, 1.5 mi below mouth Rio Verde	411885-USNM
Hylopezus perspicillatus B	Morphology	Colombia: Cordoba, Socorre, Rio Sinu, 1.5 mi below mouth Rio Verde	411883-USNM
Hylopezus perspicillatus B	Morphology	Colombia: Southern Dep. Cordoba, Upper quebr. Charrura,	787157-AMNH
Hylopezus perspicillatus B	Morphology	Colombia: Antioquia, Cauca R., Puerto Valdivia	133534-AMNH
Hylopezus perspicillatus A	Morphology	Ecuador: Rio Tepayo	331277-USNM
Hylopezus perspicillatus A	Morphology	Colombia: Choco, Rio Nuqui, Baudo Mountains, base	443346-USNM
Hylopezus perspicillatus A	Morphology	Colombia: Choco, Rio Nuqui, Baudo Mountains, base Lat 5º40	443349-USNM
Hylopezus perspicillatus A	Morphology	Colombia: Choco, Rio Jurubidá, Baudo Mountains, base Lat 5º58´	443353-USNM

Hylopezus perspicillatus A	Morphology	Colombia: Choco, Rio Jurubidá, Baudo Mountains, base Lat 5º58´	443355-USNM
Hylopezus perspicillatus A	Morphology	Colombia: Antioquia, Villa Artiaga, 7 km NE Pavarondocito	426432-USNM
Hylopezus perspicillatus A	Morphology	Colombia: Choco, Rio Jurubidá, Baudo Mountains, base Lat 5º58´	443352-USNM
Hylopezus perspicillatus A	Morphology	Colombia: Choco, Rio Nuqui, Baudo Mountains, base Lat 5º40	443348-USNM
Hylopezus perspicillatus A	Morphology	Colombia: Antioquia, Villa Artiaga, 7 km NE Pavarondocito	426433-USNM
Hylopezus perspicillatus A	Morphology	Colombia: Antioquia, Villa Artiaga, 7 km NE Pavarondocito	426434-USNM
Hylopezus perspicillatus A	Morphology	Colombia: Antioquia, Villa Artiaga, 7 km NE Pavarondocito	426435-USNM
Hylopezus perspicillatus A	Morphology	Colombia: Choco, Rio Nuqui, Baudo Mountains, base Lat 5º40	443347-USNM
Hylopezus perspicillatus A	Morphology	Colombia: Choco, Rio Jurubidá, Baudo Mountains, base Lat 5º58´	443354-USNM
Hylopezus perspicillatus A	Morphology	Colombia: Choco, Rio Nuqui, Baudo Mountains, base Lat 5º40	443350-USNM
Hylopezus perspicillatus A	Morphology	Colombia: Choco, Rio Nuqui, Baudo Mountains, base Lat 5º40	443351-USNM
Hylopezus perspicillatus A	Morphology	Ecuador: San Javier, N	492293-AMNH
Hylopezus perspicillatus A	Morphology	Ecuador: N, Pambilar	492290-AMNH
Hylopezus perspicillatus A	Morphology	Ecuador: N, Lita	492291-AMNH
Hylopezus perspicillatus A	Morphology	Ecuador: N, Cachabí	492281-AMNH
Hylopezus perspicillatus A	Morphology	Ecuador: San Javier, N	492292-AMNH
Hylopezus perspicillatus A	Morphology	Ecuador: N, Bulum	492288-AMNH
Hylopezus perspicillatus A	Morphology	Ecuador: N, Bulum	492289-AMNH
Hylopezus perspicillatus A	Morphology	Colombia: Choco, River Salaqui	113349-AMNH
Hylopezus perspicillatus A	Morphology	Colombia: N. Chocó, Rio Truandó	787156-AMNH
Hylopezus perspicillatus A	Morphology	Colombia: Choco, Baudo	123355-AMNH
Hylopezus perspicillatus A	Morphology	Colombia: N. Chocó, Upper Rio Murrí	787158-AMNH
Hylopezus perspicillatus A	Morphology	Colombia: Choco, Baudo	123352-AMNH
Hylopezus perspicillatus A	Morphology	Colombia: Choco, Baudo	123353-AMNH
Hylopezus perspicillatus A	Morphology	Colombia: Choco, Baudo	123354-AMNH
Hylopezus perspicillatus A	Morphology	Colombia: West, Narino Barbacoas	117882-AMNH
Hylopezus perspicillatus A	Vocal	Ecuador: Playa de Oro, Esmeraldas	XC98206

Hylopezus perspicillatus A	Vocal	Ecuador: Playa de Oro, Esmeraldas	XC62212
Hylopezus perspicillatus A	Vocal	Ecuador: Reserva Ecologica Cotacachi-Cayapas, Esmeraldas	XC11867
Hylopezus perspicillatus A	Vocal	Ecuador: Playa de Oro, Esmeraldas Province, Ecuador	XC112253
Hylopezus Perspicillatus A	Vocal	Ecuador: Esmeraldas, 20.0 km NW of Alto Tambo	MLS63195
Hylopezus perspicillatus	*Molecular*	Colombia: Santander, Flores Blancas	LSUMZ - 36133
Hylopezus perspicilatus	*Molecular*	Ecuador, Esmeraldas, 20 road km NNW Alto Tambo	ANSP - 17269
Hylopezus perspicilatus	*Molecular*	Ecuador, Esmeraldas, 30 km S Chontaduro; W bank Rio Verde	ANSP - 19055
Hylopezus paraensis	Morphology	Brazil: Pa. paragomimas. fazenda rio capim. cikel	58982-MPEG
Hylopezus paraensis	Morphology	Brazil: PA: Rio acará	1670-MPEG
Hylopezus paraensis	Morphology	PA: Rio Xingu. (Area 2) Caracol, Marg. Direita	65326-MPEG
Hylopezus paraensis	Morphology	PA: Rio Xingu. MARGEM DIREITA CARACOL	64919-MPEG
Hylopezus paraensis	Morphology	Brazil: Pará. mun. ourém. faz. reunida rio ducê. igarapé pedral	32407-MPEG
Hylopezus paraensis	Morphology	Brazil: Pará. mun. ourém. faz. reunida rio ducê. igarapé pedral	32408-MPEG
Hylopezus paraensis	Morphology	Brazil: Pará. senador josé porfirio. margem direita do rio xingu	55691-MPEG
Hylopezus paraensis	Morphology	Brazil: Ma-mun. carutapera. faz. sta. bárbara. rio gurupi	36922-MPEG
Hylopezus paraensis	Morphology	Brazil: Pará. rodovia belem-brasilia km 307.	18127-MPEG
Hylopezus paraensis	Morphology	Brazil: Rodovia belém-brasilia-km 92.pará	15940-MPEG
Hylopezus paraensis	Morphology	Brazil: PA -utinga	36544-MZUSP
Hylopezus paraensis	Morphology	Brazil: Pará-mum.capim-estr.bélem-brasilia km 93.	45208-MZUSP
Hylopezus paraensis	Morphology	Brazil: Pará-mum.capim-estr.bélem-brasilia km 93.	45205-MZUSP
Hylopezus paraensis	Morphology	Brazil: Pará-mum.capim-estr.bélem-brasilia km 93.	45206-MZUSP
Hylopezus paraensis	Morphology	Brazil: Pará-mum.capim-estr.bélem-brasilia km 93.	45207-MZUSP
Hylopezus paraensis	Morphology	Brazil: Utinga-bélem-pa	36543-MZUSP
Hylopezus paraensis	Vocal	Brazil: Paragominas, PA, Brazil, Bacia 549	XC86163
Hylopezus paraensis	Vocal	Brazil: Serra dos Carajás, PA	XC20410
Hylopezus paraensis	Vocal	Brazil: Belo Monte, right bank of Rio Xingu, Pará	XC18925
Hylopezus paraensis	Vocal	Brazil: Pará, Goianésia do Pará	XC155520

Hylopezus paraensis	Vocal	Brazil: Pará, 250.0 km NW of Reserva Indigena Gorotire; Redencao	MLS94535
Hylopezus paraensis	Vocal	Brazil: Pará, Floresta Nacional de Caxiuana; Estacao Cientifica Ferreira Penna	MLS127444
Hylopezus paraensis	Vocal	Brazil: Pará, Floresta Nacional de Caxiuana; Estacao Cientifica Ferreira Penna	MLS113118
Hylopezus paraensis	*Molecular*	Rio Gurupi, Carutapera, Fazenda Santa Bárbara	MPEG - 36922
Hylopezus paraensis	*Molecular*	Brazil: Rondonia, Cachoeira Nazare, W bank Rio Jiparana	FMNH - 389869
Hylopezus paraensis	*Molecular*	Rio Xingu, margem direita, Senador José Porfírio	MPEG - UHE388
Hylopezus paraensis	*Molecular*	Paragominas, Fazenda Rio Capim, CIKEL	MPEG - FRC078
Hylopezus paraensis	*Molecular*	Rio Xingu, margem direita, Caracol (área 2)	MPEG - BMP074
Hylopezus ochroleucus	Vocal	Brazil: Caetité, state of Bahia, 5 Km south from Brejinho das Ametistas	XC200963
Hylopezus ochroleucus	Vocal	Brazil: Tianguá, Tianguá, State of Ceará	XC202306
Hylopezus ochroleucus	Vocal	Brazil: Cavernas do PeruaÃ§u National Park	XC80442
Hylopezus ochroleucus	Vocal	Brazil: Araripe National Forest, Crato, Ceará State	XC201319
Hylopezus ochroleucus	Vocal	Brazil: Road to Remanso, Lençois, Chapada Diamantina, BA	XC18166
Hylopezus ochroleucus	Vocal	Brazil: Bahia, Sebastiao Laranjeiras	MLS91034
Hylopezus ochroleucus	*Molecular*	Piauí, São Raimundo Nonato, PN Serra da Capivara, Serra Vermelha	MPEG - 18943
Hylopezus ochroleucus	*Molecular*	Piauí, Caracol, PN Serra das Confusões, Projeto Cajugaia	MPEG - 18962
Hylopezus ochroleucus	*Molecular*	Piauí, Cristino Castro, PN Serra das Confusões, Baixo Japecanga	MPEG - 18984
Hylopezus ochroleucus	*Molecular*	Piauí, Cristino Castro, PN Serra das Confusões, Baixo Japecanga	MPEG - 18985
Hylopezus ochroleucus	*Molecular*	Piauí, Caracol, P. N. Serra das Confusões, Centro de Visitantes	MPEG - 20156
Hylopezus ochroleucus	*Molecular*	Morro Cabeça no Tempo, Serra Vermelha	MPEG - SRV104
Hylopezus ochroleucus	*Molecular*	Curimatá, Serra Vermelha	MPEG - SRV004
Hylopezus ochroleucus	*Molecular*	Brazil: Minas Gerais; Mocambinho, Jaíba	LGEMA - 2318
Hylopezus ochroleucus	*Molecular*	Brazil: Minas Gerais; Mocambinho, Jaíba	LGEMA - 2036
Hylopezus ocholeucus	Morphology	Brazil: Bahia, Centro oriente.	243146-AMNH
Hylopezus ocholeucus	Morphology	Brazil: Bahia, Ibianeira, Fazenda Bananeira	51162-MPEG
Hylopezus ocholeucus	Morphology	Brazil: Piaui, Morro Cabeça no Tempo, Serra Vermelha	68134-MPEG
Hylopezus ocholeucus	Morphology	Brazil: Piaui, Mun. Curimatá, Serra Vermelha	68135-MPEG

Hylopezus ocholeucus	Morphology	Brazil: Piaui, Mun. São Raimundo Nonato, PN serra da Capivara,	75481-MPEG
Hylopezus ocholeucus	Morphology	Brazil: Piaui, Mun. Caracol, PN serra das Confusões	75511-MPEG
Hylopezus ocholeucus	Morphology	Brazil: Piaui, Mun. Caracol, PN serra das Confusões	76083-MPEG
Hylopezus ocholeucus	Morphology	Brazil: Piaui, Mun. São Raimundo Nonato, PN serra da Capivara, Zabelê	76761-MPEG
Hylopezus ocholeucus	Morphology	Brazil: Piaui, Mun. Cristino Castro, PN serra das Confusões,	76770-MPEG
Hylopezus nattereri	Morphology	Brazil: Paraná, Corvo (Serra da Graciosa)	318523-AMNH
Hylopezus nattereri	Morphology	Brazil: Rio Grande do Sul, São Francisco de Penha	314615-AMNH
Hylopezus nattereri	Morphology	Argentina: Misiones, Arroyo Uruguai-i, Km 30	771188-AMNH
Hylopezus nattereri	Morphology	Argentina: Misiones, Arroyo Uruguai-i, Km 30	771189-AMNH
Hylopezus nattereri	Morphology	Argentina: Misiones, Arroyo Uruguai-i, Km 30	771187-AMNH
Hylopezus nattereri	Morphology	Argentina: Misiones, Arroyo Uruguai-i, Km 30	771186-AMNH
Hylopezus nattereri	Morphology	Argentina: Misiones, Arroyo Uruguai-i, Km 30	771185-AMNH
Hylopezus nattereri	Morphology	Argentina: Misiones, Arroyo Uruguai-i, Km 30	771184-AMNH
Hylopezus nattereri	Morphology	Argentina: Misiones, Arroyo Uruguai-i, Km 10	795287-AMNH
Hylopezus nattereri	Vocal	Brazil: Quatro Barras, Paraná State	XC90459
Hylopezus nattereri	Vocal	Brazil: Itatiaia NP, Tres Picos trail, RJ	XC62448
Hylopezus nattereri	Vocal	Paraguay: Santa Ines, San Rafael, Itapua	XC55422
Hylopezus nattereri	Vocal	Brazil: APA Capivari Monos, São Paulo, SP	XC187632
Hylopezus nattereri	Vocal	Brazil: Sitio Água da rainha , São Francisco de Paula, RS	XC109986
Hylopezus nattereri	Vocal	Brazil: São Paulo, Estacao Biologica de Boraceia	MLS63615
Hylopezus nattereri	Vocal	Brazil: Rio Grande do Sul, Faz. da Zamoreira	MLS20069
Hylopezus nattereri	Vocal	Brazil: Rio Grande do Sul, 5.0 km SE of Canela; Morro Pelado	MLS19813
Hylopezus nattereri	Vocal	Brazil: Rio Grande do Sul, 15.0 km from Sao Francisco De Paula	MLS19292
Hylopezus nattereri	Vocal	Brazil: Rio de Janeiro, Parque Nacional Itatiaia	MLS112731
Hylopezus nattereri	*Molecular*	Quatro Barras, Corvo	MPEG - CMN024
Hylopezus nattereri	*Molecular*	Condominio Alpes- São Francisco de Paula, RS	PUCRS - 3057
Hylopezus nattereri	*Molecular*	CPCN Pró-Mata, São Francisco de Paula-RS	PUCRS - 3345

Hylopezus macularius	Morphology	French Guyana: Tamanois, Mana R.	67370-ANSP
Hylopezus macularius	Morphology	French Guyana: Tamanois, Mana R.	67371-ANSP
Hylopezus macularius	Morphology	Guyana: Iwokrana Reserve; ca 41 rd. KM SW Kurupukari; 100m;	188757-ANSP
Hylopezus macularius	Morphology	Guyana: Iwokrana Reserve; Kabocalli Landing; W. Bank essequibo river	188756-ANSP
Hylopezus macularius	Morphology	Guyana: Iwokrana Reserve; ca 3 mi SW Kurupukari; 110m;	188758-ANSP
Hylopezus macularius	Morphology	Brit. Guyana: Kartabo	805770-AMNH
Hylopezus macularius	Morphology	Brit. Guyana: Kartabo	821498-AMNH
Hylopezus macularius	Morphology	Brit. Guyana: Kartabo	821496-AMNH
Hylopezus macularius	Morphology	Brit. Guyana: Kartabo	821499-AMNH
Hylopezus macularius	Morphology	Brit. Guyana: Kartabo	821497-AMNH
Hylopezus macularius	Morphology	Brit. Guyana: Kartabo	821520-AMNH
Hylopezus macularius	Morphology	Brit. Guyana: Kartabo	805769-AMNH
Hylopezus macularius	Morphology	Brit. Guyana: Ourumme	492298-AMNH
Hylopezus macularius	Morphology	Brit. Guyana: Mines district	156296-AMNH
Hylopezus macularius	Morphology	Brit. Guyana: Mines district	492296-AMNH
Hylopezus macularius	Morphology	Brit. Guyana: River carimang	492295-AMNH
Hylopezus macularius	Morphology	Brit. Guyana: River carimang	492294-AMNH
Hylopezus macularius	Morphology	Guyanaç Gunn<s Landing, 10 KM SSE	625539-USNM
Hylopezus macularius	Morphology	Brazil, Serra do navio, Rio Amapari-Amapa	515628-USNM
Hylopezus macularius	Morphology	British Guiana, Merume Mts	90596-USNM
Hylopezus macularius	Morphology	Guyana: North West; Baramita, 07º22´N, 60º29´W 125 M	586404-USNM
Hylopezus macularius	Morphology	Brazil: Amapá. alto rio araguari. mun. macapá	21181-MPEG
Hylopezus macularius	Morphology	Brazil: Amapá afluente do rio jarí mun. mazagão-amapá	29257-MPEG
Hylopezus macularius	Morphology	Brazil: Amapá areia vermelha. mun. amapá. rio araguarí.	20427-MPEG
Hylopezus macularius	Morphology	Brazil: Amapá. foz do cacouí. afluente esquerdo do rio araguarí	21235-MPEG
Hylopezus macularius	Morphology	Brazil: Amapá. alto rio araguari. margem direita. mun. macapá	21172-MPEG
Hylopezus macularius	Morphology	Brazil: Pa. flota de faro km nw faro.01° 42's 57° 12'w	64739-MPEG

Hylopezus macularius	Morphology	Brazil: Pa:alenquer. esec grão - pará. 00° 09's 55° 11'w	66053-MPEG
Hylopezus macularius	Morphology	Brazil: Amapá. mazagão. cachoeira amapá. alto rio camaipi	28744-MPEG
Hylopezus macularius	Morphology	PA: ÓBIDOS, ESEC GRÃO PARÁ	66675-MPEG
Hylopezus macularius	Morphology	PA: ÓBIDOS, ESEC GRÃO PARÁ	66676-MPEG
Hylopezus macularius	Morphology	PA: ÓBIDOS, ESEC GRÃO PARÁ	66677-MPEG
Hylopezus macularius	Morphology	PA: ÓBIDOS, ESEC GRÃO PARÁ	66678-MPEG
Hylopezus macularius	Morphology	PA: Almeirim Rebio Maicuru	66340-MPEG
Hylopezus macularius	Morphology	Brazil: Amapá Serra do navio. rio amapari-amapá	29429-MNRJ
Hylopezus macularius	Vocal	Brazil: Amazonas, 80.0 km N of Manaus	MLS74427
Hylopezus macularius	Vocal	Guyana: Upper Takutu-Upper Essequibo, 20.0 km E of Nappi Village	MLS70096
Hylopezus macularius	Vocal	Venezuela: Rio Grande; km 10; El Palmar	MLS62471
Hylopezus macularius	Vocal	Venezuela: Rio Grande; km 10.5; El Palmar	MLS62469
Hylopezus macularius	Vocal	Guyana: N of Parabara savannah	MLS54364
Hylopezus macularius	Vocal	Venezuela: 73.0 km S of Eldorado	MLS44279
Hylopezus macularius	Vocal	Venezuela: Rio Grande (sierra De Imabaca)	MLS40466
Hylopezus macularius	Vocal	Brazil: Amazonas, 80.0 km N of Manaus	ML42818
Hylopezus macularius	*Molecular*	Guyana, Iwokrama Reserve; Kobacalli Landing	ANSP - 21224
Hylopezus macularius	*Molecular*	Alenquer, ESEC Grão-Pará	MPEG - 66053
Hylopezus macularius	*Molecular*	Northwest District, Baramita	KU - B09754
Hylopezus macularius	*Molecular*	Acari Mountains, N side	KU - B10765
Hylopezus macularius	*Molecular*	Guyana: Parabara Savannah	KU - B12706
Hylopezus macularius	*Molecular*	Guyana: Barima-Waini, Baramita, In Former North West Region	USNM - 586404
Hylopezus macularius	*Molecular*	Guyana: Parabara Savannah	USNM - 616605
Hylopezus macularius	*Molecular*	Guyana: Gunn'S Landing, 10 km SSE	USNM - 625539
Hylopezus macularius	*Molecular*	Upper Takutu - Upper Essequibo, Upper Rewa River	USNM - 637111
Hylopezus macularius	*Molecular*	Upper Takutu - Upper Essequibo, Upper Rewa River	USNM - 637226
Hylopezus macularius	*Molecular*	Upper Takutu - Upper Essequibo, lower Rewa River	USNM - 637238

Hylopezus macularius	*Molecular*	FLOTA de Faro, ca 70 km NW de Faro	MPEG - CN143
Hylopezus macularius	*Molecular*	Almeirim, REBIO Maicuru	MPEG - CN901
Hylopezus macularius	*Molecular*	Óbidos, ESEC Grão-Pará	MPEG - CN1274
Hylopezus macularius	*Molecular*	Óbidos, ESEC Grão-Pará	MPEG - CN1329
Hylopezus macularius	*Molecular*	Óbidos, ESEC Grão-Pará	MPEG - CN1328
Hylopezus macularius	*Molecular*	Óbidos, ESEC Grão-Pará	MPEG - CN1332
Hylopezus fulviventris	Morphology	Ecuador: Cotapino	169720-ANSP
Hylopezus fulviventris	Morphology	Ecuador: Prov. Napo; S bank Rio Payamino, ca. 20 road km W of Coca	184722-ANSP
Hylopezus fulviventris	Morphology	Ecuador: Rio Payamino, Oriente	163682-ANSP
Hylopezus fulviventris	Morphology	Ecuador: Rio Payamino, Oriente	163683-ANSP
Hylopezus fulviventris	Morphology	Ecuador: Rio Pacayacu, Oriente	169719-ANSP
Hylopezus fulviventris	Morphology	Colombia: Rio San miguel	165179-ANSP
Hylopezus fulviventris	Morphology	Colombia: Rio San miguel	165180-ANSP
Hylopezus fulviventris	Morphology	Colombia: Rio San miguel	165181-ANSP
Hylopezus fulviventris	Morphology	Ecuador: San Jose, above	184359-AMNH
Hylopezus fulviventris	Morphology	Ecuador: E. Below San José de Sumarco	179384-AMNH
Hylopezus fulviventris	Morphology	Ecuador: Voca R, Curaray	255993-AMNH
Hylopezus fulviventris	Morphology	Ecuador: E. Rio Suno, Above avila	179382-AMNH
Hylopezus fulviventris	Vocal	Ecuador: Napo, 20.0 km W of Coca; south bank Rio Payamino	MLS78536
Hylopezus fulviventris	Vocal	Ecuador: Napo, 20.0 km W of Coca; south bank Rio Payamino	MLS78519
Hylopezus fulviventris	Vocal	Ecuador: Sucumbios, Sacha Lodge	MLS68217
Hylopezus fulviventris	Vocal	Ecuador: Sucumbv́ios, Sacha Lodge	MLS68208
Hylopezus fulviventris	Vocal	Ecuador: Napo, 1.0 km S of Puerto Napo	MLS50642
Hylopezus fulviventris	Vocal	Peru: Loreto, N. bank Rio Napo; Sucusari Camp	MLS31726
Hylopezus fulviventris	Vocal	Ecuador: Napo, Limoncocha; Rio Napo; E of Coca	MLS30302
Hylopezus fulviventris	*Molecular*	Ecuador, Napo, 20 road km W of Coca; south bank Rio Payamino	ANSP - 18744
Hylopezus fulviventris	*Molecular*	Peru, Loreto Department, Ca 54 km NNW mouth Rio Morona on east bank	LSUMZ - B43007

Hylopezus fulviventris	*Molecular*	Peru, Loreto Department, Ca 54 km NNW mouth Rio Morona on west bank	LSUMZ - B43008
Hylopezus fulviventris	*Molecular*	Peru, Loreto Department, Ca 54 km NNW mouth Rio Morona on west bank	LSUMZ - B43009
Hylopezus fulviventris	*Molecular*	Peru: Loreto ; Ca 54 km NNW mouth of Rio Morona, on east bank	LSUMZ – 42791
Hylopezus dives J	Morphology	Colombia: Antioquia, Alto Bonito	133536-AMNH
Hylopezus dives J	Morphology	Colombia: Antioquia, Alto Bonito	133535-AMNH
Hylopezus dives J	Morphology	Colombia: West, Narino Barbacoas	117884-AMNH
Hylopezus dives J	Morphology	Colombia: West, Narino Barbacoas	117886-AMNH
Hylopezus dives J	Morphology	Colombia: Cauca, San Jose	107478-AMNH
Hylopezus dives J	Morphology	Colombia: Cordoba, Quebrada Salvajin, Rio Esmeralda, Upper Rio Sinu	411877-USNM
Hylopezus dives J	Morphology	Colombia: Choco, Rio Jurubida, Baudo Mountains Lat 5º58´	443357-USNM
Hylopezus dives J	Morphology	Colombia: Valle de cauca, Punto Muchimbo, Rio San Juan,	443358-USNM
Hylopezus dives J	Morphology	Colombia: Antioquia, Villa Artiaga, 7 km NE Pavarondocito	426431-USNM
Hylopezus dives J	Morphology	Colombia: Antioquia, Villa Artiaga, 7 km NE Pavarondocito	426430-USNM
Hylopezus dives J	Morphology	Colombia: Cordoba, Socorre, Rio Sinu, 1.5 mi below mouth Rio Verde	411876-USNM
Hylopezus dives J	Morphology	Colombia: Antioquia, Villa Artiaga, 7 km NE Pavarondocito	426429-USNM
Hylopezus dives J	Morphology	Colombia: Cordoba, Quebrada Salvajin, Rio Esmeralda, Upper Rio Sinu	411875-USNM
Hylopezus dives J	Morphology	Colombia: Cordoba, Quebrada Salvajin, Rio Esmeralda, Upper Rio Sinu	411874-USNM
Hylopezus dives J	Morphology	Colombia: Choco, Rio Jurubida, pacific coast	443356-USNM
Hylopezus dives J	Vocal	Colombia: Buenaventura, Valle del Cauca	XC174797
Hylopezus dives J	Vocal	Colombia: Bahia Solano to El Valle Road, Bahia Solano	XC140772
Hylopezus dives J	Vocal	Colombia: Valle del Cauca, Lower Old Buenaventura	MLS83790
Hylopezus dives J	Vocal	Panama: Darien, Cana	MLS105095
Hylopezus dives I	Morphology	Nicaragua: Rio Grande	492276-AMNH
Hylopezus dives I	Morphology	Nicaragua: Northern, Rio Coco (Wanks River)	103387-AMNH
Hylopezus dives I	Morphology	Nicaragua: Matagalpa, Las Cuevas	102552-AMNH
Hylopezus dives I	Morphology	Nicaragua: Rio Grande	102851-AMNH
Hylopezus dives I	Morphology	Nicaragua: Rio Tuma	103601-AMNH

Hylopezus dives I	Morphology	Nicaragua: Los Sabalos, San Juan River	144043-AMNH
Hylopezus dives I	Morphology	Nicaragua: Matagalpa, Savala	102551-AMNH
Hylopezus dives I	Morphology	Nicaragua: Pena Blanca	103745-AMNH
Hylopezus dives I	Morphology	Nicaragua: Las Canas, 6 miles of Matagalpa	144042-AMNH
Hylopezus dives I	Morphology	Nicaragua: Pena Blanca	103747-AMNH
Hylopezus dives I	Morphology	Nicaragua: Pena Blanca	103746-AMNH
Hylopezus dives I	Morphology	Nicaragua: Rio Grande	492277-AMNH
Hylopezus dives I	Morphology	Nicaragua: Los sabalos	91265-USNM
Hylopezus dives I	Morphology	Nicaragua: Escondido River. 50M from bluefield	128353-USNM
Hylopezus dives I	Morphology	Nicaragua: Greytown, = Graytown (Greystown) or San Juan Del Norte?	40430-USNM
Hylopezus dives I	Vocal	Costa Rica: Pitilla Biological Station, Guancaste Conservation Area	XC6403
Hylopezus dives I	Vocal	Costa Rica: Heredia, 5.0 km S of Puerto Viejo at La Selva	MLS31389
Hylopezus dives I	Vocal	Costa Rica: Heredia, La Selva	MLS26399
Hylopezus dives I	Vocal	Panama: Darien, Cana	MLS25894
Hylopezus dives I	Vocal	Costa Rica: , 100.0 km NE of TURRIALBA; RD TO SIQUIRRES	MLS22664
Hylopezus dives	*Molecular*	Panama, Darién Province, Cana on E slope Cerro Pirré	LSUMZ - B2283
Hylopezus dives	*Molecular*	Honduras, Gracias a Dios t, Las Marias, Rio Platano, 25 km S Caribbean Sea	LSUMZ - B26087
Hylopezus dives	*Molecular*	Panama, Bocas del Toro Province, Rio Changuinola Arriba, W bank	LSUMZ - B46450
Hylopezus dives	*Molecular*	Bocas Del Toro, Tierra Oscura	USNM - 606954
Hylopezus dives	*Molecular*	Bocas Del Toro, Tierra Oscura	USNM - 612384
Hylopezus dives	*Molecular*	Honduras: Gracias a Dios ; Las Marias, on Rio Platano	LSUMZ – 26086
Hylopezus dives	*Molecular*	Costa Rica: Limón; Limón, Reserva Biológica Hitoy Cerere	LSUMZ – 82039
Hylopezus dilutus	Morphology	Venezuela: Rio Orinoco, Serra Duida, Caño Seou	270916-AMNH
Hylopezus dilutus	Morphology	Venezuela: Rio Cassiquiare, Caño Durutomoni	270915-AMNH
Hylopezus dilutus	Morphology	Venezuela: Rio Orinoco, R. bank, Mouth Rio Ocamo, R. Bank	432818-AMNH
Hylopezus dilutus	Morphology	Venezuela: Rio Cassiquiare, R. bank, Opposite El Merey	432824-AMNH
Hylopezus dilutus	Morphology	Venezuela: Rio Cassiquiare, R. bank, Opposite El Merey	432821-AMNH

Hylopezus dilutus	Morphology	Venezuela: Rio Cassiquiare, R. bank, Opposite El Merey	432822-AMNH
Hylopezus dilutus	Morphology	Venezuela: Rio Cassiquiare, R. bank, Opposite El Merey	432823-AMNH
Hylopezus dilutus	Morphology	Venezuela: Rio Cassiquiare, R. bank, Opposite El Merey	432825-AMNH
Hylopezus dilutus	Morphology	Venezuela: Rio Cassiquiare, R. bank, Opposite El Merey	432820-AMNH
Hylopezus dilutus	Morphology	Venezuela: Rio Orinoco, Serra Duida, Caño Seou	270919-AMNH
Hylopezus dilutus	Morphology	Venezuela: Rio Orinoco, R. bank, Mouth Rio Ocamo, R. Bank	432819-AMNH
Hylopezus dilutus	Morphology	Peru: Loreto, Rio Mazan	407154-AMNH
Hylopezus dilutus	Morphology	Venezuela: Rio Cassiquiare, Caño Durutomoni	270918-AMNH
Hylopezus dilutus	Morphology	Peru: Puerto Indiana, Rio Amazonas	231935-AMNH
Hylopezus dilutus	Vocal	Peru: Sabalillo, Loreto	XC20058
Hylopezus dilutus	Vocal	Peru: ExploNapo	XC102595
Hylopezus dilutus	Vocal	BRAZIL: Amazonas: Maraã, Lago Cumapi	Pers.Arc1
Hylopezus dilutus	Vocal	BRAZIL: Amazonas: Jaú National Park	Pers.Arc2
Hylopezus dilutus	*Molecular*	Maraã, Lago Cumapi	MPEG - JAP636
Hylopezus berlepschi H	Morphology	Brazil: Maica	76556-ANSP
Hylopezus berlepschi H	Morphology	Brazil: Rio Tapajós, Caxiricatuba	286766-AMNH
Hylopezus berlepschi H	Morphology	Brazil:Para; East bank Rio Xingu, 52 KM SSW Altamira	572603-USNM
Hylopezus berlepschi H	Morphology	Brazil: Mato Grosso, Mun. Alta Floresta, Rio Teles Pires Margem Esq.	51226-MPEG
Hylopezus berlepschi H	Morphology	Brazil: Mato Grosso, Mun. Paranaíta, Rio Teles Pires Margem Esq.	69331-MPEG
Hylopezus berlepschi H	Morphology	Brazil: Mato Grosso, Mun. Paranaíta, Rio Teles Pires Margem Dir	69332-MPEG
Hylopezus berlepschi H	Morphology	Brazil: Pará, Mun. Tucurui, Arresta da mata, Prox aloj. Temporario I.	36238-MPEG
Hylopezus berlepschi H	Morphology	Brazil: Pará, Carajás, Serra Norte, Manganês.	37250-MPEG
Hylopezus berlepschi H	Morphology	Brazil: Pará, Canaã dos Carajás, Mina do Sossego	72288-MPEG
Hylopezus berlepschi H	Morphology	Brazil: Pará, São Felix do Xingu, Gorotire	37123-MPEG
Hylopezus berlepschi H	Morphology	Brazil: Pará, Mun. Altamira, Rio Xingu Margem Esquerda	55490-MPEG
Hylopezus berlepschi H	Morphology	Brazil: Pará, Mun. Altamira, Rio Xingu Ilha Taboca	55491-MPEG
Hylopezus berlepschi H	Morphology	Brazil: Pará, Mun. Altamira, Rio Xingu Margem direita: Área 1	63448-MPEG

Hylopezus berlepschi H	Morphology	Brazil: Pará, Mun. Altamira, Rio Xingu Margem direita: Área 1	63449-MPEG
Hylopezus berlepschi H	Morphology	Brazil: Pará, Mun.Santarem, Retiro	55490-MPEG
Hylopezus berlepschi G	Morphology	Peru: Puerto Yessup, Junin	91233-ANSP
Hylopezus berlepschi G	Morphology	Peru: Sta Rosa, Alto Ucayali	240342-AMNH
Hylopezus berlepschi G	Morphology	Peru: Lagarta, Alto Ucayali	239269-AMNH
Hylopezus berlepschi G	Morphology	Peru: Sta Rosa, Alto Ucayali	240344-AMNH
Hylopezus berlepschi G	Morphology	Peru: Sta Rosa, Alto Ucayali	240343-AMNH
Hylopezus berlepschi G	Morphology	Bolivia: Todos os Santos, Rio chapare	140806-ANSP
Hylopezus berlepschi G	Morphology	Peru: Madre de Dios; Manu Nat. Park, Cocha Cashu	824073-AMNH
Hylopezus berlepschi G	Morphology	Peru: S. E. Astillero	146168-AMNH
Hylopezus berlepschi G	Morphology	Bolivia: Prov. Cochabamba, Todos os Santos	137176-AMNH
Hylopezus berlepschi G	Morphology	Brazil: Acre,Mun. Cruzeiro do sul, Porangaba, Rio Juruá Margem Direita	49669-MPEG
Hylopezus berlepschi G	Morphology	Brazil: Acre, Mun. Tamaturgo, Nossa senhora Aparecida, Rio Juruá	52917-MPEG
Hylopezus berlepschi	*Molecular*	Bolivia, La Paz t, Rio Beni, ca 20 km by river N. Puerto Linares	LSUMZ - B1057
Hylopezus berlepschi	*Molecular*	Bolivia, La Paz t, Rio Beni, ca 20 km by river N. Puerto Linares	LSUMZ - B1072
Hylopezus berlepschi	*Molecular*	Bolivia, Santa Cruz t, Velasco; Parque Nacional Noel Keonpff Mercado	LSUMZ - B18312
Hylopezus berlepschi	*Molecular*	Peru: Madre Dios; Hacienda Amazonia	FMNH - 322345
Hylopezus berlepschi	*Molecular*	Peru: Madre Dios; Moskitania, 13.4 km NNW of Atalaya	FMNH - 433523
Hylopezus berlepschi	*Molecular*	Rio Juruá, Marechal Taumaturgo, Nossa Senhora Aparecida	MPEG -PND325
Hylopezus berlepschi	*Molecular*	Rio Xingu, Altamira, Ilha da Taboca, UHE Belo Monte	MPEG - UHE046
Hylopezus berlepschi	*Molecular*	Rio Xingu, margem direita, Área 1	MPEG - BMP017
Hylopezus berlepschi	*Molecular*	Rio Xingu, margem direita, Área 1	MPEG - BMP024
Hylopezus berlepschi	*Molecular*	Santarém, Retiro	MPEG - PME022
Hylopezus berlepschi	*Molecular*	Paranaíta, Rio Teles Pires, margem esquerda	MPEG - TLP272
Hylopezus berlepschi	*Molecular*	Paranaíta, margem direita Rio Paranaíta, Fazenda Paranaíta	MPEG - TLP386
Hylopezus berlepschi	*Molecular*	Município de Ourilândia do Norte	MPEG - DPN158
Hylopezus berlepschi	*Molecular*	Peru: Ucayali ; SE slope Cerro Tahuayo, ca km ENE Pucallpa	LSUMZ – 11146

Hylopezus berlepschi	*Molecular*	Brazil: Pará; E. bank R.Teles Pires, 4 km from the mouth of the Rio Sao benedito	LSUMZ – 35407
Hylopezus berlepsch H	Vocal	Brazil: Pará, 250.0 km NW of Reserva Indigena Gorotire; Pinkaiti; Redencao	MLS94594
Hylopezus berlepsch H	Vocal	Brazil: Mato Grosso, S of Rio Teles Pires	MLS52297
Hylopezus berlepsch H	Vocal	Brazil: Mato Grosso, 40.0 km S of Alta Floresta	MLS48054
Hylopezus berlepsch H	Vocal	Brazil: Mato Grosso, Cristalino Ecological Institute	MLS109957
Hylopezus berlepsch H	Vocal	Brazil: Mato Grosso, Alta Floresta	MLS106054
Hylopezus berlepsch H	Vocal	Brazil: Mato Grosso, Reserva Ecologica Cristalino, Bungalow clearing	ML88888
Hylopezus berlepsch H	Vocal	Brazil: Mato Grosso, Reserva Ecologica Cristalino, Bungalow clearing	ML88887
Hylopezus berlepsch G	Vocal	Peru: Madre de Dios, Tambopata Nature Preserve	MLS48171
Hylopezus berlepsch G	Vocal	Peru: Madre de Dios, Tambopata Nature Reserve	MLS47717
Hylopezus berlepsch G	Vocal	Peru: Loreto, North bank Rio Napo; Shansho Cano	MLS30907
Hylopezus berlepsch G	Vocal	Peru: Cuzco, 2.0 km W of Pilcopata	MLS30051
Hylopezus berlepsch G	Vocal	Peru: Madre de Dios, Cocha Cashu; Manu National Park	MLS29523
Hylopezus berlepsch G	Vocal	Peru: Loreto, Rio Napo; Isla Yagua	MLS29375
Hylopezus berlepsch G	Vocal	Bolivia: Santa Cruz, Lago Caiman; Noel Kempff Mercado	MLS127024
Hylopezus berlepsch G	Vocal	Bolivia: Pando, Rutina	MLS100999
Hylopezus auricularis	Vocal	Bolivia: Hamburgo, Riberalta, Beni	XC2720
Hylopezus auricularis	Vocal	Bolivia: Puerto Hamburgo, Riberalta, Beni	XC100423
Hylopezus auricularis	Vocal	Bolivia: Puerto Hamburgo, Riberalta, Beni	XC100424
Hylopezus auricularis	Vocal	Bolivia: Puerto Hamburgo, Riberalta, Beni	XC146789
Hylopezus auricularis	*Molecular*	Bolívia: Beni; Riberalta	FMNH - 391156
Hylopezus auricularis	*Molecular*	Bolívia: Beni; Riberalta	FMNH - 391157
Hylopezus auricularis	*Molecular*	Bolívia: Beni; Riberalta	FMNH - 391158
Grallaricula nana	Morphology	Colombia: Cauca, Cerro Munchique	446635-USNM
Grallaricula nana	Morphology	Colombia: Cauca, Cerro Munchique	446636-USNM
Grallaricula nana	Morphology	Colombia: Antioquia, Sonson, Paramo	436476-USNM
Grallaricula nana	Morphology	Colombia: Antioquia, Sonson, Paramo	436475-USNM

Grallaricula nana	Morphology	Colombia: Cauca, Munchique; El Tambo	144677-ANSP
Grallaricula nana	Morphology	Colombia: Cauca, Munchique; El Tambo	142394-ANSP
Grallaricula nana	Morphology	Colombia: Cauca, San antonio; EL TAMBO	142395-ANSP
Grallaricula nana	Morphology	Colombia: Caldas, Laguneta	155176-ANSP
Grallaricula nana	Morphology	Colombia: Huila, La candela	155852-ANSP
Grallaricula nana	Vocal	Ecuador: La Sofia road, Sucumbios	XC78769
Grallaricula nana	Vocal	Peru: Bosque Paja Blanca, Chotas, Cajamarca	XC37724
Grallaricula nana	Vocal	Colombia: Páramo de Frontino	XC27433
Grallaricula nana	Vocal	Venezuela: Pico Humboldt Trail, Mérida	XC202967
Grallaricula nana	Vocal	Colombia: R. N. Rio Blanco, Caldas	XC18290
Grallaricula nana	*Molecular*	Colombia: North of Santander, PNN Tamá, Orocué	LSUMZ –960
Grallaricula flavirostris	Morphology	Colombia: Narino, Ricaurte, Pac, Side.	150783-ANSP
Grallaricula flavirostris	Morphology	Colombia: Cauca, Rio Munchique; El Tambo	142392-ANSP
Grallaricula flavirostris	Morphology	Colombia: Cauca, Rio Munchique; El Tambo	142393-ANSP
Grallaricula flavirostris	Morphology	Colombia: Caldas; La Selva	157981-ANSP
Grallaricula flavirostris	Morphology	Colombia: Cauca, Rio Munchique; El Tambo	137947-ANSP
Grallaricula flavirostris	Morphology	Colombia: Narino, Ricaurte, Pac, Side.	150784-ANSP
Grallaricula flavirostris	Morphology	Colombia: Cauca, Munchique; El Tambo	144678-ANSP
Grallaricula flavirostris	Morphology	Colombia: Cauca, La costa; El Tambo	131629-ANSP
Grallaricula flavirostris	Morphology	Colombia: Cauca, Cocal, W. Of Popayan	109636-AMNH
Grallaricula flavirostris	*Molecular*	Colombia: Antioquia, Anorí, Alto El Chaquiral	LSUMZ - 4774
Grallaria rufula	*Molecular*	Peru: Cajamarca, Quebrada Lanchal, ca 8 Km ESE Sallique	LSUMZ – 32257
Grallaria ruficapilla	*Molecular*	Colombia: Caldas; Aranzazu, Hacienda Termópilas	LSUMZ – 1666
Grallaria guatimalensis	*Molecular*	Panama: Darien, Cana on E slope Cerro Pirré	LSUMZ – 2331

Table S2**:** Habitat designations for species of antpittas analyzed in this study (P = primary; S = secondary).

Species	Habitat type
Myrmothera campanisona A	P
Myrmothera campanisona B	P
Myrmothera simplex E	P
Myrmothera simplex F	P
Myrmothera campanisona C	P
Myrmothera campanisona D	P
Hylopezus fulviventris	P
Hylopezus berlepschi G	P
Hylopezus berlepschi H	P
Hylopezus dives I	S
Hylopezus dives J	S
Hylopezus perspicillatus A	S
Hylopezus perspicillatus B	S
Hylopezus whittakeri	P
Hylopezus paraensis	P
Hylopezus dilutus	P
Hylopezus macularius	P
Hylopezus ochroleucus	S
Hylopezus auricularis	S
Grallaricula flavirostris	S
Grallaricula nana	S
Hylopezus nattereri	S

Table S3. Pairs of sympatric and allopatric antpitta taxa used to test the species recognition hypothesis (For systematic details see Carneiro et al. unpubl. ms. Chapter 1).

Sympatric pairs	**Allopatric pairs**	
A	***B***	***C***
Hylopezus perspicillatus A	*Hylopezus dives* J	*Hylopezus dives* I
Hylopezus fulviventris	*Myrmothera campanisona* C	*Myrmothera campanisona* D
Hylopezus macularius	*Myrmothera campanisona* D	*Myrmothera campanisona* C
Hylopezus paraensis	*Hylopezus berlepschi* H	*Hylopezus berlepschi* G
Myrmothera campanisona B	*Hylopezus whittakeri*	*Hylopezus paraensis*
Hylopezus dilutus	*Hylopezus fulviventris*	*Hylopezus berlepschi* G
Myrmothera campanisona C	*Hylopezus berlepschi* G	*Hylopezus berlepschi* H
Hylopezus whittakeri	*Myrmothera campanisona* A	*Myrmothera campanisona* B
Hylopezus berlepschi H	*Myrmothera campanisona* A	*Myrmothera campanisona* B

.

LITERATURE CITED

P. M. Agapow and N. J. B. Isaac. 2002. Macrocaic: revealing correlates of species richness by comparative analysis. Diversity and Distributions, 8:41–43.

Anderson, D. R. 2008. Model based inference in the life sciences: a primer on evidence. Springer, New York, NY.

Badyaev, A. V., and E. S. Leaf. 1997. Habitat associations of song characteristics in *Phylloscopus* and *Hippolais* warblers. Auk 114:40–46.

Baptista, L. F., and P. W. Trail. 1992. The role of song in the evolution of passerine diversity. Syst. Biol. 41:242–247.

Boughman, J. W. 2002. How sensory drive can promote speciation. Trends Ecol. Evol. 17:571–577.

Bowman R. I. 1979. Adaptive morphology of song dialects in Darwin's finches. J. Ornithol. 120:353–389.

Blomberg, S., T. Garland Jr, and A. Ives. 2003. Testing for phylogenetic signal in comparative data: behavioral traits are more labile. Evolution 57:717–745.

Bravo, G. A., J. V. Remsen Jr., and R. T. Brumfield. 2014. Adaptive processes drive ecomorphological convergent evolution in antwrens (Thamnophilidae). Evolution 68:2757–2774.

Bryson, R. W. Jr, J. Chaves , B. T. Smith, M. J. Miller, K. Winker, J. L. Pérez-Emán, and J. Klicka. 2014. Diversification across the New World within the 'blue' cardinalids (Aves: Cardinalidae). J. Biogeogr. 41:587–599.

Buskirk, J. 1997. Independent evolution of song structure and note structure in American wood warblers. Proc. R. Soc. Lond. B 264:755–761.

Butler, M., and A. King. 2004. Phylogenetic comparative analysis: a modeling approach for adaptive evolution. Am. Nat. 164:683–695.

Carneiro, L. S., L. P. Gonzaga, P. S. Rêgo, I. Sampaio, H. Schneider, and A. Aleixo. 2012. Systematic revision of the spotted antpitta (Grallariidae: *Hylopezus*

macularius), with description of a cryptic new species from brazilian Amazonia. Auk 129:338–351.

Catchpole, C. K., and P. J. B. Slater. 1995. Bird song: biological themes and variations. Cambridge Univ. Press, Cambridge, U.K.

Claramunt, S. 2010. Discovering exceptional diversifications at continental scales: the case of the endemic families of Neotropical suboscine passerines. Evolution 64:2004–2019.

Cooper, N., W. Jetz, and R. P. Freckleton. 2010. Phylogenetic comparative approaches for studying niche conservatism. J. Evol. Biol. 23:2529– 2539.

Crisp, M. D., and L. G. Cook. 2012. Phylogenetic niche conservatism: what are the underlying evolutionary and ecological causes? New Phytol. 196:681–694.

Derryberry, E. P., S. Claramunt, G. Derryberry, R. T. Chesser, J. Cracraft, A. Aleixo, J. Pérez-Emán, J. V. Remsen Jr., and R. T. Brumfield. 2011. Lineage diversification and morphological evolution in a large-scale continental radiation: the Neotropical ovenbirds and woodcreepers (Aves: Furnariidae). Evolution 65:2973–2986.

Derryberry, E. P., N. Seddon, S. Claramunt, J. A. Tobias, A. Baker, A. Aleixo, and R. T. Brumfield. 2012. Correlated evolution of beak morphology and song in the Neotropical woodcreeper radiation. Evolution 66:2784–2797.

Dobzhansky, T. 1951. Genetics and the origin of species. Columbia Univ. Press, New York.

Drummond, A. J., S. Y. W. Ho, M. J. Phillips, and A. Rambaut. 2006. Relaxed phylogenetics and dating with confidence. PLoS Biol. 4:e88.

Drummond, A. J., and A. Rambaut. 2007. BEAST: Bayesian evolutionary analysis by sampling trees. BMC Evol Biol. 7:214. doi: 10.1186/1471-2148-7-214.

Drummond, A. J., M. A. Suchard, D. Xie, and A. Rambaut. 2012. Bayesian phylogenetics with BEAUti and the BEAST 1.7. Mol. Biol. Evol. 29:1969–1973.

Estes, S., and S. J. Arnold. 2007. Resolving the paradox of stasis: models with

stabilizing selection explain evolutionary divergence on all timescales. Am. Nat. 169:227–244.

Farnsworth, A., and I. J. Lovette. 2005. Evolution of nocturnal flight calls in migrating wood-warblers: apparent lack of morphological constraints. J. Avian Bio. 36:337–347.

Felsenstein, J. 1973. Maximum-likelihood estimation of evolutionary trees from continuouscharacters. Am. J. Human Genet. 25: 471–492.

Felsenstein, J. 1985. Phylogenies and the comparative method. Am. Nat. 125:1–15.

Fitzpatrick, J. W. 1985. Form, foraging behavior, and adaptive radiation in the Tyrannidae. Ornithological Monographs. 36:447–4470.

Gibbs, H. L., and P. R. Grant. 1987. Oscillating selection in Darwin's finches. Nature 327:511–513.

Grant, P. R., B. R. Grant, J. A. Markert, L. F. Keller, and K. Petren. 2004. Convergent evolution of Darwin's finches caused by introgressive hybridization and selection. Evolution 58:1588–1599.

Harmon, L. J., J. A. Schulte, A. Larson, and J. B. Losos. 2003. Tempo and mode of evolutionary radiation in iguanian lizards. Science 301:961– 964.

Harmon, L. J., J. Kolbe, J. Cheverud, and J. B. Losos. 2005. Convergence and the multidimensional niche. Evolution 59:409– 421.

Harmon L. J., J. T. Weir, C. D. Brock, R. E. Glor, and W. Challenger. 2008. GEIGER: investigating evolutionary radiations. Bioinformatics 24:129– 131.

Harmon, L. J., J. B. Losos, T. J. Davies, R. G. Gillespie, J. L. Gittleman, W. B. Jennings, K. H. Kozak, M. A. McPeek, F. Moreno-Roark, T. J. Near, A. Purvis, R. E. Ricklefs, D. Schluter, J. A. Schulte II, O. Seehausen, B. Sidlauskas, O. Torres-Carvajal, J. T. Weir, and A. Ø. Mooers. 2010. Early bursts of body size and shape evolution are rare in comparative data. Evolution 64:2385–2396.

Harvey, P. H., and M. D. Pagel. 1991. The comparative method in evolutionary

biology. Oxford Univ. Press, Oxford, U.K.

Huber S. K., and J. Podos. 2006. Beak morphology and song features covary in a population of Darwin's finches (*Geospiza fortis*). Biol. J. Linn. Soc. 88:489–498.

Huelsenbeck, J.P. & Rannala, B. 2004. Frequentist properties of Bayesian posterior probabilities of phylogenetic trees under simple and complex substitution models. Systematic Biology, 53, 904–913.

Hunt, G. 2006. Fitting and comparing models of phyletic evolution: random walks and beyond. Paleobiology 32:578–601.

Ingram, T., and L. Mahler. 2013. SURFACE: detecting convergent evolution from comparative data by fitting Ornstein–Uhlenbeck models with stepwise Akaike Information Criterion. Methods Ecol. Evol. 4:416–425.

Irwin, D. E., and T. Price. 1999. Sexual imprinting, learning and speciation. Heredity 82:347–354.

Irwin, D. E., P. Alstrom, U. Olsson, and Z. M. Benowitz-Fredericks. 2001. Cryptic species in the genus *Phylloscopus* (Old World leaf warblers). Ibis 143:223–247.

Isler, M. L., P. R. Isler, and B. M. Whitney. 1998. Use of vocalizations to establish species limits in antbirds (Passeriformes: Thamnophilidae). Auk 115:577–590.

Jombart, T., Balloux, F., Dray, S., 2010a. Adephylo: new tools for investigating the phylogenetic signal in biological traits. Bioinformatics 26, 1907–1909.

Jombart, T., Pavoine, S., Devillard, S.B., Pontier, D., 2010b. Putting phylogeny into the analysis of biological traits: a methodological approach. J. Theor. Biol. 264, 693–701.

Krabbe, N., and T. S. Schulenberg. 2003. Family Rhinocryptidae (tapaculos). Pp. 748–787 *in* J. del Hoyo, A. Elliott and D. A. Christie, eds. Handbook of the Birds of the World 8. Lynx Edicions, Barcelona.

Lanfear, R., Calcott, B., Ho, S.Y.W., Guindon, S. 2012. PartitionFinder: combined

selection of partitioning schemes and substitution models for phylogenetic analyses. Mol. Biol. Evol. 29, 1695–1701.

Lerner, H. R. L., M. Meyers, H. F. James, M. Hofreiter, and R. C. Fleischer. 2011. Multilocus resolution of phylogeny and timescale in the extant adaptive radiation of Hawaiian honeycreepers. Curr. Bio. 21:1838–1844.

Lewontin, R. C. 1974. The genetic basis of evolutionary change. Columbia Univ. Press, New York.

Liou, L. W., and T. D. Price. 1994. Speciation by reinforcement of premating isolation. Evolution 48:1451–1459.

Losos, J. B. 2008. Phylogenetic niche conservatism, phylogenetic signal and the relationship between phylogenetic relatedness and ecological similarity among species. Ecol. Lett. 11:995–1003.

Losos, J. B. 2011. Convergence, adaptation, and constraint. Evolution 65:1827– 1840.

Mason, N. A., and K. J. Burns. 2015. The effect of habitat and body size on the evolution of vocal displays in Thraupidae (tanagers), the largest family of songbirds. Biol. J. Linn. Soc. 144:538–551.

Mayr, E. 1963. Animal species and evolution. Belknap Press, Cambridge, MA.

Miles, D. B., and R. E. Ricklefs. 1984. The correlation between ecology and morphology in deciduous forest passerine birds. Ecology 65:1629–1640.

Miller, M. A., W. Pfeiffer, and T. Schwartz. 2010. Creating the CIPRES Science Gateway for inference of large phylogenetic trees. Pp. 1–8 *in* Proceedings of the Gateway Computer Environments workshop, (GCE 2010), 14 November 2010, New Orleans, Louisiana. Institute of Electrical and Electronics Engineers.

Minin, V., Z. Abdo, P. Joyce, and J. Sullivan. 2003. Performance-based selection of likelihood models for phylogeny estimation. Syst. Biol. 52:674–683.

Mosimann, J. E. 1970. Size allometry: size and shape variables with characterizations of the lognormal and generalized gamma distributions. J. Am. Stat. Assoc. 65:930–

945.

Mosimann, J. E., and F. C. James. 1979. New statistical methods for allometry with application to Florida Red-winged Blackbirds. Evolution 33:444– 459.

Orme, D., R. Freckleton, G. Thomas, T. Petzoldt, S. Fritz, N. Isaac, et al. 2012. caper: Comparative Analyses of Phylogenetics and Evolution in R. R package version 0.5.http://CRAN.R-project.org/package=caper.

Palacios, M. G., and P. L. Tubaro. 2000. Does beak size affect acoustic frequencies in woodcreepers? Condor 102:553–560.

Panhuis, T. M., R. Butlin, R. M. Zuk, and T. Tregenza. 2001. Sexual selection and speciation. Trends Ecol. Evol. 16:364–371.

Paradis, E., J. Claude, and K. Strimmer. 2004. APE: analyses of phylogenetics and evolution in R language. Bioinformatics 20:289–290.

Podos, J. 2001. Correlated evolution of morphology and vocal signal structure in Darwin's finches. Nature 409:185–188.

Podos, J., J. A. Southall, and M. R. Rossi-Santos. 2004. Vocal mechanics in Darwin's finches: correlation of beak gape and song frequency. J. Exp. Biol. 207:607–619.

Posada, D. 2008. jModelTest: phylogenetic model averaging. Mol. Biol. Evol 25:1253–1256.

Price, T. 2008. Speciation in birds. Roberts and Company Publishers, Greenwood Village, CO.

Purvis, A., and A. Rambaut. 1995. Comparative analysis by independent contrasts (CAIC): an Apple Macintosh application for analyzing comparative data. Comp. Appl. Biosci. 11:247–251.

R Development Core Team. 2011. R: a language and environment for statistical computing. R Foundation for Statistical Computing, Vienna, Austria. Available at http://www.r-project.org.

Rambaut, A. , and A. J. Drummond. 2007. Tracer v1.5. Program Available at: http://beast.bio.ed.ac.uk/Tracer.

Revell, L. J., L. J. Harmon, R. B. Langerhans, and J. J. Kolbe. 2007. A phylogenetic approach to determining the importance of constraint on phenotypic evolution on the Neotropical lizard *Anolis cristatellus*. Evol. Ecol. Res. 9:261–282.

Revell, L. J. 2012. phytools: An R package for phylogenetic comparative biology (and other things). Methods Ecol. Evol. 3:217–223.

Rice, N.H. 2005. Phylogenetic relationships of antpitta genera (Passeriformes: Formicariidae). Auk. 122, 673–683.

Ronquist, F., M. Teslenko, P. van der Mark, D. L. Ayres, A. Darling, S. Höhna, B. Larget, L. Liu, M. A. Suchard, and J. P. Huelsenbeck. 2012. MrBayes 3.2: efficient Bayesian phylogenetic inference and model choice across a large model space. Syst. Biol. 61:539–542.

Ryan, M. J., and E. A. Brenowitz. 1985. The role of body size, phylogeny and ambient noise in the evolution of bird song. Am. Nat. 126:87–100.

Schulenberg, T. S. 1983. Foraging behavior, eco-morphology, and systematics of some antshrikes (Formicariidae: Thamnomanes). Wilson Bull. 95:505–521.

Seddon, N. 2005. Ecological adaptation and species recognition drives vocal evolution in Neotropical suboscine birds. Evolution 59:200–215.

Shy, E. 1983. The relation of geographical variation in song to habitat characteristics and body size in North American tanagers (Thraupinae: *Piranga*). Behav. Ecol. Sociobiol. 12:71–76.

Sidlauskas, B. 2008. Continuous and arrested morphological diversification in sister clades of characiform fishes: a phylomorphospace approach. Evolution 62:3135–3156.

Slater, G. J., S. A. Price, F. Santini, and M. E. Alfaro. 2010. Diversity versus disparity and the radiation of modern cetaceans. Proc. R. Soc. Lond. B 277:3097–3104.

Smith, B. T., and J. Klicka. 2010. The profound influence of the Late Pliocene Panamanian uplift on the exchange, diversification, and distribution of New World birds. Ecography 33:333–342.

Smith, B. T., R. W. Bryson Jr, D. D. Houston, and J. Klicka. 2012. An asymmetry in niche conservatism contributes to the latitudinal species diversity gradient in New World vertebrates. Ecol. Lett. 15:1318–1325.

Stayton, C. T. 2006. Testing hypotheses of convergence with multivariate data: morphological and functional convergence among herbivorous lizards. Evolution 60:824–841.

Tietze, D. T., J. Martens, B. S. Fischer, Y. H. Sun, A. Klussmann-Kolb, M. Packert. 2015. Evolution of leaf warbler songs (Aves: Phylloscopidae). Ecology and Evolution. 100:54–61.

Tubaro, P. L., and B. Mahler. 1998. Acoustic frequencies and body mass in New World doves. Condor 100:54–61.

Wallschläger, D. 1980. Correlation of song frequency and body weight in passerine birds. Experimentia 36:412.

Webster, N. B., T. J. M Van Dooren, M. Schilthuizen. 2012. Phylogenetic reconstruction and shell evolution of the Diplommatinidae (Gastropoda: Caenogastropoda). Mol. Phyl. Evol. 63:625–638.

Wells, M. M., and C. S. Henry. 1998. Songs, reproductive isolation and speciation in cryptic species of insects. Pp. 404–422 *in* D. J. Howard and S. H. Berlocher, eds. Endless forms: species and speciation. Oxford Univ. Press, New York.

West-Eberhard, M. J. 1983. Sexual selection, social competition, and speciation. Q. Rev. Biol. 58:155–183.

Wiens, J. J., D. D. Ackerly, A. P. Allen, B. L. Anacker, L. B. Buckley, H. V. Cornell, E. I. Damschen, T. J. Davies, J. A. Grytnes, S. P. Harrison, B. A. Hawkins, R. D. Holt, C. M. McCain, and P. R. Stephens. 2010. Niche conservatism as an emerging principle in ecology and conservation biology. Ecol. Lett. 13:1310– 1324.

Wiens, J. J., M. C. Brandley, and T. W. Reeder. 2006. Why does a trait evolve multiple times within a clade? Repeated evolution of snakelike body form in squamate reptiles. Evolution 60:123–141.

Wiley, R. H. 1991. Associations of song properties with habitats for territorial oscine birds of eastern North America. Am. Nat. 138:973–993.

Willis, E. O. 1967. The behavior of bicolored antbirds. Univ. of California Publications in Zoology, no. 79.

Zimmer, K. J., A. Whittaker, and D. C. Oren. 2001. A cryptic new species of flycatcher (Tyrannidae: *Suiriri*) from the cerrado region of central South America. Auk 118:56–78.

Capítulo 3

Revisão taxonômica de *Hylopezus* e *Mymothera* (Aves, Grallariidae), com descrição de um novo gênero da Mata Atlântica

"Taxonomic revision of *Hylopezus* and *Mymothera* (Aves, Grallariidae), with description of a new genus from Atlantic forest[3]"

[3] Esse capítulo está no formato de manuscrito e será submetido ao periódico "Zootaxa". O co-autor Gustavo Bravo não revisou a presente versão.

Taxonomic revision of *Hylopezus* and *Mymothera* (Aves, Grallariidae), with description of a new genus from Atlantic forest

Lincoln Carneiro,[1,3] Gustavo Bravo[2] and Alexandre Aleixo[3]

[1]*Curso de Pós-Graduação de Zoologia, Universidade Federal do Pará–Museu Paraense Emílio Goeldi, Belém, Pará, Brazil;* [2]*Secção de Aves, Museu de Zoologia, Universidade de São Paulo (MZUSP), Caixa Postal 42.494, CEP 04218–970, São Paulo, SP, Brasil;; and* [3]*Coordenação de Zoologia, Museu Paraense Emílio Goeldi, Caixa Postal 399, CEP 66040-170, Belém, Pará, Brazil.*

[4]Address correspondence to this author. E-mail: lincoln_carneiro@yahoo.com.br

Abstract

A dense range-wide sampling and a molecular phylogeny including *Hylopezus* and *Myrmothera* genera indicated that the *Hylopezus,* as presently configured, is polyphyletic. Our results strongly suggest that *Myrmothera* forms a monophyletic group to *H. dives*, *H. fulviventris*, *H. berlepschi,* currently placed in *Hylopezus* genus. The clade formed by, *H. auricularis*, *H. ochroleucus*, *H. withakeri*, *H. paraensis*, *H. macularius*, recovered by our phylogenetic estimation, also comprise, the type species from the genus, *H. perspicillatus*. Furthermore, the phylogeny placed the Atlantic forest taxa *H. nattereri* as an isolated lineage, not directly related to remaining *Hylopezus* and *Myrmothera*, based on this, we recommend the recognition of *H. nattereri* as a separate new genus.

Key words: antpittas, morphological, vocal, systematics, phylogeny

INTRODUCTION

The *Hylopezus* and *Myrmothera* genera are composed by small to medium-sized sedentary insectivores that inhabits forest, montane forest, bamboo, deciduous and Caatinga woodland, and scrub (Krabbe & Schulenberg, 2003). The genus *Hylopezus* is distributed throughout most of the Neotropics, Honduras to northeastern Argentina, but is largely confined to the lowlands (Krabbe and Schulenberg 2003, Carneiro et al., 2012; Remsen et al. 2015). *Myrmothera* genus inhabits both upland and seasonally flooded lowland humid forests of the Amazon Basin.

The genus *Hylopezus* currently includes 10 species, *H. perspicillatus*, *H. macularius*, *H. auricularis*, *H. dives*, *H. fulviventris*, *H. berlepschi*, *H. ochroleucus*, *H. nattereri*, *H. paraensis* and *H. whittakeri* (Krabbe and Schulenberg 2003, Carneiro et al., 2012). Ridgway (1909) describes the genus *Hylopezus*, elects *Grallaria perspicillata* (Lawrence) 1861, as type species and relocates some *Grallaria* species to this new genus. *Hylopezus*, according to Ridgway, is related to *Grallaria* Vieillot (1816), But had some morphological differences from the latter, notably the distance from anterior end to base of exposed culmen; nostril more linear and separated from frontal feathering by naked integument; bill much weaker and more slender (Ridgway 1909). Further revisions, based on morphological characters, agreed to the arrangement proposed by Ridgway (Todd 1919; Zimmer 1934; Lowery and O'Neill 1969; Galvão and Gonzaga 2011).

The genus *Myrmothera* was described by Vieillot (1816), and comprises two species, *M. campanisona* and *M. simplex*. The type species of genus is *M. campanisona*, originally described by Hermann (1783) on the genus *Myrmornis*. Sclater (1890) Synonymizes *Myrmonis* with other previously described taxa and includes in the genus proposed by Vieillot (1816), further electing him as the type species of the genus. However, the Vieillot's description is brief and contains few morphological details.

Subsequently, the monophyly of *Myrmothera* and *Hylopezus* and your close relationship to each other was recovered by several molecular studies (Krabbe *et al*., 1999, Irestedt *et al*., 2002, Chesser *et. al*, 2004, Rice, 2005 [A,B], Moyle et al. 2009, Ohlson et al. 2013), but monophyly has never been formally tested using complete

taxon (species level) sampling. Our approach, therefore, is to overlay of morphological, acoustic, and ecological characteristics on a newly completed molecular phylogeny, and then to assess the degree of differentiation and diagnosability of different clades to define and allocate species into genera. Furthermore, our objective has been to provide a genus-level taxonomic classification for species currently placed in these genera, which reflect the evolutionary history of the taxa.

METHODS

Molecular phylogeny

To infer the phylogenetic relationships within *Hylopezus* and *Myrmothera*, we sequenced 144 tissue samples (77 *Hylopezus*, 62 *Myrmothera* and 5 outgroups) from throughout their distributions (Figs 1, 2 and 3; see also Table S1 in supplementary material). Our sampling spanned the geographical distributions of all 12 currently recognized species within these genera (Krabbe & Schulenberg, 2003; Carneiro *et al*., 2012). We included in our analyzes species of the two other genera of the Grallariidae family, *Grallaricula* (*G. flavirostris* and *G. nana*) and *Grallaria* (*G. rufula*, *G. ruficapilla* and *G. guatimalensis*), as outgroups, hence covering all currently recognized genera of the family (Krabbe & Schulenberg, 2003; Rice, 2005).

The extraction procedures, PCR conditions, amplification and sequencing reactions follows (Carneiro *et al*., unpubl. ms. Chapter 1). Electropherograms were inspected, assembled in contigs and edited in Geneious 7.1.5 (Biomatters, www.geneious.com). Heterozygous sites were coded according to IUPAC when double peaks were present in both strands of the same individual's electropherograms. Sequences were aligned with MAFFT using the default parameters, and further inspected and corrected visually.

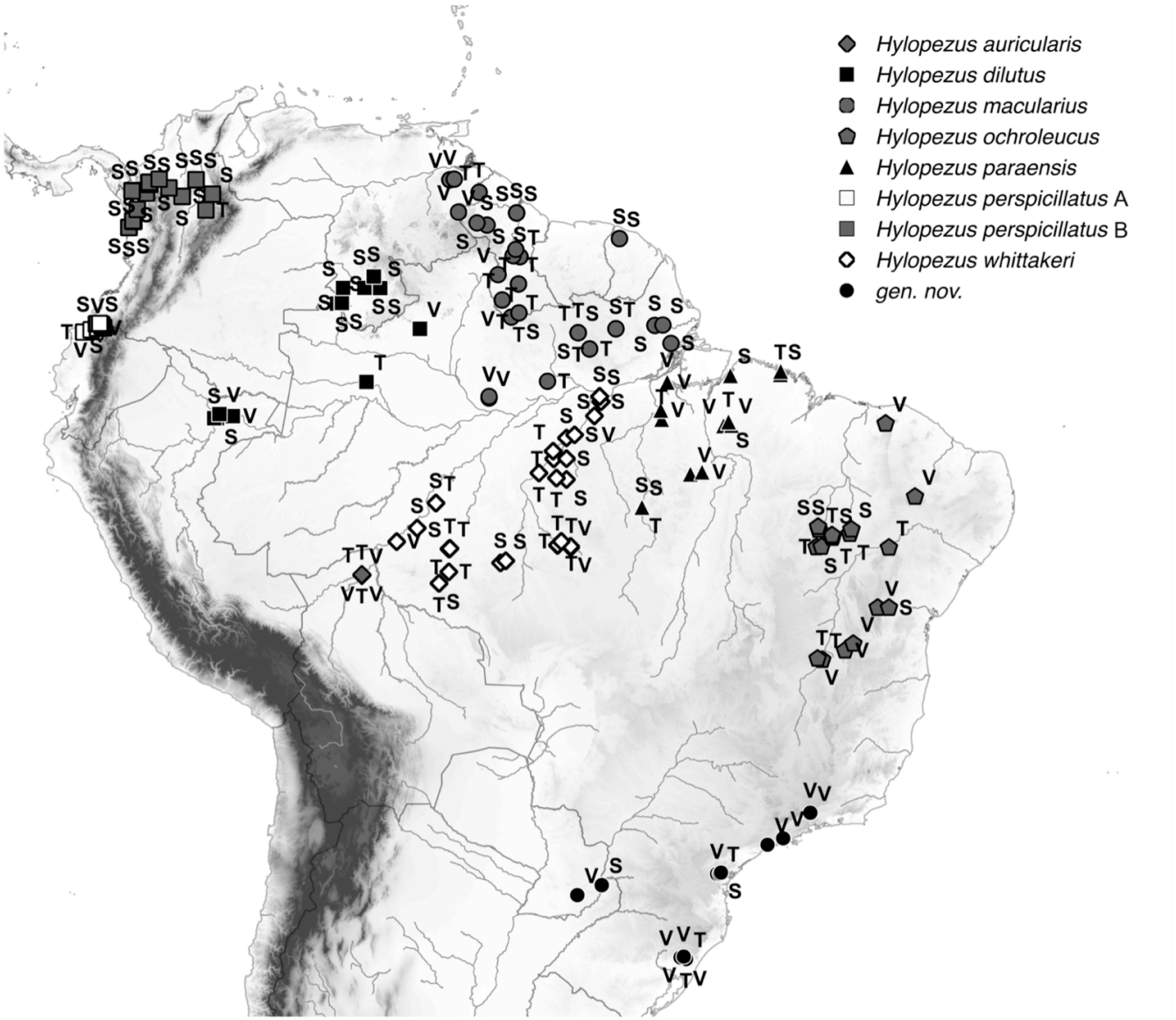

Figure 1. Geographic distribution of specimens, vocalizations, and tissues of the *Hylopezus* genus and *gen. nov*. analyzed in the present study. For population definitions of *H. perspcillatus* see results. Letters next to a symbol represent materials available for that given locality: S = skins; V = vocalizations; T = tissues. Additional locality data can be found in Appendix S1.

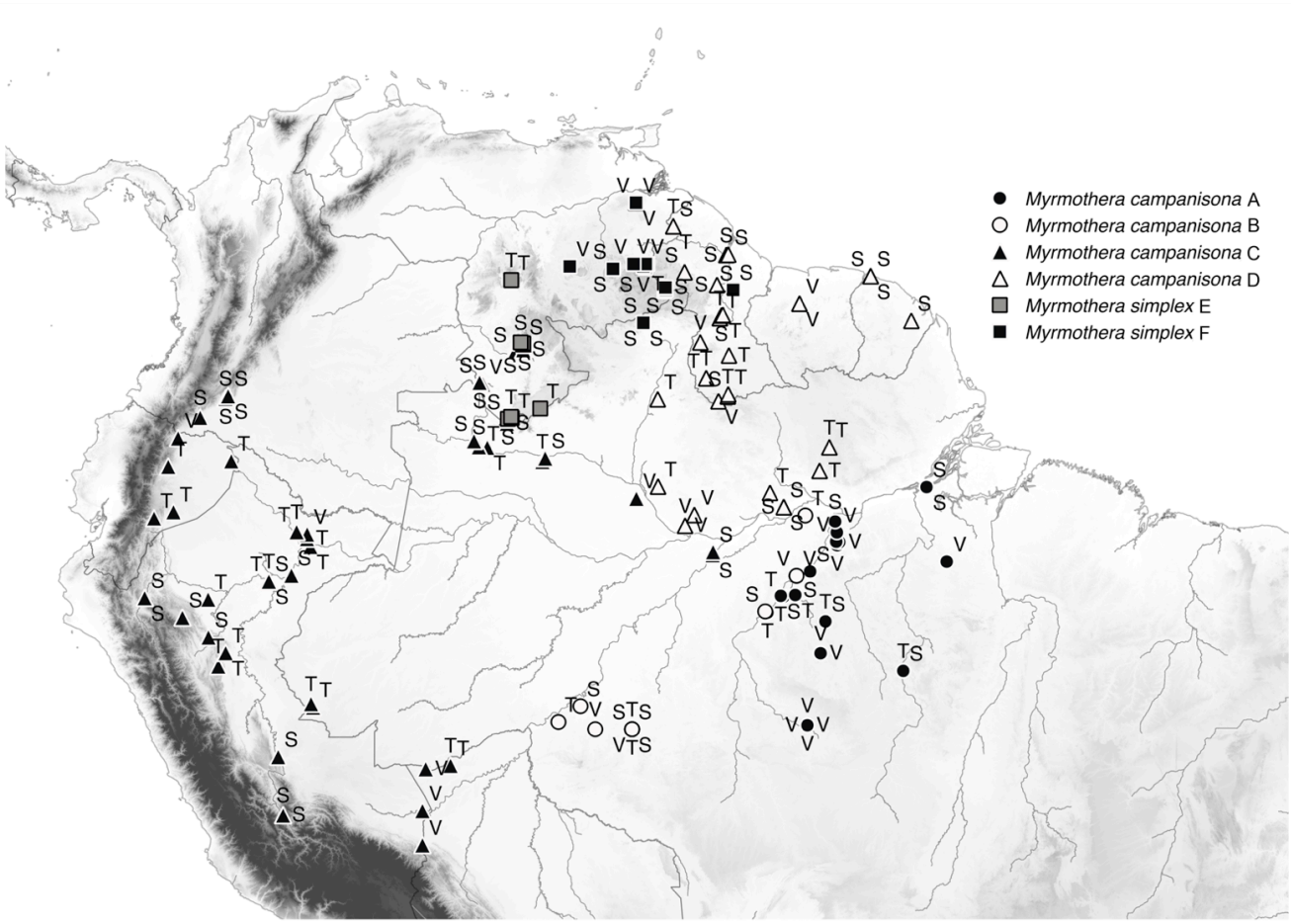

Figure 2. Geographic distribution of specimens, vocalizations, and tissues of the *Myrmothera campanisona* and *Myrmothera simplex* analyzed in the present study. For population definitions see results. Letters next to a symbol represent materials available for that given locality: S = skins; V = vocalizations; T = tissues. Additional locality data can be found in Appendix S1.

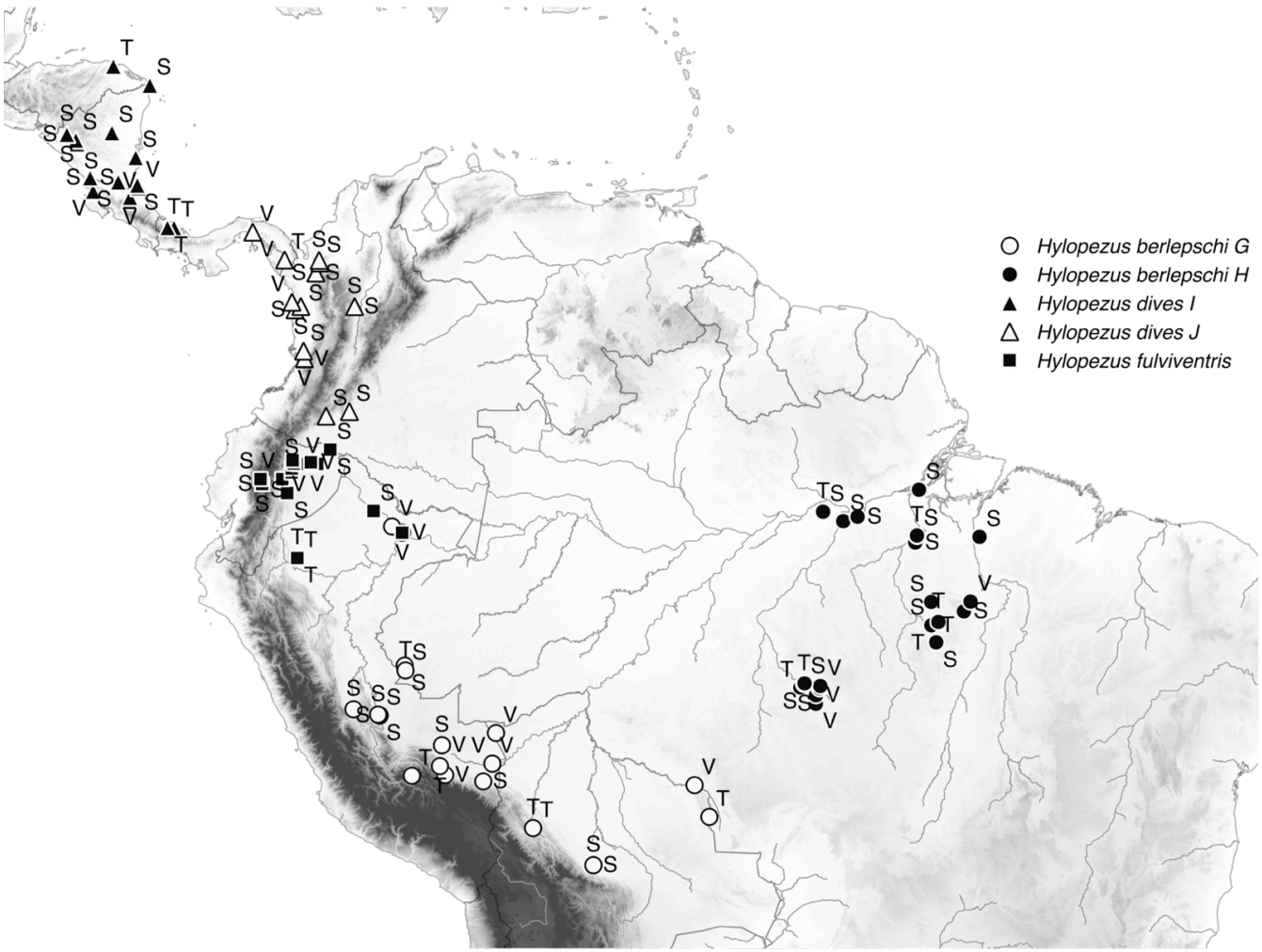

Figure 3. Geographic distribution of specimens, vocalizations, and tissues of the *Hylopezus berlepschi*, *Hylopezus dives* and *Hylopezus fulviventris* analyzed in the present study. For population definitions see results. Letters next to a symbol represent materials available for that given locality: S = skins; V = vocalizations; T = tissues. Additional locality data can be found in Appendix S1.

Species trees estimation

We reconstruct a time-calibrated multilocus species tree, including individuals from each lineage recovered by our phylogeographical estimation (Carneiro *et al*., unpubl. ms. Chapter 1), Species of the two other genera of the Grallariidae family, *Grallaricula* (*G. flavirostris* and *G. nana*) and *Grallaria* (*G. rufula*, *G. ruficapilla* and *G. guatimalensis*), were included as outgroups, hence covering all currently recognized genera of the family (Krabbe & Schulenberg, 2003; Rice, 2005). We used a Yule speciation prior and relaxed uncorrelated lognormal clock for each gene tree (Drummond et al., 2006). To calibrate our species tree, we used the ND2 substitution rate of 1.25 x 10^{-2} substitutions/site/Myr (2.5% change between lineages per Myr) from Smith & Klicka (2010). We performed two independent runs with 150 million generations each, with parameters sampled every 1000 generations, using BEAST 1.7.4 (Drummond et al., 2012). Tracer was used to check for convergence between runs, likelihood stationarity, appropriate burn-in, and adequate effective sample sizes (> 200). After discarding the first 15 million generations (10%) as burn-in, the parameter values of the samples from the posterior distribution were summarized on the maximum clade credibility tree using TreeAnnotator 1.7.4 (Drummond & Rambaut, 2007). For adittional analyses details see (Carneiro *et al*., unpubl. ms. Chapter 1).

Morphological data

We examined 311 study skins, belonging to all currently recognized lineages of the *Hylopezus* / *Myrmothera* clade recovered by our phylogeographic estimation, except *Hylopezus auricularis*, excluded from all morphological analyses due to the lack of available specimens (Table S1). Measurements of the following six morphological characters, were taken to the nearest 0.1 mm with an electronic caliper: wing length, tail length, tarsus length, bill length from the distal points of the nostrils to the tip of the bill, bill depth, and width at the distal point of the nostrils.

We quantified the measurement variation within each group (i.e., all species included in the major clades of our phylogenetic tree). To minimize measurement errors, only one person (L. Carneiro) took all measurements.

To test whether morphological differences between lineages closely related recovered by our phylogenetic analyses were statistcaly supported, we implemented the Wilcoxon

rank sum tests. Statistical analyses were performed using R 3.0.1.

Acoustic data

We analyzed 124 different recordings, from 91 localities belonging to all currently recognized species of *Hylopezus* and *Myrmothera*, except for a few lineages (see below; Table S5). The vocalizations are deposited in the following archives: MLS = Macaulay Library of Natural Sounds, Cornell Laboratory of Ornithology, Ithaca, New York; XC = Xeno-canto (www.xenocanto.org/), and PAC = Personal archives.

Two lineages recovered in the phylogeographic analyses were not included in the bioacoustics analysis due to the lack of available vocalizations, *H. perspicillatus* B and *M. simplex* E, the remaining lineages were compared using six acoustic measures (Maximum and minimum frequency of loudsong; frequency with maximum energy of loudsong; duration of first note, duration total of loudsong and number of notes per second. To measure acoustics details see (Carneiro *et al*., unpubl. ms. Chapter 2). The number of notes per loudsong and pace (Number of notes per second) were square-root transformed; all other loudsong were log-transformed prior to analysis. For each species, only one loudsong per individual was used in the analyses, to avoid pseudoreplication. Songs measurements were made using spectrograms and refer to the fundamental harmonic, which in all vocalizations analyzed was also the dominant one. Spectrograms were produced from all recordings and their structure was quantified using a variety of standard time and frequency measurements, following the method proposed by Seddon (2005) (for details see Carneiro *et al*., unpubl. ms. Chapter 2). Spectrograms and all song measurements were carried out using RAVEN PRO, version 1.5 (Cornell Laboratory of Ornithology, Ithaca, New York). Spectrograms were produced using the following settings in RAVEN (Window type: Hamming; window size: 1.300 samples; time grid: 95% overlap; and DFT size: 32.768 samples), when necessary; background noise was removed through lowpass and highpass filtering.

We assessed normality of acoustic data with Kolmogorov-Smirnov tests and used discriminant function analyses (DFA) to test for differences in the acoustic space among lineages. We combined both sexes in the analyses because there was no evidence of sexual dimorphism for any character. DFA analyses was performed in the MASS package v.7.3 in R.

RESULTS AND DISCUSSION

The BI recovered 20 evolutionary lineages within *Hylopezus* and *Myrmothera* genera, distributed in two major clades and one separate lineage with a single member, *H. nattereri* (Carneiro *et al*., unpubl. ms. Chapter 1). The 'core *Hylopezus*' clade contained 8 lineages from seven currently recognized *Hylopezus* species: *H. auricularis, H. ochroleucus, H. perspecillatus, H. macularius, H. dilutus, H. whittakeri*, and *H. paraensis* (Fig. 1), whereas the 'extended *Myrmothera*' clade comprises 11 lineages from 5 species, including 3 taxa currently allocated in *Hylopezus* (*M. campanisona*, *M. simplex*, *H. dives*, *H. berlepschi*, and *H. fulviventris*; Figs. 2 and 3).

Our reconstructions revealed all species currently recognized in the *Hylopezus* / *Myrmothera* clade as monophyletic, except for the paraphyly found within the genus *Myrmothera*. The widespread lowland Amazonian endemic *Myrmothera campanisona* includes four distinct paraphyletic lineages subdivided in two groups: one comprising Guiana Shield and Western Amazon Forest lineages (C and D), and another (A and B) comprising Eastern Amazon Forest lineages (East of Tapajos River), with the latter more closely related to the remaining species of the genus, the highland Tepui endemic *M. simplex* (Fig. 4).

Complete genetic data could not be obtained for some specimens used in our multilocus species tree analyses. In particular, we could not obtain FGB-I5 sequences from *H. dilutus*, and any nuclear data for the two divergent lineages of *H. perspicillatus* (A and B) (Fig. 4), so these lineages were represented solely from mtDNA data. Our multilocus species tree produced a time-calibrated phylogenetic reconstruction with overall high resolution and nodal support (80% of nodes with PP > 0.95; Fig. 3). Additionally, our multilocus and mtDNA chronogram topologies differed only in the placement of *H. dives* and on the relationships between the *Grallaricula* and members of the *Hylopezus* / *Myrmothera* clades (Figure 4). *Hylopezus dives* was placed as sister of *H. fulviventris* + *H. berlepschi* (multilocus species tree, PP = 0.65) or as sister to the *Myrmothera* lineages (mtDNA chronogram, PP = 0.67; Fig. 3). The multilocus species tree also yielded high support for a relationships that was poorly supported in the mtDNA reconstruction: 'core *Hylopezus*' and 'extended *Myrmothera*' clades were recovered as sister groups (Fig. 4)

The sonograms and the DFA based on the loudsong characters showed three clusters within 'core *Hylopezus*': One comprising species in the *Hylopezus macularius* complex, other formed by *H. ochroleucus*, *H. perspicillatus* and by the new genus, and a third with *Hylopezus auricularis* (Figs. 5 and 8). However the loudsong structure of new genus closely resembles that of *H. ochroleucus*, with a few misclassifications (Table 2). Though this vocal similarities could be result of convergence or retention of ancestral characters (Carneiro *et al*., unpubl. ms. Chapter 2).

On 'extended *Myrmothera*' the loudsongs are very different and were analyzed separately (Figs 9 and 10). Within the *Myrmothera* clade there is a split tendency between the loudsongs of *M. campanisona* and *M. simplex*, which is mainly associated with temporal patterns once that frequency and notes shape are quite similar (Fig. 8; Figs 6 and 7). Although there is a tendency to the formation of clusters between *M. campanisona* populations, the low percentage score of correct classification indicates that the loudsongs are very similar to each other (Figs. 6 and 9; Table 3). Within the remaining 'extended *Myrmothera*' the DFA showed two vocal clusters, one comprising *H. fulviventris and H. berlepschi* (Populations H and G), and another formed by *H. dives* (Populations I and J) (Fig. 10). There is a clear tendency of separation between the *H. dives*' populations, however there is overlap between the loudsongs of *H. berlepschi* (populations G and H) and *H. fulviventris* (Fig. 10; Table 4).

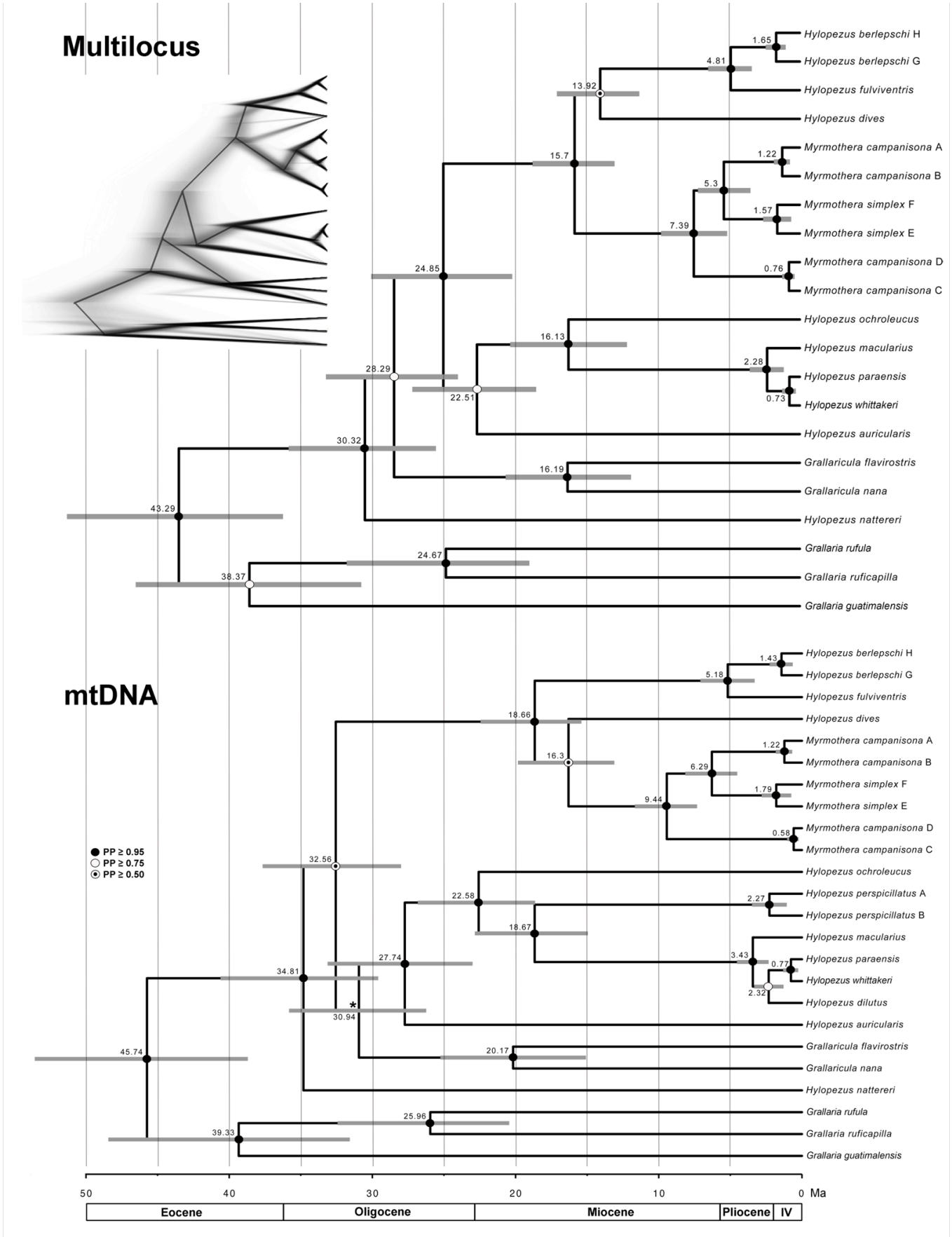
Multilocus
Hylopezus berlepschi H
Hylopezus berlepschi G
Hylopezus fulviventris
Hylopezus dives
Myrmothera campanisona A
Myrmothera campanisona B
Myrmothera simplex F
Myrmothera simplex E
Myrmothera campanisona D
Myrmothera campanisona C
Hylopezus ochroleucus
Hylopezus macularius
Hylopezus paraensis
Hylopezus whittakeri
Hylopezus auricularis
Grallaricula flavirostris
Grallaricula nana
Hylopezus nattereri
Grallaria rufula
Grallaria ruficapilla
Grallaria guatimalensis
1.65
4.81
13.92
15.7
1.22
5.3
1.57
7.39
0.76
24.85
16.13
2.28
28.29
22.51
0.73
30.32
16.19
43.29
24.67
38.37
mtDNA
PP ≥ 0.95
PP ≥ 0.75
PP ≥ 0.50
Hylopezus berlepschi H
Hylopezus berlepschi G
Hylopezus fulviventris
Hylopezus dives
Myrmothera campanisona A
Myrmothera campanisona B
Myrmothera simplex F
Myrmothera simplex E
Myrmothera campanisona D
Myrmothera campanisona C
Hylopezus ochroleucus
Hylopezus perspicillatus A
Hylopezus perspicillatus B
Hylopezus macularius
Hylopezus paraensis
Hylopezus whittakeri
Hylopezus dilutus
Hylopezus auricularis
Grallaricula flavirostris
Grallaricula nana
Hylopezus nattereri
Grallaria rufula
Grallaria ruficapilla
Grallaria guatimalensis
1.43
5.18
18.66
16.3
1.22
6.29
1.79
9.44
0.58
32.56
22.58
2.27
18.67
3.43
0.77
27.74
34.81
2.32
30.94
*
45.74
20.17
25.96
39.33
50
40
30
20
10
0 Ma
Eocene
Oligocene
Miocene
Pliocene
IV

Figure 4. Reconstructions for antpittas estimated from multilocus (species tree) and mtDNA (chronogram) datasets using *Beast. Bars indicate 95% highest posterior densities of divergence dates. The mean estimated dates are shown above nodes and the scale bar is in millions of years ago (Ma). Bayesian posterior probability (PP) support for nodes are indicated by coded dots according to the figure legend, with nodes receiving less than 0.50 support marked with an asterisk. IV = Quaternary. The inset (upper left) figure is the result of the superposition of all gene trees and has the same topology of the multilocus tree (generated by DensiTree 2.0.1).

Six pairs of closely related lineages, recovered by our phylogenetic analyses (Fig 4; *H. perspicillatus* A and B; *H. berlepschi* G and H; *H. dives* I and J; *M. campanisona* A and B; *M. campanisona* C and D; *M. simplex* E and F), had their morphological differences tested through the Wilcoxon rank sum test. Of the six pairs of lineages tested, only one, *M. campanisona* A and B, showed no significant difference in any character measurements. The remaining pairs showed significant differences in at least one morphometric character (Table 1).

The strongest morphometric difference was observed between the populations of *H. perspicillatus,* in which five of six morphometric characters tested were significantly different. (Table 1)

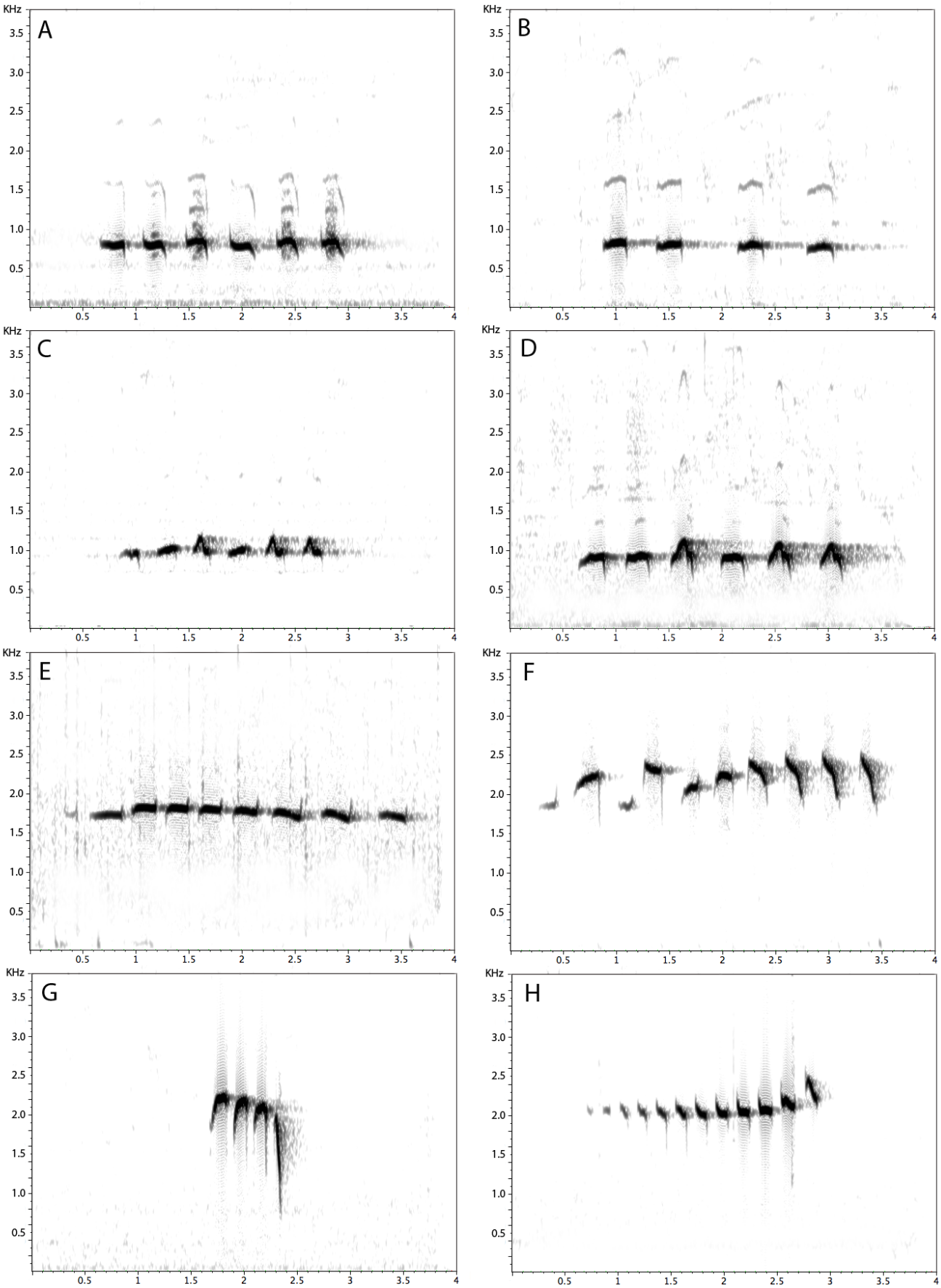

Figure 5. Representative loudsong audiospectrograms of *Hylopezus* genus and *New genus*. (A) *H. paraensis*, Caxiuanã, Pará, Brazil (MLS 127444). (B) *H. whittakeri*, Alta Floresta, Mato Grosso, Brazil

(MLS 48068). (C) *H. dilutus*, Maraã, Lago Cumapi, Amazonas, Brazil (A.A., 1 PAC). (D) *H. macularius*, Rupununi, Guyana (MLS 73054). (E) *H. perspicillatus* (Population A), Playa de Oro, Esmeraldas, Ecuador (XC 98206). (F) *H. ochroleucus*, Bahia, Sebastiao Laranjeiras, Brazil (MLS 91034). (G) *H. auricularis*, Puerto Hamburgo, Riberalta, Beni, Bolivia (XC 146789). (H) *New genus*, Rio de Janeiro, Parque Nacional Itatiaia; Trilha de Três Picos, Brazil (MLS 112731). Window type Hamming, window size 1,300 samples, time grid 95% overlap, and DFT size 32,768 samples.

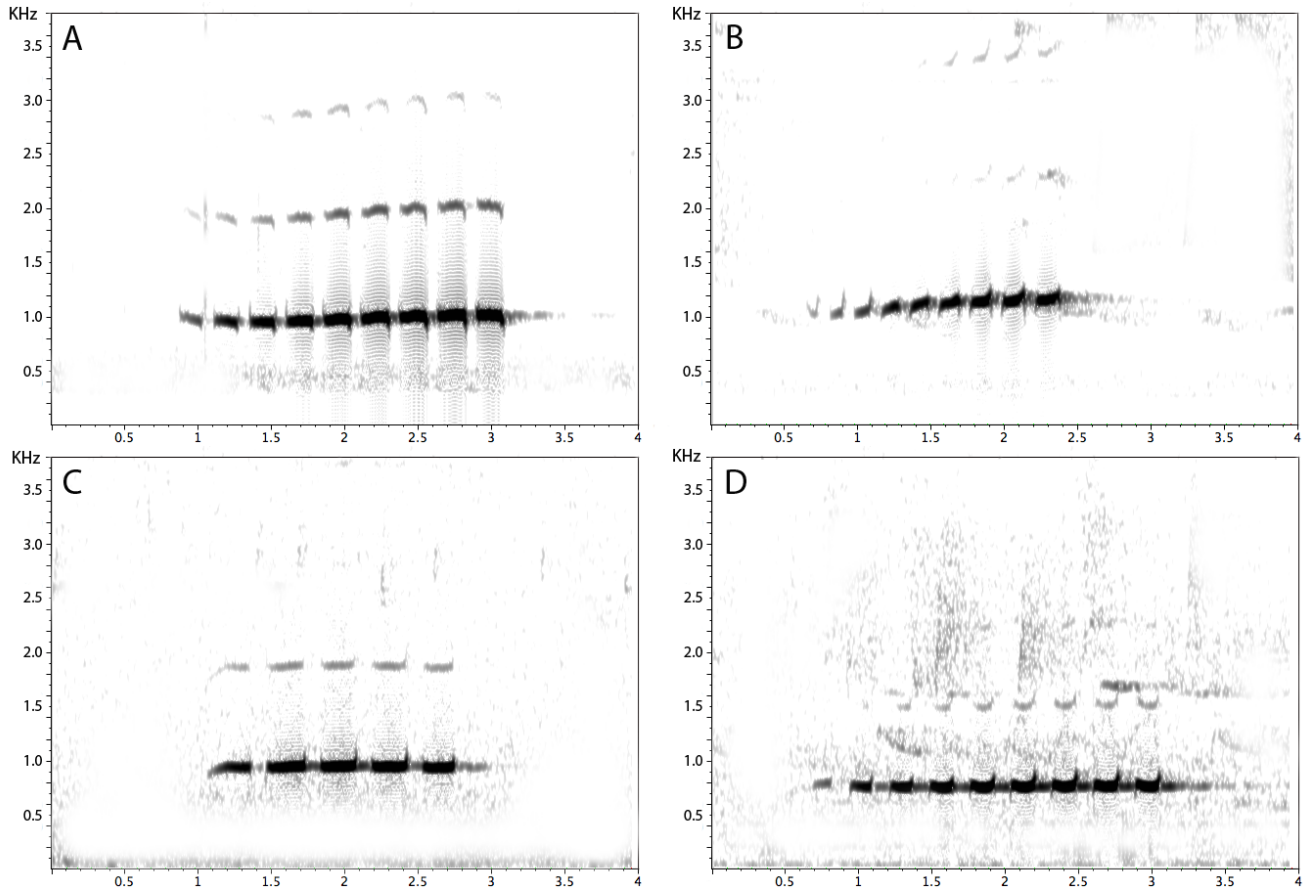

Fig. 6. Representative loudsong audiospectrograms of Populations A-D of *Mymothtera campanisona*. (A) Population A, Cristalino Jungle Lodge, Mato grosso, Brazil (XC 38478). (B) Population B, Ariquemes, Rondônia, Brazil (XC 90425). (C) Population C, Sucumbios, Ecuador (MLS 74784). (D) Population D, Nappi Village, Guyana (MLS 70074). Window type Hamming, window size 1,300 samples, time grid 95% overlap, and DFT size 32,768 samples.

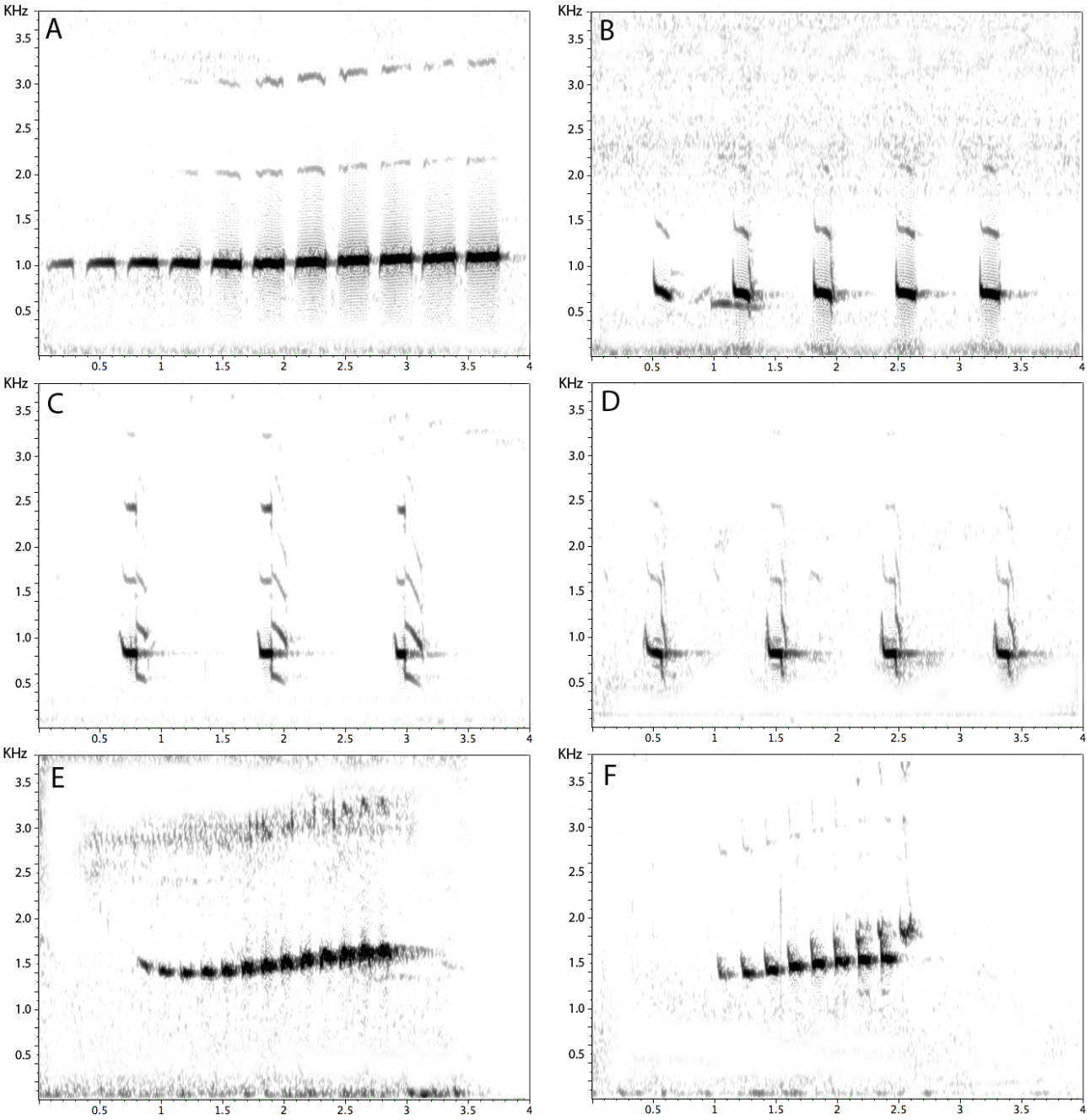

Figure 7. Representative loudsong audiospectrograms of *Myrmothera simplex*, *Hylopezus berlepschi, H. fulviventris* and *H. dives*. (A) *M. simplex* (Population F), Sierra de Lema, Venezuela (MLS 62408). (B) *H. fulviventris*, Payamino river, Napo, Ecuador (MLS 78536). (C) *H. berlepschi* (Population H), Redenção, Pará, Brazil (MLS 94594). (D) *H. berlepschi* (Population G), Madre de dios, Peru (MLS 48171). (E) *H. dives* (Population I), Heredia, Costa Rica (MLS 31389). (F) *H. dives* (Population J), Cana, Darien, Panamá (MLS 105095). Window type Hamming, window size 1,300 samples, time grid 95% overlap, and DFT size 32,768 samples.

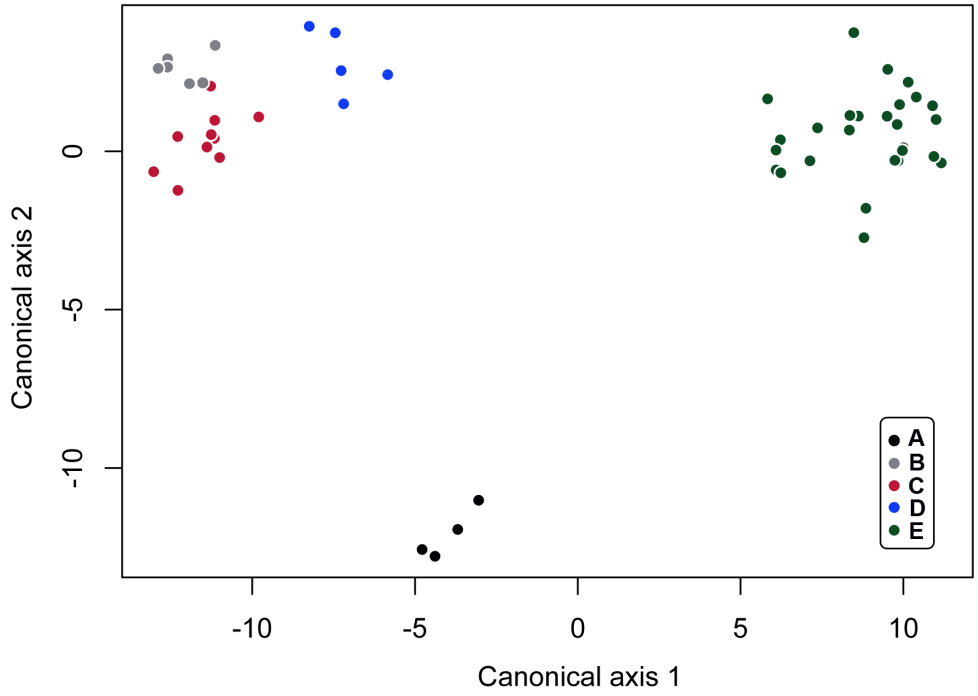

Figure.8. Graphic representation of scores of the first two axes of a discriminant function analysis based on six acoustic characters related to frequency and temporal variation (see text to details) belonging to five groups A–E as follows: A = *H. auricularis*; B = *H. ochroleucus*; C = *gen.nov*; D = *H. perspicillatus* (Population A); and E = *H. macularius* complex (*H. macularius*, *H. dilutus*, *H. whittakeri*, *H. paraensis*).

Table 2. Summary of classification accuracy obtained through a discriminant function analysis based on six acoustic characters related to frequency and temporal variation (see text to details) belonging to five groups A–E as follows: A = *H. auricularis*; B = *H. ochroleucus*; C = *gen.nov*; D = *H. perspicillatus* (Population A); and E = *H. macularius* complex (*H. macularius*, *H. dilutus*, *H. whittakeri*, *H. paraensis*). The number of tape-recordings included in the analysis is shown in parentheses.

Lineage	A	B	C	D	E	Correctness (%)
A (n=4)	4	0	0	0	0	100
B (n=6)	0	5	1	0	0	83.3
C (n=10)	0	1	9	0	0	90
D (n=5)	0	0	0	5	0	100
E (n=27)	0	0	0	0	27	100
Total (n=53)	4	6	10	5	27	94.6

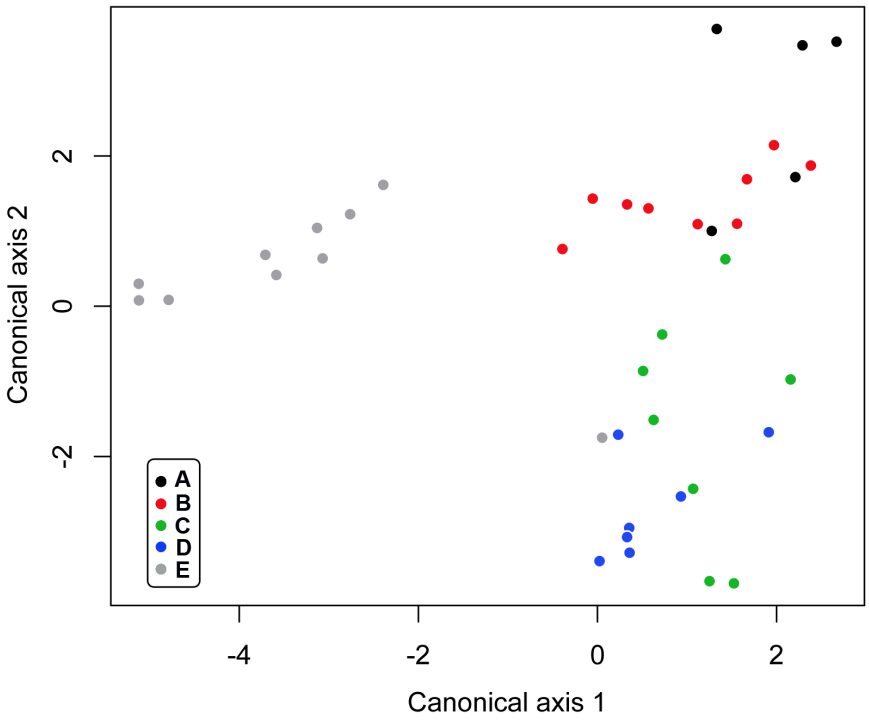

Figure 9. Graphic representation of scores of the first two axes of a discriminant function analysis based on six acoustic characters related to frequency and temporal variation (see text to details) belonging to five *Myrmothera* groups A–E as follows: A = *M. campanisona* (Population A); B = *M. campaniosna* (Population B); C = *M. campanisona* (Population C); D = *M. campanisona* (Population D); and E = *M. simplex* (Population F).

Table 3. Summary of classification accuracy obtained through a discriminant function analysis based on six acoustic characters related to frequency and temporal variation belonging to five *Myrmothera* groups A–E as follows: A = *M. campanisona* (Population A); B = *M. campaniosna* (Population B); C = *M. campanisona* (Population C); D = *M. campanisona* (Population D); and E = *M. simplex* (Population F). The number of tape-recordings included in the analysis is shown in parentheses.

Lineage	A	B	C	D	E	Correctness (%)
A (n=10)	8	2	0	0	0	80
B (n=5)	4	1	0	0	0	20
C (n=8)	1	0	5	2	0	62.5
D (n=7)	0	0	1	6	0	85.7
E (n=10)	0	0	0	1	9	90
Total (n=40)	13	3	6	9	9	72.5

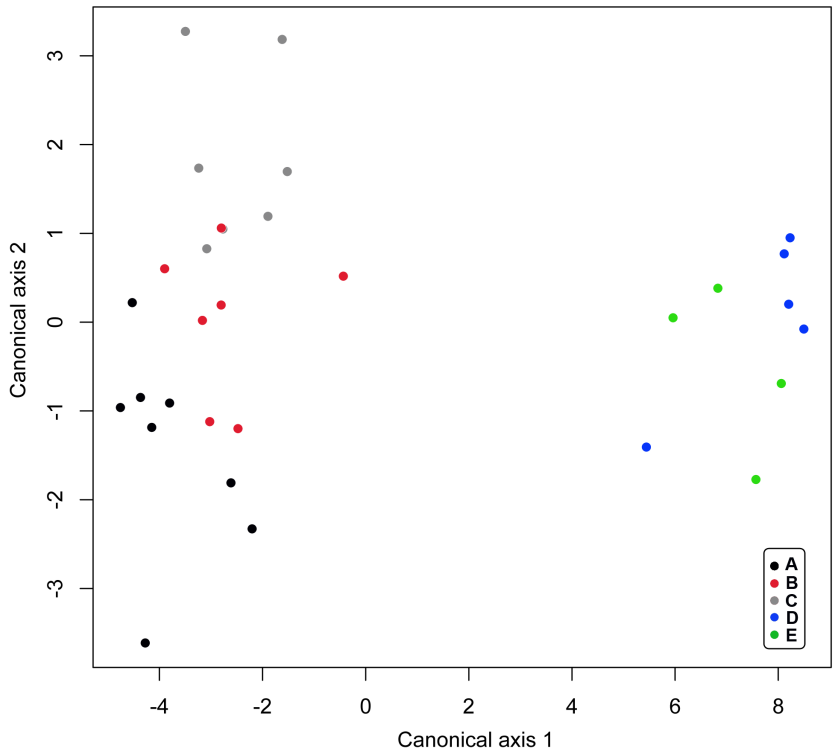

Figure 10. Graphic representation of scores of the first two axes of a discriminant function analysis based on six acoustic characters related to frequency and temporal variation belonging to five groups A–E as follows: A = *M. berlepschi* (Population G); B = *M. berlepschi* (Population H); C = *M. fulviventris*; D = *M. dives* (Population J); and E = *M. dives* (Population I).

Table 4. Summary of classification accuracy obtained through a discriminant function analysis based on six acoustic characters related to frequency and temporal variation belonging to five groups A–E as follows: A = *M. berlepschi* (Population G); B = *M. berlepschi* (Population H); C = *M. fulviventris*; D = *M. dives* (Population J); and E = *M. dives* (Population I). The number of tape-recordings included in the analysis is shown in parentheses.

Lineage	A	B	C	D	E	Correctness (%)
A (n=8)	5	3	0	0	0	62.5
B (n=7)	2	3	2	0	0	42.8
C (n=6)	0	2	4	0	0	57.1
D (n=5)	0	0	0	4	1	80
E (n=4)	0	0	0	0	4	100
Total (n=30)	8	7	6	5	4	72.5

Table 1. Mean (± SD) of morphological differences between closely related lineages recovered by our phylogenetic analyses. Statistics are derived from Wilcoxon rank sum tests; Bold denotes *P*-values that were significant ($P < 0.05$).

Trait	*H. Perspcillatus* A (n=26)	*H. Perspcillatus* B (n=23)	Statistics
Wing	76.91 ± 2.34	82.55 ± 2.06	**0.000**
Tail	30.49 ± 1.15	34.62 ± 1.41	**0.000**
Tarsus	34.17 ± 1.32	36.33 ± 1.40	**0.000**
Beak length	12.22 ± 0.56	12.8 ± 0.74	**0.001**
Beak depth	5.69 ± 0.23	6.08 ± 0.26	**0.000**
Beak width	5.47 ± 0.30	5.44 ± 0.34	0.434

Trait	*M. berlepschi* G (n=10)	*M. berlepschi* H (n=16)	Statistics
Wing	81.74 ± 1.85	80.49 ± 1.17	0.072
Tail	37.43 ± 1.73	39.6 ± 1.65	0.054
Tarsus	38.46 ± 2.10	38.31 ± 1.20	0.526
Beak length	13.15 ± 0.42	13.38 ± 0.62	0.113
Beak depth	6.08 ± 0.32	5.80 ± 0.22	**0.000**
Beak width	5.84 ± 0.25	5.71 ± 0.31	0.178

Trait	*M. campanisona* A (n=10)	*M. campanisona* B (n=9)	Statistics
Wing	80.75 ± 1.82	80.27 ± 2.07	0.538
Tail	40.40 ± 1.73	39.88 ± 1.82	0.660
Tarsus	41.665 ± 1.30	42.22 ± 1.37	0.652
Beak length	12.77 ± 0.81	12.83 ± 0.55	0.595
Beak depth	5.775 ± 0.24	5.39 ± 0.30	0.236
Beak width	5.635 ± 0.28	5.85 ± 0.30	0.413

Trait	*M. campanisona* C (n=43)	*M. campanisona* D (n=19)	Statistics
Wing	77.52 ± 2.49	78.86 ± 2.74	0.059
Tail	36.20 ± 2.19	36.23 ± 1.40	0.778
Tarsus	39.99 ± 2.29	40.80 ± 1.90	0.104
Beak length	11.95 ± 0.68	12.11 ± 0.77	0.055
Beak depth	5.68 ± 0.30	6.12 ± 0.28	**0.000**
Beak width	5.355 ± 0.43	5.635 ± 0.21	**0.006**

Trait	*M. simplex* E (n=9)	*M. simplex* F (n=25)	Statistics
Wing	84.58 ± 2.42	79.6 ± 2.21	**0.000**
Tail	49.73 ± 1.90	40.80 ± 5.11	**0.000**
Tarsus	44.73 ± 1.78	39.60 ± 3.22	**0.001**
Beak length	13.08 ± 0.58	12.85 ± 0.79	0.639
Beak depth	5.91 ± 0.25	6.02 ± 0.60	0.412
Beak width	5.25 ± 0.26	5.49 ± 0.58	0.379

Trait	*M. dives* J (n=14)	*M. dives* I (n=12)	Statistics

Wing	74.46 ± 2.38	76.55 ± 2.16	0.409
Tail	34.17 ± 1.99	34.02 ± 1.95	0.520
Tarsus	36.42 ± 1.04	35.55 ± 1.19	**0.010**
Beak length	12.66 ± 0.52	12.97 ± 0.62	0.207
Beak depth	5.17 ± 0.27	5.70 ± 0.20	**0.003**
Beak width	5.35 ± 0.25	5.12 ± 0.14	0.053

TAXONOMIC IMPLICATIONS

Despite the marked differences found in some closely related lineages, we believe that our data are not sufficiently conclusive to support accurate taxonomic decisions at a specific level, given the morphological and vocal overlay and the difficulty of diagnosing the lineages recovered by our phylogenetic analyzes.

However, at a broader level, our multilocus species tree reconstruction strongly suggests that *Myrmothera* forms a monophyletic group with three species currently placed in *Hylopezus* genus (*H. dives*, *H. fulviventris*, and *H. berlepschi* ; Fig. 4). The clade formed by *H. auricularis*, *H. ochroleucus*, *H. whittakeri*, *H. paraensis*, and *H. macularius*, recovered by the multilocus species tree, probably also comprise the type species of *Hylopezus*: *H. perspicillatus* (Fig. 4). Even though we had no success with the amplification of any nuclear markers for this taxon, it was recovered with high support within this clade according to mtDNA chronogram. Furthermore, our vocal and morphometric data also support this conclusion (Figs. 5 and 8).

Considering *H. perspicillatus* as the type species of species of *Hylopezus*, the following species must remain in this genus: *H. auricularis*, *H. ochroleucus*, *H. perspicillatus, H. macularius, H. dilutus, H. whittakeri*, and *H. paraensis*. Furthermore, the clade formed by *H. berlepschi*, *H. dives* and *H. fulviventris* renders *Myrmothera* paraphyletic, therefore merging this '*Hylopezus*' group into *Myrmothera* Hermann, 1783, solves this problem.

Finally, we also recommend the recognition of *H. nattereri* as a separate (monotypic) genus, given its phylogenetic position, vocal, and morphological diagnosability from the remaining taxa of the *Hylopezus* / *Myrmothera*.

New genus Carneiro, Bravo, and Aleixo gen. nov.

Type species. *Grallaria nattereri* Pinto, 1937.

Included species. *Grallaria nattereri* (Pinto). Speckle-breasted Antpitta

.

Diagnosis. Distinguished from other genera in Grallaridae family by breast, upper

belly and flanks with particular pattern of spotted dusky; bare orbital skin buffy white. Genetically distinct. Loudsongs structurally distinct, show whistled notes, steadily increasing in amplitude, first few slightly falling, but thereafter rising in pitch from c. 2 to c. 2·5 kHz, notes changing shape through the series. Habitat: Ground and lower growth in humid and montane forest, mature secondary woodland, and borders; often in very densely tangled vegetation and bamboo. At 1200–1900 m.

Hylopezus Ridgway, 1909

Type species. *Hylopezus perspicillatus* (Lawrence, 1861).

Included species. *Hylopezus perspicillatus* (Lawrence, 1861). Streak-chested Antpitta. *Hylopezus auricularis* (Gyldenstolpe, 1941). Masked Antpitta. *Hylopezus macularius* (Temminck, 1830) Spotted Antpitta. *Hylopezus paraensis* (Snethlage, 1910) Snethlage´s Antpitta. *Hylopezus dilutus* (Hellmayr, 1910). Zimmer´s Antpitta. *Hylopezus whittakeri* (Carneiro et al., 2012) Alta Floresta Antpitta. *Hylopezus ochroleucus* (Wied, 1831). White-browed Antpitta.

Diagnosis. Distinguished from other genera by mantle with conspicuous shaft-streaks, more olivaceous upperparts, much paler ochraceous subterminal bands of pectoral spots, and wingbars occupying the entire length of the wing. Genetically distinct. Habitat: Floor and dense undergrowth of forest, lower undergrowth of humid forest, semi-deciduous and deciduous woodland, including *caatinga* woodland.

Myrmothera Vieillot, 1816

Type species. *Myrmornim campanisonam* (Hermann, 1783).

Included species. *Myrmothera campanisona* (Hermann, 1783). Thrush-like Antpitta. *Myrmothera simplex* (Salvin and Godman, 1884). Tepui Antpitta. *Myrmothera dives* (Salvin, 1865) Thicket Antpitta. *Myrmothera fulviventris* (Sclater, 1858) White-lored Antpitta. *Myrmothera berlepschi* (Hellmayr, 1903). Amazonian Antpitta.

Diagnosis. Distinguished from other genera by show a buffy loral spot; entire upperparts olive-brown, outer webs of primaries paler; mantle without shaft-streaks,

breast and upper belly with particular patterns of streak. Genetically distinct. Loudsongs structurally distinct. Habitat: Floor and lower part of very dense undergrowth at forest edge and in overgrown clearings

Appendix. Supplementary material

Table S1. Geographic information of specimens, vocalizations, and tissues analyzed in the present study.

LINEAGE	SOURCE	LOCALITY	VOUCHER
Myrmothera simplex F	Morphology	Venezuela: Bolivar, Roraima	169839-ANSP
Myrmothera simplex F	Morphology	Venezuela: Mt. Auyan. Tepui Plateau	323541-AMNH
Myrmothera simplex F	Morphology	Venezuela: Roraima. Philipp Camp.	236690-AMNH
Myrmothera simplex F	Morphology	Venezuela: Mt. Auyan. Tepui Plateau	323544-AMNH
Myrmothera simplex F	Morphology	Venezuela: Mt. Auyan. Tepui Plateau	323543-AMNH
Myrmothera simplex F	Morphology	Venezuela: Bolivar, Serra Pacaraima, Cerro Urutami	812901-AMNH
Myrmothera simplex F	Morphology	Venezuela: Bolivar, Serra Pacaraima, Cerro Urutami	812902-AMNH
Myrmothera simplex F	Morphology	Venezuela: Bolivar, Serra Pacaraima, Cerro Urutami	812900-AMNH
Myrmothera simplex F	Morphology	Venezuela: Cerro Guaiguinima, Falda N. O.	383248-USNM
Myrmothera simplex F	Morphology	Guyana; Mount Roraima, North Slope,	626929-USNM
Myrmothera simplex F	Morphology	Guyana; Mount Roraima, North Slope,	626774-USNM
Myrmothera simplex F	Morphology	Guyana; Mount Roraima, North Slope,	626921-USNM
Myrmothera simplex F	Morphology	Guyana; Mount Roraima, North Slope,	626869-USNM
Myrmothera simplex F	Morphology	Guyana; Cuyuni-Mazaruni, Paruima, ca. 19 KM, at Mt. Holitipu,	639140-USNM
Myrmothera simplex F	Morphology	Brit. Guiana: Roraima	156333-AMNH
Myrmothera simplex F	Vocal	Venezuela: Rio Cuyuni; km 124; Sierra de Lema	MLS62408
Myrmothera simplex F	Vocal	Venezuela: At highest elevation on Escalera	MLS60984
Myrmothera simplex F	Vocal	Venezuela: Escalera, South of las Claritas	MLS60983
Myrmothera simplex F	Vocal	Venezuela: 112.0 km S of El Dorado	MLS52919
Myrmothera simplex F	Vocal	Venezuela: 112.0 km S of El Dorado	MLS52916
Myrmothera simplex F	Vocal	Venezuela: 45.0 km S of Las Claritas	MLS49522
Myrmothera simplex F	Vocal	Venezuela: 45.0 km S of Las Claritas	MLS49521
Myrmothera simplex F	Vocal	Venezuela: 25.0 km S of Las Claritas	MLS49339

Myrmothera simplex F	Vocal	Venezuela: La Escalera	MLS30418
Myrmothera simplex F	Vocal	Guyana: north slope Mt Roraima	MLS134902
Myrmothera simplex E	Morphology	Venezuela: Amazonas, Mount Duida, Desfiladero	323087-USNM
Myrmothera simplex E	Morphology	Venezuela: Mt. Duida. Sinmit Central Camp.	245926-AMNH
Myrmothera simplex E	Morphology	Venezuela: Mt. Duida. Cumbre 2. Cabeceras del Valle	270928-AMNH
Myrmothera simplex E	Morphology	Venezuela: Mt. Duida. Cabeceras del Valle	270924-AMNH
Myrmothera simplex E	Morphology	Venezuela: Mt. Duida. Valley head, Summit	270921-AMNH
Myrmothera simplex E	Morphology	Venezuela: Mt. Duida. Cumbre 13. Desfiladero	270926-AMNH
Myrmothera simplex E	Morphology	Venezuela: Mt. Duida. Cumbre 2. Cabeceras del Valle	270920-AMNH
Myrmothera simplex E	Morphology	Venezuela: Mt. Duida. Sunmit Privisional Camp.	270925-AMNH
Myrmothera simplex E	Morphology	Venezuela: Mt. Duida. Cumbre 2. Cabeceras del Valle	270923-AMNH
Myrmothera simplex E	Morphology	Venezuela: Terr. Amazonas. Valley N Base Pico Cardona	816753-AMNH
Myrmothera simplex	*Molecular*	Venezuela: Amazonas; Sierra de Tapirapeco; Cerro Tamacuari; 1270m	AMNH - 2136
Myrmothera simplex	*Molecular*	Venezuela: Amazonas; Pico Cardonas; Elev. 1250M Rainforest, Valley N. Base	AMNH - 17126
Myrmothera simplex	*Molecular*	Venezuela: Bolivar; La Escalera, KM 122 on El dorado-ST. Eleanea Road	AMNH - RDP301
Myrmothera simplex	*Molecular*	Venezuela: Amazonas; Cerro Yavi	AMNH - 213312
Myrmothera simplex	*Molecular*	Venezuela: Amazonas; Cerro de la Neblina; CAMP VII 1800-1900M	AMNH - 1440
Myrmothera simplex	*Molecular*	Venezuela: Amazonas; Cerro Yavi	AMNH - 213320
Myrmothera simplex	*Molecular*	Venezuela, Amazonas Territory, CERRO DE LA NEBLINA CAMP VII 1800M	LSUMZ - B7408
Myrmothera simplex	*Molecular*	Venezuela, Amazonas Territory, CERRO DE LA NEBLINA CAMP VII 1800M	LSUMZ - B7468
Myrmothera campanisona D	Vocal	Venezuela: 10.0 km E of Rio Grande	MLS49340
Myrmothera campanisona D	Vocal	Brazil: Amazonas, 25.0 km N of Manaus	MLS32418
Myrmothera campanisona D	Vocal	Suriname: Foengoe island	MLS2136
Myrmothera campanisona D	Vocal	Suriname: Foengoe island	MLS2131
Myrmothera campanisona D	Vocal	Guyana: Upper Takutu-Upper Essequibo, Sipu RIver	MLS134399
Myrmothera campanisona D	Vocal	Brazil: Amazonas, ZF-3, Reserva 41	MLS113138
Myrmothera campanisona D	Vocal	Guyana: Upper Takutu-Upper Essequibo, 20.0 km E of Nappi Village	MLS70074

Myrmothera campanisona C	Vocal	Ecuador: Sucumb√≠os, 12.0 km N of Lumbaqui	MLS74784
Myrmothera campanisona C	Vocal	Venezuela: Amazonas, Rio Negro region; Pica San Carlos-Solano	MLS62420
Myrmothera campanisona C	Vocal	Bolivia: La Paz, Alto Rio Madidi Camp	MLS52374
Myrmothera campanisona C	Vocal	Bolivia: Pando, SW of Cobija; Camino Mucden	MLS38929
Myrmothera campanisona C	Vocal	Brazil: Amazonas, 25.0 km N of Manaus	MLS32418
Myrmothera campanisona C	Vocal	Peru: Loreto, north bank Rio Napo; Quebrada; Sucusari	MLS29114
Myrmothera campanisona C	Vocal	Peru: Madre de Dios	MLS13288
Myrmothera campanisona C	Vocal	Brazil: Amazonas, Parque Nacional Jau	MLS117014
Myrmothera campanisona B	Vocal	Brazil: Ariquemes, Rondônia. 25km north of town	XC90425
Myrmothera campanisona B	Vocal	Brazil: Parque Nacional da Amazônia	XC90424
Myrmothera campanisona B	Vocal	Brazil: Parque Nacional da Amazônia	XC90423
Myrmothera campanisona B	Vocal	Brazil: Rondônia, Cachoeira Nazare; west bank of Rio Jiparana	MLS40235
Myrmothera campanisona B	Vocal	Brazil: Pará, Parque Nacional da Amazonia; southwest of Itaituba	MLS35671
Myrmothera campanisona A	Vocal	Brazil: Belterra, Bacia 357, PA	XC94889
Myrmothera campanisona A	Vocal	Brazil: Tapajós National Forest	XC90422
Myrmothera campanisona A	Vocal	Brazil: Cristalino Jungle Lodge, MT	XC68792
Myrmothera campanisona A	Vocal	Brazil: Cristalino Jungle Lodge, MT	XC5707
Myrmothera campanisona A	Vocal	Brazil: Cristalino Jungle Lodge, MT	XC38478
Myrmothera campanisona A	Vocal	Brazil: Novo Progresso, state of Pará	XC28243
Myrmothera campanisona A	Vocal	Brazil: Novo Progresso, state of Pará.	XC119378
Myrmothera campanisona A	Vocal	Brazil: Pará, Floresta Nacional de Tapajos; Base de Sucupira, BR-163	MLS115082
Myrmothera campanisona A	Vocal	Brazil: Pará, Floresta Nacional de Tapajos; BR-163	MLS114910
Myrmothera campanisona A	Vocal	Brazil: Mato Grosso, Cristalino Ecological Institute; Trilha da Castaneira	MLS110055
Myrmothera campanisona	*Molecular*	Brazil: Pará: FLOTA de Faro, ca 70 km NW de Faro	MPEG - CN150
Myrmothera campanisona	*Molecular*	Brazil: Pará: Juruti, Projeto Juruti/Alcoa, Platô Capiranga, trilha 196	MPEG - 0961
Myrmothera campanisona	*Molecular*	Brazil: Pará: Alenquer, ESEC Grão-Pará	MPEG - CN509
Myrmothera campanisona	*Molecular*	Brazil: Pará: Alenquer, ESEC Grão-Pará	MPEG - CN418

Myrmothera campanisona	*Molecular*	Brazil: Pará: Rio Xingu, margem direita, Caracol (área 2)	MPEG - BMP075
Myrmothera campanisona	*Molecular*	Brazil: Pará: Óbidos, Flota do Trombetas	MPEG - CN341
Myrmothera campanisona	*Molecular*	Brazil: Pará: Altamira, Floresta Nacional de Altamira	MPEG - TM008
Myrmothera campanisona	*Molecular*	Rio Juruá, Marechal Taumaturgo, Nossa Senhora Aparecida	MPEG - PNS337
Myrmothera campanisona	*Molecular*	Rio Branco, margem esquerda, Caracaraí, próximo BR 174	MPEG - MPD040
Myrmothera campanisona	*Molecular*	Brazil: Amazonas, São Gabriel da Cachoeira, PPBIO	MPEG - 20648
Myrmothera campanisona	*Molecular*	Brazil: Pará: Itaituba, margem direita Rio Tapajós, Comunidade Penedo	MPEG - 19634
Myrmothera campanisona	*Molecular*	Brazil: Pará, Jacareacanga, margem esquerda Rio Tapajós, Vila Mamãe-anã	MPEG - 18604
Myrmothera campanisona	*Molecular*	Brazil: Pará: Estern margin Rio Tapajós e direita do Jamanxin SW Itaituba	INPA - A10032
Myrmothera campanisona	*Molecular*	RR, Parque Nacional Viruá, margem esquerda do Rio Branco, "grid"	INPA - A1726
Myrmothera campanisona	*Molecular*	Brazil: Amazonas, 110 km ENE Santa Isabel do Rio Negro	INPA - A1662
Myrmothera campanisona	*Molecular*	RO, Porto Velho; margem direita do Rio Jaci; Três Praias	INPA - A4141
Myrmothera campanisona	*Molecular*	PA, Margem direita do Rio Tapajós; 147 km sudoeste de Itaituba, J	INPA - A11548
Myrmothera campanisona	*Molecular*	Guyana, Potaro-Siparuni, Iwokrama Reserve; ca. 41 road km, SW Kurupukari	ANSP - 21109
Myrmothera campanisona	*Molecular*	Guyana, Iwokrama Reserve; Kobacalli Landing	ANSP - 21242
Myrmothera campanisona	*Molecular*	Guyana, Potaro-Siparuni,Iwokrama Reserve; ca. 6-8 road mi. SW Kurupukari	ANSP - 22305
Myrmothera campanisona	*Molecular*	Ecuador, Morona-Santiago,Santiago	ANSP - 16450
Myrmothera campanisona	*Molecular*	Ecuador, Morona-Santiago,5 km SW Taisha	ANSP - 17546
Myrmothera campanisona	*Molecular*	Ecuador, Napo, Zancudo Cocha	ANSP - 18324
Myrmothera campanisona	*Molecular*	Ecuador, Napo, Pasohurco; km 57 on Hollin-Loreto Road	ANSP - 19457
Myrmothera campanisona	*Molecular*	Brazil, Rondonia, Cachoeira Nazare, W bank Rio Jiparana, 100m	FMNH - 389886
Myrmothera campanisona	*Molecular*	Brazil, Rondonia, Cachoeira Nazare, W bank Rio Jiparana, 100m	FMNH - 389885
Myrmothera campanisona	*Molecular*	Peru: Madre de Dios: Moskitania, 13.4 km NNW Atalaya	FMNH - 433464
Myrmothera campanisona	*Molecular*	Brazil, Acre, Reserva Extravista Alto Jurua, Rio Tejo,	FMNH - 395576
Myrmothera campanisona	*Molecular*	Brazil, Rondonia, Cachoeira Nazare, W bank Rio Jiparana, 100m	FMNH - 395993
Myrmothera campanisona	*Molecular*	Peru, Madre de Dios, Moskitania, 13.4 km NNW Atalaya	FMNH - 433462
Myrmothera campanisona	*Molecular*	Guyana: Parabara Savannah	KU - B12708

Myrmothera campanisona	*Molecular*	Guyana: Upper Essequibo River	USNM - 625540
Myrmothera campanisona	*Molecular*	Guyana: Parabara Savannah	USNM - 622361
Myrmothera campanisona	*Molecular*	Upper Takutu - Upper Essequibo, lower Rewa River	USNM - 637266
Myrmothera campanisona	*Molecular*	Barima-Waini, Baramita, In Former North West Region	USNM - 621449
Myrmothera campanisona	*Molecular*	Barima-Waini, Baramita, In Former North West Region	USNM - 586403
Myrmothera campanisona	*Molecular*	Gunn'S Landing, West Bank Upper Essequibo River	USNM - 616546
Myrmothera campanisona	*Molecular*	Peru, Loreto Department, S bank Maranon R., Est. Biol. Pithecia	LSUMZ - B3617
Myrmothera campanisona	*Molecular*	Bolivia, Pando Department, Nicolás Suarez; 12 km by road S of Cobija	LSUMZ - B9600
Myrmothera campanisona	*Molecular*	Bolivia, Pando Department, Nicolás Suarez; 12 km by road S of Cobija	LSUMZ - B8955
Myrmothera campanisona	*Molecular*	Peru, Loreto Department, Ca. 86 km SE Juanjui on E bank upper Rio Pauya	LSUMZ - B39839
Myrmothera campanisona	*Molecular*	Peru, Loreto Department, Ca 7 km S Jeberos	LSUMZ - B42523
Myrmothera campanisona	*Molecular*	Peru, Loreto Department, 1 km N Rio Napo, 157 km by river NNE Iquitos	LSUMZ - B2867
Myrmothera campanisona	*Molecular*	Peru, Loreto Department, 79 km WNW Contamana, ca	LSUMZ - B27991
Myrmothera campanisona	*Molecular*	Peru, Loreto Department, S Rio Amazonas, ca 10km SSW mouth Rio Napo	LSUMZ - B5066
Myrmothera campanisona	*Molecular*	Peru, Loreto Department, S bank Maranon River, Est. Biol. Pithecia.	LSUMZ - 103576
Myrmothera campanisona	*Molecular*	Peru, Loreto Department, Lower Rio Napo region, E bank Rio Yanayacu,	LSUMZ - B4346
Myrmothera campanisona	*Molecular*	Peru, Loreto Department, Lower Rio Napo region, E. bank Rio Yanayacu	LSUMZ - B4172
Myrmothera campanisona	*Molecular*	Peru, Loreto Department, 79 km WNW Contamana, ca	LSUMZ - B27987
Myrmothera campanisona	*Molecular*	Venezuela, Amazonas Territory, CERRO DE LA NEBLINA BASE CAMP 140M	LSUMZ - B7563
Mymothera Campanisona D	Morphology	Guyana: Bartica Grove	90595-USNM
Mymothera Campanisona D	Morphology	Guyana: Iwokrana Reserve; ca 41 rd. KM SW Kurupukari; 100m	188777-ANSP
Mymothera Campanisona D	Morphology	Brit. Guyana: Ourumme	51071-ANSP
Mymothera Campanisona D	Morphology	Brit. Guiana: Riv Takutu	492333-AMNH
Mymothera Campanisona D	Morphology	Brazil: R. Amazon, N. Bank, Faro: R. Jamunda, Castanhal	283954-AMNH
Mymothera Campanisona D	Morphology	Brit. Guiana: Riv Takutu	492332-AMNH
Mymothera Campanisona D	Morphology	Brit. Guiana: Tumatumari, Potaro River	125716-AMNH
Mymothera Campanisona D	Morphology	Brit. Guiana: Kartabo	805766-AMNH

Mymothera Campanisona D	Morphology	Brit. Guiana: Kartabo	805765-AMNH
Mymothera Campanisona D	Morphology	Brit. Guiana: Kartabo	805764-AMNH
Mymothera Campanisona D	Morphology	French Guiana: Jamanaio, Mana R.	233860-AMNH
Mymothera Campanisona D	Morphology	French Guiana: Jamanaio, Mana R.	233861-AMNH
Mymothera Campanisona D	Morphology	Cayenne: Ipousin, Approuaque R.	492334-AMNH
Mymothera Campanisona D	Morphology	French Guiana: Jamanaio, Mana R.	233862-AMNH
Mymothera Campanisona D	Morphology	Brazil: R. Amazon, N. Bank, Faro: R. Jamunda, Castanhal	283953-AMNH
Mymothera Campanisona D	Morphology	Brazil: R. Amazon, N. Bank, Faro: Boca R. Pirarucu	283955-AMNH
Mymothera Campanisona D	Morphology	Brazil: R. Amazon, N. Bank, Faro: R. Jamunda, Castanhal	283952-AMNH
Mymothera Campanisona D	Morphology	Brazil: R. Amazon, N. Bank, Faro: R. Jamunda, Castanhal	283951-AMNH
Mymothera Campanisona D	Morphology	Guyana; Upper Essequibo River, 01º35´N 058º38´W, 225M	625540-USNM
Mymothera Campanisona C	Morphology	Peru: Sandia, Huacamayo	103264-ANSP
Mymothera Campanisona C	Morphology	Peru: Sandia, Huacamayo	103265-ANSP
Mymothera Campanisona C	Morphology	Peru: Sandia, Huacamayo	103263-ANSP
Mymothera Campanisona C	Morphology	Peru: Shapaja; Rio Huallaga	117470-ANSP
Mymothera Campanisona C	Morphology	Peru: Dept. Loreto, S bank of Rio maraño on rio Samiria	177840-ANSP
Mymothera Campanisona C	Morphology	Peru: Dept. Loreto, S bank of Rio maraño on rio Samiria	177841-ANSP
Mymothera Campanisona C	Morphology	Peru: Lower Rio Marañon, Pomará	185760-AMNH
Mymothera Campanisona C	Morphology	Peru: Oroja, R. Amazonas	231936-AMNH
Mymothera Campanisona C	Morphology	Peru: Oroja, R. Amazonas	231937-AMNH
Mymothera Campanisona C	Morphology	Peru: N. E. Rio Negro, W. Of Moyabamba	234693-AMNH
Mymothera Campanisona C	Morphology	Peru: Boca R. Umbamba	240341-AMNH
Mymothera Campanisona C	Morphology	Peru: Pomará, Rio Maraño	182048-AMNH
Mymothera Campanisona C	Morphology	Peru: Prov. Huánuco, Chuchurras	492338-AMNH
Mymothera Campanisona C	Morphology	Peru: Mta Rosa, Alto Ucayali	240340-AMNH
Mymothera Campanisona C	Morphology	Peru: Lagarto, Alto Ucayali	239274-AMNH
Mymothera Campanisona C	Morphology	Brazil: Amazonas, Rio Maturaca	326448-USNM

Mymothera Campanisona C	Morphology	Brazil: Venezuela, Brazo Casiquiare, Cano Caripo, below	327110-USNM
Mymothera Campanisona C	Morphology	Brazil: Salto Do Hua, Rio Maturaca	326446-USNM
Mymothera Campanisona C	Morphology	Brazil: Salto Do Hua, Rio Maturaca	326449-USNM
Mymothera Campanisona C	Morphology	Guyana: North West; Baramita, 07º22´N, 60º29´W 125 M	586403-USNM
Mymothera Campanisona C	Morphology	Brazil: Venezuela, Chapazon, Brazo Casiquiare	327111-USNM
Mymothera Campanisona C	Morphology	Brazil: Serra Imeri, near Salto Do Hua	326450-USNM
Mymothera Campanisona C	Morphology	Colombia: Putumayo, Umbria	160036-ANSP
Mymothera Campanisona C	Morphology	Brazil: Amazonas, Rio Maturaca	143135-ANSP
Mymothera Campanisona C	Morphology	Venezuela: Rio Negro	8193-ANSP
Mymothera Campanisona C	Morphology	Brazil: Rio Negro, Javanari	310745-AMNH
Mymothera Campanisona C	Morphology	Brazil: Rio Madeira, Rosarinho	282119-AMNH
Mymothera Campanisona C	Morphology	Venezuela: La Laja. Rio Orinoco, Ven, MT. Duida	273000-AMNH
Mymothera Campanisona C	Morphology	Venezuela: Caño Seou. Rio Orinoco, Serra Duida	272999-AMNH
Mymothera Campanisona C	Morphology	Venezuela: Rio Cassiquiare, L. bank, El Merey	423644-AMNH
Mymothera Campanisona C	Morphology	Colombia: Caqueta, La Murelia (R. Bodoquera)	116349-AMNH
Mymothera Campanisona C	Morphology	Colombia: Caqueta, La Murelia (R. Bodoquera)	116348-AMNH
Mymothera Campanisona C	Morphology	Colombia: Bogota?	492340-AMNH
Mymothera Campanisona C	Morphology	Colombia: Caqueta, Florencia	116347-AMNH
Mymothera Campanisona C	Morphology	Colombia: Caqueta, Florencia	116346-AMNH
Mymothera Campanisona C	Morphology	Brazil: Rio Madeira, Rosarinho, Lago sampaio	282120-AMNH
Mymothera Campanisona C	Morphology	Venezuela: Playa dil Rio Bare, Mte. Duida	273003-AMNH
Mymothera Campanisona C	Morphology	Brazil: Rio Negro, São Gabriel	276106-AMNH
Mymothera Campanisona C	Morphology	Venezuela: Campamento del Medio, Mt Duida	270917-AMNH
Mymothera Campanisona C	Morphology	Brazil: Rio Negro, Cacao Pereria Igarapé	313086-AMNH
Mymothera Campanisona C	Morphology	Venezuela: La Laja. Rio Orinoco, Ven, MT. Duida	273001-AMNH
Mymothera Campanisona C	Morphology	Brazil: Rio Negro, Tatú	AMNH
Mymothera Campanisona C	Morphology	Venezuela: Rio Cassiquiare, R. bank, Opposite El Merey	423645-AMNH

Mymothera Campanisona C	Morphology	Venezuela: Rio Huaynia junction with Rio Cassiquiare, R. Bank	423646-AMNH
Mymothera Campanisona C	Morphology	Venezuela: Campamento del Medio, Mt Duida	273002-AMNH
Mymothera Campanisona C	Morphology	Brazil: Rio Negro, São Gabriel	276105-AMNH
Mymothera Campanisona C	Morphology	Venezuela: Rio Cassiquiare, L. bank, El Merey	417394-AMNH
Mymothera Campanisona C	Morphology	Venezuela: Rio Cassiquiare, R. bank, Opposite El Merey	417393-AMNH
Mymothera Campanisona C	Morphology	Peru: Rio Apurimac, Luisiana (12º39´S, 73º 44´W)	819711-AMNH
Mymothera Campanisona C	Morphology	Peru: Rio Apurimac, HDA. Luisiana, ca. 500m	788334-AMNH
Mymothera Campanisona B	Morphology	Brazil: Rio Tapajós, Limoal	288618-AMNH
Mymothera Campanisona B	Morphology	Brazil: Calama, Rio Machados (Confl. Of R. Madeira)	492336-AMNH
Mymothera Campanisona B	Morphology	Brazil: Rondonia, Mun. Porto Velho, Fazenda Rio Candeias	35156-MPEG
Mymothera Campanisona B	Morphology	Brazil: Pará, Mun. Juruti, Plato Capiranga, Trilha 196	60975-MPEG
Mymothera Campanisona B	Morphology	Brazil: Pará, Mun. Jacareacanga, Vila mamãe-anã	75730-MPEG
Mymothera Campanisona B	Morphology	Brazil: Rondonia, Cachoeira Nazaré, west bank Rio Jiparaná	39823-MPEG
Mymothera Campanisona B	Morphology	Brazil: Rondonia, Cachoeira Nazaré, west bank Rio Jiparaná	39824-MPEG
Mymothera Campanisona B	Morphology	Brazil: Rondonia, Cachoeira Nazaré, west bank Rio Jiparaná	39825-MPEG
Mymothera Campanisona B	Morphology	Brazil: Rondonia, Cachoeira Nazaré, west bank Rio Jiparaná	39826-MPEG
Mymothera Campanisona B	Morphology	Brazil: Rondonia, Cachoeira Nazaré, west bank Rio Jiparaná	39827-MPEG
Mymothera Campanisona A	Morphology	Brazil: Rio Tapajós, Igarape Brabo	286762-AMNH
Mymothera Campanisona A	Morphology	Brazil: Rio Tapajós, Aramanay	288757-AMNH
Mymothera Campanisona A	Morphology	Brazil: Rio Tapajós, Igarape Brabo	286760-AMNH
Mymothera Campanisona A	Morphology	Brazil: Pará, Mun. Itaituba, Prox. Penedo MI4	76458-MPEG
Mymothera Campanisona A	Morphology	Brazil: Pará, Rod. Transamazônica, Km 25, Rio Tapacurazinho	34421-MPEG
Mymothera Campanisona A	Morphology	Brazil: Pará, Rod. Transamazônica, Km 25, Rio Tapacurazinho	47846-MPEG
Mymothera Campanisona A	Morphology	Brazil: Pará, Rio Xingu, Caracol	65325-MPEG
Mymothera Campanisona A	Morphology	Brazil: Pará, Altamira, Flona de Altamira	63897-MPEG
Mymothera Campanisona A	Morphology	Brazil: Pará,Mun. Altamira, Rio Xingu Margem Esquerda	55488-MPEG
Mymothera Campanisona A	Morphology	Brazil: Pará,Mun. Altamira, Rio Xingu Margem Esquerda	55489-MPEG

Hylopezus whittakeri	Morphology	Brazil: Calama, Rio Machados, Confl. Of Rio Madeira	492297-AMNH
Hylopezus whittakeri	Morphology	Brazil: Rio Tapajós, Limoal	288617-AMNH
Hylopezus whittakeri	Morphology	Pará. santarém-cuiabá km 84 (santarém ruropolís).	47847-MPEG
Hylopezus whittakeri	Morphology	Mato grosso. rio aripijanã. dardanelos	34420-MPEG
Hylopezus whittakeri	Morphology	Mato grosso. rio aripijanã. dardanelos nucleo pioneiro humbolt	45606-MPEG
Hylopezus whittakeri	Morphology	RO. alvorada d'oeste linha 64 br 429 km 87	38808-MPEG
Hylopezus whittakeri	Morphology	Rondônia. cachoeira nazaré. west bank of rio jiparaná	MG39819-MPEG
Hylopezus whittakeri	Morphology	Rondônia. cachoeira nazaré. west bank of rio jiparaná	MG39820-MPEG
Hylopezus whittakeri	Morphology	Rondônia. cachoeira nazaré. west bank of rio jiparaná	MG39821-MPEG
Hylopezus whittakeri	Morphology	AM. mun. humaitá. t. i. parintintin; aldeia traíra-chororó	58757-MPEG
Hylopezus whittakeri	Morphology	brasil. pará. belterra. flona do tapajós. base sucupira.	56099-MPEG
Hylopezus whittakeri	Morphology	MT-Mun.Paranaitá, Faz. Rio Paranaitá, Margem direita do Rio Paranaitá.	MG67501-MPEG
Hylopezus whittakeri	Morphology	MT-Mun.Paranaitá, Faz. Aliança, Margem esquerda do Rio Paranaitá.	MG69333-MPEG
Hylopezus whittakeri	Morphology	MT-Mun.Paranaitá, Rio Teles Pires Margem direita.	MG69334-MPEG
Hylopezus whittakeri	Morphology	Brazil: Pará. r tapajós. fordlândia	58838-MZUSP
Hylopezus whittakeri	Morphology	Brazil: Pará. rio jamary	21895-MNRJ
Hylopezus whittakeri	Morphology	Brazil: Santarem, R. Amazon	21365-CMNH
Hylopezus whittakeri	Morphology	Brazil: Colonia de Mojui, Santarem	22035-CMNH
Hylopezus whittakeri	Morphology	Brazil: Colonia de Mojui, Santarem	22034-CMNH
Hylopezus whittakeri	Morphology	Brazil: Colonia de Mojui, Santarem	21729-CMNH
Hylopezus whittakeri	Morphology	Brazil: Colonia de Mojui, Santarem	21826-CMNH
Hylopezus whittakeri	Morphology	Brazil: Vila Braga, R. Tapajos	22994-CMNH
Hylopezus whittakeri	Morphology	Brazil: Vila Braga, R. Tapajos	23119-CMNH
Hylopezus whittakeri	Morphology	Brazil: Miriticuba, R. Tapajos	24624-CMNH
Hylopezus whittakeri	Morphology	Brazil: Santarem, R. Amazon	25166-CMNH
Hylopezus whittakeri	Morphology	Brazil: Vila Braga, R. Tapajos	313767-USMN
Hylopezus whittakeri	Vocal	Brazil: Porto Velho, Rondonia	XC189546

Hylopezus whittakeri	Vocal	Brazil: Mato Grosso, Reserva Ecologica Cristalino, Trilha de Jozias	MLS89010
Hylopezus whittakeri	Vocal	Brazil: Mato Grosso, W of Rio Cristalino, Reserva Ecologica Cristalino	MLS88479
Hylopezus whittakeri	Vocal	Brazil: Mato Grosso, S of Rio Teles Pires	MLS52318
Hylopezus whittakeri	Vocal	Brazil: Mato Grosso, 25.0 km N of Alta Floresta	MLS48111
Hylopezus whittakeri	Vocal	Brazil: Mato Grosso, 20.0 km N of Alta Floresta	MLS48068
Hylopezus whittakeri	Vocal	Brazil: Rondônia, Cachoeira Nazare; west bank of Rio Jiparana	MLS40236
Hylopezus whittakeri	Vocal	Brazil: Pará, Floresta Nacional de Tapajos; Base de Sucupira, BR-163	MLS115081
Hylopezus whittakeri	*Molecular*	Pará, Jacareacanga, margem direita Rio Tapajós, Comunidade São Martim	MPEG - 18511
Hylopezus whittakeri	*Molecular*	Pará, Itaituba, leste do Tapajós, Rio Ratão	MPEG - 18776
Hylopezus whittakeri	*Molecular*	Pará, Itaituba, leste do Tapajós, Jatobá	MPEG - 18803
Hylopezus whittakeri	*Molecular*	Pará, Jacareacanga, margem direita Rio Crepori	MPEG - 19599
Hylopezus whittakeri	*Molecular*	Alvorada d'Oeste, Linha 64, Br 429 Km 87	MPEG - 38808
Hylopezus whittakeri	*Molecular*	Cachoeira Nazaré, west bank Rio Ji-paraná	MPEG - 39819
Hylopezus whittakeri	*Molecular*	Cachoeira Nazaré, west bank Rio Ji-paraná	MPEG - 39820
Hylopezus whittakeri	*Molecular*	Cachoeira Nazaré, west bank Rio Ji-paraná	MPEG - 39821
Hylopezus whittakeri	*Molecular*	Município de Humaitá, T. Indígena Parintintin, Aldeia Traíra-Chororó	MPEG - MPD719
Hylopezus whittakeri	*Molecular*	Paranaíta, margem direita Rio Paranaíta, Fazenda Rio Paranaíta	MPEG - TLP178
Hylopezus whittakeri	*Molecular*	Paranaíta, margem direita Rio Paranaíta, Fazenda Rio Paranaíta	MPEG - TLP179
Hylopezus whittakeri	*Molecular*	Paranaíta, margem esquerda Rio Paranaíta, Fazenda Aliança	MPEG - TLP404
Hylopezus whittakeri	*Molecular*	Paranaíta, Rio Teles Pires, margem direita	MPEG - TLP095
Hylopezus perspicillatus B	Morphology	Colombia: Cordoba, Socorre, Rio Sinu, 1.5 mi below mouth Rio Verde	411881-USNM
Hylopezus perspicillatus B	Morphology	Colombia: Cordoba, Socorre, Rio Sinu, 1.5 mi below mouth Rio Verde	411887-USNM
Hylopezus perspicillatus B	Morphology	Colombia: Cordoba, Socorre, Rio Sinu, 1.5 mi below mouth Rio Verde	411886-USNM
Hylopezus perspicillatus B	Morphology	Colombia: Cordoba, Quebrada Salvajin, Rio Esmeralda, Upper Rio Sinu	411888-USNM
Hylopezus perspicillatus B	Morphology	Colombia: Cordoba, Quebrada Salvajin, Rio Esmeralda, Upper Rio Sinu	411890-USNM
Hylopezus perspicillatus B	Morphology	Colombia: Cordoba, Quebrada Salvajin, Rio Esmeralda, Upper Rio Sinu	411879-USNM
Hylopezus perspicillatus B	Morphology	Colombia: Antioquia, Hacienda Belen, 8 mi W of Segovia	402484-USNM

Hylopezus perspicillatus B	Morphology	Colombia: Antioquia, Hacienda Belen, 8 mi W of Segovia	402481-USNM
Hylopezus perspicillatus B	Morphology	Colombia: Antioquia, Hacienda Belen, 8 mi W of Segovia	402482-USNM
Hylopezus perspicillatus B	Morphology	Colombia: Antioquia, El Real, Rio Nechi	402485-USNM
Hylopezus perspicillatus B	Morphology	Colombia: Antioquia, Taraza, Rio Taraza, 12 km NW Pto. Antioquia	402486-USNM
Hylopezus perspicillatus B	Morphology	Colombia: Bolivar, Santa Rosa, Simiti, 15 mi W	398006-USNM
Hylopezus perspicillatus B	Morphology	Colombia: Bolivar, Santa Rosa, Simiti, 15 mi W	398004-USNM
Hylopezus perspicillatus B	Morphology	Colombia: Cordoba, Socorre, Rio Sinu, 1.5 mi below mouth Rio Verde	411884-USNM
Hylopezus perspicillatus B	Morphology	Colombia: Santander, Conchal, 8 mi NE, Hacienda Santana, on railroad to Wilches	411892-USNM
Hylopezus perspicillatus B	Morphology	Colombia: Santander, Conchal, 8 mi NE, Hacienda Santana, on railroad to Wilches	411891-USNM
Hylopezus perspicillatus B	Morphology	Colombia: Bolivar, Santa Rosa, Simiti, 15 mi W	398005-USNM
Hylopezus perspicillatus B	Morphology	Colombia: Bolivar, Santa Rosa, Simiti, 15 mi W	398007-USNM
Hylopezus perspicillatus B	Morphology	Colombia: Antioquia, Hacienda Belen, 8 mi W of Segovia	402483-USNM
Hylopezus perspicillatus B	Morphology	Colombia: Antioquia, Hacienda Belen, 8 mi W of Segovia	402479-USNM
Hylopezus perspicillatus B	Morphology	Colombia: Cordoba, Quebrada Salvajin, Rio Esmeralda, Upper Rio Sinu	411878-USNM
Hylopezus perspicillatus B	Morphology	Colombia: Cordoba, Quebrada Salvajin, Rio Esmeralda, Upper Rio Sinu	411889-USNM
Hylopezus perspicillatus B	Morphology	Colombia: Cordoba, Quebrada Salvajin, Rio Esmeralda, Upper Rio Sinu	411882-USNM
Hylopezus perspicillatus B	Morphology	Colombia: Cordoba, Quebrada Salvajin, Rio Esmeralda, Upper Rio Sinu	411880-USNM
Hylopezus perspicillatus B	Morphology	Colombia: Cordoba, Socorre, Rio Sinu, 1.5 mi below mouth Rio Verde	411885-USNM
Hylopezus perspicillatus B	Morphology	Colombia: Cordoba, Socorre, Rio Sinu, 1.5 mi below mouth Rio Verde	411883-USNM
Hylopezus perspicillatus B	Morphology	Colombia: Southern Dep. Cordoba, Upper quebr. Charrura,	787157-AMNH
Hylopezus perspicillatus B	Morphology	Colombia: Antioquia, Cauca R., Puerto Valdivia	133534-AMNH
Hylopezus perspicillatus A	Morphology	Ecuador: Rio Tepayo	331277-USNM
Hylopezus perspicillatus A	Morphology	Colombia: Choco, Rio Nuqui, Baudo Mountains, base	443346-USNM
Hylopezus perspicillatus A	Morphology	Colombia: Choco, Rio Nuqui, Baudo Mountains, base Lat 5º40	443349-USNM
Hylopezus perspicillatus A	Morphology	Colombia: Choco, Rio Jurubidá, Baudo Mountains, base Lat 5º58´	443353-USNM
Hylopezus perspicillatus A	Morphology	Colombia: Choco, Rio Jurubidá, Baudo Mountains, base Lat 5º58´	443355-USNM
Hylopezus perspicillatus A	Morphology	Colombia: Antioquia, Villa Artiaga, 7 km NE Pavarondocito	426432-USNM

Hylopezus perspicillatus A	Morphology	Colombia: Choco, Rio Jurubidá, Baudo Mountains, base Lat 5º58´	443352-USNM
Hylopezus perspicillatus A	Morphology	Colombia: Choco, Rio Nuqui, Baudo Mountains, base Lat 5º40	443348-USNM
Hylopezus perspicillatus A	Morphology	Colombia: Antioquia, Villa Artiaga, 7 km NE Pavarondocito	426433-USNM
Hylopezus perspicillatus A	Morphology	Colombia: Antioquia, Villa Artiaga, 7 km NE Pavarondocito	426434-USNM
Hylopezus perspicillatus A	Morphology	Colombia: Antioquia, Villa Artiaga, 7 km NE Pavarondocito	426435-USNM
Hylopezus perspicillatus A	Morphology	Colombia: Choco, Rio Nuqui, Baudo Mountains, base Lat 5º40	443347-USNM
Hylopezus perspicillatus A	Morphology	Colombia: Choco, Rio Jurubidá, Baudo Mountains, base Lat 5º58´	443354-USNM
Hylopezus perspicillatus A	Morphology	Colombia: Choco, Rio Nuqui, Baudo Mountains, base Lat 5º40	443350-USNM
Hylopezus perspicillatus A	Morphology	Colombia: Choco, Rio Nuqui, Baudo Mountains, base Lat 5º40	443351-USNM
Hylopezus perspicillatus A	Morphology	Ecuador: San Javier, N	492293-AMNH
Hylopezus perspicillatus A	Morphology	Ecuador: N, Pambilar	492290-AMNH
Hylopezus perspicillatus A	Morphology	Ecuador: N, Lita	492291-AMNH
Hylopezus perspicillatus A	Morphology	Ecuador: N, Cachabí	492281-AMNH
Hylopezus perspicillatus A	Morphology	Ecuador: San Javier, N	492292-AMNH
Hylopezus perspicillatus A	Morphology	Ecuador: N, Bulum	492288-AMNH
Hylopezus perspicillatus A	Morphology	Ecuador: N, Bulum	492289-AMNH
Hylopezus perspicillatus A	Morphology	Colombia: Choco, River Salaqui	113349-AMNH
Hylopezus perspicillatus A	Morphology	Colombia: N. Chocó, Rio Truandó	787156-AMNH
Hylopezus perspicillatus A	Morphology	Colombia: Choco, Baudo	123355-AMNH
Hylopezus perspicillatus A	Morphology	Colombia: N. Chocó, Upper Rio Murrí	787158-AMNH
Hylopezus perspicillatus A	Morphology	Colombia: Choco, Baudo	123352-AMNH
Hylopezus perspicillatus A	Morphology	Colombia: Choco, Baudo	123353-AMNH
Hylopezus perspicillatus A	Morphology	Colombia: Choco, Baudo	123354-AMNH
Hylopezus perspicillatus A	Morphology	Colombia: West, Narino Barbacoas	117882-AMNH
Hylopezus perspicillatus A	Vocal	Ecuador: Playa de Oro, Esmeraldas	XC98206
Hylopezus perspicillatus A	Vocal	Ecuador: Playa de Oro, Esmeraldas	XC62212
Hylopezus perspicillatus A	Vocal	Ecuador: Reserva Ecologica Cotacachi-Cayapas, Esmeraldas	XC11867

Hylopezus perspicillatus A	Vocal	Ecuador: Playa de Oro, Esmeraldas Province, Ecuador	XC112253
Hylopezus Perspicillatus A	Vocal	Ecuador: Esmeraldas, 20.0 km NW of Alto Tambo	MLS63195
Hylopezus perspicillatus	*Molecular*	Colombia: Santander, Flores Blancas	LSUMZ - 36133
Hylopezus perspicilatus	*Molecular*	Ecuador, Esmeraldas, 20 road km NNW Alto Tambo	ANSP - 17269
Hylopezus perspicilatus	*Molecular*	Ecuador, Esmeraldas, 30 km S Chontaduro; W bank Rio Verde	ANSP - 19055
Hylopezus paraensis	Morphology	Brazil: Pa. paragomimas. fazenda rio capim. cikel	58982-MPEG
Hylopezus paraensis	Morphology	Brazil: PA: Rio acará	1670-MPEG
Hylopezus paraensis	Morphology	PA: Rio Xingu. (Area 2) Caracol, Marg. Direita	65326-MPEG
Hylopezus paraensis	Morphology	PA: Rio Xingu. MARGEM DIREITA CARACOL	64919-MPEG
Hylopezus paraensis	Morphology	Brazil: Pará. mun. ourém. faz. reunida rio ducê. igarapé pedral	32407-MPEG
Hylopezus paraensis	Morphology	Brazil: Pará. mun. ourém. faz. reunida rio ducê. igarapé pedral	32408-MPEG
Hylopezus paraensis	Morphology	Brazil: Pará. senador josé porfirio. margem direita do rio xingu	55691-MPEG
Hylopezus paraensis	Morphology	Brazil: Ma-mun. carutapera. faz. sta. bárbara. rio gurupi	36922-MPEG
Hylopezus paraensis	Morphology	Brazil: Pará. rodovia belem-brasilia km 307.	18127-MPEG
Hylopezus paraensis	Morphology	Brazil: Rodovia belém-brasilia-km 92.pará	15940-MPEG
Hylopezus paraensis	Morphology	Brazil: PA -utinga	36544-MZUSP
Hylopezus paraensis	Morphology	Brazil: Pará-mum.capim-estr.bélem-brasilia km 93.	45208-MZUSP
Hylopezus paraensis	Morphology	Brazil: Pará-mum.capim-estr.bélem-brasilia km 93.	45205-MZUSP
Hylopezus paraensis	Morphology	Brazil: Pará-mum.capim-estr.bélem-brasilia km 93.	45206-MZUSP
Hylopezus paraensis	Morphology	Brazil: Pará-mum.capim-estr.bélem-brasilia km 93.	45207-MZUSP
Hylopezus paraensis	Morphology	Brazil: Utinga-bélem-pa	36543-MZUSP
Hylopezus paraensis	Vocal	Brazil: Paragominas, PA, Brazil, Bacia 549	XC86163
Hylopezus paraensis	Vocal	Brazil: Serra dos Carajás, PA	XC20410
Hylopezus paraensis	Vocal	Brazil: Belo Monte, right bank of Rio Xingu, Pará	XC18925
Hylopezus paraensis	Vocal	Brazil: Pará, Goianésia do Pará	XC155520
Hylopezus paraensis	Vocal	Brazil: Pará, 250.0 km NW of Reserva Indigena Gorotire; Redencao	MLS94535
Hylopezus paraensis	Vocal	Brazil: Pará, Floresta Nacional de Caxiuana; Estacao Cientifica Ferreira Penna	MLS127444

Hylopezus paraensis	Vocal	Brazil: Pará, Floresta Nacional de Caxiuana; Estacao Cientifica Ferreira Penna	MLS113118
Hylopezus paraensis	*Molecular*	Rio Gurupi, Carutapera, Fazenda Santa Bárbara	MPEG - 36922
Hylopezus paraensis	*Molecular*	Brazil: Rondonia, Cachoeira Nazare, W bank Rio Jiparana	FMNH - 389869
Hylopezus paraensis	*Molecular*	Rio Xingu, margem direita, Senador José Porfírio	MPEG - UHE388
Hylopezus paraensis	*Molecular*	Paragominas, Fazenda Rio Capim, CIKEL	MPEG - FRC078
Hylopezus paraensis	*Molecular*	Rio Xingu, margem direita, Caracol (área 2)	MPEG - BMP074
Hylopezus ochroleucus	Vocal	Brazil: Caetité, state of Bahia, 5 Km south from Brejinho das Ametistas	XC200963
Hylopezus ochroleucus	Vocal	Brazil: Tianguá, Tianguá, State of Ceará	XC202306
Hylopezus ochroleucus	Vocal	Brazil: Cavernas do PeruaÃ§u National Park	XC80442
Hylopezus ochroleucus	Vocal	Brazil: Araripe National Forest, Crato, Ceará State	XC201319
Hylopezus ochroleucus	Vocal	Brazil: Road to Remanso, Lençois, Chapada Diamantina, BA	XC18166
Hylopezus ochroleucus	Vocal	Brazil: Bahia, Sebastiao Laranjeiras	MLS91034
Hylopezus ochroleucus	*Molecular*	Piauí, São Raimundo Nonato, PN Serra da Capivara, Serra Vermelha	MPEG - 18943
Hylopezus ochroleucus	*Molecular*	Piauí, Caracol, PN Serra das Confusões, Projeto Cajugaia	MPEG - 18962
Hylopezus ochroleucus	*Molecular*	Piauí, Cristino Castro, PN Serra das Confusões, Baixo Japecanga	MPEG - 18984
Hylopezus ochroleucus	*Molecular*	Piauí, Cristino Castro, PN Serra das Confusões, Baixo Japecanga	MPEG - 18985
Hylopezus ochroleucus	*Molecular*	Piauí, Caracol, P. N. Serra das Confusões, Centro de Visitantes	MPEG - 20156
Hylopezus ochroleucus	*Molecular*	Morro Cabeça no Tempo, Serra Vermelha	MPEG - SRV104
Hylopezus ochroleucus	*Molecular*	Curimatá, Serra Vermelha	MPEG - SRV004
Hylopezus ochroleucus	*Molecular*	Brazil: Minas Gerais; Mocambinho, Jaíba	LGEMA - 2318
Hylopezus ochroleucus	*Molecular*	Brazil: Minas Gerais; Mocambinho, Jaíba	LGEMA - 2036
Hylopezus ocholeucus	Morphology	Brazil: Bahia, Centro oriente.	243146-AMNH
Hylopezus ocholeucus	Morphology	Brazil: Bahia, Ibianeira, Fazenda Bananeira	51162-MPEG
Hylopezus ocholeucus	Morphology	Brazil: Piaui, Morro Cabeça no Tempo, Serra Vermelha	68134-MPEG
Hylopezus ocholeucus	Morphology	Brazil: Piaui, Mun. Curimatá, Serra Vermelha	68135-MPEG
Hylopezus ocholeucus	Morphology	Brazil: Piaui, Mun. São Raimundo Nonato, PN serra da Capivara,	75481-MPEG
Hylopezus ocholeucus	Morphology	Brazil: Piaui, Mun. Caracol, PN serra das Confusões	75511-MPEG

Hylopezus ocholeucus	Morphology	Brazil: Piaui, Mun. Caracol, PN serra das Confusões	76083-MPEG
Hylopezus ocholeucus	Morphology	Brazil: Piaui, Mun. São Raimundo Nonato, PN serra da Capivara, Zabelê	76761-MPEG
Hylopezus ocholeucus	Morphology	Brazil: Piaui, Mun. Cristino Castro, PN serra das Confusões,	76770-MPEG
Hylopezus nattereri	Morphology	Brazil: Paraná, Corvo (Serra da Graciosa)	318523-AMNH
Hylopezus nattereri	Morphology	Brazil: Rio Grande do Sul, São Francisco de Penha	314615-AMNH
Hylopezus nattereri	Morphology	Argentina: Misiones, Arroyo Uruguai-i, Km 30	771188-AMNH
Hylopezus nattereri	Morphology	Argentina: Misiones, Arroyo Uruguai-i, Km 30	771189-AMNH
Hylopezus nattereri	Morphology	Argentina: Misiones, Arroyo Uruguai-i, Km 30	771187-AMNH
Hylopezus nattereri	Morphology	Argentina: Misiones, Arroyo Uruguai-i, Km 30	771186-AMNH
Hylopezus nattereri	Morphology	Argentina: Misiones, Arroyo Uruguai-i, Km 30	771185-AMNH
Hylopezus nattereri	Morphology	Argentina: Misiones, Arroyo Uruguai-i, Km 30	771184-AMNH
Hylopezus nattereri	Morphology	Argentina: Misiones, Arroyo Uruguai-i, Km 10	795287-AMNH
Hylopezus nattereri	Vocal	Brazil: Quatro Barras, Paraná State	XC90459
Hylopezus nattereri	Vocal	Brazil: Itatiaia NP, Tres Picos trail, RJ	XC62448
Hylopezus nattereri	Vocal	Paraguay: Santa Ines, San Rafael, Itapua	XC55422
Hylopezus nattereri	Vocal	Brazil: APA Capivari Monos, São Paulo, SP	XC187632
Hylopezus nattereri	Vocal	Brazil: Sitio Água da rainha , São Francisco de Paula, RS	XC109986
Hylopezus nattereri	Vocal	Brazil: São Paulo, Estacao Biologica de Boraceia	MLS63615
Hylopezus nattereri	Vocal	Brazil: Rio Grande do Sul, Faz. da Zamoreira	MLS20069
Hylopezus nattereri	Vocal	Brazil: Rio Grande do Sul, 5.0 km SE of Canela; Morro Pelado	MLS19813
Hylopezus nattereri	Vocal	Brazil: Rio Grande do Sul, 15.0 km from Sao Francisco De Paula	MLS19292
Hylopezus nattereri	Vocal	Brazil: Rio de Janeiro, Parque Nacional Itatiaia	MLS112731
Hylopezus nattereri	*Molecular*	Quatro Barras, Corvo	MPEG - CMN024
Hylopezus nattereri	*Molecular*	Condominio Alpes- São Francisco de Paula, RS	PUCRS - 3057
Hylopezus nattereri	*Molecular*	CPCN Pró-Mata, São Francisco de Paula-RS	PUCRS - 3345
Hylopezus macularius	Morphology	French Guyana: Tamanois, Mana R.	67370-ANSP
Hylopezus macularius	Morphology	French Guyana: Tamanois, Mana R.	67371-ANSP

Hylopezus macularius	Morphology	Guyana: Iwokrana Reserve; ca 41 rd. KM SW Kurupukari; 100m;	188757-ANSP
Hylopezus macularius	Morphology	Guyana: Iwokrana Reserve; Kabocalli Landing; W. Bank essequibo river	188756-ANSP
Hylopezus macularius	Morphology	Guyana: Iwokrana Reserve; ca 3 mi SW Kurupukari; 110m;	188758-ANSP
Hylopezus macularius	Morphology	Brit. Guyana: Kartabo	805770-AMNH
Hylopezus macularius	Morphology	Brit. Guyana: Kartabo	821498-AMNH
Hylopezus macularius	Morphology	Brit. Guyana: Kartabo	821496-AMNH
Hylopezus macularius	Morphology	Brit. Guyana: Kartabo	821499-AMNH
Hylopezus macularius	Morphology	Brit. Guyana: Kartabo	821497-AMNH
Hylopezus macularius	Morphology	Brit. Guyana: Kartabo	821520-AMNH
Hylopezus macularius	Morphology	Brit. Guyana: Kartabo	805769-AMNH
Hylopezus macularius	Morphology	Brit. Guyana: Ourumme	492298-AMNH
Hylopezus macularius	Morphology	Brit. Guyana: Mines district	156296-AMNH
Hylopezus macularius	Morphology	Brit. Guyana: Mines district	492296-AMNH
Hylopezus macularius	Morphology	Brit. Guyana: River carimang	492295-AMNH
Hylopezus macularius	Morphology	Brit. Guyana: River carimang	492294-AMNH
Hylopezus macularius	Morphology	Guyanaç Gunn<s Landing, 10 KM SSE	625539-USNM
Hylopezus macularius	Morphology	Brazil, Serra do navio, Rio Amapari-Amapa	515628-USNM
Hylopezus macularius	Morphology	British Guiana, Merume Mts	90596-USNM
Hylopezus macularius	Morphology	Guyana: North West; Baramita, 07º22´N, 60º29´W 125 M	586404-USNM
Hylopezus macularius	Morphology	Brazil: Amapá. alto rio araguari. mun. macapá	21181-MPEG
Hylopezus macularius	Morphology	Brazil: Amapá afluente do rio jarí mun. mazagão-amapá	29257-MPEG
Hylopezus macularius	Morphology	Brazil: Amapá areia vermelha. mun. amapá. rio araguarí.	20427-MPEG
Hylopezus macularius	Morphology	Brazil: Amapá. foz do cacouí. afluente esquerdo do rio araguarí	21235-MPEG
Hylopezus macularius	Morphology	Brazil: Amapá. alto rio araguari. margem direita. mun. macapá	21172-MPEG
Hylopezus macularius	Morphology	Brazil: Pa. flota de faro km nw faro.01° 42's 57° 12'w	64739-MPEG
Hylopezus macularius	Morphology	Brazil: Pa:alenquer. esec grão - pará. 00° 09's 55° 11'w	66053-MPEG
Hylopezus macularius	Morphology	Brazil: Amapá. mazagão. cachoeira amapá. alto rio camaipi	28744-MPEG

Hylopezus macularius	Morphology	PA: ÓBIDOS, ESEC GRÃO PARÁ	66675-MPEG
Hylopezus macularius	Morphology	PA: ÓBIDOS, ESEC GRÃO PARÁ	66676-MPEG
Hylopezus macularius	Morphology	PA: ÓBIDOS, ESEC GRÃO PARÁ	66677-MPEG
Hylopezus macularius	Morphology	PA: ÓBIDOS, ESEC GRÃO PARÁ	66678-MPEG
Hylopezus macularius	Morphology	PA: Almeirim Rebio Maicuru	66340-MPEG
Hylopezus macularius	Morphology	Brazil: Amapá Serra do navio. rio amapari-amapá	29429-MNRJ
Hylopezus macularius	Vocal	Brazil: Amazonas, 80.0 km N of Manaus	MLS74427
Hylopezus macularius	Vocal	Guyana: Upper Takutu-Upper Essequibo, 20.0 km E of Nappi Village	MLS70096
Hylopezus macularius	Vocal	Venezuela: Rio Grande; km 10; El Palmar	MLS62471
Hylopezus macularius	Vocal	Venezuela: Rio Grande; km 10.5; El Palmar	MLS62469
Hylopezus macularius	Vocal	Guyana: N of Parabara savannah	MLS54364
Hylopezus macularius	Vocal	Venezuela: 73.0 km S of Eldorado	MLS44279
Hylopezus macularius	Vocal	Venezuela: Rio Grande (sierra De Imabaca)	MLS40466
Hylopezus macularius	Vocal	Brazil: Amazonas, 80.0 km N of Manaus	ML42818
Hylopezus macularius	*Molecular*	Guyana, Iwokrama Reserve; Kobacalli Landing	ANSP - 21224
Hylopezus macularius	*Molecular*	Alenquer, ESEC Grão-Pará	MPEG - 66053
Hylopezus macularius	*Molecular*	Northwest District, Baramita	KU - B09754
Hylopezus macularius	*Molecular*	Acari Mountains, N side	KU - B10765
Hylopezus macularius	*Molecular*	Guyana: Parabara Savannah	KU - B12706
Hylopezus macularius	*Molecular*	Guyana: Barima-Waini, Baramita, In Former North West Region	USNM - 586404
Hylopezus macularius	*Molecular*	Guyana: Parabara Savannah	USNM - 616605
Hylopezus macularius	*Molecular*	Guyana: Gunn'S Landing, 10 km SSE	USNM - 625539
Hylopezus macularius	*Molecular*	Upper Takutu - Upper Essequibo, Upper Rewa River	USNM - 637111
Hylopezus macularius	*Molecular*	Upper Takutu - Upper Essequibo, Upper Rewa River	USNM - 637226
Hylopezus macularius	*Molecular*	Upper Takutu - Upper Essequibo, lower Rewa River	USNM - 637238
Hylopezus macularius	*Molecular*	FLOTA de Faro, ca 70 km NW de Faro	MPEG - CN143
Hylopezus macularius	*Molecular*	Almeirim, REBIO Maicuru	MPEG - CN901

Hylopezus macularius	*Molecular*	Óbidos, ESEC Grão-Pará	MPEG - CN1274
Hylopezus macularius	*Molecular*	Óbidos, ESEC Grão-Pará	MPEG - CN1329
Hylopezus macularius	*Molecular*	Óbidos, ESEC Grão-Pará	MPEG - CN1328
Hylopezus macularius	*Molecular*	Óbidos, ESEC Grão-Pará	MPEG - CN1332
Hylopezus fulviventris	Morphology	Ecuador: Cotapino	169720-ANSP
Hylopezus fulviventris	Morphology	Ecuador: Prov. Napo; S bank Rio Payamino, ca. 20 road km W of Coca	184722-ANSP
Hylopezus fulviventris	Morphology	Ecuador: Rio Payamino, Oriente	163682-ANSP
Hylopezus fulviventris	Morphology	Ecuador: Rio Payamino, Oriente	163683-ANSP
Hylopezus fulviventris	Morphology	Ecuador: Rio Pacayacu, Oriente	169719-ANSP
Hylopezus fulviventris	Morphology	Colombia: Rio San miguel	165179-ANSP
Hylopezus fulviventris	Morphology	Colombia: Rio San miguel	165180-ANSP
Hylopezus fulviventris	Morphology	Colombia: Rio San miguel	165181-ANSP
Hylopezus fulviventris	Morphology	Ecuador: San Jose, above	184359-AMNH
Hylopezus fulviventris	Morphology	Ecuador: E. Below San José de Sumarco	179384-AMNH
Hylopezus fulviventris	Morphology	Ecuador: Voca R, Curaray	255993-AMNH
Hylopezus fulviventris	Morphology	Ecuador: E. Rio Suno, Above avila	179382-AMNH
Hylopezus fulviventris	Vocal	Ecuador: Napo, 20.0 km W of Coca; south bank Rio Payamino	MLS78536
Hylopezus fulviventris	Vocal	Ecuador: Napo, 20.0 km W of Coca; south bank Rio Payamino	MLS78519
Hylopezus fulviventris	Vocal	Ecuador: Sucumbios, Sacha Lodge	MLS68217
Hylopezus fulviventris	Vocal	Ecuador: Sucumb√ios, Sacha Lodge	MLS68208
Hylopezus fulviventris	Vocal	Ecuador: Napo, 1.0 km S of Puerto Napo	MLS50642
Hylopezus fulviventris	Vocal	Peru: Loreto, N. bank Rio Napo; Sucusari Camp	MLS31726
Hylopezus fulviventris	Vocal	Ecuador: Napo, Limoncocha; Rio Napo; E of Coca	MLS30302
Hylopezus fulviventris	*Molecular*	Ecuador, Napo, 20 road km W of Coca; south bank Rio Payamino	ANSP - 18744
Hylopezus fulviventris	*Molecular*	Peru, Loreto Department, Ca 54 km NNW mouth Rio Morona on east bank	LSUMZ - B43007
Hylopezus fulviventris	*Molecular*	Peru, Loreto Department, Ca 54 km NNW mouth Rio Morona on west bank	LSUMZ - B43008
Hylopezus fulviventris	*Molecular*	Peru, Loreto Department, Ca 54 km NNW mouth Rio Morona on west bank	LSUMZ - B43009

Hylopezus fulviventris	*Molecular*	Peru: Loreto ; Ca 54 km NNW mouth of Rio Morona, on east bank	LSUMZ – 42791
Hylopezus dives J	Morphology	Colombia: Antioquia, Alto Bonito	133536-AMNH
Hylopezus dives J	Morphology	Colombia: Antioquia, Alto Bonito	133535-AMNH
Hylopezus dives J	Morphology	Colombia: West, Narino Barbacoas	117884-AMNH
Hylopezus dives J	Morphology	Colombia: West, Narino Barbacoas	117886-AMNH
Hylopezus dives J	Morphology	Colombia: Cauca, San Jose	107478-AMNH
Hylopezus dives J	Morphology	Colombia: Cordoba, Quebrada Salvajin, Rio Esmeralda, Upper Rio Sinu	411877-USNM
Hylopezus dives J	Morphology	Colombia: Choco, Rio Jurubida, Baudo Mountains Lat 5º58´	443357-USNM
Hylopezus dives J	Morphology	Colombia: Valle de cauca, Punto Muchimbo, Rio San Juan,	443358-USNM
Hylopezus dives J	Morphology	Colombia: Antioquia, Villa Artiaga, 7 km NE Pavarondocito	426431-USNM
Hylopezus dives J	Morphology	Colombia: Antioquia, Villa Artiaga, 7 km NE Pavarondocito	426430-USNM
Hylopezus dives J	Morphology	Colombia: Cordoba, Socorre, Rio Sinu, 1.5 mi below mouth Rio Verde	411876-USNM
Hylopezus dives J	Morphology	Colombia: Antioquia, Villa Artiaga, 7 km NE Pavarondocito	426429-USNM
Hylopezus dives J	Morphology	Colombia: Cordoba, Quebrada Salvajin, Rio Esmeralda, Upper Rio Sinu	411875-USNM
Hylopezus dives J	Morphology	Colombia: Cordoba, Quebrada Salvajin, Rio Esmeralda, Upper Rio Sinu	411874-USNM
Hylopezus dives J	Morphology	Colombia: Choco, Rio Jurubida, pacific coast	443356-USNM
Hylopezus dives J	Vocal	Colombia: Buenaventura, Valle del Cauca	XC174797
Hylopezus dives J	Vocal	Colombia: Bahia Solano to El Valle Road, Bahia Solano	XC140772
Hylopezus dives J	Vocal	Colombia: Valle del Cauca, Lower Old Buenaventura	MLS83790
Hylopezus dives J	Vocal	Panama: Darien, Cana	MLS105095
Hylopezus dives I	Morphology	Nicaragua: Rio Grande	492276-AMNH
Hylopezus dives I	Morphology	Nicaragua: Northern, Rio Coco (Wanks River)	103387-AMNH
Hylopezus dives I	Morphology	Nicaragua: Matagalpa, Las Cuevas	102552-AMNH
Hylopezus dives I	Morphology	Nicaragua: Rio Grande	102851-AMNH
Hylopezus dives I	Morphology	Nicaragua: Rio Tuma	103601-AMNH
Hylopezus dives I	Morphology	Nicaragua: Los Sabalos, San Juan River	144043-AMNH
Hylopezus dives I	Morphology	Nicaragua: Matagalpa, Savala	102551-AMNH

Hylopezus dives I	Morphology	Nicaragua: Pena Blanca	103745-AMNH
Hylopezus dives I	Morphology	Nicaragua: Las Canas, 6 miles of Matagalpa	144042-AMNH
Hylopezus dives I	Morphology	Nicaragua: Pena Blanca	103747-AMNH
Hylopezus dives I	Morphology	Nicaragua: Pena Blanca	103746-AMNH
Hylopezus dives I	Morphology	Nicaragua: Rio Grande	492277-AMNH
Hylopezus dives I	Morphology	Nicaragua: Los sabalos	91265-USNM
Hylopezus dives I	Morphology	Nicaragua: Escondido River. 50M from bluefield	128353-USNM
Hylopezus dives I	Morphology	Nicaragua: Greytown, = Graytown (Greystown) or San Juan Del Norte?	40430-USNM
Hylopezus dives I	Vocal	Costa Rica: Pitilla Biological Station, Guancaste Conservation Area	XC6403
Hylopezus dives I	Vocal	Costa Rica: Heredia, 5.0 km S of Puerto Viejo at La Selva	MLS31389
Hylopezus dives I	Vocal	Costa Rica: Heredia, La Selva	MLS26399
Hylopezus dives I	Vocal	Panama: Darien, Cana	MLS25894
Hylopezus dives I	Vocal	Costa Rica: , 100.0 km NE of TURRIALBA; RD TO SIQUIRRES	MLS22664
Hylopezus dives	*Molecular*	Panama, Darién Province, Cana on E slope Cerro Pirré	LSUMZ - B2283
Hylopezus dives	*Molecular*	Honduras, Gracias a Dios t, Las Marias, Rio Platano, 25 km S Caribbean Sea	LSUMZ - B26087
Hylopezus dives	*Molecular*	Panama, Bocas del Toro Province, Rio Changuinola Arriba, W bank	LSUMZ - B46450
Hylopezus dives	*Molecular*	Bocas Del Toro, Tierra Oscura	USNM - 606954
Hylopezus dives	*Molecular*	Bocas Del Toro, Tierra Oscura	USNM - 612384
Hylopezus dives	*Molecular*	Honduras: Gracias a Dios ; Las Marias, on Rio Platano	LSUMZ – 26086
Hylopezus dives	*Molecular*	Costa Rica: Limón; Limón, Reserva Biológica Hitoy Cerere	LSUMZ – 82039
Hylopezus dilutus	Morphology	Venezuela: Rio Orinoco, Serra Duida, Caño Seou	270916-AMNH
Hylopezus dilutus	Morphology	Venezuela: Rio Cassiquiare, Caño Durutomoni	270915-AMNH
Hylopezus dilutus	Morphology	Venezuela: Rio Orinoco, R. bank, Mouth Rio Ocamo, R. Bank	432818-AMNH
Hylopezus dilutus	Morphology	Venezuela: Rio Cassiquiare, R. bank, Opposite El Merey	432824-AMNH
Hylopezus dilutus	Morphology	Venezuela: Rio Cassiquiare, R. bank, Opposite El Merey	432821-AMNH
Hylopezus dilutus	Morphology	Venezuela: Rio Cassiquiare, R. bank, Opposite El Merey	432822-AMNH
Hylopezus dilutus	Morphology	Venezuela: Rio Cassiquiare, R. bank, Opposite El Merey	432823-AMNH

Hylopezus dilutus	Morphology	Venezuela: Rio Cassiquiare, R. bank, Opposite El Merey	432825-AMNH
Hylopezus dilutus	Morphology	Venezuela: Rio Cassiquiare, R. bank, Opposite El Merey	432820-AMNH
Hylopezus dilutus	Morphology	Venezuela: Rio Orinoco, Serra Duida, Caño Seou	270919-AMNH
Hylopezus dilutus	Morphology	Venezuela: Rio Orinoco, R. bank, Mouth Rio Ocamo, R. Bank	432819-AMNH
Hylopezus dilutus	Morphology	Peru: Loreto, Rio Mazan	407154-AMNH
Hylopezus dilutus	Morphology	Venezuela: Rio Cassiquiare, Caño Durutomoni	270918-AMNH
Hylopezus dilutus	Morphology	Peru: Puerto Indiana, Rio Amazonas	231935-AMNH
Hylopezus dilutus	Vocal	Peru: Sabalillo, Loreto	XC20058
Hylopezus dilutus	Vocal	Peru: ExploNapo	XC102595
Hylopezus dilutus	Vocal	BRAZIL: Amazonas: Maraã, Lago Cumapi	Pers.Arc1
Hylopezus dilutus	Vocal	BRAZIL: Amazonas: Jaú National Park	Pers.Arc2
Hylopezus dilutus	*Molecular*	Maraã, Lago Cumapi	MPEG - JAP636
Hylopezus berlepschi H	Morphology	Brazil: Maica	76556-ANSP
Hylopezus berlepschi H	Morphology	Brazil: Rio Tapajós, Caxiricatuba	286766-AMNH
Hylopezus berlepschi H	Morphology	Brazil:Para; East bank Rio Xingu, 52 KM SSW Altamira	572603-USNM
Hylopezus berlepschi H	Morphology	Brazil: Mato Grosso, Mun. Alta Floresta, Rio Teles Pires Margem Esq.	51226-MPEG
Hylopezus berlepschi H	Morphology	Brazil: Mato Grosso, Mun. Paranaíta, Rio Teles Pires Margem Esq.	69331-MPEG
Hylopezus berlepschi H	Morphology	Brazil: Mato Grosso, Mun. Paranaíta, Rio Teles Pires Margem Dir	69332-MPEG
Hylopezus berlepschi H	Morphology	Brazil: Pará, Mun. Tucurui, Arresta da mata, Prox aloj. Temporario I.	36238-MPEG
Hylopezus berlepschi H	Morphology	Brazil: Pará, Carajás, Serra Norte, Manganês.	37250-MPEG
Hylopezus berlepschi H	Morphology	Brazil: Pará, Canaã dos Carajás, Mina do Sossego	72288-MPEG
Hylopezus berlepschi H	Morphology	Brazil: Pará, São Felix do Xingu, Gorotire	37123-MPEG
Hylopezus berlepschi H	Morphology	Brazil: Pará, Mun. Altamira, Rio Xingu Margem Esquerda	55490-MPEG
Hylopezus berlepschi H	Morphology	Brazil: Pará, Mun. Altamira, Rio Xingu Ilha Taboca	55491-MPEG
Hylopezus berlepschi H	Morphology	Brazil: Pará, Mun. Altamira, Rio Xingu Margem direita: Área 1	63448-MPEG
Hylopezus berlepschi H	Morphology	Brazil: Pará, Mun. Altamira, Rio Xingu Margem direita: Área 1	63449-MPEG
Hylopezus berlepschi H	Morphology	Brazil: Pará, Mun.Santarem, Retiro	55490-MPEG

Hylopezus berlepschi G	Morphology	Peru: Puerto Yessup, Junin	91233-ANSP
Hylopezus berlepschi G	Morphology	Peru: Sta Rosa, Alto Ucayali	240342-AMNH
Hylopezus berlepschi G	Morphology	Peru: Lagarta, Alto Ucayali	239269-AMNH
Hylopezus berlepschi G	Morphology	Peru: Sta Rosa, Alto Ucayali	240344-AMNH
Hylopezus berlepschi G	Morphology	Peru: Sta Rosa, Alto Ucayali	240343-AMNH
Hylopezus berlepschi G	Morphology	Bolivia: Todos os Santos, Rio chapare	140806-ANSP
Hylopezus berlepschi G	Morphology	Peru: Madre de Dios; Manu Nat. Park, Cocha Cashu	824073-AMNH
Hylopezus berlepschi G	Morphology	Peru: S. E. Astillero	146168-AMNH
Hylopezus berlepschi G	Morphology	Bolivia: Prov. Cochabamba, Todos os Santos	137176-AMNH
Hylopezus berlepschi G	Morphology	Brazil: Acre,Mun. Cruzeiro do sul, Porangaba, Rio Juruá Margem Direita	49669-MPEG
Hylopezus berlepschi G	Morphology	Brazil: Acre, Mun. Tamaturgo, Nossa senhora Aparecida, Rio Juruá	52917-MPEG
Hylopezus berlepschi	*Molecular*	Bolivia, La Paz t, Rio Beni, ca 20 km by river N. Puerto Linares	LSUMZ - B1057
Hylopezus berlepschi	*Molecular*	Bolivia, La Paz t, Rio Beni, ca 20 km by river N. Puerto Linares	LSUMZ - B1072
Hylopezus berlepschi	*Molecular*	Bolivia, Santa Cruz t, Velasco; Parque Nacional Noel Keonpff Mercado	LSUMZ - B18312
Hylopezus berlepschi	*Molecular*	Peru: Madre Dios; Hacienda Amazonia	FMNH - 322345
Hylopezus berlepschi	*Molecular*	Peru: Madre Dios; Moskitania, 13.4 km NNW of Atalaya	FMNH - 433523
Hylopezus berlepschi	*Molecular*	Rio Juruá, Marechal Taumaturgo, Nossa Senhora Aparecida	MPEG -PND325
Hylopezus berlepschi	*Molecular*	Rio Xingu, Altamira, Ilha da Taboca, UHE Belo Monte	MPEG - UHE046
Hylopezus berlepschi	*Molecular*	Rio Xingu, margem direita, Área 1	MPEG - BMP017
Hylopezus berlepschi	*Molecular*	Rio Xingu, margem direita, Área 1	MPEG - BMP024
Hylopezus berlepschi	*Molecular*	Santarém, Retiro	MPEG - PME022
Hylopezus berlepschi	*Molecular*	Paranaíta, Rio Teles Pires, margem esquerda	MPEG - TLP272
Hylopezus berlepschi	*Molecular*	Paranaíta, margem direita Rio Paranaíta, Fazenda Paranaíta	MPEG - TLP386
Hylopezus berlepschi	*Molecular*	Município de Ourilândia do Norte	MPEG - DPN158
Hylopezus berlepschi	*Molecular*	Peru: Ucayali ; SE slope Cerro Tahuayo, ca km ENE Pucallpa	LSUMZ – 11146
Hylopezus berlepschi	*Molecular*	Brazil: Pará; E. bank R.Teles Pires, 4 km from the mouth of the Rio Sao benedito	LSUMZ – 35407
Hylopezus berlepsch H	Vocal	Brazil: Pará, 250.0 km NW of Reserva Indigena Gorotire; Pinkaiti; Redencao	MLS94594

Hylopezus berlepsch H	Vocal	Brazil: Mato Grosso, S of Rio Teles Pires	MLS52297
Hylopezus berlepsch H	Vocal	Brazil: Mato Grosso, 40.0 km S of Alta Floresta	MLS48054
Hylopezus berlepsch H	Vocal	Brazil: Mato Grosso, Cristalino Ecological Institute	MLS109957
Hylopezus berlepsch H	Vocal	Brazil: Mato Grosso, Alta Floresta	MLS106054
Hylopezus berlepsch H	Vocal	Brazil: Mato Grosso, Reserva Ecologica Cristalino, Bungalow clearing	ML88888
Hylopezus berlepsch H	Vocal	Brazil: Mato Grosso, Reserva Ecologica Cristalino, Bungalow clearing	ML88887
Hylopezus berlepsch G	Vocal	Peru: Madre de Dios, Tambopata Nature Preserve	MLS48171
Hylopezus berlepsch G	Vocal	Peru: Madre de Dios, Tambopata Nature Reserve	MLS47717
Hylopezus berlepsch G	Vocal	Peru: Loreto, North bank Rio Napo; Shansho Cano	MLS30907
Hylopezus berlepsch G	Vocal	Peru: Cuzco, 2.0 km W of Pilcopata	MLS30051
Hylopezus berlepsch G	Vocal	Peru: Madre de Dios, Cocha Cashu; Manu National Park	MLS29523
Hylopezus berlepsch G	Vocal	Peru: Loreto, Rio Napo; Isla Yagua	MLS29375
Hylopezus berlepsch G	Vocal	Bolivia: Santa Cruz, Lago Caiman; Noel Kempff Mercado	MLS127024
Hylopezus berlepsch G	Vocal	Bolivia: Pando, Rutina	MLS100999
Hylopezus auricularis	Vocal	Bolivia: Hamburgo, Riberalta, Beni	XC2720
Hylopezus auricularis	Vocal	Bolivia: Puerto Hamburgo, Riberalta, Beni	XC100423
Hylopezus auricularis	Vocal	Bolivia: Puerto Hamburgo, Riberalta, Beni	XC100424
Hylopezus auricularis	Vocal	Bolivia: Puerto Hamburgo, Riberalta, Beni	XC146789
Hylopezus auricularis	*Molecular*	Bolívia: Beni; Riberalta	FMNH - 391156
Hylopezus auricularis	*Molecular*	Bolívia: Beni; Riberalta	FMNH - 391157
Hylopezus auricularis	*Molecular*	Bolívia: Beni; Riberalta	FMNH - 391158
Grallaricula nana	*Molecular*	Colombia: North of Santander, PNN Tamá, Orocué	LSUMZ –960
Grallaricula flavirostris	*Molecular*	Colombia: Antioquia, Anorí, Alto El Chaquiral	LSUMZ - 4774
Grallaria rufula	*Molecular*	Peru: Cajamarca, Quebrada Lanchal, ca 8 Km ESE Sallique	LSUMZ – 32257
Grallaria ruficapilla	*Molecular*	Colombia: Caldas; Aranzazu, Hacienda Termópilas	LSUMZ – 1666
Grallaria guatimalensis	*Molecular*	Panama: Darien, Cana on E slope Cerro Pirré	LSUMZ – 2331

REFERENCES

Carneiro, L. S., Gonzaga, L. P., Rêgo, P. S., Sampaio, I., Schneider, H., & Aleixo, A. (2012) Systematic revision of the spotted antpitta (Grallariidae: *Hylopezus macularius*), with description of a cryptic new species from brazilian Amazonia. *The Auk*, **129**, 338–351.

Chesser, R.T., (2004) Molecular systematics of New World suboscine birds. *Mol. Phylogenet. Evol*. **32**, 11–24.

Drummond, A.J. & Rambaut, A. (2007) BEAST: Bayesian evolutionary analysis by sampling trees. *BMC Evolutionary Biology*, **7**, 214.

Drummond, A.J., Ho, S.Y.W., Phillips, M.J. & Rambaut, A. (2006) Relaxed phylogenetics and dating with confidence. *PLoS Biology*, **4**, e88.

Drummond, A.J., Suchard, M.A., Xie, D. & Rambaut, A. (2012) Bayesian phylogenetics with BEAUti and the BEAST 1.7. *Molecular Biology and Evolution*, **29**, 1969–1973.

Galvão, A. & Gonzaga, L.P. (2011) Morphological support for placement of the Wing-banded Antbird *Myrmornis torquata* in the Thamnophilidae (Passeriformes: Furnariides). *Zootaxa*, **3122**, 37–67.

Irestedt, M., Fjeldsa˚ , J., Johansson, U.S., Ericson, P.G.P., (2002) System- atic relationships and biogeography of the tracheophone suboscines (Aves: Passeriformes). *Mol. Phylogenet. Evol*. **23**, 499–512.

Krabbe, N., Agro, D.J., Rice, N.H., Jácome, M., Navarrete, L. & Sornoza, M.F. **(**1999) A new species of antpitta (Formicari- idae: *Grallaria*) from the southern Ecuadorian Andes. *Auk* **116**: 882–890.

Krabbe, N., & Schulenberg, T. S. (2003) Family Rhinocryptidae (tapaculos). *Handbook of the Birds of the World 8*. (ed. By J. del Hoyo, A. Elliott and D. A. Christie), pp. 748–787. Lynx Edicions, Barcelona.

Lowery, G.H., O'Neill, J.P. (1969). A new species of antpitta from Peru and a

revision of the subfamily Grallariinae. *Auk*. **86**, 1–12.

Moyle, R. G., Chesser, R. T., Brumfield, R. T., Tello, J. G., Marchese, D. J., & Cracraft, J. (2009) Phylogeny and Phylogenetic Classification of the Antbirds, Ovenbirds, Woodcreepers, and Allies (Aves: Passeriformes: Infraorder Furnariides). *Cladistics*, **25**, 1–5.

Ohlson J. I., M. Irestedt, P. G. P. Ericson, and J. Fjeldsa˚. (2013) Phylogeny and classification of the New World suboscines (Aves, Passeriformes). *Zootaxa*. **3613**:1–35.

Rambaut, A. & Drummond, A.J. (2007) Tracer v1.5. Available at: http://beast.bio.ed.ac.uk/Tracer.

Remsen, J.V. Jr., Areta, J.I., Cadena, C.D., Jaramillo, A., Nores, M., Pacheco, J.F., Perez-Eman, J., Robbins, M.B., Stiles, F.G., Stotz, D.F. & Zimmer, K.J. (2015) A classification of the bird species of South America. *American Ornithologists' Union*. Available at: http://www.museum.lsu.edu/~Remsen/SACCBaseline.html.

Rice, N.H., (2005a) Phylogenetic relationships of antpitta genera (Passeriformes: Formicariidae). *Auk* **122**, 673–683.

Rice, N.H., (2005b) Further evidence for paraphyly of the Formicariidae (Passeriformes). *Condor* **107**, 910–915.

Seddon, N. (2005) Ecological adaptation and species recognition drives vocal evolution in Neotropical suboscine birds. *Evolution,* **59**:200–215.

Smith, B.T. & Klicka, J. (2010) The profound influence of the Late Pliocene Panamanian uplift on the exchange, diversification, and distribution of New World birds. *Ecography*, **33**, 333–342.